UNIVERSITY OF SOUTHAMPTON

COMPLEXES OF GROUP III METAL SALTS AND TITANIUM HALIDES WITH TERTIARY PNICTOGEN OXIDE AND CROWN ETHER LIGANDS

Michael Charles Popham

Thesis submitted for the Degree of Doctor of Philosophy

Department of Chemistry

January 2003

UNIVERSITY OF SOUTHAMPTON
ABSTRACT
FACULTY OF SCIENCE
CHEMISTRY
<u>Doctor of Philosophy</u>
Complexes of Group III Metal Salts and Titanium Halides with Tertiary Pnictogen
Oxide and Crown Ether Ligands
by Michael Popham

The compounds $[Y(R_3PO)_2(EtOH)(NO_3)_3]$ (R_3 = Ph_3 or Ph_2Me), $[Y(Me_3PO)_2(H_2O)(NO_3)_3]$, $[Y(R_3PO)_3(NO_3)_3]$ (R_3 = Ph_3, Ph_2Me or Me_3) and $[Y(Ph_3PO)_4(NO_3)_2]NO_3$ were prepared by reaction of R_3PO with $Y(NO_3)_3.6H_2O$ in EtOH. Similar reactions with $Sc(NO_3)_3.5H_2O$ gave $[Sc(Ph_3PO)_2(NO_3)_3]$, $[Sc(Ph_2MePO)_3(NO_3)_3]$, $[Sc(Ph_2MePO)_4(NO_3)_2]NO_3$, $[Sc(Me_3PO)_2(EtOH)(NO_3)_3]$ and $[Sc(Me_3PO)_6][NO_3]$. Crystal structures of $[Sc(Ph_3PO)_2(NO_3)_3]$, $[Sc(Ph_2MePO)_4(NO_3)_2]NO_3$, $[Y(R_3PO)_3(NO_3)_3]$ (R_3 = Ph_3, Ph_2Me or Me_3) and $[Y(Ph_3PO)_2(EtOH)(NO_3)_3]$ are reported. Similar reactions of R_3AsO (R = Ph or Me) with $M(NO_3)_3.nH_2O$ (M = La, Sc or Y) in Me_2CO yielded the complexes $[Sc(Ph_3AsO)_2(NO_3)_3]$, $[Y(Ph_3AsO)_4(NO_3)_2]NO_3$, $[La(Ph_3AsO)_4(NO_3)_2]NO_3$ and $[La(Me_3AsO)_6](NO_3)_3$. From ethanolic solution, $[Sc(Ph_3AsO)_3(NO_3)_2]NO_3$, $[M(Ph_3AsO)_2(EtOH)(NO_3)_3]$ (M = La or Y) and $[M(Me_3AsO)_6](NO_3)_3$ (M = Y or Sc) were isolated. X-ray structures are reported for $[M(Me_3AsO)_6](NO_3)_3$ (M = Sc or Y), $[Sc(Ph_3AsO)_3(NO_3)_2]NO_3$, $[M(Ph_3AsO)_4(NO_3)_2]NO_3$ (M = Y or La) and $[La(Ph_3AsO)_2(EtOH)(NO_3)_3]$. Reactions of $YX_3.nH_2O$ (X = Cl, Br or I) with the above ligands were carried out in EtOH or Me_2CO solution. Complexes isolated include $[YX_2(Ph_3PO)_4]Z$ (X = Cl, Br or I, Z = X or PF_6), $[YX_3(Ph_2MePO)_3]$, $[YCl_2(Ph_2MePO)_4]PF_6$, $[YCl(Ph_3PO)_5][SbCl_6]_2$, $[Y(Me_3PO)_6]X_3$, $[YX_2(Ph_3AsO)_4]X$, and $[Y(Me_3AsO)_6]Cl_3$. In addition, the X-ray crystal structures of $[YCl_2(Ph_3PO)_4]Cl.2.5EtOH.H_2O$, $[YBr_2(Ph_3PO)_4]PF_6.Et_2O$ and $[Y(Me_3PO)_6]Br_3$ are reported. No reaction was observed between $YF_3.1/2H_2O$ and the same set of ligands. Studies examining complexes of $ScX_3.nH_2O$ (X = Cl, Br or I) with the same ligands were carried out. Compounds isolated include $[ScX_2(Ph_3PO)_4]X$, $[ScX_2(Ph_3AsO)_4]X$, $[ScCl(Me_3PO)_5]Cl_2$, $[Sc(Me_3PO)_6]Z_3$ (Z = Br or I) and $[Sc(Me_3AsO)_6]X_3$. X-ray crystal structures of $[ScBr_2(Ph_3PO)_4]Br$, $[ScCl_2(Ph_3AsO)_4]Cl$ and $[Sc(Me_3AsO)_6]Br_3$ are reported. All of the above complexes were characterised using a combination of analysis, conductance measurements, IR and ^1H NMR spectroscopy. Solution speciation was established by variable temperature $^{31}P-\{^1H\}$ and either ^{89}Y or ^{45}Sc NMR spectroscopy.

The compounds $[ScCl([15]\text{-crown-5})(MeCN)][SbCl_6]_2$, $[ScCl_2([15]aneS_2O_3)][FeCl_4]$ and $[ScCl_2([18]\text{-crown-6})][FeCl_4]$ were made by reaction of $[ScCl_3(thf)_3]$, a halide abstractor and the appropriate ligand in MeCN, the two crown ether (CE) complexes characterised by X-ray crystallography. All three complexes were identified by analysis, IR, ^1H and ^{45}Sc NMR spectroscopy. Hydrolysis of these complexes afforded $[ScCl_3(H_2O)_3].crown$, with $[ScCl_3(H_2O)_3].[18]\text{-crown-6}$ identified by X-ray crystallography. Similar compounds were isolated by direct reaction of $ScCl_3.6H_2O$ and CE's in ethanol, including $[ScCl_3(H_2O)_3]_n.(CE)$ (n = 1 or 2, CE = [18]-crown-6; n = 2, CE = [15]-crown-5, [12]-crown-4). Finally, reactions of $Sc(NO_3)_3.5H_2O$ with CE ligands in ethanol were studied, revealing complexes exhibiting a diverse range of structural type. X-ray crystal structures are reported for $[Sc(H_2O)_2(NO_3)_3].([12]\text{-crown-4})_2$, $[Sc(H_2O)_4(NO_3)_2]NO_3.[15]\text{-crown-5}$, $[Sc_2(NO_3)_2(H_2O)_6(OH)_2](NO_3)_2.[12]\text{-crown-4}$ and $[Sc_2(NO_3)_4(H_2O)_4(OH)_2][Na([12]\text{-crown-4})_2](NO_3).(H_2O)_3$. The Ti(IV) complexes of the same CE ligands were investigated, with compounds of the type $[TiX_4(\eta^2\text{-CE})]$ (X = Cl, Br, CE = [18]-crown-6, [15]-crown-5; X = Br, CE = [12]-crown-4) and $[TiCl_4([15]aneS_2O_3)]$ prepared from TiX_4 and the ligand in anhydrous toluene. Compounds were characterised by analysis, IR, UV/visible and ^1H NMR spectroscopy. Products were readily hydrolysed, with examples identified by X-ray crystallography, namely $[([18]\text{-crown-6})Cl_3Ti(\mu\text{-O})TiCl_3([18]\text{-crown-6})]$ and the tetramer $[\{TiOCl_2([15]\text{-crown-5})\}_4]$. Reaction did not occur when TiI_4 was treated with the CE under the same experimental conditions.

Acknowledgements

Contents

Chapter 3 – Complexes of Yttrium Halides with Tertiary Phosphine and Arsine Oxide Ligands   84

Chapter 4 – Complexes of Scandium Halides with Tertiary Phosphine and Arsine Oxide Ligands   118

Chapter 5 – Complexes of Scandium Halides with Crown Ether Ligands   152

Chapter 6 – Complexes of Titanium Halides with Crown Ether Ligands   189

Chapter 7 – Appendix   214

List of Figures

Chapter 1 – Introduction

Chapter 2 – Complexes of Group III Nitrates with Tertiary Phosphine and Arsine Oxide Ligands

clear resolution of both resonances apparent.

Chapter 3 – Complexes of Yttrium Halides with Tertiary Phosphine and Arsine Oxide Ligands

Chapter 4 – Complexes of Scandium Halides with Tertiary Phosphine and Arsine Oxide Ligands

Chapter 5 – Complexes of Scandium Halides with Crown Ether Ligands

.CH$_3$OH.

Chapter 6 – Complexes of Titanium Halides with Crown Ether Ligands

List of Tables

Chapter 3 – Complexes of Yttrium Halides with Tertiary Phosphine and Arsine Oxide Ligands

Chapter 4 – Complexes of Scandium Halides with Tertiary Phosphine and Arsine Oxide Ligands

Chapter 5 – Complexes of Scandium Halides with Crown Ether Ligands

Chapter 6 – Complexes of Titanium Halides with Crown Ether Ligands

Chapter 7 – Appendix

Abbreviations

Techniques

IR	Infrared	FT	Fourier Transform
NMR	Nuclear Magnetic Resonance	UV/Vis	Ultra violet/visible
Λ_m	Molar Conductance		

Spectroscopy

δ	Chemical Shift	ppm	Parts per million
Hz	Hertz	$\{^1H\}$	Proton decoupled
Q	Quadrupolar moment	I	Nuclear Spin
D_p	Relative receptivity to ^1H	$W_{1/2}$	Half height width
D_c	Relative receptivity to ^{13}C	(s)	Singlet
(d)	Doublet	(t)	Triplet
vw	Very weak	w	Weak
m	Medium	s	Strong
vs	Very strong	br	Broad
e.s.d	Estimated standard deviation	sh	Shoulder
adp	Atomic Displacement Parameter	U	Volume
DR	Diffuse Reflectance	μ	Magnetic moment

Ligands

DPPM	Bis(diphenylphosphino)methane
[12]-crown-4	1,4,7,10-tetraoxacyclododecane
[15]-crown-5	1,4,7,10,13-pentaoxacyclopentadecane
[18]-crown-6	1,4,7,10,13,16-hexaoxacyclooctadecane
[15]aneS$_2$O$_3$	1,4-dithia-7,10,13-trioxacyclopentadecane
[18]aneS$_2$O$_4$	1,4-dithia-7,10,13,16-tetraoxacyclooctadecane
bipy	2,2'-bipyridine
terpy	2,2':6',2"-terpyridine
phen	1,10-phenanthroline
en	Ethylenediamine
EDTA	Ethylenediamine tetraacetate
acac	Acetylacetonate

DOTA	1,4,7,10-tetraazacyclododecane-1,4,7,10-tetraacetic acid		
pz	Pyrazol-1yl		

Groups

M	Metal centre	L	Donor ligand
E	Donor atom	X	Halide
R	Alkyl/Aryl substituent	Me	Methyl
Et	Ethyl	Pr	Propyl
Bu	Butyl	Ph	Phenyl

Solvents

MeCN	Acetonitrile	$MeNO_2$	Nitromethane
Me_2CO	Acetone	$EtNO_2$	Nitroethane
THF	Tetrahydrofuran	Et_2O	Diethyl ether
DMF	N,N-Dimethylformamide	EtOH	Ethanol
DMSO	Dimethylsulfoxide	DCM	Dichloromethane

Other

Mins	Minutes	s	Seconds
d	Days	H	Hours
mmol	Millimoles	*o*	Ortho
TEMPO	2,2,6,6-tetramethylpiperidin-1-oxyl		

Chapter 1

Introduction

1.1 Coordination Chemistry

Within this study, reactions of Group III metal salts and titanium(IV) halides with an array of hard donor ligands are investigated to probe the coordination chemistry of these systems, focusing particularly on the behaviour of species in solution. Explanations of selected concepts and terminologies inherent in the area follow.

1.1.1 Classification of Lewis Acids and Bases

In 1913, G. N. Lewis reported a classification system for chemical substances, defining ligands as 'bases' and the reagents they bond with as 'acids'.[1] The definitions were: -

Lewis Acid ⟶ Electron Pair Acceptor

Lewis Base ⟶ Electron Pair Donor

Whilst useful, this system did not offer information as to whether a given combination of metal and ligand would react to form a stable complex. As a result, in 1958 the Chatt-Ahrland system for classification of metals was developed, with two classes of metal defined:-[2]

Class A → The metal forms stable complexes with 1st row donor elements (eg N, O)

Class B → The metal forms stable complexes with 2nd row donor elements (eg P, S)

The system allowed prediction of the reactivity of two reagents and hence was an improvement upon the system proposed by Lewis. However, the system was fallible in certain cases. For example, transition metals may exhibit different oxidation states, with their reactivity altering significantly as a result. Therefore, their classification may change, a situation not allowed for by the system.

In 1968, the classification system employed today was developed by Pearson to accommodate changes in oxidation state.[3] The following categories were defined: -

Hard Base → donor with high electronegativity, low polarisability, stable to oxidation

Soft Base → donor with low electronegativity, high polarisability, readily oxidised

Hard Acid → acceptor with high positive charge density, low polarisability

Soft Acid → acceptor with low positive charge density and high polarisability

Strong interactions occur when a hard acid reacts with a hard base, combining high charge separation components with low polarisability, resulting in bonds that are ionic in character. For example, Sc^{3+}, a hard acid, readily interacts with hard donor ligands of the type OR_2. In contrast, soft acids react with soft bases to give bonds that are largely covalent in character. In such examples, the charge separation is much less than for a hard/hard interaction, whilst both constituents are easily polarised. Within this study, the majority of reactions involve hard/hard interactions. However, several attempts were made to bond softer ligands to the hard Group III metals. In such cases, there is a potential mismatch in the electronic properties of the acid and the base, with interactions much less stable than either a hard/hard or soft/soft interaction as a result.

1.1.2 Geometries

A study of the coordination chemistry of a given system probes the geometries of compounds produced. With the development of single crystal X-ray diffraction (see 7.1.5), both the detailed geometry and the 'coordination number' around a given metal centre can be easily determined.

The coordination number (CN) is defined as the number of ligands within the primary coordination sphere. A wide range of values is possible, with a maximum value of 12 achievable.[4] The coordination number is dependent on three factors: -

1.   Radius of the central atom or ion.
2.   Steric interactions between the ligands.
3.   Electronic interactions.

In general, higher coordination numbers are observed for larger ionic radii, such as those in the 5th and 6th periods of the Periodic Table, particularly those towards the

left of the d-block. In this region, in addition to a large radius, the ions have few d electrons meaning they can accept more electrons from Lewis bases. The 'smaller' the steric bulk of the ligands, the higher the coordination number is likely to be, as more ligands can be accommodated in a given area.[4]

For a given coordination number, the arrangement of ligands around the metal centre will be in a given geometry (although the angles may not be the idealised values). Table 1.1 lists simple geometries, observed for coordination numbers ranging from 2 to 5, whilst Figure 1.2 gives examples of geometries encountered for complexes with a coordination number of 6 or more.

Further information can be given in the description of a geometry. For example, a compound of formula MX_4Y_2 may be either a 'cis' or 'trans' isomer, whilst complexes of the type MX_3Y_3 could be either the 'mer' or 'fac' isomer (Fig. 1.1).

Table 1.1 Common geometries observed around metal centres with a coordination number of 2 to 5.

Coordination Number	Geometries Commonly Observed
2	Linear
3	Trigonal Planar
4	Tetrahedral, Square Planar
5	Trigonal Bypyramidal, Square Pyramidal

Cis   Trans   Mer   Fac
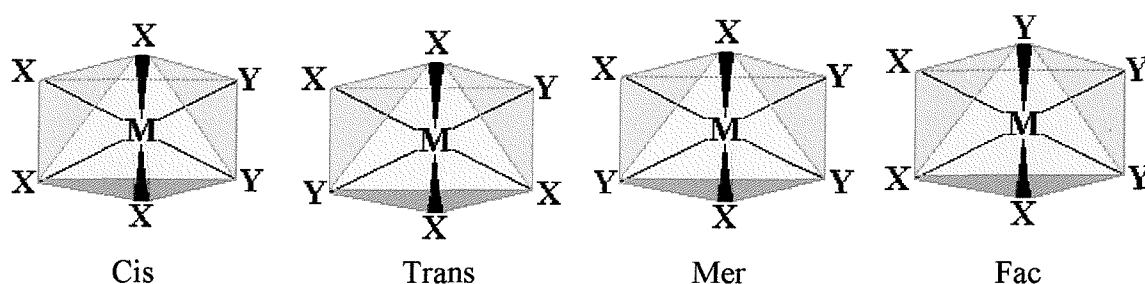
Fig. 1.1 Diagrams showing 'cis' and 'trans' isomers for complexes of the type MX_4Y_2 and the 'mer' and 'fac' isomers of compounds with the formula MX_3Y_3. Shading indicates 'faces' of the octahedron.
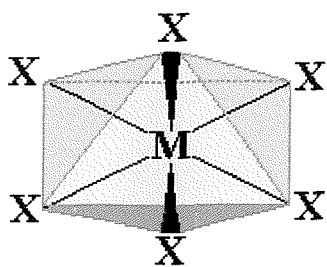
CN = 6 'Octahedral'
eg $[Ti(H_2O)_6]^{3+}$
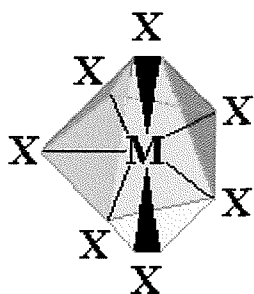
CN = 7 'Pentagonal bipyramidal'
(Pentagonal arrangement of five
ligands with two ligands
perpendicular to this plane).
eg IF_7
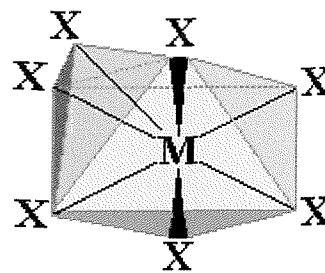
CN = 7 'Capped Octahedral'
(As for Octahedral, with a further
ligand occupying one face).
eg $[NbOF_6]^{3-}$
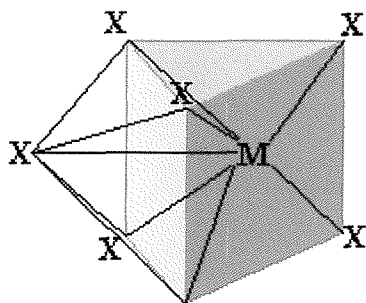
CN = 7 'Capped Trigonal Prism'
(Trigonal Prism with a further
ligand occupying one face).
eg $[NbF_7]^{2-}$
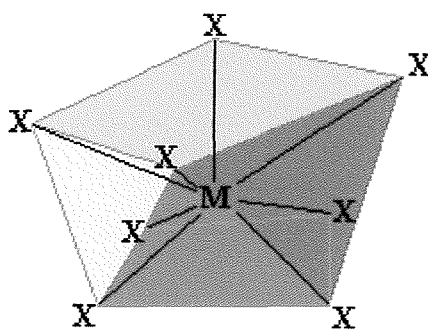
CN = 8 'Square Antiprism
eg $[XeF_8]^{2-}$
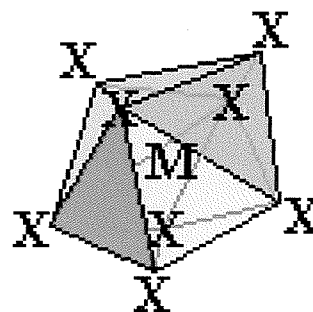
CN = 8 'Dodecahedral'
eg $[Zr(acac)_2(NO_3)_2]$
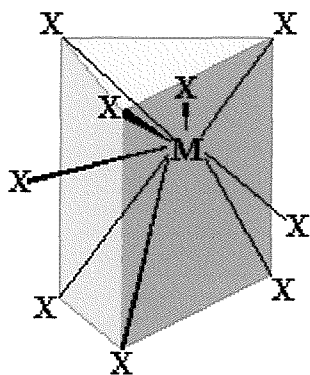
CN = 9 'Tricapped Trigonal Prism' eg $[ReH_9]^{2-}$

Fig. 1.2 Selected geometries encountered for coordination numbers six to nine. M represents the central metal ion, whilst X corresponds to a ligand. Shading has been used to indicate 'faces' of the shape described.

1.2 The Metal Centres

This study focuses on the coordination chemistry of the Group III metals scandium, yttrium and lanthanum, along with investigations into the first row transition metal, titanium.

1.2.1 Scandium

Scandium was first discovered in 1879 by the Swedish scientist Lars Frederick Nilson.[5] Until the turn of the century, when studies into the properties of the element began in earnest, scandium received little attention from within the scientific community, with debates over whether it should be classified as a rare earth, along with an apparent rarity of the metal hindering research. Even when study had commenced, there were difficulties in obtaining sufficient quantities of the metal with a high degree of purity.[5] The first structure determination was for $Sc(acac)_3$, reported in 1926, following which no further structural data were reported until the early 1950's.[6] In the 1940's, during research of the Manhattan project, rare earths were discovered as products of nuclear fission. This lead to development of ion-exchange methods, meaning larger quantities of scandium could be isolated. As a result, more extensive research began.[5] A review details the advances made in the chemistry of scandium in the first twenty years following the development of these ion-exchange methods, a period in which many fundamental areas were examined to some extent.[7]

In recent years, interest in the coordination chemistry of scandium has increased significantly, yet it is still a little studied element, having received the least attention of the 3d elements.[8] Three main reasons explain the lack of study. Firstly, the element is still relatively expensive - whilst the element is not rare, it is evenly distributed throughout the earth's crust, meaning no rich ores exist.[9] Secondly, the element only exhibits a single oxidation state in aqueous solution, Sc(III), meaning scandium is not usually classified as a transition metal. Scandium(III) has the electronic structure $[Ar]3d^04s^0$. This is diamagnetic and colourless, meaning both magnetic and d-d UV/visible spectroscopic probes, two important spectroscopic tools of the coordination chemist, are not of use.[9] Coupled with the high lability of many scandium complexes, these factors have limited studies. A third source of problems

was the misconception that the hard metal centre would not bond to soft ligands, meaning that little study in this area was conducted. However, in the past decade, a number of such examples have been reported, including the phosphine complexes $[Sc[C(PMe_2)_2PMe_2]_3]$ and $[ScCl_2(thf)[N(SiMe_2CH_2PPr^i_2)_2]])$.[9, 10]

Despite not initially appearing an attractive element for study, several properties make scandium an interesting metal to the coordination chemist. Firstly, Sc^{3+} has an ionic radius of 0.68 Å (for the six-coordinate centre), making it larger than any M^{3+} ions of the 3d transition metals, meaning relatively high coordination numbers (CN = 8 or 9) are often met in its chemistry.[9, 11] Early studies suggested that a coordination number of six was standard, with an octahedral geometry the norm, making the coordination chemistry appear less appealing. However, through single crystal X-ray diffraction studies, it has been revealed that the relatively small scandium metal centre can accommodate coordination spheres of between three and nine (although examples of the latter are rare, $[Sc(NO_3)_3(H_2O)_3]$ and $[NO]_2^+[Sc(NO_3)_5]^{2-}$ being the only compounds reported).[6] Examples of structures with a coordination number of 3 are only encountered when the ligands are extremely bulky. For example, the complex $[Sc[N(SiMe_3)_2]_3]$ has been reported.[12] Whilst variation in coordination number is now acknowledged, complexes with a six-coordinate scandium centre are still the most common. Simple examples relevant to this study include $[ScCl_3(thf)_3]$ and $[ScCl_3(H_2O)_3]$, both of which exhibit a *mer*-octahedral geometry.[13, 14]

The difficulties caused by the unsuitability of Sc(III) for certain spectroscopic studies are partially overcome by both the increasing use of single crystal X-ray diffraction in modern chemistry (although reported structures containing Sc are still limited), and the ease with which scandium NMR spectra can be obtained. ^{45}Sc is quadrupolar (I = 7/2) but has only a moderate quadrupole moment (Q = -0.22 x 10^{-28} m^2). The nucleus is one of the most sensitive NMR nuclei (D_c = 1709) and has 100% natural abundance.[15] Despite being little used, ^{45}Sc NMR spectroscopy gives a suitable probe for studying behaviour in solution, although line broadening can cause some problems. ^{45}Sc NMR spectroscopy has been used extensively throughout this project and is described in more detail in section 1.4.2.

Scandium is a hard metal ion (see 1.1) and hence readily coordinates with ligands donating through oxygen, nitrogen or the lighter halides. Scandium has a well developed nitrogen and oxygen donor chemistry.[8] Recent advances in these areas include the isolation of hydrated scandium triflate $Sc(O_3SCF_3)_3.9H_2O$,[16] characterisation of $[Sc(thf)_2(H_2O)Cl_3]$,[17] the first structural determination of a scandium ammine complex, namely $(NH_4)_2[Sc(NH_3)I_5]$,[18] and the synthesis of $[Sc\{N(SiHMe_2)_2\}_3(thf)]$.[19] In contrast, few complexes are known with soft ligands such as those based on sulphur or phosphorus.[8] An example is the compound $[Sc[C(PMe_2)_2SiMe_3]_3]$.[20] Interest in scandium chemistry is increasing, with many applications developed recently. For example, scandium complexes, particularly scandium triflate, have been employed in olefin polymerisation catalysis and sol-gel preparations for oxide materials (for the preparation of thin-film materials or high purity oxide materials).[21, 22] Scandium triflate has also been used as a catalyst for a wide range of organic synthesis reactions, (eg. Michael addition, Aldol reactions) acting as a Lewis acid in aqueous conditions.[23, 24]

1.2.2 Yttrium

The chemistry of yttrium is at a more advanced stage than that of scandium despite the fact that, as for scandium, research into its coordination chemistry did not truly begin until 1950. However, yttrium is still the least studied 4d element. In common with the other Group III metals, only a single oxidation state, Y(III), is accessible in solution. The reason for Y^{3+} being favoured is obvious when the electronic configuration is considered, as it allows the ion to have the stable configuration of krypton $(Y^{3+} = [Kr]4d^0 5s^0)$.[25] Hence, Y(III) has no d-electrons, meaning UV/visible spectroscopy will not show d-d transitions, whilst magnetic probes are also ineffectual owing to the diamagnetic nature of the ion.

The yttrium-89 nucleus is suitable for NMR spectroscopy, having $I = \frac{1}{2}$, being 100% abundant in nature and exhibiting a reasonable receptivity $(D_c = 0.668)$. However it has a low magnetic moment $(\mu = -0.2370)$, which, combined with its lack of a

quadrupolar relaxation mechanism, gives rise to long relaxation times and can make spectra difficult to obtain (see 1.4.1).[15]

As for scandium, the metal favours six-coordinate compounds, with the octahedral geometry prevalent. However, variation in coordination number is seen, with the reasonably large ionic radius of 0.88 Å able to accommodate more than 6 ligands.[11] For example, ten-coordinate Y has been identified, with the nitrate salt, $Y(NO_3)_3.4H_2O$ and $[Y(NO_3)_3(terpy)(H_2O)]$.terpy.3MeCN recently reported examples.[26]

As would be expected given the hard nature of the Y(III) ion, an extensive nitrogen and oxygen donor chemistry has been developed, including some particularly relevant examples with tertiary pnictogen oxides (see 2.1 for a detailed description of these studies).[27, 28, 29] Recent advances in these areas include studies of $YCl_3.6H_2O$ with both bipy and phen ligands, with structures reported for $[Y(bipy)(H_2O)_6]$ $Cl_3.bipy.2H_2O$, $[Y(bipy)(H_2O)_6]Cl_3$ and $[Y(phen)_2(H_2O)_3Cl]Cl_2.H_2O$,[30] whilst complexes with terpy have also been reported, including $[Y(terpy)_3][ClO_4]_3$.[31] Owing to a 'hard/soft mismatch', examples with soft donor ligands are less common, although research in this area is growing. Interest in the chemistry of yttrium has increased significantly in recent years, with a range of applications reported. For example, numerous studies involving oxide materials have been conducted with a view to producing thin-film coatings.[32] Reports of yttrium containing species being adopted as catalysts for ethene polymerisation are known, with the complexes $[rac\text{-}Me_2Si\text{-}2\text{-}SiMe_3\text{-}4\text{-}CMe_3C_5H_2)_2YR]$ (R = C_6F_5, CH_3) and $[N,N'\text{-}R_2\text{-}L\text{-}N''\text{-}(CH_2)_2NBu^t]\text{-}Y(CH_2SiMe_3)_2$ (R = Me or Pr^I, L = 1,4,7-triazacyclononane) recently reported examples.[33, 34, 35] Another application recently pioneered was receptor-mediated radiotherapy (using a complex of the ^{90}Y isotope with $DOTAH_4$ (Fig. 1.3).[36] A review of the use of radioisotopes in both diagnosis and therapy details further complexes of yttrium used in medicine.[37]
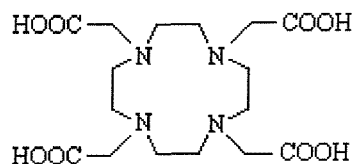
Fig. 1.3 The chelating ligand DOTAH$_4$.[36]

1.2.3 Lanthanum

In common with other Group III metals, lanthanum exhibits a single oxidation state, La(III), the electronic configuration of [Xe]5d^{0}6s^0 conferring stability to the ion. With a radius of 1.06 Å, the lanthanum ion is larger than any of the lanthanide elements (defined as the fourteen elements following lanthanum in the periodic table).[38] The large radius means lanthanum can accomplish coordination numbers as high as 12 when ligands contain close pairs of donor atoms. For example, [La(NO$_3$)$_6$]$^{3-}$ has been identified.[8] As observed for the other lanthanide elements, La forms stable complexes with oxygen donor ligands, particularly those which chelate such as EDTAH$_4$. For example [La(OH$_2$)$_4$EDTAH].3H$_2$O has been identified.[38] Numerous other complexes of lanthanum with chelating oxygen ligands have been characterised, including [La(acac)$_3$].EtOH.3H$_2$O.[39] Lanthanum also forms stable complexes with monodentate oxygen donor ligands, an example particularly relevant to this study being [La(Ph$_3$PO)$_4$(NO$_3$)$_3$].Me$_2$CO (Fig. 1.4).[40] In common with the lighter Group III metals, lanthanum has a well developed nitrogen donor chemistry, again forming stable complexes with both chelating and monodentate ligands.[38] For example, the compounds [La(en)$_4$CF$_3$SO$_3$]$^{2+}$ and [{LaCl$_2$(EtOH)$_2$(bipy)$_2$}$_2$(μ-Cl)$_2$] have been identified.[31, 41]
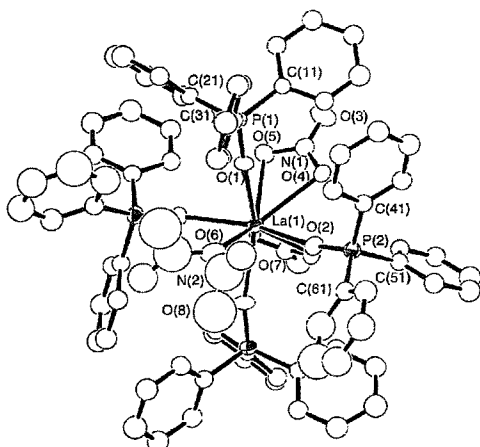
Fig. 1.4 View of [La(NO$_3$)$_3$(Ph$_3$PO)$_4$].Me$_2$CO, revealing a ten-coordinate La centre.[40]

As seen for yttrium and scandium, La(III) lacks d-electrons and is diamagnetic. In contrast to its lighter group III congeners, the ^{139}La nucleus is not generally suitable for NMR spectroscopic studies, with excessive line broadening common (^{139}La is 99.9% abundant, I = 7/2, D_c = 336, Q = 0.21 x 10^{-28} cm^2). However, certain systems exhibit peak widths narrow enough to allow the NMR resonances to be observed, such as aqueous LaX$_3$ solutions (X = Cl$^-$, Br$^-$, I$^-$, NO$_3^-$, ½[SO$_4$]$^{2-}$ or ClO$_4^-$) and as a result, limited ^{139}La studies have been carried out to date.[11]

1.2.4 Titanium

Titanium is the ninth most abundant element in the earth's crust and is the second most common d-block element, only iron being more abundant. It exists in two major ores, namely ilmenite (FeTiO$_3$) and rutile (TiO$_2$), the latter used extensively in the paint industry as a white pigment.[42] Titanium shows a preference for a +4 oxidation state, as exhibited in both ores, in which its four valence electrons are removed presenting a d^0 electronic configuration.[42, 43] Complexes containing Ti(III) and Ti(II) are also known, examples of the former being far more common (eg. [TiCl$_3$(MeCN)$_3$], trans-[TiCl$_2$(THF)$_4$][ZnCl$_3$(THF)]) than Ti(II) compounds.[44] These lower oxidation state titanium centres are often prone to oxidation, explaining the higher frequency of Ti(IV) compounds observed.[42, 43] Titanium (IV) halides readily

complex with hard oxygen donor ligands (eg. $TiCl_4(OMe_2)_2$,) and nitrogen donors (eg. $TiF_2(NMe_2)_2]_4$).[45, 46] In addition, complexes with soft donor ligands are known. For example, the 8-coordinate compounds $[TiBr_4\{o\text{-}C_6H_4(PMe_2)_2\}_2]$, $[TiBr_4\{o\text{-}C_6H_4(AsMe_2)_2\}_2]$ and the 6-coordinate $[TiCl_4\{MeS(CH_2)_2SMe\}]$ have all been characterised by single crystal X-ray diffraction.[47, 48]

Irrespective of oxidation state, the favoured coordination number of titanium is six, although as shown above, variable coordination spheres are observed.[49, 50] Indeed, Ti(IV) complexes are known to demonstrate coordination numbers as low as four (in monomeric $TiCl_4$) and as high as eight ($[Ti(NO_3)_4]$).[51] Titanium NMR was not used for solution speciation in this study, owing to both the poor solubility of the complexes synthesised and the apparent poor properties of the nucleus (whilst both ^{47}Ti and ^{49}Ti are reasonably abundant (7.3 and 5.5% respectively) and are quite sensitive (D_c = 0.864 and 1.18), in practice it is often extremely difficult to obtain spectra, especially in exchanging systems).[11]

1.3 The Ligands

A discussion of ligand classes used in this project and methods for their preparation is presented here.

1.3.1 Phosphine Oxides

Phosphine oxides are ideal ligands for probing the preferred coordination numbers of the Group III metals, with a high affinity to the metal centres being of great importance. Much of this can be ascribed to the fact that oxygen (for which these elements show their greatest affinity) is the bonding atom.[28, 52, 53] However, the exact nature of bonding within R_3PO ligands is still not known, despite being a topic of much discussion for some time. Phosphine and arsine oxide ligands both show a high affinity for a wide range of metals. Indeed, complexes of the most thoroughly studied of these ligands, triphenylphosphine oxide, have been reported with nearly all of the metals in the periodic table. For example, with lithium, the lightest metal, the

compound [LiI(Ph$_3$PO)$_4$].Ph$_3$PO has been reported, whilst at the heavier end of the scale, the complex [HgCl$_2$(μ_2-Ph$_3$AsO)$_2$HgCl$_2$] has been identified.[54]

Little doubt surrounds the bonding when the ligand coordinates to a metal centre with the oxygen of the phosphine oxide coordinating to the metal as a σ-donor. In contrast, a universally accepted bonding model for the PO component in uncoordinated ligands has still not been reported. Until the early 1980's, the PO bond for a tertiary phosphine oxide ligand was considered as somewhere in between the extreme forms shown in Figure 1.5. The left-hand structure is inaccurate as there is evidence that there are not full charges on either atom,[55] whilst phosphorus has insufficient orbitals for the right-hand model to be correct. To explain these problems, a model proposing backbonding from O to low lying empty d orbitals of phosphorus was adopted but is now outdated.

$$P^+ \!\!-\!\! O^- \quad \longleftrightarrow \quad P == O$$
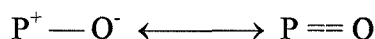
Fig. 1.5 The now outdated representation of the PO bond for 'free' phosphine oxide ligands.

A thorough review of literature concerning the nature of the bonding in phosphine oxides has been published,[55] arriving at the conclusion that the PO bond is best described by one of the following definitions: -

1. 'The PO bond is a double strength bond, formulated as P=O. This representation implies that i) there are three electron pairs between P and O composed of a σ bond between P and O and two π backbonds between lone pairs on O and acceptor orbitals on P which are antibonding in character with respect to the other ligands on P and ii) the electron density of the bonds is strongly skewed towards O so that there is a high degree of positive charge on P and negative on O'.[55]

2. 'The PO bond is a double strength bond, formulated as P=O. This representation implies that i) there are three electron pairs between P and O composed of three π bonds (Fig. 1.6, Part A) from P to A and that ii) the electron density of the bonds is strongly skewed towards O so that there is a high degree of positive charge on P and negative on O'.[55]

3. 'The PO bond is a double strength bond, formulated as P=O. This representation implies that i) there are four electron pairs between P and O composed of a σ bond between P and O and three backbonds from lone pairs on O to the P atom (Fig. 1.6, Part B) and ii) the electron density of the bonds is strongly skewed towards O so that there is a high degree of positive charge on P and negative on O'.[55]

At some point in the future it is likely that the exact nature of the PO bond will be known, but currently these definitions seem the most likely solutions.

A   **B**
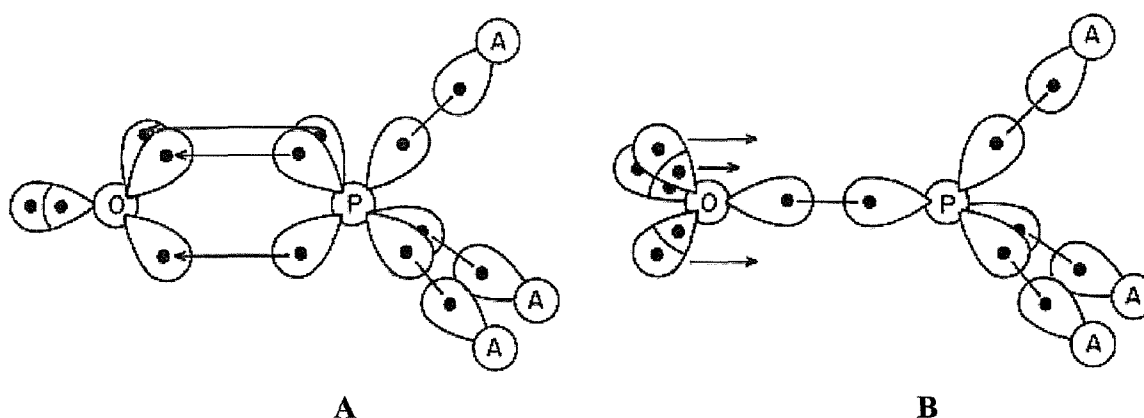
Fig. 1.6 Proposed bonding models for the A_3PO ligand.[56]

Alongside the high affinity of Group III metals for phosphine oxide ligands, a second benefit of using these reagents for determination of the preferred coordination polyhedra of the Group III metals is the ease of observation of ^{31}P-$\{^1H\}$NMR spectra, with the properties of the nucleus well suited to NMR spectroscopic studies (see Section 7.1.4). In addition to characteristic shifts allowing solution speciation, coupling patterns to ^{89}Y and, in high symmetry environments, ^{45}Sc, offer information as to the number of ligands coordinated to the metal centre and hence the precise metal speciation.

A third advantage is characteristic changes observed in the PO strectching frequency upon coordination to the Group III metal centre. The value of v(PO) is seen to

decrease relative to the 'free' ligand. This behaviour is caused by an increase in σ-bonding coupled with a decrease in the π bonding component.[29]

It should be borne in mind when using phosphine oxide ligands that following coordination to a metal centre, the ligand exhibits a 'bent' M-O-P linkage due to lone pair repulsion on the oxygen atom. Whilst this does not hinder bonding, the ligands do require more space than if they were linear. Hence, it is possible that fewer ligands could be coordinated to a given metal centre than if linear ligands were employed.

A wide range of methods exist for the synthesis of phosphine oxide ligands, and the most commonly used routes are described here.[57] The most obvious method is by oxidation of a phosphine reagent, with several routes possible.

Air oxidation in the presence of a suitable catalyst is often adopted. For example, Ph_3P can be converted quantitatively into its oxide by treatment with oxygen in the presence of $Ph_4P^+Cl^-$.[58] Similarly, stirring Ph_3P with nickelocene in benzene in the presence of oxygen affords Ph_3PO in a 90% yield.[57]

A second method employed is oxidation by a peroxy compound. Fig. 1.7 shows oxidation of a diphosphine to afford a diphosphine dioxide ligand by this route.[59] However, whilst effective, there is a risk of explosion (due to peroxides) when adopting this method, meaning extreme care must be taken during synthesis.
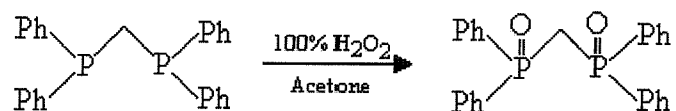
Fig. 1.7 Hydrogen peroxide oxidation of DPPM.[59]

Similar oxidation methods using other inorganic oxidants exist. For example, in this study, iodine oxidation of a phosphine in toluene solution was used, proceeding as shown in Figure 1.8 (note that the intermediate marked 'A' has not been isolated).

$$R_3P \ + \ I_2 \ \longrightarrow \ R_3PI_2 \ \xrightarrow{OH^-} \ R_3P \begin{array}{c} ^{OH} \\ \diagdown_{OH} \end{array} \ + \ 2HI \ \longrightarrow \ R_3P{=}O \ +H_2O$$

A
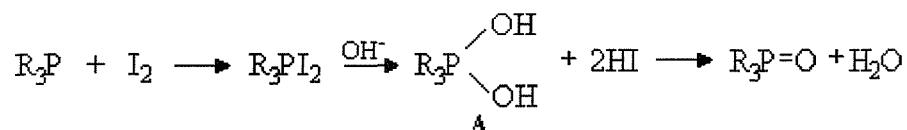
Fig. 1.8 Iodine oxidation of a phosphine to form a phosphine oxide ligand.[55]

1.3.2 Arsine Oxides

As seen for their phosphorus analogues, arsine oxides prove excellent ligands for formation of compounds of Group III metals. Figure 1.9 shows the structure of a ligand used commonly throughout this study, triphenylarsine oxide.
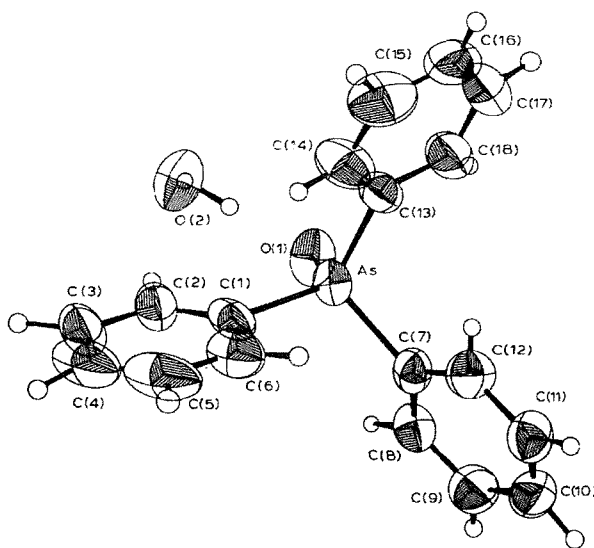
Fig. 1.9 The crystal structure of $Ph_3AsO.H_2O$, showing the atom numbering scheme.[53]

The arsenic derivatives are seen to bond more strongly than their phosphorus congeners, as would be predicted owing to larger dipole moments. For example, Me_3PO exhibits a dipole moment of 4.39 D, compared to 5.12 D for Me_3AsO. Similarly, Ph_3AsO has a dipole moment of 5.50 D compared to 4.51 D for Ph_3PO.[60, 61]

In contrast to ^{31}P, the ^{75}As nucleus is of little use for NMR spectroscopy owing to its quadrupolar properties. Arsine oxide ligands do exhibit a characteristic change in

v(AsO) upon coordination to a metal centre, making infra-red spectroscopy a useful tool for quick identification of complex formation. The value of v(AsO) is seen to increase, contrasting with the behaviour of phosphine oxides for which v(PO) is seen to decrease on coordination. When either ligand coordinates, the σ-bond strength in the pnictogen – oxygen bond is expected to increase, whilst the π-bonding component decreases. The rise in v(AsO) is attributed to an increased importance of σ-bonding.[29]

As for phosphine oxides, there are numerous synthetic routes for the preparation of arsine oxide ligands.[62] Oxidation by either hydrogen peroxide or potassium permanganate are commonly used methods, often giving excellent yields.[63, 64] Iodine oxidation has also proved a successful strategy.[65]

1.3.3 Crown Ethers

Crown ethers are macrocyclic polyethers. A range of compounds is possible by variation in ring size, the arrangement of donor atoms and alteration of the carbon 'backbone' (eg by addition of rigid o-phenylene groups.[66] Examples of variations are shown in Figure 1.10. In addition to demonstrating how the ligands vary, these examples allow explanation of the nomenclature used for crown ethers. The left-hand compound is known as [18]-crown-6. The number in brackets corresponds to the total number of atoms in the macrocyclic ring. The word describes the ligand type (in this case a crown, the name derived from the resemblance of the saturated puckered ring to a crown) whilst the final digit is the number of oxygen atoms in the ring. Groups added to the carbon chain precede this description. For example, the right hand complex is known as dibenzo-[18]-crown-6.
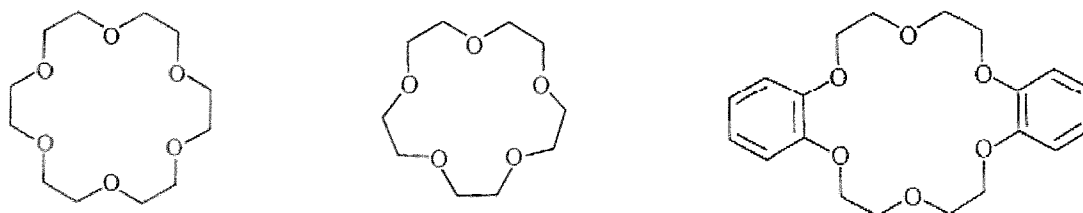
Fig. 1.10 Examples of crown ether ligands. [18]-crown-6, [15]-crown-5 and dibenzo-[18]-crown-6 are pictured (from left to right).

The first reported crown ether ligands were discovered by Lüttringhaus in 1937 during a study investigating medium and large size rings.[67] However, it was not until 1967 that Pedersen reported the formation of stable complexes between crown ethers and alkali metals.[68] The ligands were found to selectively complex alkali and alkaline earth metal ions, leading to numerous studies into their use in separations, solubilisations and ion transport.[69] The selectivity can be apportioned to several major factors. Firstly, 'hole-size selectivity' is of great importance. A close match between the crown cavity and the radius of the cation encourages a stable complex. For example, [18]-crown-6 (cavity 2.6 – 3.2 Å) is seen to form a particularly stable complex with K^+ (radius 2.66 Å).[70] The number and nature of the donor atoms also has considerable effect. Ideally, the number of donor atoms will at least be equal to the coordination number of the cation with the appropriate solvent molecules. The nature of donor atom is obviously of importance. As a general rule, replacement of an oxygen atom with a different donor atom, such as nitrogen or sulphur, will reduce the affinity of the crown for alkali metal ions but often increase affinity towards the softer transition metal cations.[71] A fourth factor governing stability of complexes is addition of rigid cyclic groups to the ring structure, with the effect changing markedly with the nature of the group. For example, benzene rings make the ligand more rigid than the unsubstituted crown, whilst cyclohexyl groups have relatively little effect on ligand / ion stability because they do not greatly alter the flexibility of the ring.[72] Other factors contributing to the ease of complex formation are both the entropy and enthalpies of solvation, along with the conformational preferences of the ligand.[70]

Through a combination of the above factors, different crown ether ligands show greater affinity towards different metal ions. For example, [18]-crown-6 selectively binds alkali metals in the following order: - $K^+ > Rb^+ > Cs^+, Na^+ > Li^+$.[11] Complexes of crown ethers have been reported for a wide range of metal ions. Pedersen reported complexes with Group I and II metals in 1967, since when reactions with transition metal ions have been investigated.[68] An good demonstration of the depth of study of transition metal / crown ether complexes have received is given by examining complexes with metal halides - for the entire first row of the transition metal series, complexes with crown ether ligands have been structurally determined.[73]

Additionally, reactions with the lanthanide and actinide metals have been studied, with structurally characterised examples reported. For example, the structures of $[La(NO_3)_3([18]\text{-crown-6})]$, $[La(ClO_4)_2([18]aneS_2O_4)(H_2O)]^+$ and $[Eu(NO_3)_3([12]\text{-crown-4})]$ have all been reported.[74, 75, 76]

Two main methods of crown ether synthesis exist, namely template synthesis and high dilution synthesis. Template mediated cyclisations essentially use a metal ion to hold the macrocycle framework in place whilst the cyclisation reaction occurs, greatly improving the final yield of product when compared to synthesis in the absence of the template ion. Fig. 1.11 shows a potassium ion acting as a template for synthesis of [18]-crown-6. High dilution synthesis uses large volumes of solvent, with low concentrations of reagents. As a result, cyclisation is favoured over polymerisation.
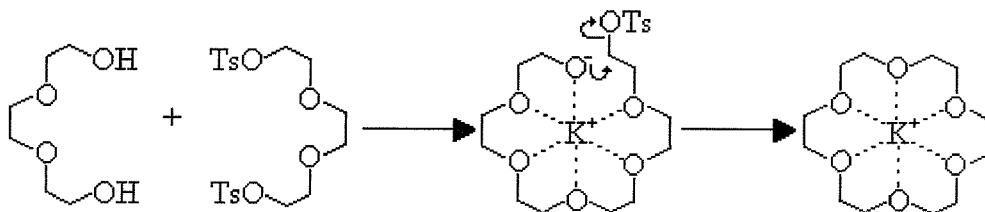
Fig. 1.11 Example of 'templated' crown ether synthesis.[69]

Synthetic strategies for crown ether syntheses may involve displacement of halide ions from a dihaloalkane by a dianion derived from a diol.[69] A typical example is given in Fig. 1.12. Adaptation of the reagents used can greatly alter the final yield. Strategies commonly adopted include use of sulphonate esters as leaving groups (instead of halides), use of a different base (NaH, KOH and Me_3COK are popular alternatives to NaOH) and alteration in solvent, with tetrahydrofuran, DMSO and butanol typical examples.[69]
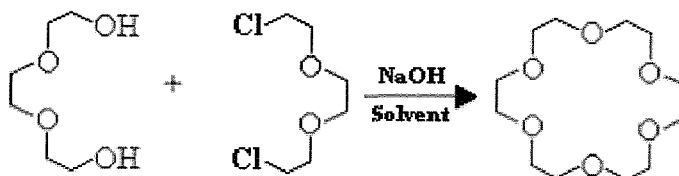
Fig. 1.12 A typical synthetic route for the synthesis of [18]-crown-6.

Synthesis of macrocyclic ligands containing oxygen and sulfur atoms is also well established. For example, Fig. 1.13 shows a synthetic route to the ligand [15]aneS$_2$O$_3$.[77]
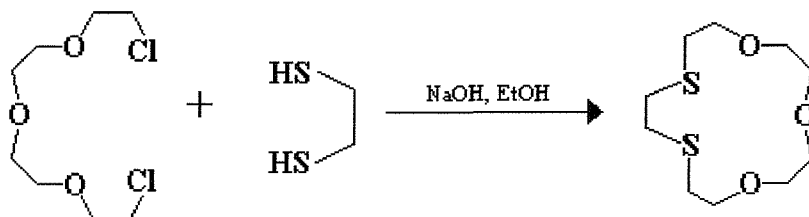
Fig. 1.13 Synthetic route to the ligand [15]aneS$_2$O$_3$.[77]

Crown ethers are excellent ligands for a wide range of metal ions. A description of compounds with the lanthanide metals and titanium are given in Sections 5.1 and 6.1 respectively. Here, complexes with the transition metals are discussed. A good example of the versatility of these ligands is given when the first row transition metal chlorides are considered – complexes have been identified by single crystal X-ray diffraction for every element.[73] For example, reaction of manganese bromide with [12]-crown-4 affords [Mn([12]-crown-4)$_2$][Br$_3$]$_2$, the crowns coordinated through all four oxygens to give an 8-coordinate Mn centre (Fig. 1.14).[78] A second example is the chromium complex [CrCl$_3$.H$_2$O(η^2-[15]-crown-5)], exhibiting hydrogen bonding to the coordinated water from four of the crown oxygens, in addition to bonding between the crown and the chromium centre.[79]
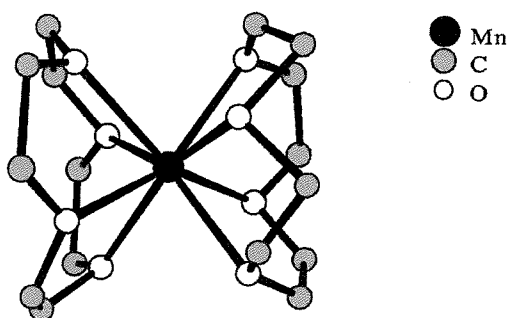
Fig. 1.14 View of the complex [Mn([12]-crown-4)$_2$][Br$_3$]$_2$.[78]

1.4 Characterisation Techniques

Standard characterisation and synthetic techniques are described in Chapter 7, the appendix. This includes IR spectroscopy, ^{1}H, ^{13}C and ^{31}P NMR spectroscopy, single crystal X-ray diffraction, UV/Visible spectroscopy and molar conductance measurements. Here, less common spectroscopic probes are discussed, namely ^{45}Sc and ^{89}Y NMR spectroscopy.

1.4.1 ^{89}Y NMR spectroscopy

The experimental procedures adopted are detailed in Section 7.1.4. The properties of the ^{89}Y nucleus make NMR spectroscopy possible - it is 100% abundant in nature, exhibits a reasonable receptivity (D_c = 0.668) and has I = ½. However, the nucleus has a low magnetic moment (μ = -0.2370), which combined with the lack of a quadrupolar relaxation mechanism gives rise to long relaxation times, making spectra harder to obtain.[15, 80] Studies incorporating solution state ^{89}Y NMR spectroscopy are not common. However, sufficient studies have been conducted to give an insight into how different chemical environments affect the ^{89}Y NMR spectrum. The shift scale runs across approximately 600 ppm. For example, [YCl$_6$]$^{3-}$ appears at 240 ppm (in nitrobenzene solution), whilst at the other end of the scale, [(MeC$_5$H$_4$)$_3$Y(THF)] appears at –371 ppm.[80, 81] The spectrum of [Y(EDTA)]$^-$ in aqueous solution exhibits a resonance at 126 ppm whilst [Y(O$_2$CMe)$_3$] appears at 37 ppm.[81]

1.4.2 ^{45}Sc NMR spectroscopy

The experimental procedures employed for ^{45}Sc NMR spectroscopy are detailed in Section 7.1.4. The scandium-45 nucleus is quadrupolar (I = 7/2) but only has a moderate quadrupole moment (Q = -0.22 x 10^{-28}), is 100% abundant in nature and is very sensitive (D_c = 1709), making spectra relatively easy to obtain.[15, 80] However, despite being a suitable nucleus, examples of ^{45}Sc NMR spectroscopy studies are not common in the literature. Several examples relevant to this study have been reported. For example, Kirakosyan et al. have examined scandium complex formation in non-aqueous solutions by ^{45}Sc NMR spectroscopy, including complexes of Ph$_3$PO and trimethylphosphate with ScCl$_3$ (see 4.1).[82] Examples of chemical shifts from this

report include $[ScF_6]^{3-}$ at δ 2.3, $[ScCl_6]^{3-}$ at δ 249, $[ScBr_6]^{3-}$ at δ 288, exhibiting the effect of heavier halides on chemical shift. The study also includes shifts for ions of the type $[ScCl_{6-n}L_n]$ (L = OP(OMe)$_3$), shown in Table 1.2, demonstrating the shift to lower frequency observed as chloride groups are displaced by the oxygen donor ligand. Also quoted are $[Sc(DMSO)_6]^{3+}$ at δ 44 and cis-$[ScCl_3(DMSO)_3]$ at δ 164. A summary of many early ^{45}Sc NMR spectroscopy studies is given in 'NMR and the Periodic Table', including chemical shifts for a range of 0.1 molar aqueous solutions (eg. $Sc_2(SO_4)_3$ has δ 9.1).[15] Further studies include those by Willey et al., examining the solution state chemistry of scandium(III) with crown ether ligands (discussed in Chapter 5), whilst Korovin et al. have published multinuclear NMR studies into extraction of scandium from hydrochloric acid solutions using tributyl phosphate.[83, 84] The species $[Sc(NCS)_6]^{3-}$ exhibits a resonance at 27 ppm whilst $[Sc(acac)_3]$ appears at 89 ppm.[81]

Table 1.2 Examples of ^{45}Sc NMR shifts for ions of the type $[ScCl_{6-n}L_n]$ in MeCN solution (L = OP(OMe)$_3$).[82]

'Complex'	Chemical Shift (ppm)
$ScCl_6^{3-}$	249.0
cis-$ScCl_4L_2^-$	169.5
cis-$ScCl_3L_3$	139.0
cis-$ScCl_2L_4^+$	87.6
$ScClL_5^{2+}$	33.0
ScL_6^{3+}	-20.7

1.5 Aims of the Study

The study investigates a series of hard/hard interactions probing the coordination chemistry of Group III metals and titanium with an array of oxygen donor ligands. Specifically: -

• Complexes of $M(NO_3)_3.nH_2O$ (M = Y, Sc or La) with tertiary pnictogen oxide ligands were synthesised to examine the geometries of such compounds. No previous examples of structurally characterised tertiary arsine oxide / lanthanide nitrate complexes exist, whilst scandium nitrate / phosphine oxide structures have never previously been reported. In addition, this study allowed comparison of the ligating behaviour of R_3PO and R_3AsO to Group III metal centres.

• Similar studies were conducted using hydrated yttrium and scandium halides. In addition to the above factors, this allowed comparison of the affinity of these metal centres for nitrate and halide groups.

• Reactions of hydrated scandium salts with crown ether ligands were investigated to examine the relative affinity of Sc(III) for water and crown ethers. Analogous reactions were conducted using the anhydrous $[ScCl_3(thf)_3]$ as a precursor to offer comparative results. In addition, this provided more synthetically challenging chemistry, with the products being extremely moisture sensitive.

• For comparison, reactions of titanium(IV) with crown ether ligands were studied, using TiX_4 (X = Cl, Br or I) as a precursor. The decomposition of these compounds when exposed to moisture was also examined.

• Throughout this study, multinuclear NMR spectroscopy was used to monitor behaviour of complexes in solution where appropriate and to allow solution speciation where possible.

1.6 References

1. G. N. Lewis, *J. Am. Chem. Soc.*, 1913, **35**, 1448.

2. J. Chatt, S. Ahrland, N. R. Davies, *Q. Rev. Chem. Soc.*, 1958, **12**, 265.

3. R. G. Pearson, *J. Chem. Educ.*, 1968, **45**, 581.

4. *Inorganic Chemistry, 3^{rd}Edition*, Eds. D. F. Shriver, P. W. Atkins, Oxford University Press, Oxford, 1999, p 212.

5. C. T. Horovitz, *Scandium – Its Occurrence, Chemistry, Physics, Metallurgy, Biology and Technology*, Academic Press Inc., London, 1975.

6. P. R. Meehan, D. A. Aris, G. R. Willey, *Coord. Chem. Rev.*, 1999, **181**, 121.

7. G. A. Melson, R. W. Stotz, *Coord. Chem. Rev.*, 1971, **7**, 133.

8. F. A. Hart in *Comprehensive Coordination Chemistry I*, Eds. G. Wilkinson, R. D. Gillard, J. A. McCleverty, Volume 3, Pergamon Press, Oxford, 1987, p 1060.

9. S. A. Cotton, *Polyhedron*, 1999, **18**, 1691.

10. F. Nief, *Coord. Chem. Rev.*, **178-180**, 13.

11. F. A. Cotton, G. Wilkinson, P. L. Gaus, *Basic Inorganic Chemistry*, 3rd Edition, Wiley, London, 1988.

12. E. C. Alyea, D. C. Bradley, R. G. Copperthwaite, *J. Chem. Soc. Dalton Trans.*, 1972, 1580.

13. J. L. Atwood, K. D. Smith, *J. Chem. Soc., Dalton. Trans.*, 1974, 921.

14. G. R. Willey, P. R. Meehan, M. D. Rudd, M. G. B. Drew, *J. Chem. Soc., Dalton Trans.*, 1995, 3175.

15. R. K. Harris, B. E. Mann, *NMR and the Periodic Table*, Academic Press, London, 1978.

16. C. B. Castellani, O. Carugo, M. Giusti, N. Sardone, *Eur. J. Solid State Inorg. Chem.*, 1995, **32**, 1089.

17. G. R. Willey, P. R. Meehan, M. G. B. Drew, *Polyhedron*, 1997, **16**, 3485.

18. M. Simon, G. Meyer, *Z. Krist*, 1996, **211**, 327.

19. R. Anwander, O. Runte, J. Eppinger, G. Gerstberger, E. Herdtweck, M. Spiegler, *J. Chem. Soc., Dalton Trans.*, 1998, 847.

20. H. H. Karsch, G. Ferazin, O. Steigelmann, H. Kooijman, W. Hiller, A. Schier, P. Bissinger, *J. Organomet. Chem.*, 1994, **482**, 151.

21. S. Hajela, W. P. Schaefer, J. E. Bercaw, *J. Organomet. Chem.*, 1999, **532**, 45.

22. D. Grosso, P. A. Sermon, *J. Mater. Chem.*, 2000, **10**, 359.

23. For a review, see S. Kobayashi, *Eur. J. Org. Chem.*, 1999, 15.

24. M. Nakajima, Y. Yamaguchi, S. Hashimoto, *Chem. Commun.*, 2001, 1596.

25. G. A. Melson, N. P. Crawford, *J. Chem. Soc.*, 1970, 141.

26. P. C. Junk, C. J. Kepert, B. W. Skelton, A. H. White, *Aust. J. Chem.*, 1999, **52**, 497 and A. K. Boudalis, V. Nastopoulos, A. Terzis, C. P. Raptopoulou, S. P. Perlepes, *Z. Naturforsch*, 2001, **56b**, 112.

27. D. R. Cousins, F. A. Hart, *J. Inorg. Nucl. Chem.*, 1967, **29**, 1745.

28. D. R. Cousins, F. A. Hart, *J. Inorg. Nucl. Chem.*, 1967, **29**, 2965.

29. D. R. Cousins, F. A. Hart, *J. Inorg. Nucl. Chem.*, 1968, **30**, 3009.

30. L. I. Semenova, B. W. Skelton, A. H. White, *Aust. J. Chem.*, 1999, **52**, 551.

31. L. I. Semenova, A. N. Sobolev, B. W. Skelton, A. H. White, *Aust. J. Chem.*, 1999, **52**, 519.

32. W. J. Evans, M. S. Sollberger, *Inorg. Chem.*, 1988, **27**, 4417.

33. E. B. Coughlin, J. E. Bercaw, *J. Am. Chem. Soc.*, 1992, **114**, 7606.

34. S. Bambirra, D. van Leusen, A. Meetsma, B. Hessen, J. H. Teuben, *Chem. Commun.*, 2001, 637.

35. W. J. Evans, J. L. Shreeve, R. J. Doedens, *Inorg. Chem.*, 1993, **32**, 245.

36. Y. H. Jang, M. Blanco, S. Dasgupta, D. A. Keire, J. E. Shively, W. A. Goddard, *J. Am. Chem. Soc.*, 1999, **121**, 6142.

37. K. J. Jankowski, D. Parker, *Advances in Metals in Medicine*, 1993, **1**, 29.

38. F. A. Cotton, G. Wilkinson, *Advanced Inorganic Chemistry*, 5th Edition, Wiley, London, 1988.

39. T. J. Wenzel, *Polyhedron*, 1985, **4**, 369.

40. W. Levason, E. H. Newman, M. Webster, *Polyhedron*, 2000, **19**, 2697.

41. P. H. Smith, K. N. Raymond, *Inorg. Chem.*, 1985, **24**, 3469.

42. R. J. H. Clark in *Comprehensive Inorganic Chemistry*, Eds. J. C. Bailar Jr., H. J. Emeleus, R. S. Nyholm, A. F. Trotman-Dickenson, Volume 3, Pergamon Press, Oxford, 1973.

43. R. J. H. Clark, *The Chemistry of Titanium and Vanadium*, Elsevier, Amsterdam, 1968.

44. K. G. Caulton, *Inorg. Chem.*, 1984, **23**, 3289.

45. L. K. Tan, S. Brownstein, *Inorg. Chem.*, 1984, **23**, 1353.

46. P. P. Power, *J. Am. Chem. Soc.*, 1983, **105**, 2927.

47. W. Levason, B. Patel, G. Reid, V.-A. Tolhurst, M. Webster, *J. Chem. Soc., Dalton Trans.*, 2000, 3001.

48. R. Hart, W. Levason, B. Patel, G. Reid, *Eur. J. Inorg. Chem.*, 2001, 2927.

49. D. S. Barratt, C. A. McAuliffe in *Comprehensive Coordination Chemistry*, Eds. G. Wilkinson, R. D. Gillard, J. A. McCleverty, Volume 3, Pergamon Press, Oxford, 1987, p 324.

50. D. L. Kepert, *The Early Transition Metals*, Academic Press, London, 1972.

51. C. D. Garner, S. C. Wallwork, *J. Chem. Soc. (A)*, 1966, 1496.

52. G. Valle, G. Casotto, P. L. Zanonato, B. Zarli, *Polyhedron*, 1986, **5**, 2093.

53. V. K. Belsky, *J. Organomet. Chem.*, 1981, **213**, 435

54. For a review, see P. L. Goggin in *Comprehensive Coordination Chemistry*, Eds. G. Wilkinson, R. D. Gillard, J. A. McCleverty, Volume 2, Pergamon Press, Oxford, 1987, p 497.

55. D. G. Gilheany in *The Chemistry of Organophosphorus Compounds*, ed. F. R. Hartley, Wiley, New York, 1992, Volume 2, p 2.

56. R. P. Messmer, *J. Am. Chem. Soc.*, 1991, **113**, 433.

57. For a review of methods, see A. K. Bhattacharya, N. K. Roy in *The Chemistry of Organophosphorus Compounds*, ed. F. R. Hartley, Wiley, New York, 1992, Volume 2, p 197.

58. R. K. Poddar, U. Agarwala, *Inorg. Nucl. Chem. Lett.*, 1973, **9**, 785.

59. W. Hewertson, *Chem. Abstr.*, 1970, **73**, 56570k.

60. R. R. Carlson, D. W. Meek, *Inorg. Chem.*, 1974, **13**, 1741.

61. R. S. Armstrong, M. J. Aroney, R. J. W. LeFevre, R. K. Pierens, J. D. Saxby, C. J. Wilkins, *J. Chem. Soc.*, 1969, 2735.

62. For a review, see G. O. Doak, L. D. Freeman in *Organometallic Compounds of Arsenic, Antimony and Bismuth*, Wiley, New York, 1970, Chapter 5

63. E. R. H. Jones, F. G. Mann, *J. Chem. Soc.*, 1958, 294.

64. R. L. Shriner, C. N. Wolf, *Org. Syn.*, 1963, **4**, 910.

65. H. Bauer, *J. Am. Chem. Soc.*, 1945, **67**, 591.

66. *Comprehensive Coordination Chemistry I*, Eds. G. Wilkinson, R. D. Gillard, J. A. McCleverty, Volume 2, Pergamon Press, Oxford, 1987, p 915.

67. A. Lüttringhaus, *Ann. Chem.*, 1937, **528**, 181.

68. C. J. Pedersen, *J. Am. Chem. Soc.*, 1967, **89**, 2495 & 7017.

69. For a review see ref. 66 or E. Weber, F. Vögtle in *Crown Ethers and Analogs*, Eds. S. Patai, Z. Rappoport, Wiley, New York, 1989, p 207.

70. G. W. Gokel, D. M. Goll, C. Minganti, L. Echegoyen, *J. Am. Chem. Soc.*, 1983, **105**, 6786.

71. H. K. Frensdorff, *J. Am. Chem. Soc.*, 1971, **93**, 600.

72. R. M. Izatt, R. E. Terry, B. L. Haymore, L. D. Hanson, J. K. Dalley, A. G. Avondet, J. J. Christensen, *J. Am. Chem. Soc.*, 1976, **98**, 7620.

73. For a review, see V. K. Belsky, B. M. Bulychev, *Russ. Chem. Rev.*, 1999, **68**, 119.

74. J. D. J. Backer-Dirks, J. E. Cooke, A. M. R. Galas, J. S. Ghotra, C. J. Gray, F. A. Hart, M. B. Hursthouse, *J. Chem. Soc., Dalton Trans.*, 1980, 2191.

75. M. Ciampolini, C. Mealli, N. Nardi, *J. Chem. Soc., Dalton Trans.*, 1980, 376.

76. J.–C. G. Bünzli, B. Klein, D. Wessner, N. W. Alcock, *Inorg. Chim. Acta*, 1982, **59**, 269.

77. J. S. Bradshaw, G. Y. Hui, B. L. Haymore, J. J. Christensen, *J. Heterocyclic Chem.*, 1973, **10**, 1.

78. B. B. Hughes, R. C. Haltiwanger, C. G. Pierpoint, M. Hampton, G. L. Blackmer, *Inorg. Chem.*, 1980, **19**, 1801.

79. T. Ernst, K. Dehnicke, H. Goessmann, D. Fenske, *Z. Naturforsch., B Chem. Sci.*, 1990, **45**, 967.

80. *Multinuclear NMR*, Ed. J. Mason, Plenum, New York, 1987, p195.

81. D. Rehder in *Transition Metal NMR*, P. S. Pregosin (Ed.), Elsevier, New York, 1991, Ch. 1, p4.

82. G. A. Kirakosyan, V. P. Tarasov, Y. A. Bulsaev, *Magn. Reson. Chem.*, 1989, **27**, 103.

83. Y. V. Korovin, S. B. Randerevich, Y. N. Pogorelov, S. V. Bodaratskii, *Koord. Khim.*, 1996, **22**, 597.

84. G. R. Willey, P. R. Meehan, *Inorg. Chim. Acta*, 1999, **284**, 71.

Chapter 2

Complexes of Group III Nitrates with Tertiary Phosphine and Arsine Oxide Ligands

2.1 Introduction

Lanthanide ions complex readily with phosphine and arsine oxide ligands, largely due to the negative charge on the oxygen atom produced by the canonical form RX^+-O^- (X = As or P).[1] This provides an electrostatic charge to the cation ligand bond energy, favouring coordination (discussed in Section 1.3.1).[2-4] This affinity was first recognised when the compound $[EuCl_3(Ph_3PO)_3]$ was reported in 1964.[5] Shortly afterwards, a range of phosphine and arsine oxide complexes was reported in a series of papers detailing synthesis and characterisation (largely by IR spectroscopy and microanalysis of C, H and N levels).[2,6,7] Of direct interest were complexes of the type $[M(NO_3)_3L_2(EtOH)]$, $[M(NO_3)_3L_3]$ and $[M(NO_3)_2L_4]NO_3$ (where M = yttrium or a lanthanide, L = Ph_3PO or Ph_3AsO), synthesised by reaction of the hydrated nitrate with the ligand in either ethanol or acetone.[2,6] Concentrating specifically on compounds of yttrium and lanthanum with triphenylphosphine oxide, the compounds reported by Hart *et al.* are detailed in Table 2.1, with the PO stretch reported also described. Several of these compounds were reproduced during this investigation to probe behaviour in solution and to allow further characterisation in the solid state.

Table 2.1 Complexes of $M(NO_3)_3.6H_2O$ (M = Y or La) with Ph_3PO reported by Hart *et al.*[6]

Complex	Ph_3PO:Metal	Solvent	PO stretch
$[La(NO_3)_3(Ph_3PO)_2]EtOH$	2:1	EtOH	1142 + 1153
$[Y(NO_3)_3(Ph_3PO)_2]EtOH$	2:1	EtOH	1151 + 1171
$[La(NO_3)_3(Ph_3PO)_3]$	3:1	EtOH	1147
$[Y(NO_3)_3(Ph_3PO)_3]$	3:1	EtOH	1153 + 1161
$[La(NO_3)_3(Ph_3PO)_3].2Me_2CO$	3:1	Me_2CO	1140sh + 1149
$[Y(NO_3)_3(Ph_3PO)_3].2Me_2CO$	3:1	Me_2CO	1151 + 1163
$[La(NO_3)_2(Ph_3PO)_4]NO_3.Me_2CO$	4:1	Me_2CO	1159
$[Y(NO_3)_2(Ph_3PO)_4]NO_3$	4:1	EtOH	1150

Since these early studies, phosphine oxides have become popular ligands for determination of the preferred coordination polyhedra of the lanthanide series, although very few NMR studies have been carried out.[8] Along with the advantage conferred by their easy coordination to the trivalent metal ions, the ease of observation of ^{31}P-$\{^{1}H\}$ NMR spectra makes them attractive. The nucleus is 100% abundant, having $I = \frac{1}{2}$, a reasonable receptivity ($D_p = 0.0663$) and a fairly high magnetic moment ($\mu = 1.9581$).[9] When coordinated to a suitable metal centre (such as ^{89}Y or ^{45}Sc), coupling patterns may be observed revealing the number of ligands bonded. In contrast, ^{75}As is of little use for study by NMR spectroscopy owing to its quadrupolar properties, with no resonances observed for low symmetry environments such as R_3AsO.[9]

Both pnictogen oxides exhibit characteristic changes in the X-O stretching frequency upon co-ordination (X = As or P). When the ligand bonds to the lanthanide ion, the σ-bonding component is expected to increase whilst the π-bond strength decreases. The $v(AsO)$ increases on complexation, whilst the value of $v(PO)$ decreases relative to the 'free' ligand, indicating a stronger σ-bonding contribution in the former.[6] This is predicted, since arsenic is less electronegative, hence allowing more electron density to be centred on the oxygen atom.

The reactions of pnictogen oxides with lanthanide ions provide an active area of research with much work concentrating on the use of phosphine oxide ligands in the extraction and separation of ions.[10,11] However, despite significant study in this context, few examples have been structurally characterised,[3,12,13] whilst speciation in solution has received only very scant attention.[1,8] In particular, little is known about complexes with scandium or yttrium, with no complexes of the former structurally characterised.[14-16] Of the examples that have been structurally characterised, $[Ce(Ph_3PO)_3(NO_3)_3]$,[13] $[La(Ph_3PO)_3(NO_3)_3].xCH_2Cl_2$ (Fig. 2.1),[13] $[Eu(Ph_3PO)_3(NO_3)_3]$,[3] $[Nd(Ph_3PO)_3(NO_3)_3]$[17] and $[Sm(Ph_3PO)_3(NO_3)_3]$[18] are directly relevant to the work in this thesis. Examples of X-ray structures of bis(phosphine oxide)-ethanol adducts reported include $[Eu(Ph_3PO)_2$ $(NO_3)_3(EtOH)]$ and $[Ce(Ph_3PO)_2(NO_3)_3(EtOH)]$,[3,13] whilst $[Lu(Ph_3PO)_4(NO_3)_2]NO_3$ offers an example of a structurally characterised tetrakis(phosphine oxide) complex of

lanthanum nitrate.[13] No previous examples of structurally characterised tertiary arsine oxide / lanthanide nitrate compounds have been reported in the literature.
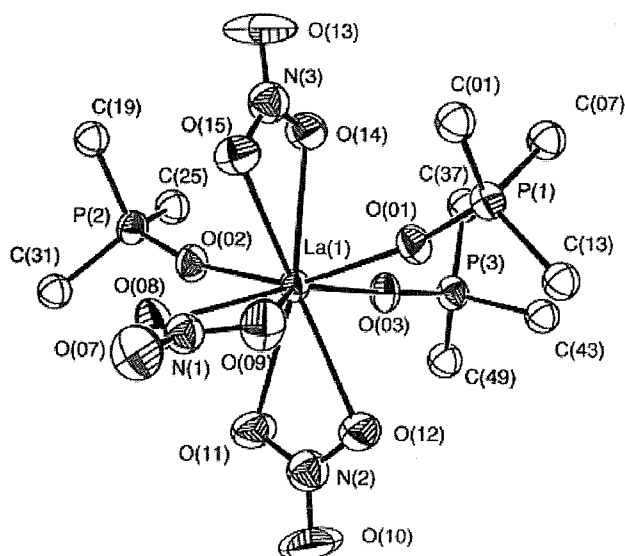
Fig. 2.1 View of $[La(Ph_3PO)_3(NO_3)_3].xCH_2Cl_2$, showing the atom numbering scheme.[13] Phenyl groups are removed for clarity.

The aims of this study were numerous. Firstly, previous work in this area by Hart *et al.* had only identified complexes by IR spectroscopy and analysis. No studies looking at behaviour in solution had been conducted, whilst structural data was very limited with no examples of a Group III metal nitrate/tertiary arsine oxide complex reported previously. With the aid of a wide range of spectroscopic techniques, full characterisation would be possible, including solution speciation. Hence, by comparison with previous work in this area, a complete picture of the coordination chemistry of Group III metal nitrates with these ligands would be formed. Furthermore, these studies would allow comparison of the ligating power of R_3PO and R_3AsO. Finally, results would reveal any differences in the coordination chemistry of Sc, Y and La centres, with the large variation in ionic radii likely to result in different products under similar reaction conditions.

2.2 Results and Discussion

2.2.1 Complexes of yttrium nitrate with triphenylphosphine oxide

Reaction of yttrium nitrate hexahydrate with either one or two molar equivalents of Ph_3PO in boiling ethanol afforded the complex $[Y(Ph_3PO)_2(EtOH)(NO_3)_3]$, whilst reaction of a 1 : 4 ratio of metal to ligand in warm ethanol yielded the tris species, $[Y(Ph_3PO)_3(NO_3)_3]$. A third complex in the series, $[Y(Ph_3PO)_4(NO_3)_2]NO_3$, was produced by reaction of the metal salt with six molar equivalents of triphenylphosphine oxide in ice-cold ethanol. All the compounds were poorly soluble in ethanol, precipitating out of solution when refrigerated, making the syntheses relatively straightforward. The complexes formed had the same stoichiometries as reported by Hart et $al.$ in a paper describing reactions of the same system.[2]

Infrared spectroscopy showed a reduction in $v(PO)$ in all three compounds, compared with the vibration in the free ligand (1195 cm^{-1}). The weakening of the P-O bond was most prominent in the tetrakis(phosphine oxide) species ($v(PO)$ = 1154 cm^{-1}, compared to 1150 cm^{-1} reported by Hart, the difference presumably due to both the improved resolution of modern IR spectrometers and the fact that whilst in this work, CsI plates were used for Nujol mulls, Hart employed KBr discs).[2] The ionic nitrate present in this compound could be identified by the weak band at 830 cm^{-1} (absent in the other spectra), assigned as the v_2 mode of NO_3^-.[19] The 'free' nitrate has D_3h symmetry, with IR active bands observed at 834 (A_2"[v_2]), 1361 (E'[v_3]) and 755 (E'[v_4]). In addition, three Raman active bands exist, namely (A_1'[v_1]), (E'[v_3]) and (E'[v_4]).[19] Upon coordination, whether in a monodentate or bidentate mode, the symmetry drops to C_2v (Fig. 2.2). Distinguishing between the monodentate and bidentate modes of coordination can prove difficult as both have the same symmetry. However, it is possible by examining the separation of the first two stretching bands, with the difference being greater for bidentate NO_3 groups. In practice this is hard if the bond is primarily ionic in nature as the separation becomes less.[20] Within these studies, bands were often obscured by resonances of the R_3EO ligands (E = P or As). In addition, Nujol peaks can obscure nitrate bands, hence CsI pressed discs were used in several samples later in these studies.
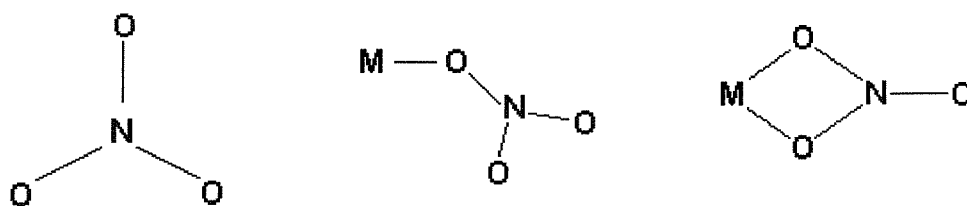
Fig. 2.2 Diagrams showing the loss of symmetry of a nitrate group upon coordination to a metal centre. 'Free' ion (Left) has D_{3h} symmetry, whilst both monodentate and bidentate modes of coordination (Centre and Right) exhibit lower symmetry (the latter being C_{2v}).

$[Y(Ph_3PO)_3(NO_3)_3]$ was seen to have $v(PO) = 1168$ and 1154 cm^{-1} (compared to 1161 and 1153 cm^{-1} in the literature),[2] whilst the spectrum of $[Y(Ph_3PO)_2(EtOH)(NO_3)_3]$ had $v(PO) = 1171$ and 1155 cm^{-1} (compared to 1171 and 1151 cm^{-1}).[2] Ethanol was identified by the broad band at 3300 cm^{-1}, assigned as $v(OH)$, and its presence was confirmed by the characteristic resonances in the ^1H NMR spectrum.

The ^{31}P-$\{^1H\}$ NMR spectrum of $[Y(Ph_3PO)_2(EtOH)(NO_3)_3]$ at 300 K showed a singlet at δ 37.0 ppm. Cooling to 200 K allowed coupling with ^{89}Y to be observed. Following addition of TEMPO as a relaxation agent, an ^{89}Y NMR spectrum was recorded, showing a triplet at δ -35.8 $(^2J(^{31}P-^{89}Y) = 11$ Hz), confirming that two triphenylphosphine oxide ligands were co-ordinated to the metal centre. The molar conductance of a 10^{-3} mol dm^{-3} solution in dry dichloromethane was measured, with $\Lambda_m = 10$ ohm^{-1} cm^2 mol^{-1}, indicating the compound is a non-electrolyte in solution, as predicted.[21]

$[Y(Ph_3PO)_3(NO_3)_3]$ exhibited a ^{31}P-$\{^1H\}$NMR spectrum consisting of two phosphorus resonances at δ 36.5 and 33.9. Initially, the possibility that the two resonances were caused by inequivalent phosphine oxides (as seen in the crystal structure of the solvated species, which shows a T-shaped arrangement of the ligands – see Fig. 2.5) was considered, although this theory was rejected because the relative intensities of the two resonances were approximately $1.5 : 1$, rather than a $2 : 1$ ratio which would fit this model. Furthermore, dilution of the solution saw the relative intensities change. An ^{89}Y

NMR spectrum of this solution at 200 K (Fig. 2.3) revealed two resonances of similar intensity, a quartet at δ –35.7 ($^2J(^{31}P-^{89}Y) = 9$ Hz), and a quintet at δ –2.0 ($^2J(^{31}P-^{89}Y) = 12$ Hz), corresponding to the tris and tetrakis(phosphine oxide) species respectively, demonstrating that in solution [Y(Ph$_3$PO)$_3$(NO$_3$)$_3$] exists as a mixture of [Y(Ph$_3$PO)$_3$(NO$_3$)$_3$] and [Y(Ph$_3$PO)$_4$(NO$_3$)$_2$]NO$_3$ (a third (unidentified) yttrium species must exist in order to mass balance the system). Addition of Ph$_3$PO to the solution saw three resonances in the ^{31}P-{^{1}H}NMR spectrum at 300 K, at δ 26.0 ('free' ligand), 33.9 and 36.5. The intensity of the resonance at 36.5 increased relative to the resonance at 33.9, suggesting that the former can be attributed to the tetrakis(phosphine oxide) species whilst also indicating that the 8- and 9-coordinate species are fluxional in solution.

The molar conductance, $\Lambda_m = 13$ ohm^{-1} cm^2 mol^{-1} (for a 10 mol dm^{-3} solution in CH$_2$Cl$_2$), a value in between that of a non-electrolyte and a 1:1 electrolyte, was consistent with the NMR data ($\Lambda_m = 22.5$ ohm^{-1} cm^2 mol^{-1} for a standard solution of ^{n}Bu$_4$NBF$_4$). Addition of excess Ph$_3$PO to either solution saw the molar conductance increase to that of a 1: 1 electrolyte ($\Lambda_m = 24$ ohm^{-1} cm^2 mol^{-1}).
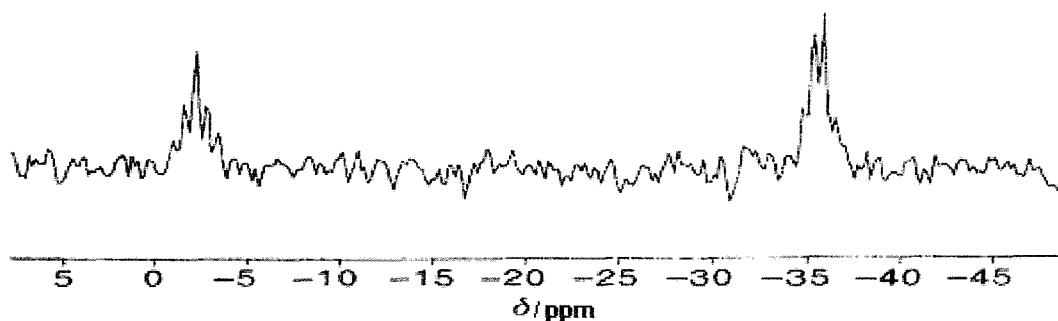
Fig. 2.3 The ^{89}Y NMR spectrum at 200 K of [Y(Ph$_3$PO)$_3$(NO$_3$)$_3$], showing resolution of both the quintet and quartet resonances.

A solution of [Y(Ph$_3$PO)$_4$(NO$_3$)$_2$]NO$_3$ exhibited a very similar ^{31}P-{^{1}H} NMR spectrum to that of [Y(Ph$_3$PO)$_3$(NO$_3$)$_3$], with resonances at δ 26.0 (Ph$_3$PO), 33.3 and 36.5. The 'free' ligand peak was present because of dissociation in solution, with the complex existing in solution as a mixture of the tris and tetrakis(phosphine oxide) species. Multinuclear NMR data for all three compounds are summarised in Table 2.2.

Table 2.2 Multinuclear NMR spectroscopy data for complexes of yttrium(III) nitrate with triphenylphosphine oxide.

Complex	δ (^{31}P-{^{1}H})	δ (^{89}Y)	^2J(^{31}P-^{89}Y)/Hz	T/K
[Y(Ph$_3$PO)$_3$(NO$_3$)$_3$]	33.3 (d)	-35.7 (quartet)	9	240
[Y(Ph$_3$PO)$_4$(NO$_3$)$_2$]NO$_3$	35.7 (d)	-2.0 (quintet)	12	240
[Y(Ph$_3$PO)$_2$(EtOH)(NO$_3$)$_3$]	37.0 (d)	-35.8 (triplet)	11	200

The crystal structure of [Y(Ph$_3$PO)$_2$(EtOH)(NO$_3$)$_3$] is shown in Fig. 2.4, with selected bond lengths and angles given in Table 2.3. The Y atom is nine-coordinate, with the nitrate groups bonded in the bidentate symmetrical mode of co-ordination for this anion.[22] If the nitrate groups are replaced conceptually with monodentate ligands, the structure can be described as distorted *mer*-(pseudo)octahedral, with *cis* Ph$_3$PO ligands. The Y-O(P) bond lengths are significantly shorter than in the structure of [Ce(Ph$_3$PO)$_2$(EtOH)(NO$_3$)$_3$],[13] (Y-O(P) = 2.25(2) and 2.27(1) Å, Ce-O(P) = 2.36(2) and 2.39(2) Å). The bonds are shorter than the difference in radii of the respective M^{3+} ions, possibly due to the more concentrated charge density on yttrium (Ionic radii: - Y^{3+} = 0.88 Å, Ce^{3+} = 1.03 Å).[23]
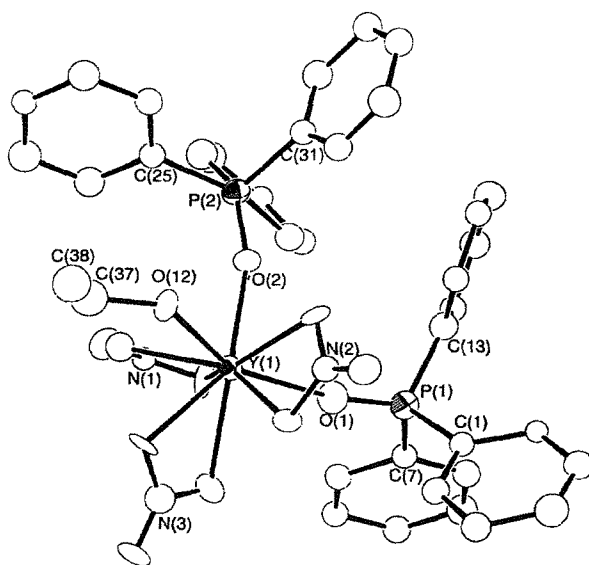
Fig. 2.4 The structure of [Y(Ph$_3$PO)$_2$(EtOH)(NO$_3$)$_3$], showing the atom numbering scheme adopted. Thermal ellipsoids are drawn at 40% probability, with hydrogen atoms omitted for clarity.

Table 2.3 Selected bond lengths (Å) and angles (°) for the structure of [Y(Ph$_3$PO)$_2$(EtOH)(NO$_3$)$_3$].

Y(1)-O(1)	2.25(2)	O(1)-P(1)	1.50(2)
Y(1)-O(2)	2.27(1)	O(2)-P(2)	1.50(1)
Y(1)-O(N)	2.39(2)-2.47(1)	Y(1)-O(12)	2.40(2)
N-O$_c$[a]	1.22(2)-1.33(2)	N-O$_f$[a]	1.25(2), 1.20(2), 1.21(2)
O(1)-Y(1)-O(2)	89.2(6)	Y(1)-O(1)-P(1)	170(1)
O(1)-Y(1)-O(12)	149.8(6)	Y(1)-O(2)-P(2)	164(1)
O(2)-Y(1)-O(12)	79.8(5)	O$_c$-N-O$_c$	113(2)-115(2)
O$_c$-Y(1)-O$_c$	52.1(5)-52.9(6)		

[a] O$_c$ refers to oxygen atoms coordinated to yttrium centre, O$_f$ corresponds to 'free' oxygen atoms, bonded only to N.

The structure of [Y(Ph$_3$PO)$_3$(NO$_3$)$_3$].xCH$_2$Cl$_2$ (Fig. 2.5), (discussed here in preference to that solved for crystals isolated from the non-solvated form because of the stronger data and lower R value) also shows nine-coordinate yttrium. Selected bond lengths and angles are given in Table 2.4. The nitrate groups bond in the bidentate symmetrical mode. The N-O(Y) bond lengths are longer than in the 'free' ion, and the N$_c$-O-N$_c$ angles are smaller than the expected 120° for an uncoordinated ion. If the bidentate NO$_3$ ligands are regarded as monatomic ligands, the structure is (pseudo)-octahedral, with the phosphine oxides in a *mer* arrangement. The structure of the non-solvated complex has the same stereochemistry as the solvated form, with similar bond lengths and angles. When compared to the complex [La(Ph$_3$PO)$_3$(NO$_3$)$_3$].xCH$_2$Cl$_2$ (Fig. 2.2), it is immediately apparent that the Y-O(P) bond lengths are considerably shorter than for the lanthanum complex, largely due to the smaller radius of Y^{3+}(Y-O(P) = 2.269(5) to 2.284(5) Å, La-O(P) = 2.41(2) to 2.44(1) Å).[13]

Attempts to grow crystals of [Y(Ph$_3$PO)$_4$(NO$_3$)$_2$]NO$_3$ from a range of solvents proved unsuccessful, with the tris(phosphine oxide) species preferentially crystallising out of the solutions.
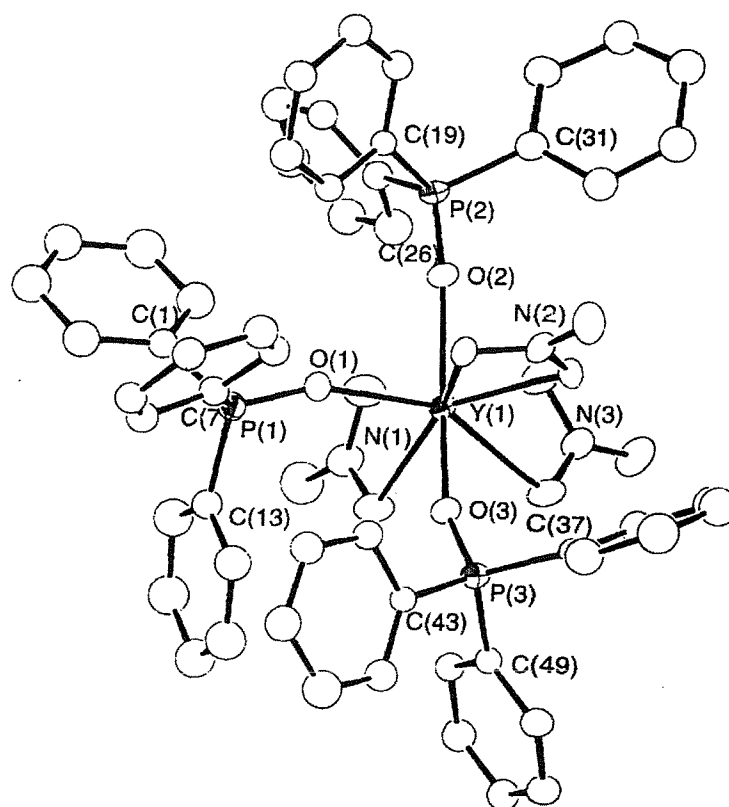
Fig. 2.5 The coordination polyhedron around Y in [Y(Ph₃PO)₃(NO₃)₃].xCH₂Cl₂.
Thermal ellipsoids are drawn at 40% probability, with hydrogen atoms omitted for clarity.

Table 2.4 Selected bond lengths (Å) and angles (°) for the structure of [Y(Ph₃PO)₃(NO₃)₃].xCH₂Cl₂.

Y(1)-O(1)	2.269(5)	O(1)-P(1)	1.503(5)
Y(1)-O(2)	2.284(5)	O(2)-P(2)	1.484(5)
Y(1)-O(3)	2.283(5)	O(3)-P(3)	1.498(5)
Y(1)-O(N)	2.403(5)-2.506(5)	P-C	1.789(7)-1.807(8)
N-O$_c$	1.254(8)-1.271(8)	N-O$_f$	1.215(8), 1.235(8), 1.220(8)
O(1)-Y(1)-O(2)	83.4(2)	Y(1)-O(1)-P(1)	156.8(3)
O(1)-Y(1)-O(3)	86.2(2)	Y(1)-O(2)-P(2)	173.7(3)
O(2)-Y(1)-O(3)	149.5(2)	Y(1)-O(3)-P(3)	162.6(3)
O$_c$-N-O$_c$	116.0(7)-116.7(6)	O$_c$-Y(1)-O$_c$	51.5(2)-52.1(2)

Attempts to synthesise Ph₃PS compounds by the same methods were unsuccessful, irrespective of ratio of ligand to metal, showing the poor affinity of the softer phosphine sulphide for the hard yttrium centre.

2.2.2 Complexes of yttrium nitrate with diphenylmethylphosphine oxide

Reaction of Ph_2MePO with $Y(NO_3)_3.6H_2O$ in a 3 : 1 ratio in boiling ethanol gave $[Y(Ph_2MePO)_3(NO_3)_3]$, whilst reaction of a 1 : 1 ratio gave poor yields of $[Y(Ph_2MePO)_2(EtOH)(NO_3)_3]$, which was always slightly contaminated with a small quantity of the tris(phosphine oxide) species. Hence, despite several attempts, an analytically pure sample could not be obtained. Attempts to obtain a 4 : 1 complex in the solid state were unsuccessful, although evidence for this species in solution was seen in the multinuclear NMR spectra.

The $v(PO)$ vibrations in the complexes were intense, with a shift to lower frequency compared to that of the 'free' ligand, indicating coordination of the phosphine oxide to the metal centre. $[Y(Ph_2MePO)_3(NO_3)_3]$ had $v(PO)$ = 1150 cm^{-1}, whilst the bis(phosphine oxide) complex exhibited $v(PO)$ = 1155 cm^{-1} (compared to 1172 cm^{-1} in the 'free' ligand). The coordinated ethanol in $[Y(Ph_2MePO)_2(EtOH)(NO_3)_3]$ was evident by the broad band at 3300 cm^{-1} and confirmed by the characteristic resonances in the ^1H NMR spectrum. The molar conductances of the bis and tris(phosphine oxide) complexes were low (Λ_m = 7.5 and 4.5 $ohm^{-1}\,cm^2\,mol^{-1}$ respectively), showing that both were non-electrolytes. Addition of an excess of the phosphine oxide to the solution of $[Y(Ph_2MePO)_3(NO_3)_3]$ saw the value of Λ_m rise to 22.0 $ohm^{-1}\,cm^2\,mol^{-1}$, consistent with a 1 : 1 electrolyte, suggesting "$[Y(Ph_2MePO)_4(NO_3)_2]NO_3$" had been formed *in situ*.

In contrast to its triphenylphosphine analogue, the $^{31}P-\{^1H\}$ NMR spectrum of $[Y(Ph_2MePO)_3(NO_3)_3]$ at ambient temperature showed only a single resonance at δ 36.6, which resolved into a doublet when cooled to 200 K. The observation that the phosphine oxides were equivalent by NMR (whilst not so in the crystal structure) indicated fluxionality in solution. The ^{89}Y NMR spectrum at 200 K showed a binomial quartet ($^2J(^{31}P-^{89}Y)$ = 10 Hz), confirming that three phosphine oxide ligands were coordinated to the metal centre. Addition of an excess of Ph_2MePO to the same solution saw a shift in the $^{31}P-\{^1H\}$ NMR spectrum to δ 38.3 ppm, with the ^{89}Y NMR spectrum exhibiting a quintet at δ + 6.0 ppm ($^2J(^{31}P-^{89}Y)$ = 10 Hz), indicating complete conversion to a tetrakis(phosphine oxide) species.

[Y(Ph$_2$MePO)$_2$(EtOH)(NO$_3$)$_3$] showed a doublet at δ 37.7 in the ^{31}P-{^{1}H}NMR spectrum, with the ^{89}Y NMR spectrum of the same solution having a triplet at δ -37.6 ppm (^2J(^{31}P-^{89}Y) = 8 Hz). The NMR data are summarised in Table 2.5.

Table 2.5 Multinuclear NMR spectroscopic data for complexes of yttrium(III) nitrate with diphenylmethylphosphine oxide.

Complex	δ (^{31}P-{^{1}H})	δ (^{89}Y)	^2J(^{31}P-^{89}Y)/Hz	T/K
[Y(Ph$_2$MePO)$_3$(NO$_3$)$_3$]	36.6 (d)	-26.2 (quartet)	10	220
[Y(Ph$_2$MePO)$_2$(EtOH)(NO$_3$)$_3$]	37.7 (d)	-37.6 (triplet)	8	200
[Y(Ph$_2$MePO)$_4$(NO$_3$)$_2$]NO$_3$[a]	38.3 (d)	+6.0 (triplet)	10	200

[a] *In situ* from a solution of [Y(Ph$_2$MePO)$_3$(NO$_3$)$_3$], with an excess of Ph$_2$MePO added.

The structure of [Y(Ph$_2$MePO)$_3$(NO$_3$)$_3$] (Fig. 2.6), shows nine-coordinate yttrium with a (pseudo)-octahedral structure (if the nitrate groups are conceptually replaced with monodentate ligands), with the phosphine oxides in a *mer* arrangement. Selected bond lengths and angles are given in Table 2.6. The Y-O-P angles are significantly smaller than for the structures of [Y(Ph$_3$PO)$_2$(EtOH)(NO$_3$)$_3$] and [Y(Ph$_3$PO)$_3$(NO$_3$)$_3$].xCH$_2$Cl$_2$, and are larger than for the complex [Y(Me$_3$PO)$_3$(NO$_3$)$_3$] (below) (Y-O-P (ave.): Ph$_3$PO = 166°, Ph$_2$MePO = 156°, Me$_3$PO = 146°). It is apparent that these angles increase with a greater number of phenyl rings in the phosphine oxide ligand, probably because of steric effects. The bond lengths Y-O(P) and P-O showed little variation between all four reported yttrium nitrate – phosphine oxide structures reported in this study.
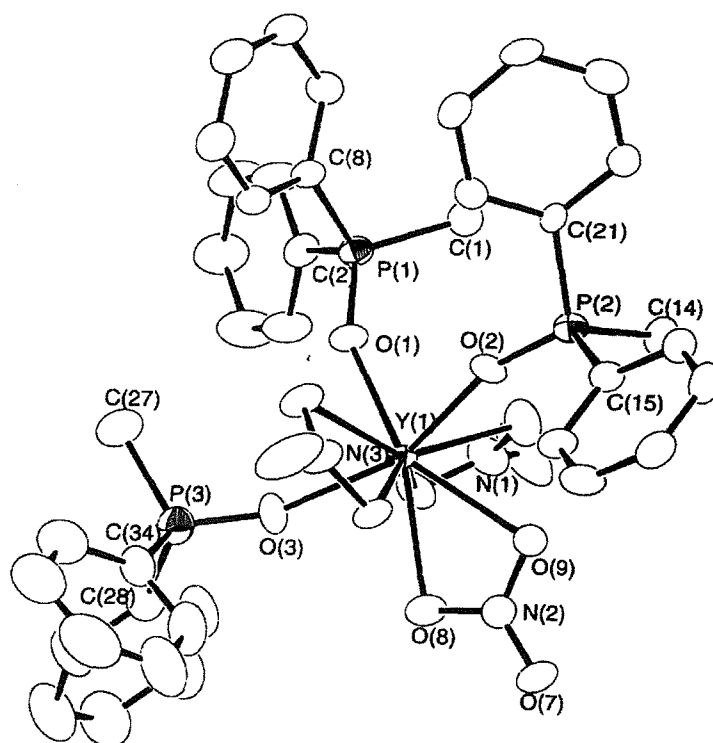
Fig. 2.6 The coordination polyhedron around Y in [Y(Ph₂MePO)₃(NO₃)₃]. Thermal ellipsoids are drawn at 40% probability, with hydrogen atoms omitted for clarity.

Table 2.6 Selected bond lengths (Å) and angles (°) for the structure of [Y(Ph₂MePO)₃(NO₃)₃].

Y(1)-O(1)	2.258(3)	O(1)-P(1)	1.510(3)
Y(1)-O(2)	2.248(4)	O(2)-P(2)	1.513(4)
Y(1)-O(3)	2.252(4)	O(3)-P(3)	1.494(4)
Y(1)-O(N)	2.413(5)-2.491(4)	P-C	1.773(6)-1.815(7)
N-O$_c$	1.255(6)-1.279(5)	N-O$_f$	1.221(6), 1.232(5), 1.209(6)
O(1)-Y(1)-O(2)	84.1(1)	Y(1)-O(1)-P(1)	154.3(3)
O(1)-Y(1)-O(3)	84.2(1)	Y(1)-O(2)-P(2)	157.9(2)
O(2)-Y(1)-O(3)	153.5(1)	Y(1)-O(3)-P(3)	157.3(3)
O$_c$-N-O$_c$	115.8(5)-116.4(6)	O$_c$-Y(1)-O$_c$	50.9(1)-52.4(1)

2.2.3 Complexes of yttrium nitrate with trimethylphosphine oxide

$Y(NO_3)_3.6H_2O$ reacted with three molar equivalents of Me_3PO in warm ethanol to produce $[Y(Me_3PO)_3(NO_3)_3]$. Reaction of a 1 : 1 molar ratio of ligand to metal salt in boiling ethanol yielded $[Y(Me_3PO)_2(H_2O)(NO_3)_3]$ rather than the ethanol adduct that might be expected in light of the reactions with Ph_3PO and Ph_2MePO described earlier. A tetrakis(phosphine oxide) complex could not be isolated, despite evidence for its existence in both multinuclear NMR and conductivity experiments. Reaction of an 8 : 1 ratio of Me_3PO : Y and also addition of excess free ligand to an ethanolic solution of the tris(phosphine oxide) compound afford solid $[Y(Me_3PO)_3(NO_3)_3]$ following concentration of the reaction solutions.

The water present in the bis(phosphine oxide) complex was apparent from a strong, very broad band at $v = 3400$ cm^{-1} and a second band at 1650 cm^{-1}. The $v(PO)$ vibration appeared as an intense band at $v = 1140$ cm^{-1} ($v(PO)$ in 'free' $Me_3PO = 1161$ cm^{-1}). The complex $[Y(Me_3PO)_3(NO_3)_3]$ had $v(PO) = 1146$ cm^{-1}.

The $^{31}P-\{^1H\}$ NMR spectrum of $[Y(Me_3PO)_3(NO_3)_3]$ at 200 K showed a doublet at δ 48.3 ppm. The corresponding ^{89}Y NMR spectrum exhibited a quartet at δ −17.7 ($^2J(^{31}P-^{89}Y) = 6$ Hz). Addition of excess free ligand to this solution led to formation of a tetrakis(phosphine oxide) complex *in situ*, identified by a quintet at δ -0.3 ppm ($^2J(^{31}P-^{89}Y) = 8$ Hz). The $^{31}P-\{^1H\}$ NMR resonance had shifted to δ 52.0, although the coupling was ill-defined. The molar conductance data fitted with these results, $\Lambda_m = 6$ ohm^{-1}cm^{2}mol^{-1} initially (typical of a non-electrolyte), rising to 20 ohm^{-1}cm^{2}mol^{-1} following addition of 'free' ligand, suggesting dissociation of one nitrate group from the metal centre.

$[Y(Me_3PO)_2(H_2O)(NO_3)_3]$ exhibited a poorly resolved doublet at δ 51.0 ppm in the $^{31}P-\{^1H\}$ NMR spectrum. However, the ^{89}Y resonance was a triplet at δ -12.0 ppm, distinguishing between this complex and the tris(phosphine oxide) species in solution. Multinuclear NMR data are summarised in Table 2.7.

Table 2.7 Multinuclear NMR spectroscopic data for complexes of yttrium(III) nitrate with trimethylphosphine oxide.

Complex	δ (^{31}P-{^{1}H})	δ (^{89}Y)	^2J(^{31}P-^{89}Y)/Hz	T/K
[Y(Me$_3$PO)$_3$(NO$_3$)$_3$]	48.3 (d)	-17.7 (quartet)	6	200
"[Y(Me$_3$PO)$_4$(NO$_3$)$_2$]NO$_3$"[a]	52.0 (d)[b]	-0.3 (quintet)	8	200
[Y(Me$_3$PO)$_2$(H$_2$O)(NO$_3$)$_3$]	51.0 (d)[b]	-12.0 (triplet)	$ca.$ 12	200

[a] $In\ situ$ from a solution of [Y(Me$_3$PO)$_3$(NO$_3$)$_3$], with an excess of Me$_3$PO added.

[b] Coupling was poorly resolved.

The structure of [Y(Me$_3$PO)$_3$(NO$_3$)$_3$] was determined (Fig. 2.7) and selected bond lengths and angles are given in Table 2.8. As for the other structurally determined yttrium nitrate / phosphine oxide compounds in this study, the metal centre is nine-coordinate and the structure can be described as (pseudo)-octahedral. However, for the Me$_3$PO complex, the phosphine oxides adopt a fac arrangement, contrasting with the mer arrangement seen for [Y(Ph$_2$MePO)$_3$(NO$_3$)$_3$] and [Y(Ph$_3$PO)$_3$(NO$_3$)$_3$].xCH$_2$Cl$_2$. The average M-O-P angle of 146.5° is significantly smaller than for [Y(Ph$_3$PO)$_3$ (NO$_3$)$_3$].xCH$_2$Cl$_2$ (Y-O-P(ave.) = 164.4°), presumably due to the smaller bulk of Me groups compared to Ph groups.
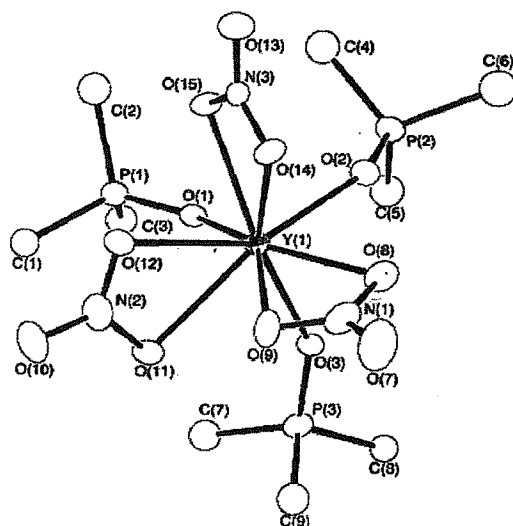
Fig. 2.7 The structure of [Y(Me$_3$PO)$_3$(NO$_3$)$_3$] showing the atom labelling scheme for the molecule centred on Y (1). Thermal ellipsoids are drawn at 40%.

Table 2.8 Selected bond lengths (Å) and angles (°) for the structure of [Y(Me₃PO)₃(NO₃)₃].

Y(1)-O(1)	2.281(7)	Y(2)-O(4)	2.270(6)
Y(1)-O(2)	2.279(7)	Y(2)-O(5)	2.251(7)
Y(1)-O(3)	2.262(7)	Y(2)-O(6)	2.258(7)
Y(1)-O(N)	2.441(7)-2.520(8)	Y(2)-O(N)	2.463(8)-2.525(7)
P(n)-O(n) (n = 1-6)	1.495(7)-1.521(7)	N-O$_f$	1.21(1)-1.25(1)
N-O$_c$	1.26(1)-1.30(1)		
O(1)-Y(1)-O(2)	86.0(2)	O(4)-Y(2)-O(5)	82.5(2)
O(1)-Y(1)-O(3)	82.9(2)	O(4)-Y(2)-O(6)	86.8(3)
O(2)-Y(1)-O(3)	84.3(2)	O(5)-Y(2)-O(6)	86.1(2)
Y(1)-O(1)-P(1)	149.9(4)	Y(2)-O(4)-P(4)	149.3(4)
Y(1)-O(2)-P(2)	140.2(4)	Y(2)-O(5)-P(5)	147.8(4)
Y(1)-O(3)-P(3)	147.0(4)	Y(2)-O(6)-P(6)	144.5(4)
O$_c$-N-O$_c$	115(1)-119(1)	O$_c$-Y(1)-O$_c$	51.2(2)-52.5(2)

2.2.4 Complexes of scandium nitrate with triphenylphosphine oxide

Irrespective of the ratio of reagents, reaction of Sc(NO₃)₃.5H₂O with triphenylphosphine oxide in ethanol produced colourless crystals of [Sc(Ph₃PO)₂(NO₃)₃]. This contrasts with the analogous yttrium system (see 2.2.1) for which three different compounds were seen to form. The smaller radius of Sc³⁺ (0.68 Å) compared to Y³⁺ (0.88 Å) offers explanation, with steric hindrance limiting the number of ligands that the former can accomodate.[23]

Both multinuclear NMR spectra and conductivity studies showed no evidence of other species in solution when excess ligand was added. The complex had $Λ_m$ = 2.0 ohm⁻¹ cm² mol⁻¹, with addition of excess Ph₃PO having no significant effect, suggesting that no new species were formed in solution. The ³¹P-{¹H} NMR spectrum at 300 K was a singlet at δ 37.7 ppm, with no coupling resolved upon cooling to 200 K, presumably due to the fast quadrupolar relaxation of the scandium nucleus. At ambient temperature, the ⁴⁵Sc spectrum of the complex revealed a broad resonance at δ - 7.5 ($W_½$ = 900 Hz). Addition of excess Ph₃PO saw no changes to either spectrum, besides the appearance of a 'free' ligand resonance at δ 26.0 ppm (NMR spectra are summarised in Table 2.9).

Table 2.9 Multinuclear NMR data for the scandium nitrate / tertiary phosphine oxide system.

Complex	δ ($^{31}P-\{^1H\}$)	δ (^{45}Sc)	$^2J(^{31}P-^{45}Sc)$/Hz	T/K
$[Sc(Ph_3PO)_2(NO_3)_3]$	37.7	-7.5	Not Observed	300
$[Sc(Ph_2MePO)_3(NO_3)_3]$	39.5	-4.0	Not Observed	300
$[Sc(Ph_3MePO)_4(NO_3)_2]NO_3$	38.7	-36.0 (br)	Not Observed	240
$[Sc(Me_3PO)_2(EtOH)(NO_3)_3]$	54.8	-2.5	Not Observed	300
$[Sc(Me_3PO)_6][NO_3]_3$ [a]	62.0 (octet)	+5.0	20	300
"$[Sc(Me_3PO)_5(NO_3)](NO_3)_2$" [b]	64.7	+11.5	Not Observed	300

[a] Solution made up in $MeNO_2$ – 10% CD_3NO_2, with an excess of Me_3PO added.

[b] *In situ* from $[Sc(Me_3PO)_6][NO_3]_3$, with the solution made up in $MeNO_2$ – 10% CD_3NO_2

The structure of $[Sc(Ph_3PO)_2(NO_3)_3]$ is shown in Fig. 2.8, with selected bond lengths and angles presented in Table 2.10. The scandium centre is eight-coordinate, with the nitrates bound in the same symmetrical bidentate mode seen for the yttrium nitrate-phosphine oxide structures described earlier. The structure can be described as pseudo-trigonal bipyramidal, with the phosphine oxides in axial and equatorial positions. As expected, the Sc-O bond lengths are considerably shorter than in similar yttrium structures, owing to the small radius of the scandium centre (Sc-O(P) = 2.047(7) and 2.068(7) Å, for the complex $[Y(NO_3)_3(Ph_3PO)_2(EtOH)]$, Y-O(P) = 2.25(2) to 2.27(1) Å). The Sc-O(2)-P(2) bond is almost linear (178.5°), owing to the lack of steric hindrance, whilst Sc-O(1)-P(1) was slightly bent (165.1°).
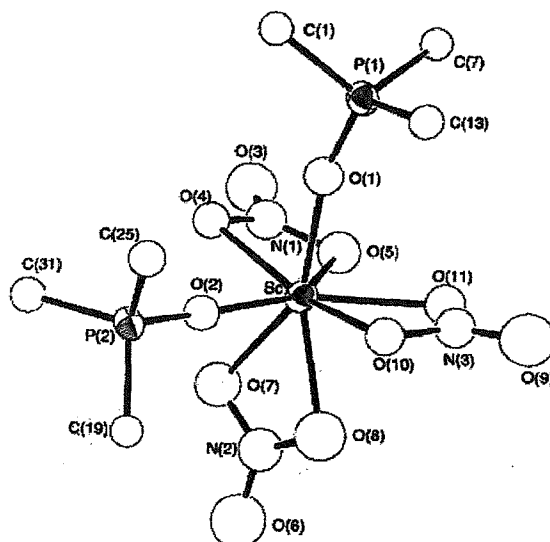
Fig. 2.8 The coordination polyhedron around Sc in [Sc(Ph₃PO)₂(NO₃)₃]. Phenyl C atoms not bonded to P have been omitted for clarity. Thermal ellipsoids are drawn at the 50% probability level and H atoms are omitted.

Table 2.10 Selected bond lengths (Å) and angles (°) for the structure of [Sc(NO₃)₃(Ph₃PO)₂].

Sc-O(1)	2.068(7)	O(1)-P(1)	1.497(8)
Sc-O(2)	2.047(7)	O(2)-P(2)	1.513(7)
Sc-O(N)	2.205(8)-2.311(7)	P-C	1.77(1)-1.81(1)
N-O$_c$	1.264(12)-1.280(11)	N-O$_f$	1.208(11)-1.216(12)
O(1)-Sc-O(2)	90.7(3)	Sc-O(1)-P(1)	165.1(5)
Sc-O(2)-P(2)	178.5(5)	O$_c$-N-O$_c$	112.0(10)-114.4(9)
O$_c$-Sc-O$_c$	55.2(3)-57.1(3)		

2.2.5 Complexes of scandium nitrate with diphenylmethylphosphine oxide

Reaction of hydrated scandium(III) nitrate with four or more molar equivalents of diphenylmethylphosphine oxide in ethanol afforded white crystals of $[Sc(Ph_2MePO)_4(NO_3)_2]NO_3$. When $Sc(NO_3)_3.5H_2O$ was reacted with one or two molar equivalents of the ligand in boiling ethanol, concentration of the reaction mixture afforded a sticky solid. If this product was washed with ice-cold diethyl ether, poor yields of $[Sc(Ph_2MePO)_3(NO_3)_3]$ were produced. The spectroscopic evidence points to this being a nine-coordinate scandium complex, which is very rare,[24] although owing to its high solubility, crystals of the complex could not be obtained to prove this unambiguously.

For both compounds, $v(PO) = 1153$ cm^{-1}. The IR spectrum of the 4 : 1 complex includes a weak band at 831 cm^{-1}, indicating the presence of an ionic nitrate. This feature was absent for the tris(phosphine oxide) species, indicating that all three nitrate groups were coordinated.

The low value of $\Lambda_m = 8.0$ ohm^{-1} cm^2 mol^{-1} for a 10^{-3} mol dm^{-3} CH_2Cl_2 solution of $[Sc(Ph_2MePO)_4(NO_3)_2]NO_3$ initially seemed strange in light of the crystal structure obtained, but the NMR studies showed that in solution the complex existed as a mixture of non-conducting tris(phosphine oxide) species, as well as the 4 : 1 complex (expected to be a 1 : 1 electrolyte). Addition of excess Ph_2MePO saw Λ_m rise towards 22 ohm^{-1} cm^2 mol^{-1}, showing the equilibrium position shift towards $[Sc(Ph_2MePO)_4(NO_3)_2]NO_3$.

At ambient temperature, the $^{31}P-\{^1H\}$ NMR spectrum of $[Sc(Ph_2MePO)_4(NO_3)_2]NO_3$ was a single broad resonance at δ 38.5 ($W_{1/2} = 700$ Hz). Cooling to 250 K saw a strong peak at δ 38.7, with weaker resonances at δ 39.5 and 29.2 (Ph_2MePO). Addition of free ligand saw the major peak grow, indicating that this was due to the 4 : 1 species. The ^{45}Sc NMR spectrum at ambient temperature showed broad, partially overlapping resonances at δ –4 and –33. Cooling the solution saw these converge further, producing a very broad asymmetric resonance, due to the effect of the scandium quadrupole. Upon addition of excess ligand, the peak at δ –33 increased in intensity, denoting that this

was due to the tetrakis(phosphine oxide) species, although the resonance caused by the tris(phosphine oxide) complex was always present. The ^{31}P-$\{^{1}$H$\}$ spectrum of [Sc(Ph$_2$MePO)$_3$(NO$_3$)$_3$] was more simple, with a single resonance at δ 39.5, whilst the ^{45}Sc spectrum also showed a single peak at δ – 7.5 ($W_{1/2}$ = 350 Hz). A summary of the NMR spectroscopic data are presented in Table 2.9.

The structure of [Sc(Ph$_2$MePO)$_4$(NO$_3$)$_2$]NO$_3$ is depicted in Fig. 2.9, with selected bond lengths and angles given in Table 2.11. The scandium centre is eight-coordinate, with nitrate groups again bonded in the symmetrical bidentate mode. Replacement of the nitrate groups with monodentate ligands produces an octahedral structure, with *trans* nitrates. The average Sc-O-P bond angle is smaller than seen for the structure of [Sc(Ph$_3$PO)$_2$(NO$_3$)$_3$] (161.5° compared with 172°).
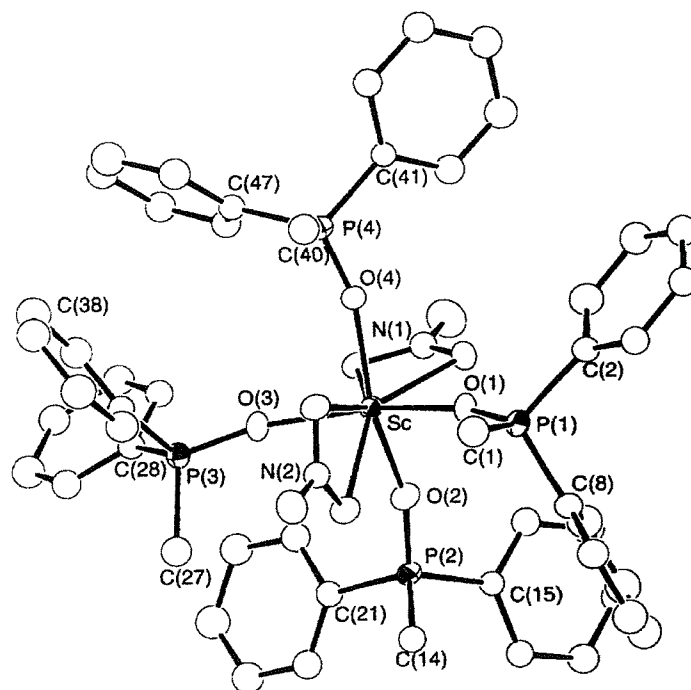
Fig. 2.9 The structure of the cation in [Sc(Ph$_2$MePO)$_4$(NO$_3$)$_2$]NO$_3$.xCH$_2$Cl$_2$. Thermal ellipsoids are drawn at 40% probability, with H atoms omitted for clarity.

Table 2.11 Selected bond lengths (Å) and angles (°) for the structure of

$[Sc(Ph_2MePO)_4(NO_3)_2]NO_3.xCH_2Cl_2$

Sc-O(1)	2.099(6)	O(1)-P(1)	1.493(6)
Sc-O(2)	2.097(6)	O(2)-P(2)	1.505(6)
Sc-O(3)	2.090(6)	O(3)-P(3)	1.502(6)
Sc-O(4)	2.088(6)	O(4)-P(4)	1.504(6)
Sc-O(N)	2.311(6)-2.425(6)	P-C	1.782(9)-1.822(9)
N-O$_c$	1.257(9)-1.277(9)	N-O$_f$	1.214(9), 1.219(9)
O(1)-Sc-O(2)	93.8(2)	Sc-O(1)-P(1	162.7(4)
O(1)-Sc-O(4)	91.7(2)	Sc-O(2)-P(2)	159.6(4)
O(2)-Sc-O(3)	93.5(2)	Sc-O(3)-P(3)	161.3(4)
O(3)-Sc-O(4)	92.2(2)	Sc-O(4)-P(4)	162.4(4)
O$_c$-N-O$_c$	114.4(7), 116.5(7)	O$_c$-Sc-O$_c$	54.8(2), 53.3(2)

2.2.6 Complexes of scandium nitrate with trimethylphosphine oxide

When $Sc(NO_3)_3.5H_2O$ was reacted with a large excess of Me_3PO (six to ten molar equivalents) in ice-cold ethanol, the white solid $[Sc(Me_3PO)_6][NO_3]_3$ was obtained, with microanalysis confirming this stoichiometry and supported by infrared spectroscopy and molar conductance data. Reaction of equimolar quantities of ligand and metal salt gave a very poor yield of $[Sc(Me_3PO)_2(EtOH)(NO_3)_3]$, which could conceivably have a nine-coordinate metal centre, although in the absence of X-ray studies this could not be confirmed.

For the ethanol adduct, $v(PO) = 1152$ cm^{-1} (compared to 1161 cm^{-1} in the free ligand). A broad band at $v = 3200$ cm^{-1} indicated the presence of the alcohol, whilst the absence of a band at ca. 830 cm^{-1} showed that all three nitrates were coordinated. The spectrum of $[Sc(Me_3PO)_6][NO_3]_3$ was simple, with $v(PO) = 1104$ cm^{-1}, the low wavenumber explained by stronger Sc-O bonds owing to the high charge on the metal centre. The three ionic nitrate groups were identified by peaks at 1361 (v_3), 1298 (v_1) and 834 (v_2) cm^{-1}.[19]

The molar conductance of a 10^{-3} mol dm^{-3} solution of $[Sc(Me_3PO)_6][NO_3]_3$ was measured in nitromethane (the compound had poor solubility in chlorocarbons, acetone and ethanol), with $\Lambda_m = 157$ ohm^{-1} cm^2 mol^{-1}, consistent with a 2 : 1 electrolyte,[21]

suggesting the complex had decomposed, possibly to $[Sc(Me_3PO)_5(NO_3)][NO_3]_2$. Addition of excess phosphine oxide saw Λ_m rise to 250 ohm^{-1} cm^2 mol^{-1}, typical of a 3 : 1 electrolyte,[21] showing that all three nitrate groups were ionic. The multinuclear NMR spectra confirmed this dissociation in solution. At 300 K, the ^{31}P-$\{^1H\}$ NMR spectrum contained a broad singlet at δ 64.7, with a shoulder at 62.0, as well as a weaker resonance at δ 43.0 (free ligand), with the integrals approximately 5.3 : 1. Cooling to 245 K saw sharpening of the peaks, but as the solvent has a melting point of 244 K, lower temperature studies could not be conducted. Addition of a ten-fold excess of ligand saw the coordinated ligand peak shift to δ 62.0, with coupling to ^{45}Sc observed as an eight-line pattern under higher resolution $(^2J(^{31}P-^{45}Sc) = 20$ Hz). This peak must correspond to $[Sc(Me_3PO)_6][NO_3]_3$, with the regular octahedral symmetry slowing the quadrupolar relaxation and allowing coupling to be observed (see Fig. 2.10). The ^{45}Sc NMR spectrum of the initial solution contained a broad resonance at δ 11.8 $(W_½ = 450$ Hz), with a sharp, weaker peak at δ 5.0. However, no coupling was resolved in the ^{45}Sc NMR spectrum. Addition of Me_3PO saw the broad feature disappear.

The ^{31}P-$\{^1H\}$ NMR spectrum of $[Sc(Me_3PO)_2(EtOH)(NO_3)_3]$ was more simple, with a singlet at δ 54.8. The ^{45}Sc NMR spectrum had a single resonance at δ – 2.5. Addition of up to four equivalents of free ligand saw no new complexes formed.
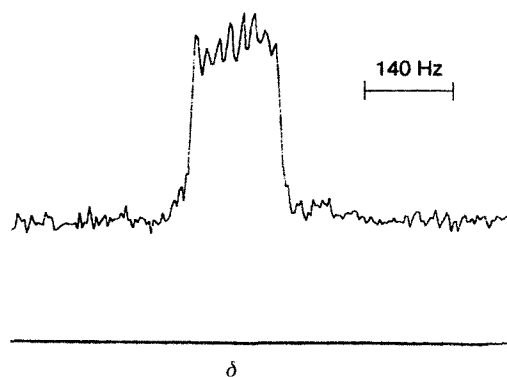
Fig. 2.10 The ^{31}P-$\{^1H\}$ NMR resonance of $[Sc(Me_3PO)_6]^{3+}$ in a $MeNO_2$ solution of $[Sc(Me_3PO)_6](NO_3)_3$ containing an excess of Me_3PO.

Attempts to grow crystals of $[Sc(Me_3PO)_6](NO_3)_3$ from a nitromethane solution of the complex were unsuccessful. However, in related work, very poor crystals were obtained from $MeNO_2$ with an excess of Me_3PO present. X-ray data were collected of one of these crystals but refinement was unsatisfactory (crystal data given below*). The cation had an octahedral geometry, similar to that of $[Sc(Me_3AsO)_6](NO_3)_3$ (see 2.2.10). [25]

(* $[Sc(Me_3AsO)_6](NO_3)_3$. Crystal data: monoclinic, $a = 10.975(3)$, $b = 11.150(3)$, $c = 15.463(6)$ Å, $\beta = 90.58(1)°$, $U = 1892.1$ Å^3. Space group $= P2_1$ (no. 4), $Z = 2$, $T = 120$ K. Refinement also attempted in $P\bar{1}$ (No. 2) and $P2_1/n$ (no. 14), giving the same chemical answer.)

2.2.7 Complexes of yttrium nitrate with triphenylarsine oxide

When $Y(NO_3)_3.6H_2O$ was reacted with two molar equivalents of triphenylarsine oxide in boiling ethanol, $[Y(Ph_3AsO)_2(EtOH)(NO_3)_3]$ was produced. In boiling acetone, using a 3 : 1 ratio of ligand to metal salt, the product was $[Y(Ph_3AsO)_4(NO_3)_2]NO_3.Me_2CO$. Attempts to isolate a lower Ph_3AsO:Y ratio complex from acetone (by slow evaporation of a 1 : 1 mixture) were unsuccessful, although a third compound was identified *in situ* by ^{89}Y NMR spectroscopy.

Coordination of the ligand was apparent in the IR spectra by a characteristic increase (and often splitting) of the AsO stretching mode.[2,6] The 'free' ligand exhibits $\nu(AsO)$ as a broad, intense peak at 878 cm^{-1}, whilst the spectrum of the ethanol adduct $[Y(Ph_3AsO)_2(EtOH)(NO_3)_3]$, saw $\nu(AsO) = 932$ and 910 cm^{-1}. Ethanol was apparent as a broad band at $\nu = 3300$ cm^{-1}, its presence confirmed in the ^1H NMR spectrum. The tetrakis(arsine oxide) complex had a single intense band caused by the As-O stretch at $\nu = 911$ cm^{-1}. The peak at $\nu = 1703$ cm^{-1} confirmed the presence of acetone in the compound (also visible in the ^1H NMR spectrum by the singlet at δ 2.15 ppm), whilst a weak band at $\nu = 831$ cm^{-1} corresponded to the ionic nitrate.

A 10^{-3} ml dm^{-3} dichloromethane solution of $[Y(Ph_3AsO)_2(EtOH)(NO_3)_3]$ was found to have $\Lambda_m = 2.0$ ohm^{-1} cm^2 mol^{-1}, a value typical of a non-electrolyte, consistent with the

suggested stoichiometry. $[Y(Ph_3AsO)_4(NO_3)_2]NO_3.Me_2CO$ had $\Lambda_m = 28$ ohm^{-1} cm^2 mol^{-1}, remaining unchanged upon addition of excess ligand. This indicates that no compound forms in solution with further Ph_3AsO ligands coordinated and that the compound does not decompose in chlorocarbon solvents (in contrast to the phosphine oxide analogue). The ^{89}Y NMR spectrum confirmed this, showing a single peak at δ 21 ppm at room temperature.

Table 2.12 ^{89}Y NMR spectroscopic data for complexes of yttrium(III) nitrate with tertiary arsine oxide ligands.

Complex	$\delta(^{89}Y)$	T/K
$[Y(Ph_3AsO)_2(EtOH)(NO_3)_3]$	+1.0	180
$[Y(Ph_3AsO)_4(NO_3)_2]NO_3.Me_2CO$	+21	300
"$[Y(Ph_3AsO)_3(NO_3)_3]$"	+18	200
$[Y(Me_3AsO)_6](NO_3)_3$	+133	200

No ^{89}Y NMR resonance was observed at room temperature in solutions of $[Y(Ph_3AsO)_2(EtOH)(NO_3)_3]$. Cooling to 200 K with a long collection time saw two peaks, a strong feature at δ 20 ppm ($[Y(Ph_3AsO)_4(NO_3)_2]NO_3$) and a weaker resonance at δ 0.5 ppm. Addition of excess Ph_3AsO caused disappearance of the latter peak, which was thus attributed to $[Y(Ph_3AsO)_2(EtOH)(NO_3)_3]$.

The ^{89}Y NMR spectrum of a solution of a 1 : 1 ratio reaction mixture that had been evaporated to dryness and redissolved in CH_2Cl_2 showed possible evidence of $[Y(Ph_3AsO)_3(NO_3)_3]$ with a peak at δ 18 ppm evident (along with the tetrakis(arsine oxide) species and $Y(NO_3)_3.nH_2O$). However, the compound responsible for the resonance at δ 18 ppm could not be separated and purified.

Attempts to grow crystals of $[Y(Ph_3AsO)_2(EtOH)(NO_3)_3]$ were unsuccessful. However, given the data obtained, along with the structures of the analogous $[La(Ph_3AsO)_2(EtOH)(NO_3)_3]$ (Fig. 2.15) and the similar $[Y(Ph_3PO)_2(EtOH)(NO_3)_3]$, it

seems likely the yttrium is nine-coordinate. The structure of [Y(Ph$_3$AsO)$_4$(NO$_3$)$_2$]NO$_3$.1/2H$_2$O was determined (Fig. 2.11), with selected bond lengths and angles given in Table 2.13. The structure has an eight-coordinate yttrium centre, with the bidentate nitrates approximately perpendicular to each other. The coordination geometry is similar to that of [Sc(Ph$_2$MePO)$_4$(NO$_3$)$_2$]NO$_3$ (see Fig. 2.9) and [Lu(Ph$_3$PO)$_4$(NO$_3$)$_2$]NO$_3$.[13]
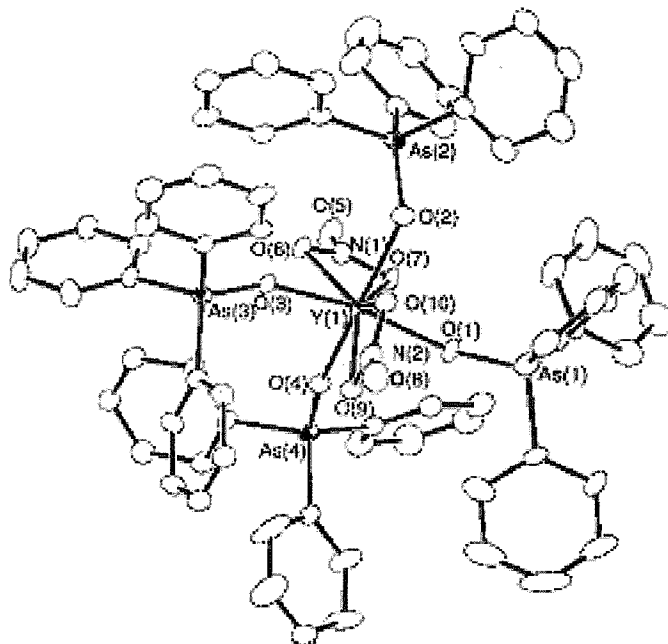
Fig. 2.11 The structure of the cation in [Y(Ph$_3$AsO)$_4$(NO$_3$)$_2$]NO$_3$.1/2H$_2$O. Thermal ellipsoids are drawn at 30% probability, with H atoms omitted for clarity.

Table 2.13 Selected bond lengths (Å) and angles (°) for the structure of [Y(Ph$_3$AsO)$_4$(NO$_3$)$_2$]NO$_3$.1/2H$_2$O.

Y-O(1)	2.212(4)	O(1)-As(1)	1.493(6)
Y-O(2)	2.233(4)	O(2)-As(2)	1.505(6)
Y-O(3)	2.228(4)	O(3)-As(3)	1.502(6)
Y-O(4)	2.228(4)	O(4)-As(4)	1.504(6)
Y-O(N)	2.458(4)-2.506(4)	As-C	1.901(7)-1.922(6)
O(1)-Y-O(2)	90.4(2)	Y-O(1)-As(1)	164.5(3)
O(1)-Y-O(4)	88.5(2)	Y-O(2)-As(2)	147.3(3)
O(2)-Y-O(3)	97.1(2)	Y-O(3)-As(3)	156.1(2)
O(3)-Y-O(4)	93.3(2)	Y-O(4)-As(4)	160.6(2)
O$_c$-Y-O$_c$	51.3(1), 51.5(1)		

Comparing this system with the analogous phosphine oxide complex results indicates that Ph₃AsO coordinates more strongly to $Y(NO_3)_3.6H_2O$ than Ph₃PO. Whilst a tris(arsine oxide) compound could not be isolated, $[Y(Ph_3PO)_3(NO_3)_3]$ was the preferred complex for reactions with Ph₃PO.

2.2.8 Complexes of yttrium nitrate with trimethylarsine oxide

Reaction of trimethylarsine oxide with hydrated yttrium nitrate in a $\geq 6:1$ ratio in ice cold ethanol yielded $[Y(Me_3AsO)_6](NO_3)_3$. No evidence was seen for further complexes in this system. The compound was insoluble in chlorocarbons, ethanol or acetone, so solution studies were conducted in nitromethane and nitroethane (the latter used when low temperature studies below 245 K were required).

The IR spectrum of this complex was simple, exhibiting $v(AsO) = 877$ or 926 cm^{-1} (it is difficult to distinguish between $v(AsO)$ and AsMe₃ rocking modes which occur at similar frequencies) and identifying ionic nitrate groups by strong bands at 1358 (v_3) and 836 (v_2) cm^{-1}.[19] The molar conductance of a 10^{-3} mol dm^{-3} solution in MeNO₂ was measured, with $\Lambda_m = 180$ ohm^{-1}cm^{2}mol^{-1} (in the region of a 2 : 1 electrolyte), suggesting decomposition in solution. Addition of ligand caused Λ_m rise to 240 ohm^{-1} cm^2 mol^{-1} (3 : 1 electrolyte), showing the homoleptic cation had formed.

^{89}Y NMR spectroscopy of the compound at 200 K in EtNO₂ showed a broad resonance at δ 112. Addition of excess ligand produced a single sharp peak at 133 ppm, assignable to $[Y(Me_3AsO)_6][NO_3]_3$. The resonance at 112 ppm was tentatively attributed to exchanging $[Y(Me_3AsO)_{6-n}(NO_3)_n]^{(3-n)+}$ species.

The structure of the hexakis(arsine oxide) complex was determined (Fig. 2.12), with selected bond lengths and angles given in Table 2.14. The structure exhibited octahedral geometry, with the Y-O distances showing little variation from those seen for $[Y(Ph_3AsO)_4(NO_3)_2]NO_3$ (Fig. 2.11). The Y-O-As angles were smaller than for the triphenylarsine oxide compound, as might be predicted given the smaller steric bulk of methyl groups (Y-O-As (ave.) = 139.0 c.f. 157.1° for $[Y(Ph_3AsO)_4(NO_3)_2]NO_3$).
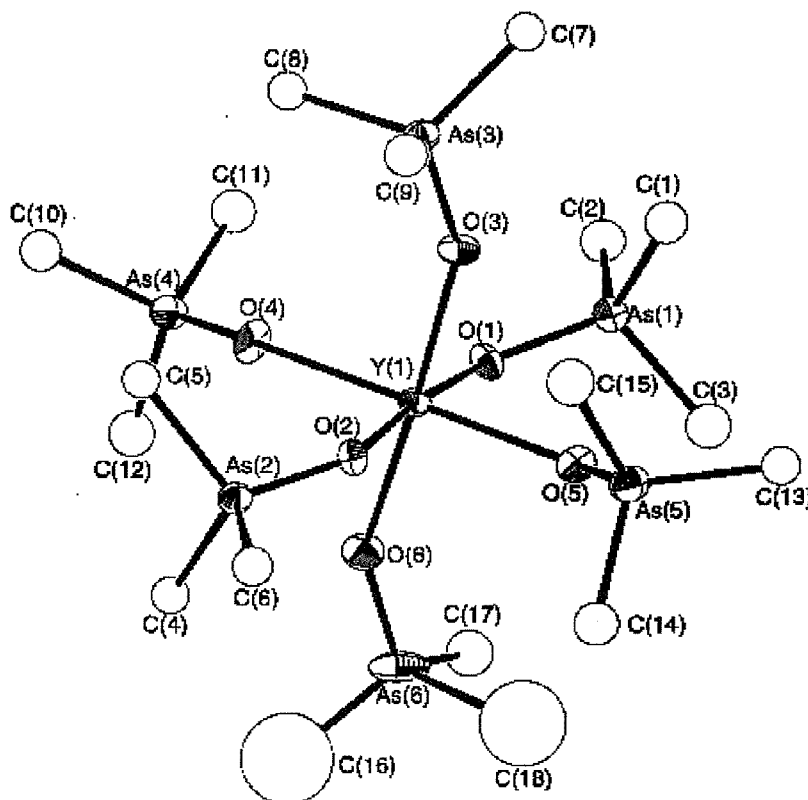
Fig. 2.12 The structure of the cation in $[Y(Me_3AsO)_6](NO_3)_3$. Thermal ellipsoids are drawn at 30% probability. H atoms omitted for clarity.

Table 2.14 Selected bond lengths (Å) and angles (°) for the structure of $[Y(Me_3AsO)_6](NO_3)_3$.

Y-O(1)	2.242(10)	Y-O(4)	2.221(9)
Y-O(2)	2.248(10)	Y-O(5)	2.253(9)
Y-O(3)	2.202(10)	Y-O(6)	2.209(11)
As(n) – O(n)	1.65(1)-1.70(1)	As-C	1.82(4)-2.04(4)
Y-O(1)-As(1)	131.3(5)	Y-O(2)-As(2)	134.0(5)
Y-O(3)-As(3)	149.1(6)	Y-O(4)-As(4)	142.3(6)
Y-O(5)-As(5)	130.0(5)	Y-O(6)-As(6)	147.1(6)
O-Y-O	86.7(4)-96.3(4)	O-As-C	108.0(6)-113.4(7)

The fact that $[Y(Me_3AsO)_6](NO_3)_3$ was the only product isolated from the $Y(NO_3)_3.6H_2O$ / Me_3AsO system contrasted strongly with reactions of $Y(NO_3)_3.6H_2O$ and Me_3PO, where the highest ligand : metal ratio complex detected was

$[Y(Me_3PO)_4(NO_3)_2]NO_3$. This indicated that the arsine oxide has a higher affinity for the yttrium centre than the phosphine oxide analogue.

2.2.9 Complexes of scandium nitrate with triphenylarsine oxide

Reaction of $Sc(NO_3)_3.5H_2O$ with 3 equivalents of Ph_3AsO in boiling ethanol yielded colourless crystals of $[Sc(Ph_3AsO)_3(NO_3)_2]NO_3$. A 1 : 1 molar ratio in warm acetone afforded an impure sample of $[Sc(Ph_3AsO)_2(NO_3)_3]$ (contaminated with $Sc(NO_3)_3.5H_2O$ which could not be removed).

The IR spectrum of the tris(arsine oxide) complex showed a broad $v(AsO)$ stretch at 899 cm^{-1} (compared with 878 cm^{-1}) in the 'free' ligand), along with a sharp band at 834 cm^{-1}, corresponding to the v_2 vibration of the ionic nitrate. The spectrum of the impure $[Sc(Ph_3AsO)_2(NO_3)_3]$ exhibited $v(AsO)$ 898 cm^{-1}, and also had a weak resonance at 834 cm^{-1}. However, this was attributed to residual $Sc(NO_3)_3.5H_2O$.

The molar conductances of 10^{-3} mol dm^{-3} solutions in CH_2Cl_2 were measured, with the tris(arsine oxide) compound having $\Lambda_m = 27$ ohm^{-1}cm^{2}mol^{-1}, typical of a 1 : 1 electrolyte. Addition of excess ligand did not affect this value, indicating no higher Ph_3AsO : Sc complexes form *in situ*. $[Sc(Ph_3AsO)_2(NO_3)_3]$ had $\Lambda_m = 8$ ohm^{-1}cm^{2}mol^{-1}, rising to 22 ohm^{-1}cm^{2}mol^{-1} following addition of Ph_3AsO, showing conversion to $[Sc(Ph_3AsO)_3(NO_3)_2]NO_3$.

^{45}Sc NMR spectroscopic data on $[Sc(Ph_3AsO)_3(NO_3)_2]NO_3$ showed a broad resonance at δ 31.9 ppm. No change was seen following addition of further triphenylarsine oxide. The spectrum of "$[Sc(Ph_3AsO)_2(NO_3)_3]$" also contained the peak at 31.9 ppm, along with a second, broad feature at δ 14.0, the latter attributed to the bis(arsine oxide) species. Addition of Ph_3AsO caused this resonance to disappear.

The structure of the cation of $[Sc(Ph_3AsO)_3(NO_3)_2]NO_3$ is depicted in Fig. 2.13, with bond lengths and angles given in Table 2.15. The scandium centre is seven-coordinate and can be described as pseudo-trigonal bypyramidal, with the nitrates in equatorial positions.
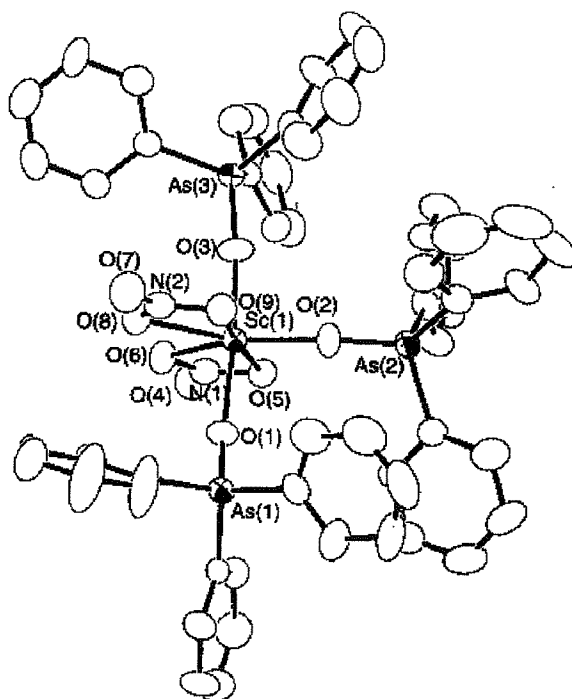
Fig. 2.13 The structure of the cation in $[Sc(Ph_3AsO)_3(NO_3)_2]NO_3$. Thermal ellipsoids are drawn at 30% probability. H atoms have been omitted for clarity.

Table 2.15 Selected bond lengths (Å) and angles (°) for the structure of $[Sc(Ph_3AsO)_3(NO_3)_2]NO_3$.

Sc-O(1)	2.030(4)	Sc-O(6)	2.256(5)
Sc-O(2)	1.999(4)	Sc-O(8)	2.267(5)
Sc-O(3)	1.996(4)	Sc-O(9)	2.251(5)
Sc-O(5)	2.250(5)	As(1)-O(1)	1.669(4)
As(2)-O(2)	1.665(4)	As(3)-O(3)	1.659(4)
As-C	1.877(7)-1.925(8)	N-O$_c$	1.258(7)-1.287(8)
N-O$_f$	1.222(8), 1.217(8)		
O(1)-Sc-O(2)	93.4(2)	O(1)-Sc-O(3)	171.4(2)
O(2)-Sc-O(3)	94.2(2)	O(5)-Sc-O(6)	56.2(2)
O(8)-Sc-O(9)	56.8(2)	Sc-O(1)-As(1)	149.2(3)
Sc-O(2)-As(2)	153.1(3)	Sc-O(3)-As(3)	176.4(3)
O-As-C	106.1(3)-113.1(3)	C-As-C	106.6(3)-112.4(3)

Comparison of these results with those for reactions of scandium nitrate with triphenylphosphine oxide (see 2.2.2) suggest that Ph_3AsO coordinates more strongly

than Ph_3PO. No evidence for a tris(phosphine oxide) complex was seen, whilst $[Sc(Ph_3AsO)_3(NO_3)_2]NO_3$ was the preferred compound for the arsine oxide system.

2.2.10 Complexes of scandium nitrate with trimethylarsine oxide

The reaction of hydrated scandium nitrate with trimethylarsine oxide in ice cold ethanol formed $[Sc(Me_3AsO)_6][NO_3]_3$. No other complexes could be isolated from these reagents, irrespective of ligand : metal ratio.

The IR spectrum was simple, with $v(AsO) = 925$ or 873 cm^{-1} (one band corresponds to a $AsMe_3$ rocking mode but it is difficult to distinguish between the two). Ionic nitrate groups were also identified by bands at 1364 and 836 cm^{-1}.[19] The molar conductance (measured for a 10^{-3} mol dm^{-3} solution in $MeNO_2$) was 157 ohm^{-1}cm^{2}mol^{-1} prior to addition of Me_3AsO, rising to 220 ohm^{-1}cm^{2}mol^{-1} afterwards, suggesting some decomposition in solution. The ^{45}Sc NMR spectrum showed a broad resonance at *ca.* 58 ppm, with a sharper feature superimposed at δ 56.0. Addition of excess ligand produced total conversion to the 56 ppm species. The sharper peak (caused by a cubic environment of the ^{45}Sc nucleus) was attributed to $[Sc(Me_3AsO)_6](NO_3)_3$, with the broader peak assigned to decomposition products of the type $[Sc(Me_3AsO)_{6-n}(NO_3)_n]^{(3-n)+}$. This behaviour in solution is similar to that observed for the phosphine oxide analogue (see 2.2.6) and $[Y(Me_3AsO)_6](NO_3)_3$.

The structure of $[Sc(Me_3AsO)_6](NO_3)_3$ was determined (Fig. 2.14) with selected bond angles and lengths given in Table 2.16. The methyl groups attached to As(3) were slightly disordered. The scandium centre is six co-ordinate with an octahedral geometry. Sc-O-As angles are smaller than for those in $[Sc(Ph_3AsO)_3(NO_3)_2]$ $NO_3.H_2O$ (137.1° c.f. 169.6°).
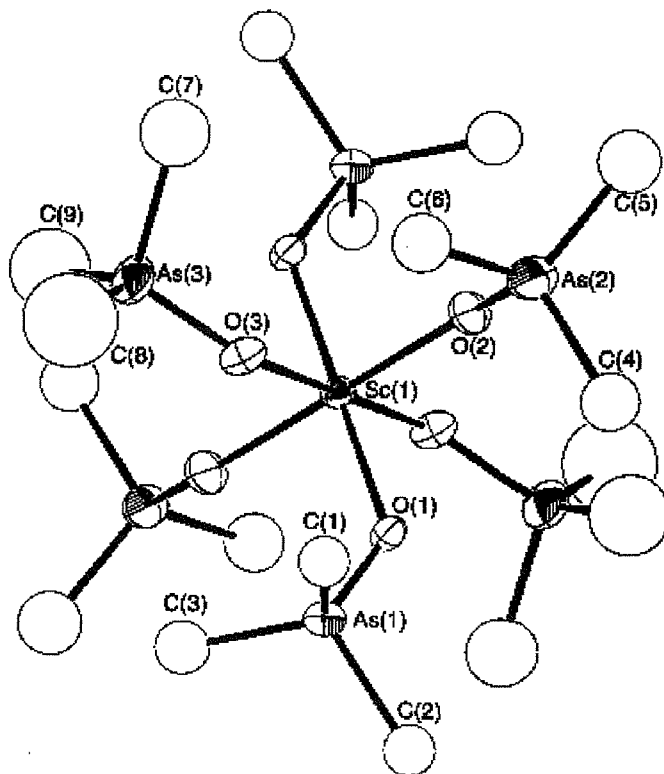
Fig. 2.14 The structure of the cation in [Sc(Me₃AsO)₆](NO₃)₃, showing the atom numbering scheme. Thermal ellipsoids are drawn at 30% probability, with H atoms omitted for clarity.

Table 2.16 Selected bond lengths (Å) and angles (°) for the structure of [Sc(Me₃AsO)₆](NO₃)₃.

Sc-O(1)	2.100(8)	As(1)-O(1)	1.662(8)
Sc-O(2)	2.064(8)	As(2)-O(2)	1.649(9)
Sc-O(3)	2.097(8)	As(3)-O(3)	1.650(8)
As-C	1.86(4)-1.99(2)		
Sc-O(1)-As(1)	132.6(4)	Sc-O(2)-As(2)	144.3(6)
Sc-O(3)-As(3)	134.3(5)	O-Sc-O	88.5(3)-91.5(3)
O-As-C	107.2(6)-112.1(6)	C-As-C	99(1)-123(2)

2.2.11 Complexes of lanthanum nitrate with triphenylarsine oxide

$[La(Ph_3AsO)_2(EtOH)(NO_3)_3]$ was formed when $La(NO_3)_3.6H_2O$ was reacted with two molar equivalents of Ph_3AsO in boiling ethanol. Reaction of a 1 : 3 molar ratio of lanthanum nitrate hexahydrate with triphenylarsine oxide in boiling acetone afforded $[La(Ph_3AsO)_3(NO_3)_3].Me_2CO$. A third complex in the series, $[La(Ph_3AsO)_4(NO_3)_2]$ $NO_3.Me_2CO$, was produced from reaction of a 6 : 1 molar ratio of Ph_3AsO to $La(NO_3)_3.6H_2O$ in acetone.

Infrared spectroscopy showed some variation in $v(AsO)$ between the three compounds. $[La(Ph_3AsO)_2(EtOH)(NO_3)_3]$ had $v = 908$ and 888 cm^{-1}, whilst the tris and tetrakis (arsine oxide) complexes had broader bands at $v = 890$ and 891 cm^{-1} respectively. Ethanol was apparent by a broad band at 3400 cm^{-1} in the IR spectrum of the ethanol adduct, whilst acetone was apparent by bands at 1702 cm^{-1} ($[La(Ph_3AsO)_3$ $(NO_3)_3].Me_2CO$) and 1707 cm^{-1} ($[La(Ph_3AsO)_4(NO_3)_2]NO_3.Me_2CO$).

^{139}La NMR spectroscopy was of little use for this system, the nucleus having $I = 7/2$ and a quadrupole moment of 0.21 x 10^{-28} cm^2, leading to fast relaxation and unobservably broad resonances.[9] ^{1}H and ^{13}C-{^{1}H} NMR spectroscopy proved insensitive to coordination of the ligands, although both confirmed the solvents present in the compounds.

Molar conductance measurements showed both $[La(Ph_3AsO)_2(EtOH)(NO_3)_3]$ ($\Lambda_m = 4$ ohm^{-1}cm^{2}mol^{-1}) and $[La(Ph_3AsO)_3(NO_3)_3]$ ($\Lambda_m = 4$ ohm^{-1}cm^{2}mol^{-1}) to be non-electrolytes for 10^{-3} mol dm^{-3} solutions in anhydrous CH_2Cl_2. Addition of excess ligand saw Λ_m rise to values consistent with a 1 : 1 electrolyte for both complexes. $[La(Ph_3AsO)_4(NO_3)_2]NO_3.Me_2CO$ had $\Lambda_m = 21$ ohm^{-1}cm^{2}mol^{-1}, showing it is a 1 : 1 electrolyte and suggesting that the other two complexes had been converted to a tetrakis(arsine oxide) species by the addition of Ph_3AsO. Addition of ligand to the tetrakis(arsine oxide) compound saw no significant change in Λ_m, indicating that no higher Ph_3AsO : La compounds exist. The results for $[La(Ph_3AsO)_4(NO_3)_2]$

$NO_3.Me_2CO$ contrast with those for $[La(Ph_3PO)_4(NO_3)_3]$, which completely decomposes in solution to $[La(Ph_3PO)_3(NO_3)_3]$ and Ph_3PO.[13]

The structure of $[La(Ph_3AsO)_2(EtOH)(NO_3)_3]$ was determined (Fig. 2.15), with selected bond lengths and angles given in Table 2.17. The lanthanum centre was found to be nine-coordinate with three bidentate nitrate groups. If the nitrate groups are considered monodentate, the geometry is *mer*-(pseudo)-octahedral. The structure is isomorphous with the analogous Ph_3PO complexes of Sm,[18] Eu,[3] and Ce.[13]
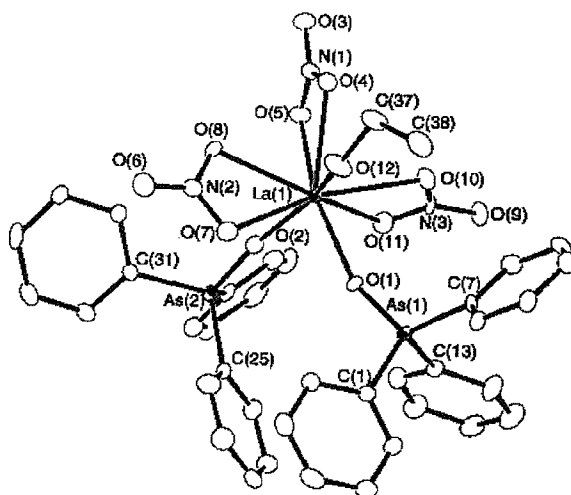
Fig. 2.15 The structure of $[La(Ph_3AsO)_2(EtOH)(NO_3)_3]$, showing the atom numbering scheme. Thermal ellipsoids are drawn at 30% probability. H atoms omitted for clarity.

Table 2.17 Selected bond lengths (Å) and angles (°) for the structure of $[La(Ph_3AsO)_2(EtOH)(NO_3)_3]$.

La-O(1)	2.347(7)	La-O(8)	2.592(7)
La-O(2)	2.324(8)	La-O(10)	2.581(7)
La-O(4)	2.640(7)	La-O(11)	2.615(8)
La-O(5)	2.608(8)	La-O(12)	2.552(7)
La-O(7)	2.664(7)	As-C	1.896(12)-1.932(9)
As(1)-O(1)	1.670(7)	As(2)-O(2)	1.671(7)
O(1)-La-O(2)	92.0(3)	O(1)-La-O(12)	80.1(3)
O(2)-La-O(12)	149.5(3)	O(4)-La-O(5)	48.4(2)
O(7)-La-O(8)	48.7(2)	O(10)-La-O(11)	49.5(3)
La-O(1)-As(1)	159.2(4)	La-O(2)-As(2)	164.0(5)
O-As-C	107.5(4)-114.6(4)	C-As-C	106.9(4)-110.6(5)

The structure of $[La(Ph_3AsO)_4(NO_3)_2]NO_3.2Me_2CO$ was determined (Fig. 2.16), with selected bond lengths and angles given in Table 2.18. The cation is structurally similar to $[Y(Ph_3AsO)_4(NO_3)_2]NO_3$ (Fig. 2.11), with an eight-coordinate metal centre in a (pseudo)-octahedral geometry. The bidentate nitrates are in *trans* positions and are mutually perpendicular. Whilst two acetones were present in the crystal structure, microanalysis suggests that only one solvent molecule is present in the bulk material. The analogous phosphine oxide cation has been reported, albeit with a different anion.[26] Comparison of this cation with $[La(Ph_3AsO)_4(NO_3)_2]^+$ shows La-O(As) to be significantly shorter than La-O(P) (2.340(5) to 2.361(5) Å c.f. 2.449(8) to 2.695(8) Å). $[La(Ph_3PO)_4(NO_3)_3]$ has also been characterised, with a nine-coordinate lanthanum centre (one nitrate group is monodentate).[13]
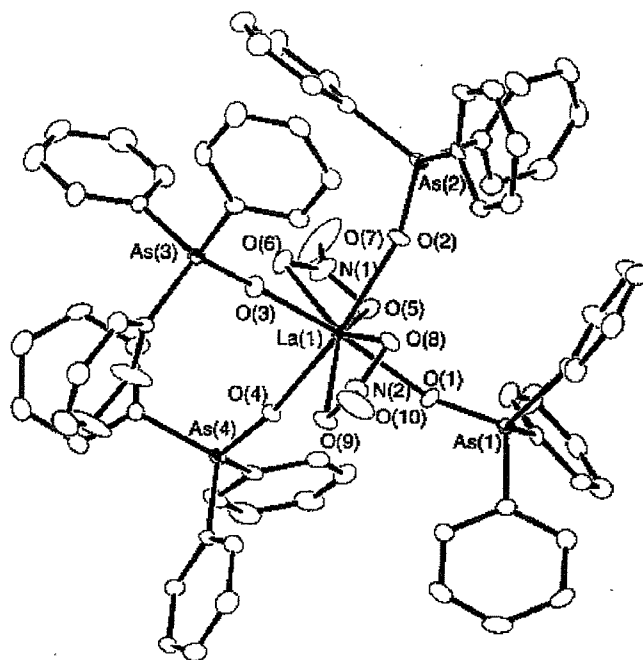
Fig. 2.16 The structure of the cation in $[La(Ph_3AsO)_4(NO_3)_2]NO_3.2Me_2CO$, showing the atom numbering scheme. Thermal ellipsoids are drawn at 30% probability. H atoms have been omitted for clarity.

Table 2.18 Selected bond lengths (Å) and angles (°) for the structure of

$[La(Ph_3AsO)_4(NO_3)_2]NO_3.2Me_2CO$.

La-O(1)	2.361(5)	La-O(5)	2.635(5)
La-O(2)	2.343(4)	La-O(6)	2.641(5)
La-O(3)	2.340(5)	La-O(8)	2.651(5)
La-O(4)	2.347(4)	La-O(9)	2.656(5)
As(1)-O(1)	1.660(5)	As(2)-O(2)	1.661(4)
As(3)-O(3)	1.658(5)	As(4)-O(4)	1.660(4)
As-C	1.907(7)-1.921(7)	N-O$_f$	1.206(8), 1.218(8)
N-O$_c$	1.250(8)-1.270(7)		
O(1)-La-O(2)	94.9(2)	O(1)-La-O(4)	89.3(2)
O(2)-La-O(3)	89.8(2)	O(3)-La-O(4)	92.3(2)
O(5)-La-O(6)	48.1(2)	O(8)-La-O(9)	48.1(1)
La-O(2)-As(2)	162.8(3)	La-O(1)-As(1)	160.0(3)
La-O(3)-As(3)	175.7(3)	La-O(4)-As(4)	167.5(3)
O-As-C	107.0(3)-112.8(3)		

2.2.12 Complexes of lanthanum nitrate with trimethylarsine oxide

Reaction of lanthanum nitrate hexahydrate with 6 molar equivalents trimethylarsine oxide in ice cold ethanol produced $[La(Me_3AsO)_6](NO_3)_3$. In addition, reaction in a 1 : 2 molar ratio in boiling ethanol afforded $[La(Me_3AsO)_2(H_2O)(NO_3)_3]$. Attempts to synthesise $[La(Me_3AsO)_4(NO_3)_3]$ (identified as a decomposition product of $[La(Me_3AsO)_6](NO_3)_3$ in nitromethane) in bulk were unsuccessful.

The infrared spectrum of $[La(Me_3AsO)_6](NO_3)_3$ contained $v(AsO)$ = 864 cm^{-1}. Ionic nitrate groups were apparent by bands at 1359 and 836 cm^{-1}. The IR spectrum was very similar to that of both the yttrium and scandium congeners, suggesting the complex shares a similar six-coordinate metal centre. The spectrum of $[La(Me_3AsO)_2(H_2O)(NO_3)_3]$ had $v(AsO)$ = 875 cm^{-1}, with water apparent from broad band at *ca.* 3400 cm^{-1} and a sharp band at 1620 cm^{-1}. Confirmation of the presence of water comes from the ^{1}H NMR spectrum. The presence of water rather than ethanol has been seen previously in the complex $[Y(Me_3PO)_2(H_2O)(NO_3)_3]$ (see 2.2.1).

Attempts to grow crystals of $[La(Me_3AsO)_6](NO_3)_3$ yielded several crystals which upon refinement were identified as the decomposition product $[La(Me_3AsO)_4(NO_3)_3]$.

However, the data were of poor quality, with refinement unsatisfactory. The La centre was nine-coordinate, with one of the nitrate groups monodentate (see below*).

(*[La(Me$_3$AsO)$_4$(NO$_3$)$_3$]. Crystal data: monoclinic, a = 10.278(3), b = 12.034(4), c = 12.030(2) Å, β = 97.42(2)°, U = 1475.4(6) Å^3. Space group = $P2_1$ (no. 4), Z = 2, T = 150 K. R = 0.14 for 2381 I_o > 4$\sigma(F_o)$ and 237 parameters.)

2.2.13 Reaction schemes

Y(NO$_3$)$_3$.6H$_2$O +

Ph$_3$PO → [Y(Ph$_3$PO)$_2$(EtOH)(NO$_3$)$_3$]
Ph$_3$PO → [Y(Ph$_3$PO)$_3$(NO$_3$)$_3$]
Ph$_3$PO → [Y(Ph$_3$PO)$_4$(NO$_3$)$_2$]NO$_3$

Ph$_2$MePO → [Y(Ph$_2$MePO)$_3$(NO$_3$)$_3$]
Ph$_2$MePO → [Y(Ph$_2$MePO)$_2$(EtOH)(NO$_3$)$_3$]

Me$_3$PO → [Y(Me$_3$PO)$_3$(NO$_3$)$_3$]
Me$_3$PO → [Y(Me$_3$PO)$_2$(H$_2$O)(NO$_3$)$_3$]

Ph$_3$AsO → [Y(Ph$_3$AsO)$_2$(EtOH)(NO$_3$)$_3$]
Ph$_3$AsO → [Y(Ph$_3$AsO)$_4$(NO$_3$)$_2$]NO$_3$.Me$_2$CO

Me$_3$AsO → [Y(Me$_3$AsO)$_6$](NO$_3$)$_3$
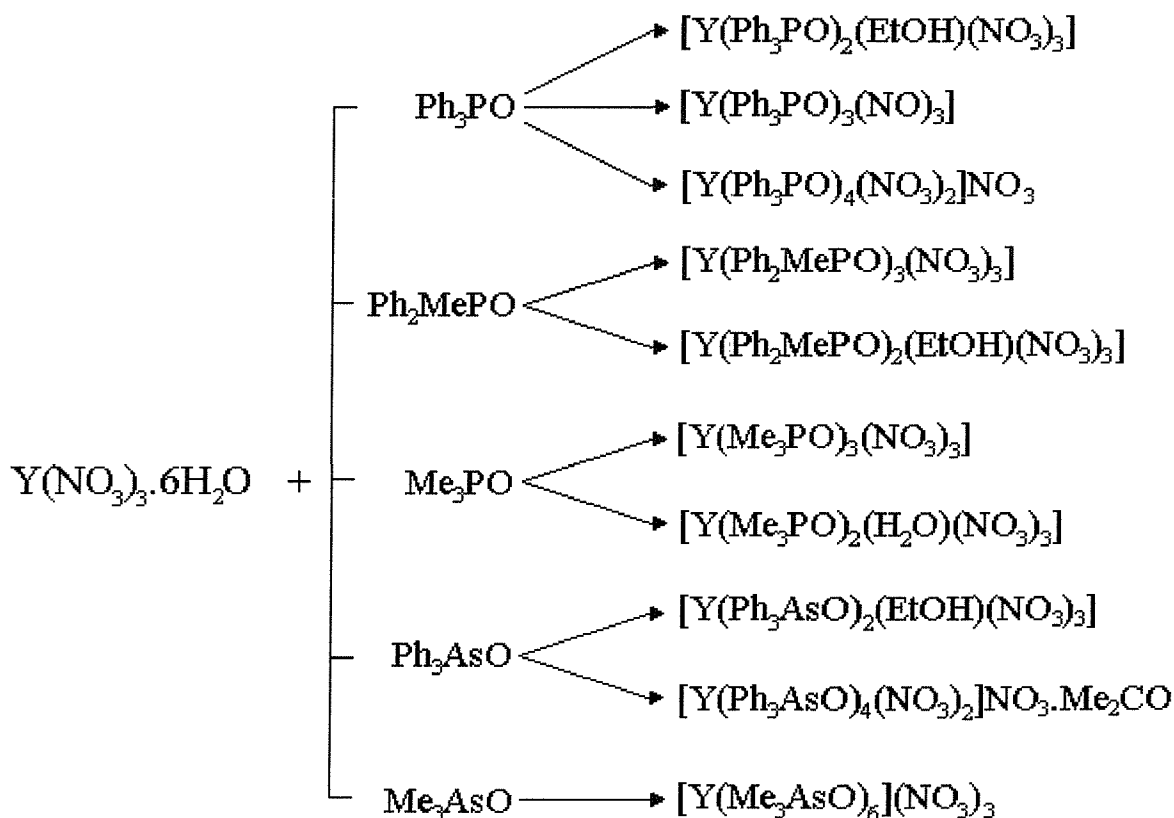
Fig. 2.17 Reaction scheme showing all products isolated from reaction of yttrium(III) nitrate with the R$_3$EO ligands examined in this study.

$$Sc(NO_3)_3.5H_2O \quad + \quad \begin{cases} Ph_3PO \longrightarrow [Sc(Ph_3PO)_2(NO)_3] \\ \\ Ph_2MePO \begin{cases} [Sc(Ph_2MePO)_3(NO_3)_3] \\ [Sc(Ph_2MePO)_4(NO_3)_2]NO_3 \end{cases} \\ \\ Me_3PO \begin{cases} [Sc(Me_3PO)_2(EtOH)(NO_3)_3] \\ [Sc(Me_3PO)_6](NO_3)_3 \end{cases} \\ \\ Ph_3AsO \begin{cases} [Sc(Ph_3AsO)_2(NO_3)_3] \\ [Sc(Ph_3AsO)_3(NO_3)_2]NO_3 \end{cases} \\ \\ Me_3AsO \longrightarrow [Sc(Me_3AsO)_6](NO_3)_3 \end{cases}$$
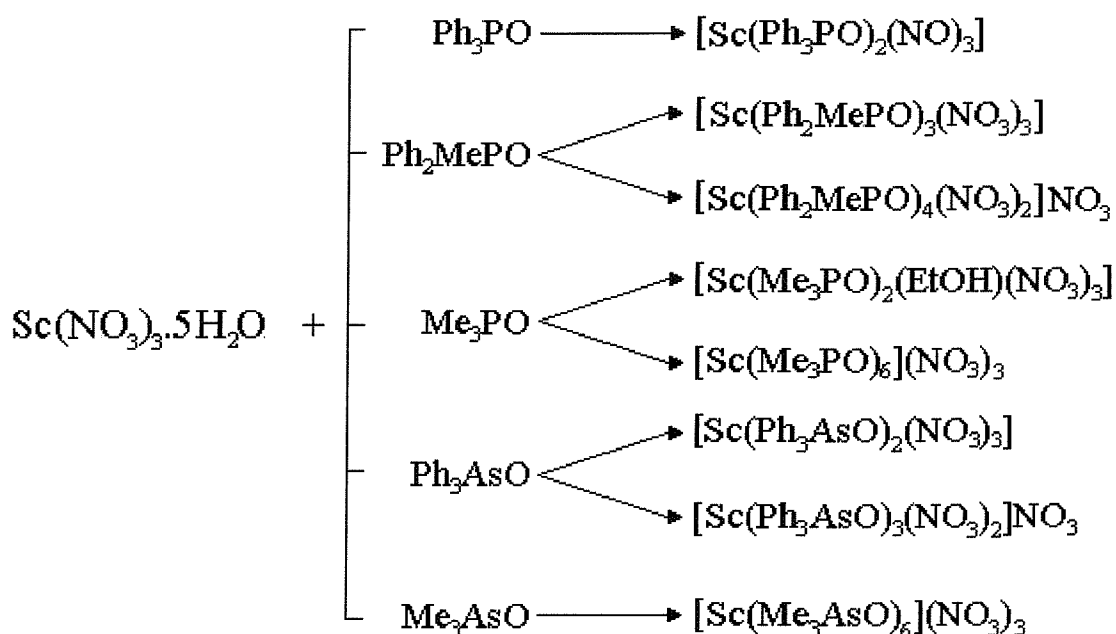
Fig. 2.18 Reaction scheme showing all products isolated from reaction of scandium(III) nitrate with R_3EO ligands within this study.

$$La(NO_3)_3.6H_2O \quad + \quad \begin{cases} Ph_3AsO \begin{cases} [La(Ph_3AsO)_2(EtOH)(NO_3)_3] \\ [La(Ph_3AsO)_3(NO_3)_3].Me_2CO \\ [La(Ph_3AsO)_4(NO_3)_2]NO_3.Me_2CO \end{cases} \\ \\ Me_3AsO \begin{cases} [La(Me_3AsO)_6](NO_3)_3 \\ [La(Me_3AsO)_2(H_2O)(NO_3)_3] \end{cases} \end{cases}$$
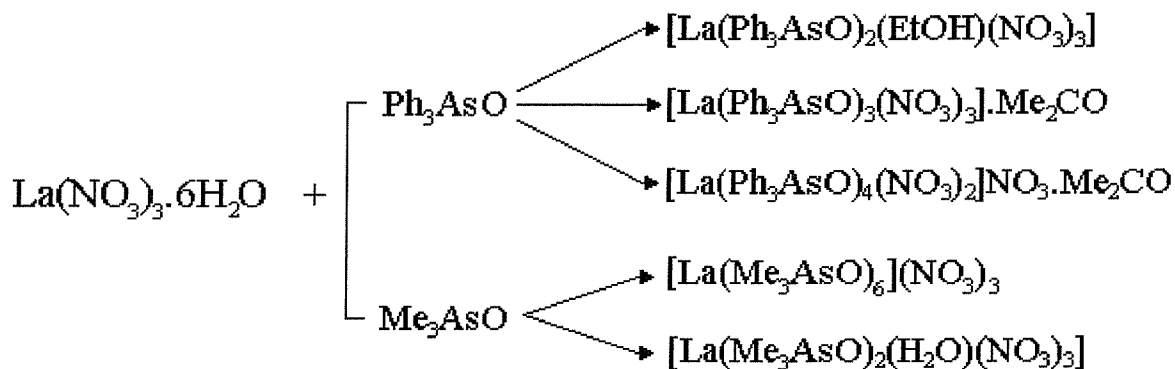
Fig. 2.19 Scheme indicating products formed when hydrated lanthanum(III) nitrate was reacted with Ph_3AsO or Me_3AsO.

2.3 Conclusions

A range of complexes exist in the $M(NO_3)_3$ / R_3XO systems (M = Y, Sc or La and X = As or P), with significant variation dependent on the reaction conditions, the metal in question and ligand type. The first structurally characterised examples of tertiary arsine oxide / lanthanide nitrate complexes are reported, whilst scandium nitrate / phosphine oxide complexes are described for the first time.

The results allow comparison of the ligating properties of R_3AsO and R_3PO with Sc(III), Y(III) and La(III) nitrate metal centres. It is apparent that tertiary arsine oxide ligands coordinate more strongly than their phosphine oxide congeners, resulting in higher ratio ligand to metal species being formed. For example, when Ph_3PO is reacted with yttrium nitrate, $[Y(Ph_3PO)_3(NO_3)_3]$ is the favoured product, whilst reaction of $Y(NO_3)_3.6H_2O$ with Ph_3AsO yields $[Y(Ph_3AsO)_4(NO_3)_2]NO_3$, with no tris(arsine oxide) complex isolated. Similarly, reaction with Me_3PO yields $[Y(Me_3PO)_2(H_2O)(NO_3)_3]$ or $[Y(Me_3PO)_3(NO_3)_3]$, whilst reaction with Me_3AsO affords only $[Y(Me_3AsO)_6][NO_3]_3$. Examination of the dipole moments of the ligands suggest that R_3AsO would indeed be stronger donors, the arsine oxides having more electron density centred on the oxygen atom (Ph_3AsO = 5.50 D c.f. Ph_3PO = 4.51 D; Me_3AsO = 5.12 D c.f. Me_3PO = 4.39 D).[27,28]

Crystallographic results also indicate that arsine oxide ligands complex more strongly than the analogous phosphine oxide ligands, with M-O(As) consistently shorter than M-O(P). Comparison of Ln-O(X) distances (X = P or As) for other lanthanide metals in related work leads to the same conclusion.[18,26,29,30] It is also apparent that the average M-O-X angles (X = As or P, M = Sc or Y) are larger as the steric bulk of R increases in the ligand. For example, for the compound $[Y(Ph_3PO)_3(NO_3)_3].xCH_2Cl_2$, Y-O-P(ave.) = 164.4°, whilst for $[Y(Me_3PO)_3(NO_3)_3]$, Y-O-P(ave.) = 146.5°).

Multinuclear NMR studies revealed interesting behaviour in solution. Many of the pure compounds isolated in the solid state exist as mixtures of species in solution. $^{31}P-\{^1H\}$ NMR demonstrated that exchange with free R_3PO is slow on the NMR timescale at

ambient temperatures. However, the complexes are labile and readily interchange in solution.

2.4 Experimental

$Y(NO_3)_3.6H_2O$, Ph_3PO, Ph_2MePO and Ph_3AsO were purchased from Aldrich Chemical Company, Me_3PO from ALFA, $Sc(NO_3)_3.5H_2O$ from Strem and $La(NO_3)_3.6H_2O$ from BDH. Me_3AsO was synthesised by H_2O_2 oxidation of Me_3As in diethyl ether and purified by sublimation *in vacuo*.[31]

2.4.1 Complexes of yttrium nitrate with tertiary phosphine oxides

[Y(Ph₃PO)₃(NO₃)₃]

Yttrium nitrate hexahydrate (0.38 g, 1.0 mmol) and Ph_3PO (1.11 g, 4.0 mmol) were dissolved separately in warm (60 °C) ethanol (20 cm^3). The solutions were mixed, then stirred for 1 h. The solution was evaporated to *ca.* 10 cm^3 then refrigerated overnight. The white solid formed was filtered off and dried *in vacuo*. Yield 0.93 g, 91%. (Found: C, 58.1; H, 3.7; N, 3.7. Calc. for $C_{54}H_{45}N_3O_{12}P_3Y$: C, 58.4; H, 4.1; N, 3.8%). IR (cm^{-1}) (Nujol mull): 1500w, 1437m, 1311w, 1187w, 1168s (PO), 1154s (PO), 1121m, 1092m, 1031w, 815m, 745s, 725m and 690w. ^{31}P-{^1H} NMR (300 K, CH_2Cl_2): δ 36.5 and 33.9. ^{89}Y NMR (300 K): not observed. A_m (CH_2Cl_2, 10^{-3} mol dm^{-3}) = 13 ohm^{-1} cm^2 mol^{-1}.

[Y(Ph₂MePO)₃(NO₃)₃]

Yttrium nitrate hexahydrate (0.38 g, 1.0 mmol) and Ph_2MePO (0.65 g, 3.0 mmol) were dissolved in warm (60 °C) ethanol (15 cm^3). After 3 h, the solution was cooled and refrigerated overnight, yielding a white, crystalline solid which was filtered off and dried *in vacuo*. Yield 74%. (Found: C, 50.2; H, 4.1; N, 4.5. Calc. for $C_{39}H_{39}N_3O_{12}P_3Y$: C, 50.7; H, 4.3; N, 4.6%). IR (cm^{-1}) (Nujol mull): 1500w (sh), 1450m, 1306w, 1300w (sh), 1172w (sh), 1150s (PO), 1126s, 1105m, 1035m, 895w, 883w, 781m, 745m, 716w, 696w and 668m. ^{31}P-{^1H} NMR (300 K, CH_2Cl_2): δ 36.6. ^{89}Y NMR (300 K): δ -22br. ^1H NMR (300 K, $CDCl_3$): δ 7.2-7.7m [30H], 1.95(d, $^2J_{PH}$ 13.5 Hz)[9H]. A_m (CH_2Cl_2, 10^{-3} mol dm^{-3}) = 4 ohm^{-1} cm^2 mol^{-1}.

[Y(Me$_3$PO)$_3$(NO$_3$)$_3$]

The method used was as for above, but using Me$_3$PO (0.28 g, 3.0 mmol). A white solid was isolated. Yield 33%. (Found: C, 19.1; H, 4.8; N, 7.5. Calc. for C$_9$H$_{27}$N$_3$O$_{12}$P$_3$Y: C, 19.6; H, 4.9; N, 7.6%). IR (cm^{-1}) (Nujol mull): 1308m, 1171 (sh), 1146s (PO), 1120 (sh), 1036m, 949s, 863m, 819w, 390m and 365w. ^{31}P-{^{1}H} NMR (300 K, CH$_2$Cl$_2$): δ 48.3. ^{89}Y NMR (300 K): δ -17.0(s). ^{1}H NMR (300 K, CDCl$_3$): δ 1.65(d, $^2J_{PH}$ 13.6 Hz). Λ_m (CH$_2$Cl$_2$, 10^{-3} mol dm^{-3}) = 6 ohm^{-1} cm^2 mol^{-1}.

[Y(Ph$_3$PO)$_2$(EtOH)(NO$_3$)$_3$]

Yttrium nitrate hexahydrate (0.38 g, 1.0 mmol) and Ph$_3$PO (0.28 g, 1.0 mmol) were dissolved in boiling ethanol (15 cm^3). After 15 min, the solution was cooled and refrigerated overnight, yielding a white, crystalline solid which was filtered off and dried *in vacuo*. Yield 0.46 g, 53%. (Found: C, 52.3; H, 4.1; N, 4.8. Calc. for C$_{38}$H$_{36}$N$_3$O$_{12}$P$_2$Y: C, 52.0; H, 4.1; N, 4.8%). IR (cm^{-1}) (Nujol mull): 3300 (br), 1500w, 1314m, 1171s (PO), 1155s (PO), 1120m, 1039m, 1032 (sh), 816w, 692m and 539s. ^{31}P-{^{1}H} NMR (300 K, CH$_2$Cl$_2$): δ 37.0. ^{89}Y NMR (300 K): not observed. ^{1}H NMR (300 K, d$_6$-acetone): δ 7.1-7.6(m), 3.56 (quartet, J=7) and 1.11 (t, J=7 Hz). Λ_m (CH$_2$Cl$_2$, 10^{-3} mol dm^{-3}) = 10 ohm^{-1} cm^2 mol^{-1}.

[Y(Ph$_2$MePO)$_2$(EtOH)(NO$_3$)$_3$]

The method used was as for above, but using Ph$_2$MePO (0.22 g, 1.0 mmol). Yield 0.40 g, 53%. (Found: C, 46.4; H, 4.0; N, 4.8. Calc. for C$_{28}$H$_{32}$N$_3$O$_{12}$P$_2$Y: C, 44.6; H, 4.3; N, 5.6%).* IR (cm^{-1}) (Nujol mull): 3300 (br), 1591w, 1300 (br), 1181 (sh), 1155s (PO), 1126m, 1109m, 1073w, 998w, 969w, 893m, 881m, 816m, 779w, 741s, 693s, 513m, 504s and 398w. ^{31}P-{^{1}H} NMR (300 K, CH$_2$Cl$_2$): δ 37.7. ^{89}Y NMR (300 K): not observed. ^{1}H NMR (300 K, d$_6$-acetone): δ 7.6-7.9(m)[20H], 3.60 (q, J=7)[2H], 2.05 (d, $^2J_{PH}$ = 14)[6H] and 1.15 (t, J=7 Hz)[3H]. Λ_m (CH$_2$Cl$_2$, 10^{-3} mol dm^{-3}) = 7 ohm^{-1} cm^2 mol^{-1}.

* See text, section 2.2.2

[Y(Me₃PO)₂(H₂O)(NO₃)₃]

A solution of $Y(NO_3)_3.6H_2O$ (0.38 g, 1 mmol) in boiling ethanol (15 cm³) was added to Me_3PO (0.09 g, 1 mmol) in ethanol (10 cm³). The solution was concentrated to *ca.* 10 cm³, cooled and refrigerated for 24 h. A white solid was formed, which was filtered off and dried *in vacuo*. Yield 36%. (Found: C, 14.5; H, 3.9; N, 8.7. Calc. for $C_6H_{20}N_3O_{12}P_2Y$: C, 15.1; H, 4.2; N, 8.7%). IR (cm⁻¹) (Nujol mull): 3400 (br) s, 1650m, 1297s, 1160 (sh) (PO), 1140s (PO), 1083m, 1034m, 951s, 866m, 816m, 745m, 605 (br), 391m, 371m and 333w. $^{31}P-\{^1H\}$ NMR (300 K, CH_2Cl_2): δ 50.5. ^{89}Y NMR (300 K): not observed. ^1H NMR (300 K, d₆-acetone): δ 1.45(d, $^2J_{PH}$ = 13.6 Hz). $Λ_m$ (CH_2Cl_2, 10^{-3} mol dm⁻³) = 7 ohm⁻¹ cm² mol⁻¹.

[Y(Ph₃PO)₄(NO₃)₂]NO₃

A solution of yttrium nitrate hexahydrate (0.19 g, 0.5 mmol) in ice-cold ethanol (5 cm³) was added to a solution of Ph₃PO (0.84 g, 3.0 mmol) in ethanol (15 cm³) at 0 °C. A white crystalline solid was filtered off after 1 h and dried *in vacuo*. Yield 0.35 g, 51%. (Found: C, 62.0; H, 4.0; N, 3.2. Calc. for $C_{72}H_{60}N_3O_{13}P_4Y$: C, 62.3; H, 4.3; N, 3.0%). IR (cm⁻¹) (Nujol mull): 1520w, 1298m, 1154s (PO), 1121s, 1091m, 1031w, 997w, 971w, 830w, 816w, 742m, 692m, 542s, 416w and 308w. $^{31}P-\{^1H\}$ NMR (300 K, CH_2Cl_2): δ 36.5, 33.3 and 26.0. ^{89}Y NMR (300 K): not observed. $Λ_m$ (CH_2Cl_2, 10^{-3} mol dm⁻³) = 14 ohm⁻¹ cm² mol⁻¹.

2.4.2 Complexes of scandium nitrate with tertiary phosphine oxides

[Sc(Ph₃PO)₂(NO₃)₃]

A boiling solution of $Sc(NO_3)_3.5H_2O$ (0.23 g, 1.0 mmol) in ethanol (20 cm³) was added to a solution of Ph₃PO (0.83 g, 3.0 mmol) in ethanol (10 cm³). The solution was concentrated to *ca.* 15 cm³ then refrigerated for 24h. White crystals were filtered off and dried *in vacuo*. Yield 0.26 g, 33%. (Found: C, 54.5; H, 4.0; N, 5.1. Calc. for $C_{36}H_{30}N_3O_{11}P_2Sc$: C, 54.9; H, 3.8; N, 5.3%). IR (cm⁻¹) (Nujol mull): 1591m, 1527w, 1299s, 1284s, 1167s (PO), 1141s, 1123m, 1009w, 808s, 747m, 692m and 542s. $^{31}P-\{^1H\}$ NMR (300 K, CH_2Cl_2): δ 37.7. ^{45}Sc NMR (300 K, CH_2Cl_2): δ -7.5 ($W_{1/2}$ = 900 Hz). $Λ_m$ (CH_2Cl_2, 10^{-3} mol dm⁻³) = 2 ohm⁻¹ cm² mol⁻¹.

[Sc(Ph₂MePO)₄(NO₃)₂]NO₃

Made as above, using Ph_2MePO (0.86 g, 4.0 mmol) with $Sc(NO_3)_3.5H_2O$ (0.23 g, 1.0 mmol). Yield 0.66 g, 60%. (Found: C, 56.9; H, 5.0; N, 3.7. Calc. for $C_{52}H_{52}N_3O_{13}P_4Sc$: C, 57.0; H, 4.7; N, 3.8%). IR (cm⁻¹) (Nujol mull): 1591w, 1299m, 1153s (PO), 1125m, 1108m, 1073m, 1037w, 996w, 889s, 831w, 818w, 744s, 711s, 694s, 507s, 479m, 453m, 425w, 400w and 277m. ^{31}P-$\{^1H\}$ NMR (300 K, CH_2Cl_2): δ 38.5 ($W_{1/2}$ = 700 Hz); (220 K) δ 39.6vw, 38.7s and 29.2vw. ^{45}Sc NMR (300 K, CH_2Cl_2): δ -3.5 ($W_{1/2}$ = 500 Hz) and -33 ($W_{1/2}$ = 10000 Hz). ^1H NMR (300 K, $CDCl_3$): δ 7.6-7.9m[40H], 2.10 (d, $^2J_{PH}$ = 12 Hz)[12H]. $Λ_m$ (CH_2Cl_2, 10^{-3} mol dm⁻³) = 8 ohm⁻¹ cm² mol⁻¹.

[Sc(Ph₂MePO)₃(NO₃)₃]

A solution of $Sc(NO_3)_3.5H_2O$ (0.23 g, 1.0 mmol) in boiling ethanol (20 cm³) was added to a solution of Ph_2MePO (0.43 g, 2.0 mmol) in ethanol (10 cm³). The solution was concentrated to *ca.* 5 cm³ and refrigerated for 24 h. A sticky solid was formed, the supernatant liquid decanted off and the solid washed with ice-cold diethyl ether (5 cm³). The resultant white solid was dried *in vacuo*. Yield 0.25 g, 28%. (Found: C, 53.2; H, 4.4; N, 4.6. Calc. for $C_{39}H_{39}N_3O_{12}P_3Sc$: C, 53.3; H, 4.5; N, 4.8%). IR (cm⁻¹) (Nujol mull): 1590w, 1302s, 1153s (PO), 1090w, 1025w, 971w, 890m, 814w, 777m, 692m, 502s, 422w, 400w and 287m. ^{31}P-$\{^1H\}$ NMR (300 K, CH_2Cl_2): δ 39.5. ^{45}Sc NMR (300 K, CH_2Cl_2): δ -4.0 ($W_{1/2}$ = 350 Hz). ^1H NMR (300 K, $CDCl_3$): δ 7.7-7.9m[30H], 2.10 (d, $^2J_{PH}$ = 12 Hz)[9H].

[Sc(Me₃PO)₂(EtOH)(NO₃)₃]

A boiling solution of $Sc(NO_3)_3.5H_2O$ (0.35 g, 1.5 mmol) in ethanol (20 cm³) was added to a solution of Me_3PO (0.14 g, 1.5 mmol) in ethanol (10 cm³). The solution was evaporated to dryness then redissolved in the minimum n-butanol and refrigerated for 24 h. A cream coloured sticky solid was formed which was discarded, with the mother liquor allowed to evaporate slowly, producing colourless crystals. Filtered off and dried *in vacuo*. Yield 0.05 g, 10%. (Found: C, 20.4; H, 5.1; N, 9.6. Calc. for $C_8H_{24}N_3O_{12}P_2Sc$: C, 20.8; H, 5.6; N, 9.1%). IR (cm⁻¹) (Nujol mull): 3200 (br), 1312m, 1152s (PO), 1112m, 1026w, 956m, 866w, 815w, 534w, 485w, 430w, 372w and 327w.

^{31}P-$\{^1$H$\}$ NMR (300 K, CH$_2$Cl$_2$): δ 54.8. ^{45}Sc NMR (300 K, CH$_2$Cl$_2$): δ -2.5 ($W_{1/2}$ = 600 Hz). ^{1}H NMR (300 K, CDCl$_3$): δ 0.9 (t, J=7)[3H], 1.6 (d, $^2J_{PH}$ = 10)[18H] and 3.6 (quartet, J=7 Hz)[2H].

[Sc(Me$_3$PO)$_6$][NO$_3$]$_3$

A solution of Sc(NO$_3$)$_3$.5H$_2$O (0.23 g, 1.0 mmol) in ice-cold ethanol (20 cm^3) was added to a solution of Me$_3$PO (0.53 g, 6.0 mmol) in ethanol (10 cm^3). A white precipitate was seen to form immediately. The reaction mixture was refrigerated for 24 h, filtered and the solid dried *in vacuo*. Yield 0.43 g, 57%. (Found: C, 26.9; H, 6.6; N, 5.2. Calc. for C$_{18}$H$_{54}$N$_3$O$_{15}$P$_6$Sc: C, 27.6; H, 6.9; N, 5.4%). IR (cm^{-1}) (Nujol mull): 1361m, 1298m, 1156 (sh), 1104vs (PO), 958s, 891w, 870s, 834s, 760m, 681w, 423m, 371m, 363m and 350w. ^{31}P-$\{^1$H$\}$ NMR (300 K, MeNO$_2$): δ 64.7, 62.0 (sh) and 43.0. ^{45}Sc NMR (300 K, MeNO$_2$): δ 11.4 ($W_{1/2}$ = 450 Hz) and 5.0 ($W_{1/2}$ = 180 Hz). ^{1}H NMR (300 K, CD$_3$NO$_2$): δ 2.6 (d, $^2J_{PH}$ = 13) and 2.4 (d, $^2J_{PH}$ = 13 Hz). Λ_m (MeNO$_2$, 10^{-3} mol dm^{-3}) = 157 ohm^{-1} cm^2 mol^{-1}.

2.4.3 Complexes of yttrium nitrate with triphenylarsine oxide

[Y(Ph$_3$AsO)$_2$(EtOH)(NO$_3$)$_3$]

A solution of yttrium nitrate hexahydrate (0.38 g, 1 mmol) in boiling ethanol (10 cm^3) was added to a solution of triphenylarsine oxide (0.64 g, 2 mmol) in ethanol (15 cm^3). The solution was cooled, then refrigerated for 24 h, following which the white solid was filtered off and dried *in vacuo*. Yield 0.34 g, 37%. (Found: C, 46.8; N, 4.3; H, 3.9. Calc. for C$_{38}$H$_{36}$As$_2$N$_3$O$_{12}$Y: C, 47.3; N, 4.4; H, 3.8%). IR (cm^{-1}) (CsI disc): 3420(br), 3065w, 2989w, 1494s, 1463s, 1441s, 1323s, 1090s, 1045m, 1036m, 999m, 933s (AsO), 910s (AsO), 877m, 818m, 745s, 691s, 479s, 459m, 373s, 359s. ^{89}Y NMR (300 K): Not observed (200 K) 0.5 (br), 21.0 (w). ^{1}H NMR (300 K, CDCl$_3$): δ 7.4-7.6(m)[30H], 3.70 (quartet, J = 7)[2H] and 1.17 (t, J = 7 Hz)[3H]. Λ_m (CH$_2$Cl$_2$, 10^{-3} mol dm^{-3}) = 2 ohm^{-1} cm^2 mol^{-1}.

[Y(Ph₃AsO)₄(NO₃)₂]NO₃.Me₂CO

A boiling solution of yttrium nitrate hexahydrate (0.38 g, 1 mmol) in acetone (10 cm^3) was added to a solution of triphenylarsine oxide (0.97 g, 3 mmol) in boiling acetone (5 cm^3). The solution was refrigerated for 24 h, following which the white crystalline solid was filtered off and dried *in vacuo*. Yield 0.58 g, 35%. (Found: C, 54.3; N, 2.8; H, 3.8. Calc. for $C_{75}H_{66}As_4N_3O_{14}Y$: C, 55.3; N, 3.0; H, 4.1%). IR (cm^{-1}) (CsI disc): 3050w, 1706m, 1465s, 1441s, 1362s, 1314s, 1227w, 1186m, 1163w, 1089m, 1038w, 999w, 914br,s (AsO), 832m, 821m, 744s, 692s, 479s, 458s, 357s. ^{89}Y NMR (300 K): δ 21. ^{1}H NMR (300 K, CDCl₃): δ 7.15-7.65(m)[60H], 2.15(s)[6H]. A_m (CH₂Cl₂, 10^{-3} mol dm^{-3}) = 28 ohm^{-1} cm^2 mol^{-1}.

[Y(Me₃AsO)₆](NO₃)₃

Yttrium nitrate hexahydrate (0.19 g, 0.5 mmol) was dissolved in ice-cold ethanol (10 cm^3) and added to a solution of trimethylarsine oxide (0.41 g, 3 mmol) in ethanol (5 cm^3) with the resultant solution stirred for 1 h. Concentrated to *ca.* 10 cm^3 and refrigerated for 24 h, affording a white solid. This was filtered off and dried *in vacuo*. Yield 0.29 g, 53%. (Found: C, 19.6; N, 3.9; H, 4.9. Calc. for $C_{18}H_{54}As_6N_3O_{15}Y$: C, 19.8; N, 3.9; H, 5.0%). IR (cm^{-1}) (CsI disc): 3010w, 1642w, 1358s, 1270m, 1095m, 926s, 877vs, 836s, 650s, 353s, 288m. ^{89}Y NMR (200 K, EtNO₂/CDCl₃): δ 112, +excess Me₃AsO 133. ^{1}H NMR (300 K, CD₃NO₂): δ 2.55(s). ^{13}C{^{1}H}NMR (300 K, MeNO₂/CD₃NO₂): 15.0(s). A_m (MeNO₂, 10^{-3} mol dm^{-3}) = 180 ohm^{-1} cm^2 mol^{-1}, with excess Me₃AsO = 240.

2.4.4 Complexes of scandium nitrate with triphenylarsine oxide

[Sc(Ph₃AsO)₃(NO₃)₂]NO₃

A solution of Sc(NO₃)₃.5H₂O (0.23 g, 1 mmol) in boiling ethanol (10 cm^3) was added to a solution of triphenylarsine oxide (0.97 g, 3 mmol) in absolute ethanol (10 cm^3). The solution was stirred for 1 h, cooled then refrigerated for 24 h. The white crystalline solid formed was filtered off and dried *in vacuo*. Yield 0.50 g, 42%. (Found: C, 53.4; N, 3.3; H, 3.7. Calc. for $C_{54}H_{45}As_3N_3O_{12}Sc$: C, 54.1; N, 3.5; H, 3.8%). IR (cm^{-1}) (CsI disc): 3065w, 1521s, 1485m, 1441s, 1362s, 1298m, 1163w, 1089s, 1026m, 999m,

948w, 899br, s (AsO), 832w, 812m, 743s, 691s, 478s, 418m, 368s, 357s. ^{45}Sc NMR (300 K): δ 31.9 ($W_{1/2}$ = 5200 Hz). ^{1}H NMR (300 K, CDCl$_3$): δ 7.4-7.8(m). Λ_m (CH$_2$Cl$_2$, 10^{-3} mol dm^{-3}) = 27 ohm^{-1} cm^2 mol^{-1}.

[Sc(Ph$_3$AsO)$_2$(NO$_3$)$_3$]

A solution of Sc(NO$_3$)$_3$.5H$_2$O (0.23 g, 1 mmol) in warm acetone (10 cm^3) was added to a solution of triphenylarsine oxide (0.32 g, 1 mmol) in acetone (10 cm^3). A white solid was seen to form but redissolved. The solution was taken to dryness *in vacuo*, with the resultant residue washed with Et$_2$O (20 cm^3) then extracted with CH$_2$Cl$_2$ (10 cm^3) and filtered. The filtrate was evaporated to dryness. Yield 0.08 g. Sample not analytically pure (see results and discussion). IR (cm^{-1}) (CsI disc): 3443br*, 1636m*, 1520m, 1441m, 1357s*, 1186w, 1089m, 1027m, 999m, 898 br, s (AsO), 834w*, 813m, 743s, 692s, 479m, 413m, 365m, 284m (* attributed to Sc(NO$_3$)$_3$.nH$_2$O impurity). ^{45}Sc NMR (300 K): δ 14.0 ($W_{1/2}$ = 3500 Hz). ^{1}H NMR (300 K, CDCl$_3$): δ 7.4-7.8(m). Λ_m (CH$_2$Cl$_2$, 10^{-3} mol dm^{-3}) = 8 ohm^{-1} cm^2 mol^{-1}.

[Sc(Me$_3$AsO)$_6$](NO$_3$)$_3$

Sc(NO$_3$)$_3$.5H$_2$O (0.17 g, 0.75 mmol) was dissolved in ice-cold ethanol (10 cm^3). A solution of Me$_3$AsO (0.61 g, 4.5 mmol) in ethanol (10 cm^3) was added with the mixture stirred for 1 h. Concentration to *ca.* 10 cm^3 followed by refrigeration overnight yielded a white solid which was filtered off and dried *in vacuo*. Yield 0.18 g, 38%. (Found: C, 20.3; N, 4.6; H, 5.1. Calc. for C$_{18}$H$_{54}$As$_6$N$_3$O$_{15}$Sc: C, 20.7; N, 4.0; H, 5.2%). IR (cm^{-1}) (CsI disc): 3010w, 1648w, 1364s, 1269m, 1111m, 1048w, 925s, 873vs, 848s, 836sh, 648s, 396s, 303m. ^{45}Sc NMR (300 K, MeNO$_2$/CD$_3$NO$_2$): δ 58.0 ($W_{1/2}$ = 1200 Hz), +excess Me$_3$AsO 56.0 ($W_{1/2}$ = 80 Hz). ^{1}H NMR (300 K, CD$_3$NO$_2$): δ 2.3(s). ^{13}C-{^{1}H}NMR (300 K, MeNO$_2$/CD$_3$NO$_2$): 15.0(s). Λ_m (MeNO$_2$, 10^{-3} mol dm^{-3}) = 157 ohm^{-1} cm^2 mol^{-1}, with excess Me$_3$AsO = 220.

2.4.5 Complexes of lanthanum nitrate with tertiary arsine oxide ligands

[La(Ph₃AsO)₂(EtOH)(NO₃)₃]

A solution of $La(NO_3)_3.6H_2O$ (0.43 g, 1 mmol) in boiling ethanol (20 cm^3) was added to a solution of Ph_3AsO (0.64 g, 2 mmol) in ethanol (10 cm^3). The solution was evaporated to *ca.* 10 cm^3, cooled then refrigerated for 24 h. The white solid was filtered off then dried *in vacuo*. Yield 0.56 g, 58%. (Found: C, 45.6; N, 3.7; H, 3.5. Calc. for $C_{38}H_{36}As_2LaN_3O_{12}$: C, 45.0; N, 4.1; H, 3.6%). IR (cm^{-1}) (CsI disc): 3400 (br), 1477s, 1307s, 1186w, 1089s, 1032m, 999m, 908s, 888s (AsO), 820m, 743s, 691s, 478s, 457m, 368s, 361s. ^{1}H NMR (300 K, CDCl$_3$): δ 7.3-7.8m[30H], 3.70 (quartet, J = 7)[2H] and 1.20 (t, J = 7 Hz)[3H]. Λ_m (CH$_2$Cl$_2$, 10^{-3} mol dm^{-3}) = 4.0 ohm^{-1} cm^2 mol^{-1}.

[La(Ph₃AsO)₃(NO₃)₃].Me₂CO

A solution of lanthanum nitrate hexahydrate (0.22 g, 0.5 mmol) in boiling acetone (10 cm^3) was added to a solution of triphenylarsine oxide (0.48 g, 1.5 mmol) in acetone (10 cm^3). The solution was evaporated to *ca.* 10 cm^3, cooled then refrigerated for 24 h. The colourless crystalline solid was filtered off, then dried *in vacuo*. Yield 0.55 g, 85%. (Found: C, 50.4; N, 2.6; H, 3.7. Calc. for $C_{57}H_{51}As_3La$ N_3O_{13}: C, 50.7; N, 3.1; H, 3.8%). IR (cm^{-1}) (CsI disc): 3054w, 1702w, 1486s, 1454s, 1442s, 1363s, 1304s, 1226w, 1185w, 1163w, 1089m, 1070w, 1033m, 999w, 924w, 890s (AsO), 821m, 747s, 693s, 533m, 478s, 359s. ^{1}H NMR (300 K, CDCl$_3$): δ 7.20-7.65(m)[45H], 2.15(s)[6H]. Λ_m (CH$_2$Cl$_2$, 10^{-3} mol dm^{-3}) = 4 ohm^{-1} cm^2 mol^{-1}.

[La(Ph₃AsO)₄(NO₃)₂]NO₃.Me₂CO

A solution of $La(NO_3)_3.6H_2O$ (0.43 g, 1.0 mmol) in boiling acetone (10 cm^3) was added to a solution of Ph_3AsO (1.9 g, 6.0 mmol) in acetone (30 cm^3). The mixture was left to stand at room temperature for 24 h producing colourless crystals which were filtered off then dried *in vacuo*. Yield 1.23 g, 73%. (Found: C, 53.2; N, 2.5; H, 4.2. Calc. for $C_{75}H_{66}As_4LaN_3O_{14}$: C, 53.6; N, 2.6; H, 3.8%). IR (cm^{-1}) (CsI disc): 3059w, 1707m, 1442s, 1361s, 1313s, 1228m, 1189m, 1089s, 1050w, 1036w, 999m, 925sh, 891s (AsO), 836w, 820m, 746s, 693s, 614w, 479s, 366s. ^{1}H NMR (300 K, CDCl$_3$): δ 7.2-7.7(m) [60H], 2.15(s)[6H]. Λ_m (CH$_2$Cl$_2$, 10^{-3} mol dm^{-3}) = 21 ohm^{-1} cm^2 mol^{-1}.

[La(Me₃AsO)₆](NO₃)₃

Lanthanum nitrate hexahydrate (0.43 g, 1.0 mmol) was dissolved in acetone (10 cm^3) and added to a solution of trimethylarsine oxide (0.27 g, 2.0 mmol) in acetone (10 cm^3). Refrigeration for 24 h afforded a white solid which was filtered off and dried *in vacuo*. Yield 0.21 g, 55%. (Found: C, 19.2; N, 4.2; H, 4.9. Calc. for $C_{18}H_{54}As_6LaN_3O_{15}$: C, 19.0; N, 3.7; H, 4.8%). IR (cm^{-1}) (CsI disc): 2936w, 1653w, 1359s, 1269w, 1091m, 987w, 924s, 864vs, 847s, 836sh, 647s, 317s, 279m. ^{1}H NMR (300 K, CD₃NO₂): δ 2.3(s). ^{13}C-{^{1}H}NMR (200 K, EtNO₂/CD₃NO₂): 15.0(s). A_m (MeNO₂, 10^{-3} mol dm^{-3}) = 121 ohm^{-1} cm^2 mol^{-1}, with excess Me₃AsO = 285.

[La(Me₃AsO)₂(H₂O)(NO₃)₃]

Boiling ethanolic solutions of La(NO₃)₃.6H₂O (0.43 g, 1.0 mmol) and Me₃AsO (0.27 g, 2.0 mmol) were added together and stirred for 1 h. Refrigeration overnight saw precipitation of a white solid which was filtered off and dried *in vacuo*. Yield 0.12 g, 20%. (Found: C, 12.4; N, 6.4; H, 3.6. Calc. for $C_6H_{20}O_{12}As_2N_3La$: C, 11.7; N, 6.8; H, 3.3%). IR (cm^{-1}) (CsI disc): 3400br, 3095w, 1620m, 1455m, 1407m, 1358m, 1322w, 1287s, 1266w, 1040m, 924m, 875s, 860s, 850m, 822w, 736m, 644m, 595w, 323s, 285sh. ^{1}H NMR (300 K, CD₃NO₂): δ 2.2(s)[18H], 2.6(s)[2H]. A_m (CH₂Cl₂, 10^{-3} mol dm^{-3}) = 4 ohm^{-1} cm^2 mol^{-1}.

2.4.6 Crystallographic studies

Details of the crystallographic data collection and refinement parameters are given in Table 2.19.

[Y(Ph₃PO)₂(EtOH)(NO₃)₃]

Plate-like crystals were grown by slow evaporation of a concentrated solution of the complex, with data collected on the Nonius CCD diffractometer at 150 K. The structure was solved using DIRDIF,[32] with the data refined[33] on *F* with isotropic atomic displacement parameters (adp's) for the C and N atoms, owing to the small amount of observed data. Hydrogen atoms were placed in calculated positions for phenyl groups.

$[Y(Ph_3PO)_3(NO_3)_3].xCH_2Cl_2$ and $[Y(Ph_3PO)_3(NO_3)_3]$

Both sets of crystals were grown by vapour diffusion of Et_2O into a solution of the compound in CH_2Cl_2 in a freezer, resulting in colourless plate-like crystals. The non-solvated crystal gave weaker data, so the discussion and comparisons in the text refer to the solvated example. CH_2Cl_2 molecules became apparent during the later stages of refinement, and were included in the model with a refined population. H atoms were included in the final model in calculated positions (d(C-H) = 0.95 Å), significantly improving the fit to the data. Refinement on F^2 was conducted using SHELXL 97^{34} with Y, N, O and P atoms anisotropic, and C, H and Cl atoms isotropic.

$[Y(Ph_2MePO)_3(NO_3)_3]$

Small colourless needle crystals were grown by vapour diffusion of Et_2O into a solution of the complex in CH_2Cl_2, with the crystallising cell placed in a freezer. Data was collected using a Nonius CCD diffractometer at 150 K. Full-matrix least squares refinement on F was carried out in TEXSAN.^{33} Many plausible H atoms were seen in the Fourier difference synthesis and all were included in calculated positions (d(C-H) = 0.95 Å). All non-H atoms were treated as anisotropic.

$[Y(Me_3PO)_3(NO_3)_3]$

Several large, colourless crystals were grown by vapour diffusion of Et_2O into a solution of the compound in CH_2Cl_2 at room temperature. During refinement, some C atoms were seen to become non-positive definite when anisotropic and hence, all C atoms were retained with isotropic adp values. No H atoms were introduced as a result. The space group $P\bar{1}$ (no. 2) with $Z = 4$ initially caused concern but the Niggli cell did not indicate missed symmetry and whilst the coordinates of the two Y atoms of the asymmetric unit look to be related, this did not extend to the other atoms and hence, no smaller cell was identified.

$[Sc(Ph_3PO)_2(NO_3)_3]$

The crystal used was isolated during the preparation of the compound, following refrigeration of the reaction mixture. Later electron-density maps identified some

phenyl H atoms, with no solvate groups shown. H atoms were introduced in calculated positions (d(C-H) = 0.95 Å) and full matrix least-squares refinement[34] was carried out on F^2. The absolute configuration of the selected crystal was established (Flack parameter[35] 0.01(9)).

[Sc(Ph₂MePO)₄(NO₃)₂]NO₃·xCH₂Cl₂

Crystals were grown by vapour diffusion of light petroleum (bp 40-60 °C) into a solution of the complex in CH_2Cl_2. The solvate molecules were first seen in the later electron-density maps but gave large U values. The population of CH_2Cl_2 was adjusted to give Cl atom adp values similar to those of Sc and P atoms. Phenyl H atoms were added in calculated positions (d(C-H) = 0.95 Å) and full-matrix least-squares refinement was carried out[34] on F^2. The largest peaks in the residual electron density were close to Cl atoms.

[Y(Ph₃AsO)₄(NO₃)₂]NO₃·1/2H₂O

Vapour diffusion of diethyl ether into a CH_2Cl_2 solution of the compound (cell held in refrigerator) yielded small, colourless block crystals. Data was collected using a Nonius CCD diffractometer at 150 K. Refinement was carried out using the TEXSAN package.[33] All non-H atoms were refined anisotropically. The anions are described as one disordered group with the N located on a centre of symmetry and a second general (two-fold) NO_3 with a site occupation of 0.5.

[Y(Me₃AsO)₆](NO₃)₃·H₂O

Small crystals were grown by vapour diffusion of Et_2O into a nitromethane solution of the complex. Data was collected on the CCD diffractometer and solved using SHELXL 97.[34] The space group is described as Pn rather than the centrosymmetric space group $P2/n$. Attempts to solve the structure in $P2/n$ yielded unsatisfactory results, and the coordinates could not be transformed. Refinement was as a racemic twin. Restraints were applied to two of the three nitrate groups (N-O and O···O).

[Sc(NO₃)₂(Ph₃AsO)₃]NO₃.H₂O

$[Sc(NO_3)_2(Ph_3AsO)_3]NO_3.H_2O$

Crystals were grown by vapour diffusion of Et₂O into a solution of the complex in CH₂Cl₂. Data was collected using the Nonius CCD diffractometer at 150K. Refinement on F was conducted using SHELXL 97.[34] All non-hydrogen atoms were refined anisotropically, with all hydrogen atoms added in calculated positions, except for the OH⁻ hydrogen which was not observed. Refinement of the occupancy of the solvated anions NO₃⁻ and OH⁻ showed each to have occupancy of a half, hence leaving the charges of the metallic cationic species balanced.

$[Sc(Me_3AsO)_6](NO_3)_3$

Small crystals were formed by vapour diffusion of diethyl ether into a nitromethane solution of the compound (sealed container in a freezer at *ca.* -15°C). Refinement in TEXSAN[33] was straightforward.

$[La(Ph_3AsO)_2(NO_3)_3(EtOH)]$

The crystal used was obtained by vapour diffusion of Et₂O into a solution of the complex in CH₂Cl₂. Data was collected using a Rigaku AFC7S diffractometer at 150 K. The structure was solved using DIRDIF[32] and the data refined[33] on F. All non-H atoms were refined anisotropically.

$[La(Ph_3AsO)_4(NO_3)_2]NO_3.2Me_2CO$

Colourless block crystals were isolated from the synthesis. Data was collected on the Nonius CCD diffractometer. Refinement using SHELXL 97[34] was routine, with two solvate molecules appearing in the later stages of refinement. All non-hydrogen atoms were refined anisotropically.

Table 2.19 Crystallographic data collection and refinement parameters

	[Y(Ph₃PO)₂(EtOH)(NO₃)₃]	[Y(Ph₃PO)₃(NO₃)₃].xCH₂Cl₂ᵉ	[Y(Ph₃PO)₃(NO₃)₃]	[Y(Ph₂MePO)₃(NO₃)₃]	[Y(Me₃PO)₃(NO₃)₃]
Formula	$C_{38}H_{36}N_3O_{12}P_2Y$	$C_{54}H_{45}N_3O_{12}P_3Y + xCH_2Cl_2$	$C_{54}H_{45}N_3O_{12}P_3Y$	$C_{39}H_{39}N_3O_{12}P_3Y$	$C_9H_{27}N_3O_{12}P_3Y$
Formula weight	877.57	1109.79 + x84.93ᵉ	1109.79	923.58	551.15
Crystal system	Monoclinic	Monoclinic	Monoclinic	Monoclinic	Triclinic
Space group	$P2_1/n$ (No. 14)	$P2_1/n$ (No. 14)	$P2_1/c$ (No. 14)	$P2_1/n$ (No. 14)	$P\bar{1}$ (No. 2)
a / Å	16.975(2)	11.118(2)	11.170(6)	20.111(1)	14.578(10)
b / Å	10.745(2)	19.342(3)	11.411(4)	10.8636(4)	15.394(23)
c / Å	22.024(3)	27.244(3)	41.504(6)	20.648(1)	10.567(22)
α / °	90	90	90	90	99.99(14)
β / °	105.877(8)	94.57(2)	93.48(3)	106.830(2)	93.03(11)
γ / °	90	90	90	90	96.91(9)
U / ų	3863.8(9)	5839.8(16)	5280.3(3.5)	4318.0(4)	2312.0(6.2)
Z	4	4	4	4	4
μ(Mo-K$_\alpha$) / cm⁻¹	16.61	13.1ᵉ	12.61	15.26	27.94
No. of unique reflections	6286	10255	9809	8832	8145
No. of obs. reflections ᵃ	1765	10255	2941	4609	5513
No. of parameters/restraints	300/0	409/0	356/0	523/0	415/0
R ᵇ	0.097	0.0656	0.087	0.0623	0.060
wR_2 ᶜ	-	0.2206	-	-	-
wR ᵈ	0.095	-	0.095	0.0422	0.062

ᵃ Observed if $[I_o > 2\sigma(I_o)]$ ᵇ $R = \sum (|F_{obsi}| - |F_{calci}|) / \sum |F_{obsi}|$ ᶜ $wR_2 = [\sum w(F_{obs}^2 - F_{calc}^2)^2 / \sum w(F_{obs}^2)^2]^{1/2}$ ᵈ $wR = \sqrt{[\sum w_i(|F_{obsi}| - |F_{calci}|)^2 / \sum w_i|F_{obsi}|^2}$ ᵉ $x = 1.78$

Table 2.19 (cont.) Crystallographic data collection and refinement parameters

	$[Sc(Ph_3PO)_2(NO_3)_3]$	$[Sc(Ph_2MePO)_4(NO_3)_2]NO_3.xCH_2Cl_2$	$[Y(Ph_3AsO)_4(NO_3)_2]NO_3.1/2H_2O$	$[Y(Me_3AsO)_6](NO_3)_3.H_2O$
Formula	$C_{36}H_{30}N_3O_{11}P_2Sc$	$C_{52}H_{52}N_3O_{13}P_4Sc.xCH_2Cl_2$ ($x = 1.3$)	$C_{72}H_{61}As_4N_3O_{13.5}Y$	$C_{18}H_{56}As_6N_3O_{16}Y$
Formula weight	787.53	$1095.85 + x84.93$	1572.83	1109.10
Crystal system	Monoclinic	Monoclinic	Triclinic	Monoclinic
Space group	Pn (No. 7)	$P2_1/n$ (No. 14)	$P\bar{1}$ (No. 2)	Pn (No. 7)
a / Å	10.249(5)	13.712(5)	13.2731(2)	11.1136(5)
b / Å	10.628(4)	23.412(4)	14.4205(2)	11.4594(5)
c / Å	17.289(5)	18.650(4)	20.1717(5)	15.9320(9)
α / °	90	90	104.293(7)	90
β / °	100.76(3)	98.40(2)	96.302(9)	91.088(2)
γ / °	90	90	112.06(1)	90
U / Å^3	1850.0(12)	5922.9(2.9)	3378.2(1)	2028.7(2)
Z	2	4	2	2
μ(Mo-K$_\alpha$) / cm^{-1}	3.49	4.1 ($x = 1.3$)	28.74	63.45
No. of unique reflections	2704	10398	11685	6448
R_{int}	0.200	0.088	0.064	0.088
No. of obs. reflections [a]	2704	10398	9012	4413
No. of parameters/restraints	284/2	428/0	832/6	244/14
R [b]	0.0515	0.0846	0.057	0.064
wR_2 [c]	0.1546	0.3322	0.158	0.161
wR [d]	-	-	-	-

[a] Observed if $[I_o > 2\sigma(I_o)]$ [b] $R = \sum (|F_{obs}|_i - |F_{calc}|_i) / \sum |F_{obs}|_i$ [c] $wR_2 = [\sum w(F_{obs}^2 - F_{calc}^2)^2 / \sum w(F_{obs}^2)^2]^{1/2}$ [d] $wR = \sqrt{[\sum w_i(|F_{obs}|_i - |F_{calc}|_i)^2 / \sum w_i |F_{obs}|_i^2}$

Table 2.19 (cont.) Crystallographic data collection and refinement parameters

	$[Sc(Ph_3AsO)_3(NO_3)_2]NO_3.H_2O$	$[Sc(Me_3AsO)_6](NO_3)_3$	$[La(Ph_3AsO)_2(EtOH)(NO_3)_3]$	$[La(Ph_3AsO)_4(NO_3)_2]NO_3,2Me_2CO$
Formula	$C_{54}H_{47}As_3N_3O_{13}Sc$	$C_{18}H_{54}As_6N_3O_{15}Sc$	$C_{38}H_{36}As_2LaN_3O_{12}$	$C_{78}H_{72}As_4LaN_3O_{15}$
Formula weight	1215.67	1047.12	1015.45	1730.03
Crystal system	Triclinic	Monoclinic	Monoclinic	Triclinic
Space group	$P\bar{1}$ (No. 2)	$P2_1/n$ (No. 14)	$P2_1/n$ (No. 14)	$P\bar{1}$ (No. 2)
a / Å	10.9069(2)	10.9800(4)	17.239(3)	14.8068(1)
b / Å	12.7505(4)	11.2665(4)	10.904(2)	15.6295(1)
c / Å	22.2281(7)	15.7688(7)	21.907(4)	18.3401(1)
α / °	84.792(2)	90	90	65.9821(6)
β / °	81.577(2)	90.833(2)	104.32(2)	80.3764(5)
γ / °	73.000(1)	90	90	86.7683(4)
U / Å^3	2920.5(1)	1950.5(1)	3990.0(12)	3821.96(5)
Z	2	2	4	2
μ(Mo-K$_\alpha$) / cm^{-1}	18.73	52.98	27.82	63.45
No. unique reflections	10179	3421	6940	17165
R_{int}	0.038	0.085	0.099	0.079
No. of obs. reflections [a]	6562	2040	5347	10440
No. parameter/restraints	642/0	126/13	506/0	910/0
R [b]	0.066	0.091	0.081	0.056
wR_2 [c]	0.220	0.275	0.271	0.209
wR [d]	-	-	-	0.063

[a] Observed if $[I_o > 2\sigma(I_o)]$ [b] $R = \sum (|F_{obs}|_i - |F_{calc}|_i) / \sum |F_{obs}|_i$ [c] $wR_2 = [\sum w(F_{obs}^2 - F_{calc}^2)^2/\sum w(F_{obs}^2)^2]^{1/2}$ [d] $wR = \sqrt{[\sum w_i(|F_{obs}|_i - |F_{calc}|_i)^2 / \sum w_i|F_{obs}|_i^2}$ [e] Observed if $[I_o > 4\sigma(I_o)]$

2.5 References

1. F. A. Hart in *Comprehensive Coordination Chemistry I*, Eds. G. Wilkinson, R. D. Gillard and J. A. McCleverty, Volume 3, Pergamon Press, Oxford, 1987, p 1068.

2. D. R. Cousins and F. A. Hart, *J. Inorg. Nucl. Chem.*, 1967, **29**, 1745.

3. G. Valle, G. Casotto, P. L. Zanonato and B. Zarli, *Polyhedron*, 1986, **5**, 2093.

4. V. K. Belsky, *J. Organomet. Chem.*, 1981, **213**, 435.

5. L. R. Melby, N. J. Rose, E. Abramson and J. C. Carris, *J. Am. Chem. Soc.*, 1964, **86**, 5117.

6. D. R. Cousins and F. A. Hart, *J. Inorg. Nucl. Chem.*, 1967, **29**, 2965.

7. D. R. Cousins and F. A. Hart, *J. Inorg. Nucl. Chem.*, 1968, **30**, 3009.

8. T. S. Lobana in *The Chemistry of Organophosphorus Compounds*, Ed. F. R. Hartley, Wiley, New York, 1992, Volume 2, p. 409.

9. R. K. Harris and B. E. Mann, *NMR and the Periodic Table*, Academic Press, London, 1978.

10. Z. Pikramenou, *Coord. Chem. Rev.*, 1997, **164**, 189.

11. C. E. Housecroft, *Coord. Chem. Rev.*, 1995, **138**, 27.

12. A. M. G. Massabni, M. L. R. Gibran and O. A. Serra, *Inorg. Nucl. Chem. Lett.*, 1978, **14**, 419.

13. W. Levason, E. H. Newman and M. Webster, Unpublished work.

14. N. P. Crawford and G. Melson, *J. Chem. Soc. A*, 1969, 1049.

15. F. Kutek and B. Durek, *Collect. Czech. Chem. Commun.*, 1970, **35**, 3768.

16. C. M. Mikulski, N. M. Karayannis and L. L. Pytlewski, *J. Less Common Metals*, 1977, **51**, 201.

17. H. Chunhui, L. Genbei, Z. Yongfen, J. Tianzhu and X. Guangxian, *Beijing Dax. Xue., Zir. Kex.*, 1985, 12 (*Chem. Abstr.*, 1987, **106**, 167758x).

18. J. Sakamoto and C. Miyake, *Kidouri* (Rare Earths), 1993, **22**, 154 (*Chem. Abstr.*, 1995, **122**, 278608y).

19. S. D. Ross, *Inorganic Infrared and Raman Spectra*, McGraw Hill, London, 1972, Chapter 4.

20. K. Nakamoto, *Infrared Spectra of Inorganic and Coordination Compounds*, 2nd Edition, Wiley, London, 1970, p171.

21. W. J. Geary, *Coord. Chem. Rev.*,1971, 7, 81.

22. N. N. Greenwood and A. Earnshaw, *Chemistry of the Elements*, Pergamon, Oxford, 1984, p541.

23. F. A. Cotton, G. Wilkinson and P. L. Gaus, *Basic Inorganic Chemistry*, 3rd Edition, Wiley, London, 1995.

24. F. Nief, *Coord. Chem. Rev.*, 1998, **178-180**, 13.

25. N. J. Hill, L.-S. Leung, W. Levason, M. Webster, *Inorg. Chim. Acta.*, 2003, **343**, 90.

26. D.-L. Long, H.-M. Hu, J.-T. Chen, J.-S. Huang, *Acta Crystallogr. Sect. C*, 1999, **55**, 1662.

27. R. R. Carlson, D. W. Meek, *Inorg. Chem.*, 1974, **13**, 1741.

28. R. S. Armstrong, M. J. Aroney, R. J. W. LeFevre, R. K. Pierens, J. D. Saxby, C. J. Wilkins, *J. Chem. Soc.*, 1969, 2735.

29. R. R. Ryan, E. M. Larson, G. F. Payne, J. R. Peterson, *Inorg. Chim. Acta.*, 1987, **131**, 267.

30. U. Cassellato, R. Graziani, U. Russo, B. Zarli, *Inorg. Chim. Acta*, 1989, **166**, 9.

31. A. Merijanian, R. A. Zingaro, *Inorg. Chem.*, 1966, 5, 187.

32. P. T. Beurskens, G. Admiraal, G. Beurskens, W. P. Bosman, S. Garcia-Granda, R. O. Gould, J. M. M. Smits and C. Smykalla, The DIRDIF program system, University of Nijmegen, 1992.

33. TEXSAN, Single crystal structure analysis software, Version 1.7-1, Molecular Structure Corporation, The Woodlands, TX, 1995.

34. G. M. Sheldrick, SHELXL 97, Crystal structure refinement program, University of Göttingen, 1997.

35. H. D. Flack, *Acta Crystallogr., Sect. A*, 1983, **39**, 876.

Chapter 3

Complexes of Yttrium Halides with Tertiary Phosphine and Arsine Oxide Ligands

3.1 Introduction

The first lanthanide–phosphine oxide complex, $[EuCl_3(Ph_3PO)_3]$, was reported in 1964,[1] prompting numerous investigations probing similar systems with the other lanthanide elements.[2-5] For example, Hart *et al.* synthesised $[MCl_3(Ph_3PO)_3]$ (M = Nd, Sm) by reaction of $MCl_3.nH_2O$ with three molar equivalents Ph_3PO in ethanol.[4] In addition, the synthesis of '$[MCl_3(Ph_3PO)_4].EtOH$' (M= Sm, Nd) is described using a 6:1 molar ratio of ligand to metal, suggesting seven-coordinate metal centres.[4] Whilst yttrium is not literally a lanthanide metal, its properties are similar, and often investigations into the lanthanide elements also include the Group III ion.[2-4] However, very little study has been conducted examining yttrium halide complexes of R_3EO ligands (E = As or P). Reviews report that lanthanide halides form compounds of the type $[M(Ph_3PO)_nCl_3]$ (n = 3 or 4), being non-conductors in solution and implying six or seven coordinate metal centres.[6,7] However, closer inspection of the original sources reveals that often several lanthanide metals have been examined with the results taken as representative of the entire series and often yttrium.[4,5,8] Actual data on yttrium halide compounds is sparse, with no complexes structurally characterised and no examinations of behaviour in solution.[9]

Yttrium halide complexes have been reported with a range of coordinated solvents. For example, the polymeric THF complex $[YCl_3(THF)_2]_\infty$ has been structurally characterised.[10]
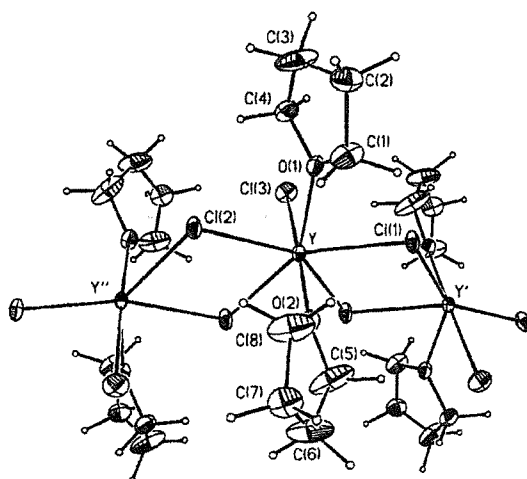
Fig. 3.1 View of the polymeric THF complex $[YCl_3(THF)_2]_\infty$.[10]

Investigations of compounds of polyalcohols with YCl_3 have also been published.[11] For example, the complex $[Y\{(OHCH_2)_3CN(CH_2CH_2OH)_2\}Cl_2(MeOH)]Cl$ was synthesised (Fig. 3.2).[11] The molecular adduct $[YCl_3(H_2O)_2(MeCN)_2]$ was isolated by treatment of yttrium chloride with thionyl chloride in acetonitrile solution. The geometry around the seven-coordinate yttrium centre was pentagonal bipyramidal.[12]
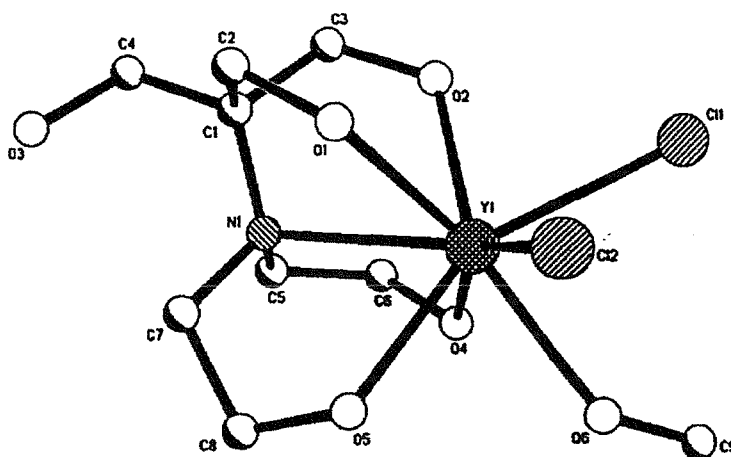
Fig. 3.2 View of the cation $[Y\{(OHCH_2)_3CN(CH_2CH_2OH)_2\}Cl_2(MeOH)]^+$.[11]

Complexes demonstrating nitrogen donor ligands coordinating to yttrium halides have been reported, a simple example being the pyridine compound $[YCl_3(py)_4]$ for which the structure has been determined, revealing a seven coordinate metal centre.[13] Amine complexes have also been investigated. For example, the compound $[YI(N,N'-bis(4-antipyrylmethylidene)ethylenediamine)_3]I_2$ has been isolated (Fig. 3.3).[14] Complexes of $YX_3.nH_2O$ (X = Cl, Br or I) with 2,2'-bipyridine N,N'-dioxide are known, whilst several other investigations into complexes with Schiff bases have been conducted.[15,16]
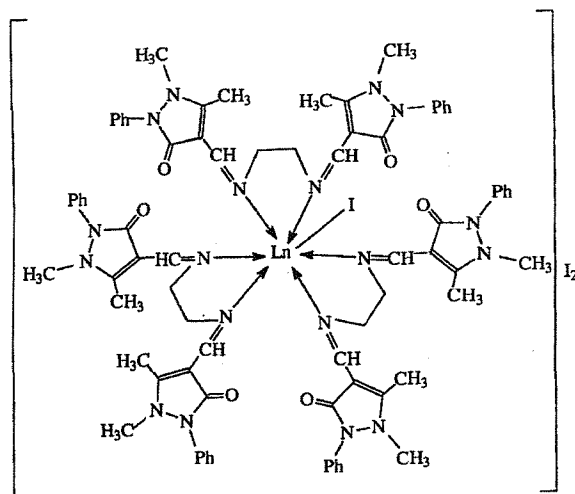
Fig. 3.3 Proposed structure of the complex compound [YI(N,N'-bis(4-antipyrylmethylidene)ethylenediamine)$_3$]I$_2$ (Ln = Y).[14]

In this study, the primary aim was to develop a thorough picture of how yttrium halides interact with R$_3$EO ligands. Previous studies examining reactions of lanthanide chlorides had not looked at YCl$_3$.6H$_2$O in any depth so this study also aimed to fill this void. No previous compounds of this type had been structurally characterised and no investigations of behaviour in solution had been conducted. Results would allow further comparison of the ligating power of R$_3$PO and R$_3$AsO, whilst also giving information on the relative affinity of yttrium for the different halides and nitrate groups (by comparison with previous results). The coordination chemistry should vary significantly from that of yttrium nitrate given the monodentate nature of the halides.

3.2 Results and Discussion

3.2.1 Complexes of yttrium halides with triphenylphosphine oxide

Reaction of yttrium chloride hexahydrate with four molar equivalents of Ph_3PO in ice-cold ethanol yielded white $[YCl_2(Ph_3PO)_4]Cl$. If the same reaction was carried out in the presence of NH_4PF_6, the product was $[YCl_2(Ph_3PO)_4]PF_6$. Products of the type $[YX_2(Ph_3PO)_4]Z$ (X = Br or I, Z = X or PF_6) were isolated from analogous reactions using $YBr_3.6H_2O$ or $YI_3.8H_2O$, the iodo-complexes appearing pale yellow in colour. Whilst the isolated chloro- and bromo-complexes were air and moisture stable, the iodo-complexes darken in colour after exposure to air, probably due to liberation of diiodine. No reaction was observed for $YF_3.1/2H_2O$ with Ph_3PO, even after extended reaction times. When $[YCl_2(Ph_3PO)_4]^+$ was mixed with Ph_3PO in anhydrous CH_2Cl_2 in the presence of two molar equivalents $SbCl_5$, $[YCl(Ph_3PO)_5][SbCl_6]_2$ was formed. Further addition of antimony pentachloride in the presence of excess ligand failed to form a hexakis(phosphine oxide) product. Even when a lower Ph_3PO : Y ratio was used, no tris(phosphine oxide) compounds could be isolated in the solid state although evidence for $[YX_3(Ph_3PO)_3]$ was found in solution.

The infrared spectrum of $[YCl_2(Ph_3PO)_4]Cl$ exhibited $v(PO)$ as a very strong band at 1150 cm^{-1}. The spectrum of $[YCl_2(Ph_3PO)_4]PF_6$ was similar, with the anion apparent by characteristic v_3 (v(P-F)) and v_4 ($\delta(PF_2)$) PF_6^- vibrations at 839 and 559 cm^{-1}.[17] The $v(PO)$ was observed at 1140 cm^{-1} for $[YBr_2(Ph_3PO)_4]Br$, the hexafluorophosphate complex having $v(PO)$ = 1147 cm^{-1}. $[YI_2(Ph_3PO)_4]I$ showed $v(PO)$ = 1136 cm^{-1} whilst $[YI_2(Ph_3PO)_4]PF_6$ had $v(PO)$ = 1144 cm^{-1}. The $v(PO)$ band moves to higher frequency along the halide series I → Br → Cl, as the strength of the (M)-O-P bond increases. This effect is caused by more electropositivity concentrated on the metal centre with increasing electronegativity of the halide. The spectrum of $[YCl(Ph_3PO)_5][SbCl_6]_2$ had $v(PO)$ = 1141 cm^{-1}, noticeably lower than for $[YCl_2(Ph_3PO)_4]Cl$ ($v(PO)$ = 1150 cm^{-1}). A characteristic strong band at 347 cm^{-1} identified $[SbCl_6]^-$.[18]

The ^{31}P-$\{^1H\}$ NMR spectrum of $[YCl_2(Ph_3PO)_4]Cl$ in dichloromethane showed three resonances at δ 36.0, 34.5 and 27.0 ppm ('free' ligand), with the two former peaks

resolved as doublets due to coupling with ^{89}Y $(^2J(^{31}P\text{-}^{89}Y) = 12$ Hz). Addition of excess ligand saw the peak at 34.5 disappear, suggesting this was attributable to [YCl₃(Ph₃PO)₃], with the peak at 36.0 caused by the tetrakis(phosphine oxide) species. No ^{89}Y NMR spectrum was observed at ambient temperature (a feature common to all the $[YX_2(Ph_3PO)_4]^+$ compounds reported here). Cooling the solution to 200 K showed two multiplets, a quintet at δ 192 ppm (with intensities agreeing with the theoretical 1:4:6:4:1 binomial pattern) corresponding to [YCl₂(Ph₃PO)₄]Cl (Fig. 3.4) and a quartet at δ 242 ppm. Following addition of Ph₃PO, the latter disappeared, leading to its assignment as *fac*-[YCl₃(Ph₃PO)₃]. The multinuclear NMR spectra for [YCl₂(Ph₃PO)₄]PF₆ were similar except for a binomial septet present at δ -145 ppm in the $^{31}P\text{-}\{^1H\}$ NMR spectrum, characteristic of the hexafluorophosphate counter-ion. When two molar equivalents of triphenylphosphine oxide were added to this solution, weak features appeared in the $^{31}P\text{-}\{^1H\}$ NMR spectrum at δ 37.5 and 40.0 ppm, which when compared to data obtained from isolated [YCl(Ph₃PO)₅][SbCl₆]₂ (see Table 3.3), can be assigned as the pentakis(phosphine oxide) cation, suggesting a competitive equilibrium exists between Cl⁻ and Ph₃PO for coordination to the Y centre. The molar conductance of 10^{-3} mol dm⁻³ solutions of [YCl₂(Ph₃PO)₄]Z (Z = Cl or PF₆) in dichloromethane were consistent with 1 : 1 electrolytes.
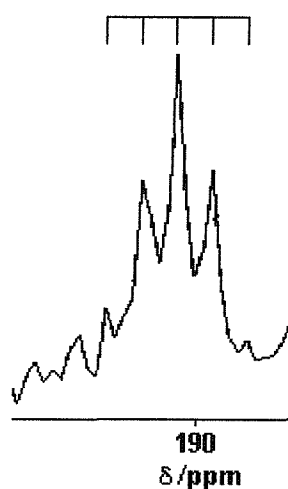
Fig. 3.4 The ^{89}Y NMR spectrum of *trans*-[YCl₂(Ph₃PO)₄]Cl, showing a quintet at δ 192 ppm.

The X-ray structure of $[YCl_2(Ph_3PO)_4]Cl.2.5EtOH.H_2O$ (Fig. 3.5), shows an octahedral geometry around the metal centre, with *trans* chlorides. The angles at Y are close to the idealized values. The Y-O distances are very similar to those observed for $[YBr_2(Ph_3PO)_4]PF_6$ (Table 3.2), whilst the Y-O-P angles are larger than observed for $[Y(Me_3PO)_6]Br_3$ (Y-O-P (ave.) = 171.0 c.f. 147.8°). Selected bond lengths and angles are given in Table 3.1.
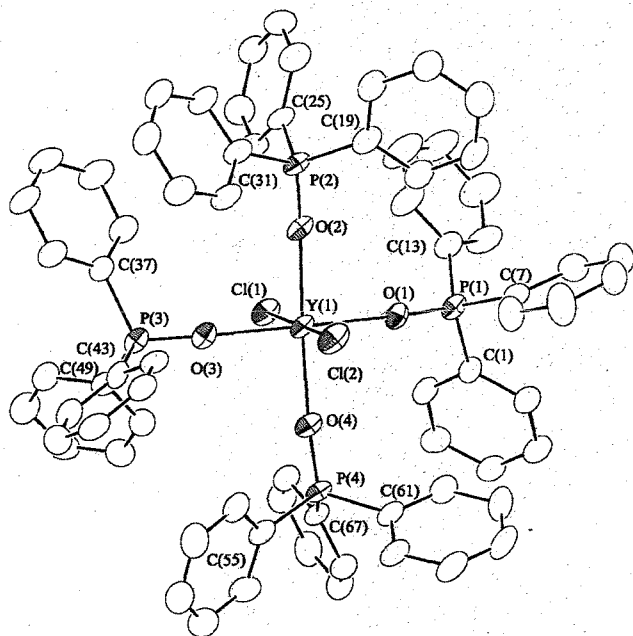
Fig. 3.5 The structure of the cation in $[YCl_2(Ph_3PO)_4]Cl.2.5EtOH.H_2O$. H atoms are omitted for clarity. Ellipsoids are drawn at 40% probability.

Table 3.1 Selected bond lengths (Å) and angles (°) for the structure of $[YCl_2(Ph_3PO)_4]Cl.2.5EtOH.H_2O$.

Y-O(1)	2.225(7)	Y-O(3)	2.231(7)
Y-O(2)	2.220(7)	Y-O(4)	2.230(7)
O(n)-P(n)	1.509(7)-1.514(8)	P-C	1.764(12)-1.809(12)
Y-Cl(1)	2.620(3)	Y-Cl(2)	2.616(3)
O(1)-Y-O(2)	87.9(3)	O(2)-Y-O(3)	91.9(3)
O(1)-Y-O(3)	174.2(3)	O(2)-Y-O(4)	177.1(3)
O(1)-Y-O(4)	90.2(3)	O(3)-Y-O(4)	90.1(3)
Cl(1)-Y-Cl(2)	177.03(10)	Y-O(1)-P(1)	167.5(5)
Y-O(2)-P(2)	172.4(5)	Y-O(3)-P(3)	170.1(5)
Y-O(4)-P(4)	174.0(5)		

The ^{31}P-$\{^1$H$\}$ NMR spectrum of [YCl(Ph$_3$PO)$_5$][SbCl$_6$]$_2$ in dichloromethane contained two doublets at δ 37.5 and 40.0 ppm ($^2J(^{31}$P-^{89}Y) = 10 and 11 Hz respectively), the ratio of integrals being 4 : 1, corresponding to the two different phosphorous environments in the octahedral cation. The corresponding ^{89}Y NMR spectrum at 200 K exhibited a sextet at δ 179 ppm. A doublet of quintets is predicted from theory, but, owing to the similar ^{89}Y-^{31}P couplings of the axial and equatorial phosphine oxides and ill-defined outer lines, an apparent 'sextet' was observed.

Addition of an excess of SbCl$_5$ to the above solution (in an attempt to produce a hexakis(phosphine oxide) species) caused decomposition, with multiple resonances in the ^{31}P-$\{^1$H$\}$ NMR spectrum appearing. One peak at δ 47.0 ppm was attributed to [SbCl$_5$(Ph$_3$PO)], agreeing with the literature value for this complex.[19] This was confirmed by running the ^{31}P-$\{^1$H$\}$ NMR spectrum of a solution of Ph$_3$PO and SbCl$_5$ in dry DCM (revealing the same resonance).

The ^{31}P-$\{^1$H$\}$ NMR spectrum of [YBr$_2$(Ph$_3$PO)$_4$]Br contained a doublet at δ 36.5 ppm ($^2J(^{31}$P-^{89}Y) = 11 Hz), along with a weak resonance at 35.5 ppm. Cooling the solution to 200 K saw the weak feature resolved into a doublet. Addition of Ph$_3$PO removed the peak at 35.5 ppm, suggesting it could be due to [YBr$_3$(Ph$_3$PO)$_3$]. The ^{89}Y NMR spectrum of the solution at 200 K, prior to addition of excess ligand, exhibited a binomial quintet at δ 220 ppm, caused by coupling to four equivalent Ph$_3$PO ligands. A second ^{89}Y NMR resonance, assignable to [YBr$_3$(Ph$_3$PO)$_3$] was not observed, presumably due to a low abundance of the species and the poor sensitivity of ^{89}Y. The spectra for [YBr$_2$(Ph$_3$PO)$_4$]PF$_6$ were similar, the ^{31}P-$\{^1$H$\}$ NMR spectrum containing a doublet at 36.0 ppm and a binomial septet at –145 ppm (PF$_6^-$). [YBr$_2$(Ph$_3$PO)$_4$]Br and [YBr$_2$(Ph$_3$PO)$_4$]PF$_6$ had Λ_m = 20 and 19 ohm^{-1}cm^{2}mol^{-1} for a 10^{-3} mol dm^{-3} dichloromethane solution, corresponding to 1 : 1 electrolytes.

The structure of [YBr$_2$(Ph$_3$PO)$_4$]PF$_6$.Et$_2$O was determined (Fig. 3.6), revealing a *trans*-octahedral geometry around the yttrium centre. The Y-O values were very close to those seen for [YCl$_2$(Ph$_3$PO)$_4$]Cl (above) (Y-O = 2.221(4) to 2.233(5) Å (for the

bromo-complex) c.f. 2.220(7) to 2.231(7) Å) and those observed for [Y(Me$_3$PO)$_6$]Br$_3$ (Y-O = 2.217(4) to 2.233(4)). The Y-X distances (X = Cl or Br) of the varied by 0.14 Å, closely reflecting the difference in ionic radii of the two halogens. The Y-O-P angles were significantly more acute than for the [YCl$_2$(Ph$_3$PO)$_4$]$^+$ cation, presumably due to the greater steric bulk of the bromide atoms (Y-O-P(ave.) = 161.4 c.f. 171.0°). A selection of bond lengths and angles are given in Table 3.2.
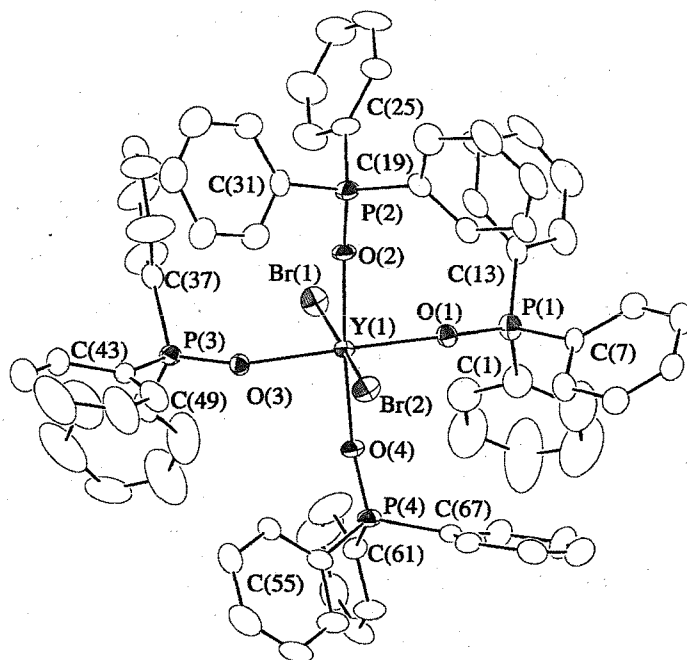
Fig. 3.6 Structure of the cation in [YBr$_2$(Ph$_3$PO)$_4$]PF$_6$.Et$_2$O showing the atom numbering scheme. Thermal ellipsoids are drawn at the 40 % probability level with H atoms omitted for clarity.

Table 3.2 Selected bond lengths (Å) and angles (°) for the structure of [YBr$_2$(Ph$_3$PO)$_4$]PF$_6$.Et$_2$O.

Y-O(1)	2.221(5)	Y-O(3)	2.233(5)
Y-O(2)	2.220(4)	Y-O(4)	2.221(4)
O(n)-P(n)	1.501(4)-1.506(5)	P-C	1.779(7)-1.811(8)
Y-Br(1)	2.775(1)	Y-Br(2)	2.794(1)
O(1)-Y-O(2)	89.2(2)	O(2)-Y-O(3)	95.0(2)
O(1)-Y-O(4)	88.2(2)	O(3)-Y-O(4)	88.4(2)
Br(1)-Y-Br(2)	174.67(4)	Y-O(1)-P(1)	166.7(3)
Y-O(2)-P(2)	172.5(3)	Y-O(3)-P(3)	155.9(3)
Y-O(4)-P(4)	161.4(3)		

The ^{31}P-{^{1}H} NMR spectrum of [YI$_2$(Ph$_3$PO)$_4$]I showed a doublet at δ 37.5 ppm whilst [YI$_2$(Ph$_3$PO)$_4$]PF$_6$ exhibits a similar doublet at δ 37.0 ppm, along with a binomial septet at –145 ppm, characteristic of the PF$_6^-$ anion. The ^{89}Y NMR spectrum of the same solutions at 200 K each contained a binomial quintet at δ 245 ppm, caused by coupling of the yttrium centre to four equivalent Ph$_3$PO ligands. If left to stand, the solutions turned dark brown due to liberation of diiodine. This was accompanied by the appearance of new resonances in the ^{31}P-{^{1}H} NMR spectrum. The new products were not identified. In the absence of oxygen, no change in colour was observed. The molar conductances of 10^{-3} mol dm^{-3} dichloromethane solutions of both [YI$_2$(Ph$_3$PO)$_4$]I and [YI$_2$(Ph$_3$PO)$_4$]PF$_6$ were measured, Λ_m = 25 and 23 ohm^{-1} cm^2 mol^{-1} respectively.

Addition of 5 molar equivalents of Ph$_3$PO to a dichloromethane solution containing the [YI$_2$(Ph$_3$PO)$_4$]$^+$ cation led to a broadening of the ^{31}P-{^{1}H} NMR resonance, suggesting rapid intermolecular exchange at ambient temperature. Cooling to 180 K gave a spectrum containing a strong peak at δ 26.0 (Ph$_3$PO), a weak doublet at 37.0 ([YI$_2$(Ph$_3$PO)$_4$]$^+$), two intense doublets at 37.5 and 38.0, assigned as [YI(Ph$_3$PO)$_5$]$^{2+}$ (ratio of integrals 4 : 1, no ^{31}P-^{31}P couplings were observed due to long P-O-Y-O-P distance), and some very weak, unassigned features. The ease of formation of this pentakis(phosphine oxide) species in solution by addition of Ph$_3$PO contrasts with the bromo-complexes, where it was not seen at all and the chloro-complex where it required SbCl$_5$ addition. This is consistent with the easier displacement of the softer iodide from the oxophilic metal centre.

Table 3.3 Multinuclear NMR spectroscopic data for complexes of yttrium(III) halides with triphenylphosphine oxide.

Complex	δ $(^{31}P\text{-}\{^1H\})$	δ (^{89}Y)	$^2J(^{31}P\text{-}^{89}Y)/Hz$	T/K
[YCl$_2$(Ph$_3$PO)$_4$]Cl	36.0 (d)	192 (quintet)	13	200
[YCl$_2$(Ph$_3$PO)$_4$]PF$_6$	36.0 (d)	192 (quintet)	13	200
[YCl$_3$(Ph$_3$PO)$_3$]^a	34.5 (d)	242 (quartet)	12	200
[YCl(Ph$_3$PO)$_5$][SbCl$_6$]$_2$	37.5 (d), 40.0 (d)	179 (multiplet)	11, 10	200
[YBr$_2$(Ph$_3$PO)$_4$]Br	36.5 (d)	220 (quintet)	11	200
[YBr$_2$(Ph$_3$PO)$_4$]PF$_6$	36.0 (d)	220 (quintet)	11	200
[YI$_2$(Ph$_3$PO)$_4$]I	37.5 (d)	245 (quintet)	11	200
[YI$_2$(Ph$_3$PO)$_4$]PF$_6$	37.0 (d)	245 (quintet)	11	200

^{a} Identified in solution only.

3.2.2 Complexes of yttrium halides with diphenylmethylphosphine oxide

In contrast to the YX$_3$ / Ph$_3$PO system, reaction of yttrium halides with diphenylmethylphosphine oxide in ethanol or acetone yielded [YX$_3$(Ph$_2$MePO)$_3$] (X = Cl, Br or I), irrespective of the ligand to metal ratio used. In the presence of NH$_4$PF$_6$, reaction of YCl$_3$.6H$_2$O with four molar equivalents Ph$_2$MePO yielded [YCl$_2$(Ph$_2$MePO)$_4$]PF$_6$. Synthesis of the analogous bromide complex was not attempted, whilst no pure iodide complex could be isolated from the YI$_3$.8H$_2$O / NH$_4$PF$_6$ / Ph$_2$MePO system.

The IR spectrum of [YCl$_3$(Ph$_2$MePO)$_3$] exhibited v(PO) = 1148 cm^{-1}. The bromide compound had v(PO) = 1144 cm^{-1} whilst the spectrum of [YI$_3$(Ph$_2$MePO)$_3$] contained v(PO) = 1140 cm^{-1}, showing the same trend with halide as observed for the Ph$_3$PO system (see 3.2.1). The spectrum of [YCl$_2$(Ph$_2$MePO)$_4$]PF$_6$ had v(PO) = 1151 cm^{-1}, with the PF$_6^-$ anion identified by a strong bands at 840 and 559 cm^{-1}.[17]

At ambient temperature, the $^{31}P\text{-}\{^1H\}$ NMR spectrum of [YCl$_3$(Ph$_2$MePO)$_3$] in dichloromethane solution showed a singlet at δ 40.0 ppm. Cooling the solution to 200 K allowed observation of a poorly defined doublet (caused by coupling with ^{89}Y). At the same temperature, a binomial quartet was apparent in the ^{89}Y NMR spectrum at δ

256 ppm, due to coupling to three equivalent ^{31}P atoms, indicating a *fac* geometry. Addition of a large excess of ligand altered the ^{31}P-{^{1}H} NMR spectrum at room temperature with broad resonances present at δ 29 (Ph$_2$MePO) and *ca*. 40 ppm. Cooling the solution to 200 K led to sharpening of these resonances, with an additional peak evident at δ 41.0 ppm. ^{89}Y NMR spectroscopy of the same solution revealed a quintet at δ 190 ppm in addition to the quartet at δ 256 ppm. Comparison of this resonance with that observed for [YCl$_2$(Ph$_3$PO)$_4$]Cl (Table 3.3) and that of [YCl$_2$(Ph$_2$MePO)$_4$]PF$_6$ (Table 3.4), along with the fact that four phosphine oxide ligands must be coordinated to the yttrium to generate this pattern led to assignment of this species as [YCl$_2$(Ph$_2$MePO)$_4$]$^+$. The ^{31}P-{^{1}H} NMR spectrum of [YCl$_2$(Ph$_2$MePO)$_4$]PF$_6$ contained a doublet at δ 40.5 ppm, along with a binomial septet at δ -145 ppm (PF$_6^-$). Cooling the solution to 185 K showed weaker resonances at δ 29.0 (Ph$_2$MePO) and 40.0 ppm ([YCl$_3$(Ph$_2$MePO)$_3$]) in addition to the doublet at δ 40.5 ppm, indicating an equilibrium was present. The ^{89}Y NMR spectrum of this solution at 185 K exhibited a quintet at δ 192 ppm. The molar conductance of [YCl$_3$(Ph$_2$MePO)$_3$] was measured for a 10^{-3} mol dm^{-3} solution in dichloromethane, with Λ_m = 2 ohm^{-1} cm^2 mol^{-1}, a value indicating it is a non-electrolyte in solution. Addition of Ph$_2$MePO saw Λ_m rise to 22 ohm^{-1} cm^2 mol^{-1}, a value typical of a 1 : 1 electrolyte, consistent with conversion to [YCl$_2$(Ph$_2$MePO)$_4$]Cl. Λ_m was 20 ohm^{-1} cm^2 mol^{-1} for a 10^{-3} mol dm^{-3} solution of [YCl$_2$(Ph$_2$MePO)$_4$]PF$_6$ in dichloromethane, showing it is a 1 : 1 electrolyte in solution.

Table 3.4 Multinuclear NMR spectroscopic data for complexes of yttrium(III) halides with diphenylmethylphosphine oxide.

Complex	δ (^{31}P-{^{1}H})	δ (^{89}Y)	^2J(^{31}P-^{89}Y)/Hz	T/K
[YCl$_3$(Ph$_2$MePO)$_3$]	40.0 (d)	256 (quartet)	10	200
[YCl$_2$(Ph$_2$MePO)$_4$]PF$_6$	41.5 (d)	192 (quintet)	10	185
[YBr$_3$(Ph$_2$MePO)$_3$]	40.0 (d)	299 (quartet)	11	185
[YBr$_2$(Ph$_2$MePO)$_4$]Br^a	41.0 (d)	220 (quintet)	11	185
[YI$_3$(Ph$_2$MePO)$_3$]	41.5 (d)	354^b	14	180

^{a} Observed in solution only ^{b} Coupling not resolved

[YBr$_3$(Ph$_2$MePO)$_3$] contained a doublet at δ 40.0 ppm in the ^{31}P-{^{1}H} NMR spectrum. Addition of excess ligand led to broad resonances at δ 29.0 and 40.0 ppm, the former assigned to 'free' Ph$_2$MePO. Cooling this solution to 200 K led to sharpening of both resonances and observation of coupling to ^{89}Y present in the latter. In addition, a second doublet at 41.0 ppm was observed, corresponding to [YBr$_2$(Ph$_2$MePO)$_4$]$^+$. The ^{89}Y NMR spectrum of the initial solution exhibited a binomial quartet at δ 299 ppm, caused by coupling to three equivalent phosphine oxide ligands, consistent with a *fac* geometry (Fig. 3.7). Following addition of excess Ph$_2$MePO, a quintet was observed at δ 220 ppm, confirming formation of a *trans*-tetrakis(phosphine oxide) species in solution. [YBr$_3$(Ph$_2$MePO)$_3$] had Λ_m = 7 ohm^{-1} cm^2 mol^{-1} for a 10^{-3} mol dm^{-3} solution in CH$_2$Cl$_2$. Addition of Ph$_2$MePO saw this value rise to 19 ohm^{-1}cm^{2}mol^{-1}, consistent with a 1 : 1 electrolyte, giving further evidence of conversion to [YBr$_2$(Ph$_2$MePO)$_4$]Br in solution.

Fig. 3.7 The ^{89}Y NMR spectrum of [YBr$_3$(Ph$_2$MePO)$_3$] showing a quartet at δ 299 ppm. The poor signal to noise ratio observed is due to the poor sensitivity of ^{89}Y and the modest solubility of the complex at 200 K.

The ^{31}P-{^{1}H} NMR spectrum of [YI$_3$(Ph$_2$MePO)$_3$] at room temperature contained a very broad resonance at δ 41.5 ppm. Cooling the solution resulted in sharpening of the peak, resolving to a doublet at 190 K (^2J(^{89}Y-^{31}P) = 14 Hz). Several weaker

resonances were seen at higher frequency. Addition of excess Ph_2MePO produced a peak at δ 29.0 ppm (Ph_2MePO) along with a very broad feature at *ca.* 40 ppm. At 190 K, the features were still broad, although along with the 'free' ligand peak, two doublets at δ 41.5 and 42.0 ppm were apparent, the former assigned to $[YI_3(Ph_2MePO)_3]$, the latter provisionally to $[YI_2(Ph_2MePO)_4]^+$ by comparison to the spectra for the chloride and bromide species. The ^{89}Y NMR spectrum at 180 K of $[YI_3(Ph_2MePO)_3]$ showed a broad resonance at δ 354 ppm. No coupling could be resolved but by comparison of the shifts with those of $[YCl_3(Ph_2MePO)_3]$ and $[YBr_3(Ph_2MePO)_3]$ (Table 3.4) it seems probable this was due to the tris(phosphine oxide) species. The molar conductance for a 10^{-3} mol dm^{-3} dichloromethane solution was 5 ohm^{-1} cm^2 mol^{-1}, typical of a non-electrolyte. Attempts to grow crystals of any $[YX_3(Ph_2MePO)_3]$ species by vapour diffusion of Et_2O into a CH_2Cl_2 solution or by slow evaporation of an ethanolic solution of the product were unsuccessful.

3.2.3 Complexes of yttrium halides with trimethylphosphine oxide

Reaction of $YX_3.nH_2O$ (X = Cl, Br or I) with six molar equivalents of Me_3PO in ethanol yielded compounds of the type $[Y(Me_3PO)_6]X_3$. The complexes were insoluble in acetone, ethanol, chlorocarbon solvents and were decomposed by DMF and DMSO. However, the compounds were slightly soluble in nitromethane, allowing solution studies. The IR spectra of all three compounds were simple and superimposable, exhibiting $v(PO)$ = 1110 cm^{-1} (compared to 1161 cm^{-1} for uncomplexed Me_3PO).

The $^{31}P-\{^1H\}$ NMR spectra were similar, $[Y(Me_3PO)_6]Cl_3$ having a doublet at δ 54.0 ppm $(^2J(^{31}P-^{89}Y)$ = 9 Hz), whilst both the bromide and iodide exhibited doublets at δ 55.0 ppm. The poor solubility of the complexes in $MeNO_2$ meant ^{89}Y NMR spectra were extremely difficult to obtain. A multiplet with an ill-defined coupling pattern at δ 133 ppm was observed for $[Y(Me_3PO)_6]Cl_3$, whilst no resonances could be observed for the bromo- or iodo-complexes. The molar conductivities for 10^{-3} mol dm^{-3} solutions in $MeNO_2$ were measured. $[Y(Me_3PO)_6]Cl_3$ had Λ_m = 225 ohm^{-1} cm^2 mol^{-1}, $[Y(Me_3PO)_6]Br_3$ showed Λ_m = 207 ohm^{-1} cm^2 mol^{-1} whilst for $[Y(Me_3PO)_6]I_3$,

$\Lambda_m = 228$ ohm^{-1} cm^2 mol^{-1}. All three values were consistent with a 3 : 1 electrolyte in MeNO$_2$.[20]

Table 3.5 Multinuclear NMR spectroscopic data for complexes of yttrium(III) halides with trimethylphosphine oxide and trimethylarsine oxide.

Complex	δ (^{31}P-{^{1}H})	δ (^{89}Y)	^2J(^{31}P-^{89}Y)/Hz	T/K
[Y(Me$_3$PO)$_6$]Cl$_3$	54.0 (d)	133 (m)[a]	9	245
[Y(Me$_3$PO)$_6$]Br$_3$	55.0 (d)	Not observed[b]	9	245
[Y(Me$_3$PO)$_6$]I$_3$	55.0 (d)	Not observed[b]	9	245
[Y(Me$_3$AsO)$_6$]Cl$_3$	Not Applicable	135 (s)	Not Applicable	200[c]

[a] Coupling not resolved

[b] No resonance observed owing to poor solubility of complex

[c] Solvent used EtNO$_2$ / d$_6$-Me$_2$CO

The structure of [Y(Me$_3$PO)$_6$]Br$_3$ was determined by single crystal X-ray diffraction (Fig. 3.8). Selected bond lengths and angles are given in Table 3.6. The cation had octahedral geometry with six Me$_3$PO ligands coordinated to the yttrium centre. The metal centre is located on a centre of symmetry, with O-Y-O angles close to idealised values. Whilst the Y-O distances show little variation, the Y-O-P angles do vary significantly (142.1(3) to 158.8(3)°). These angles were noticeably smaller than seen for the Ph$_3$PO / YX$_3$ structures described in Section 3.2.1, due to the smaller steric bulk of the methyl groups in the present species.
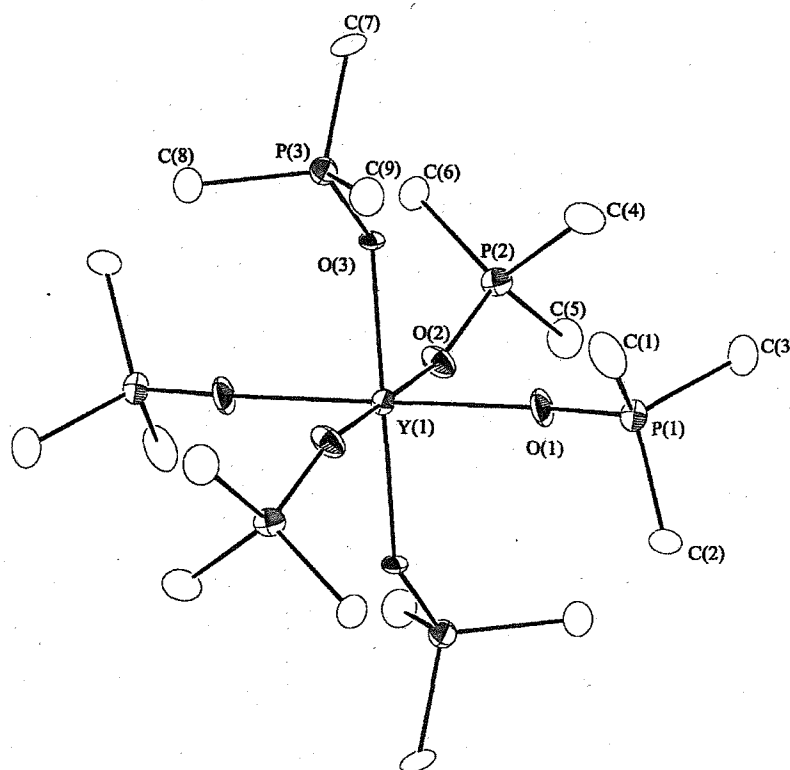
Fig. 3.8 Structure of the cation in $[Y(Me_3PO)_6]Br_3$, showing the atom numbering scheme. Thermal ellipsoids are drawn at the 40% probability level with H atoms omitted for clarity.

Table 3.6 Selected bond lengths (Å) and angles (°) for $[Y(Me_3PO)_6]Br_3$.

Y-O(1)	2.221(4)	P(1)-O(1)	1.513(5)
Y-O(2)	2.217(4)	P(2)-O(2)	1.520(5)
Y-O(3)	2.233(4)	P(3)-O(3)	1.517(4)
P-C	1.759(7)-1.785(7)		
Y-O(1)-P(1)	158.8(3)	O(1)-Y-O(2)	89.6(2)
Y-O(2)-P(2)	142.4(3)	O(1)-Y-O(3)	91.6(2)
Y-O(3)-P(3)	142.1(3)	O(2)-Y-O(3)	90.9(2)

These results contrast with those for the $Y(NO_3)_3$ / Me_3PO system (Chapter 2), for which $[Y(Me_3PO)_3(NO_3)_3]$ and $[Y(Me_3PO)_4(NO_3)_2]NO_3$ were prepared but no hexakis(phosphine oxide) compound could be isolated. Yttrium halides form complexes of the type $[Y(Me_3PO)_6]X_3$ (X = Cl, Br or I), irrespective of ligand : metal ratio used, with lower L : M ratios giving poorer yields of $[Y(Me_3PO)_6]X_3$. This

behaviour demonstrates that the oxophilic Y(III) centre shows greater affinity for nitrate groups than halides.

3.2.4 Complexes of yttrium chloride with diphosphine dioxide ligands

Reaction of $YCl_3.6H_2O$ with $Ph_2P(O)CH_2P(O)Ph_2$ (DPPM-O_2) in boiling ethanol afforded the white complex [YCl_2(DPPM-O_2)$_2$]Cl. When o-$C_6H_4\{P(O)Ph_2\}_2$ was used as the ligand in the same conditions, the product was [YCl_2(o-$C_6H_4\{P(O)Ph_2\}_2)_2$]Cl. These appear to be the first reported examples of complexes of yttrium with diphosphine dioxide ligands.

The IR spectra confirmed coordination of the ligand, [YCl_2(DPPM-O_2)$_2$]Cl containing v(PO) = 1167 cm^{-1}. [YCl_2(o-$C_6H_4\{P(O)Ph_2\}_2)_2$]Cl had v(PO) = 1171 cm^{-1} (compared to 1200 cm^{-1} in the 'free' ligand). Both compounds were 1 : 1 electrolytes in dichloromethane, [YCl_2(DPPM-O_2)$_2$]Cl giving A_m = 21 ohm^{-1} cm^2 mol^{-1} and [YCl_2(o-$C_6H_4\{P(O)Ph_2\}_2)_2$]Cl giving A_m = 19 ohm^{-1} cm^2 mol^{-1}.

The $^{31}P-\{^1H\}$ NMR spectrum of [YCl_2(o-$C_6H_4\{P(O)Ph_2)_2$]Cl at room temperature revealed a broad resonance at 36.0 ppm. Cooling the solution to 200 K saw resolution to a doublet ($^2J(^{31}P-^{89}Y)$) = 7 Hz). The ^{89}Y NMR spectrum at the same temperature showed a quintet at δ 210 ppm ($^2J(^{89}Y-^{31}P)$ = 7 Hz), showing coupling to four equivalent ^{31}P atoms. NMR spectroscopy on the [YCl_2(DPPM-O_2)$_2$]Cl was more limited owing to poor solubility in dichloromethane. However, at 200 K, the $^{31}P-\{^1H\}$ NMR spectrum contained a broad resonance at ca. 32 ppm, with the corresponding ^{89}Y NMR spectrum showing an ill-resolved multiplet at δ 213 ppm (Table 3.7).

Table 3.7 Multinuclear NMR spectroscopic data for complexes of yttrium chloride hexahydrate with diphosphine dioxide ligands.

Complex	δ ($^{31}P-\{^1H\}$)	δ (^{89}Y)	$^2J(^{31}P-^{89}Y)$/Hz	T/K
[YCl_2(o-$C_6H_4\{P(O)Ph_2)_2$]Cl	36.0 (d)	210 (quintet)	7	200
[YCl_2(DPPM-O_2)$_2$]Cl	32.0^a	213 (multiplet)^a	-	200

^{a} Coupling not clearly resolved

3.2.5 Complexes of yttrium halides with triphenylarsine oxide

Reaction of $YCl_3.6H_2O$ with four molar equivalents Ph_3AsO in boiling ethanol afforded $[YCl_2(Ph_3AsO)_4]Cl$. When $YBr_3.6H_2O$ was used, the product was $[YBr_2(Ph_3AsO)_4]Br$. In contrast, the same reaction using $YI_3.8H_2O$ yielded the polyiodide complex $[YI_2(Ph_3AsO)_4]I_5$ (confirmed by microanalysis). As for the Ph_3PO system (see 3.2.1), the chloro- and bromo-complexes were air stable, whilst the iodo-complex was moisture sensitive. Several attempts to isolate analytically pure $[YI_2(Ph_3PO)_4]I$ were unsuccessful.

Infrared spectroscopy of the complexes showed the characteristic rise in $v(AsO)$ upon coordination.[2, 3] $[YCl_2(Ph_3AsO)_4]Cl$ had $v(AsO) = 894$ cm^{-1}, compared to 878 cm^{-1} in the 'free' ligand. The bromo- and iodo-compounds contained $v(AsO) = 893$ cm^{-1}.

The ^{89}Y NMR spectrum of $[YCl_2(Ph_3AsO)_4]Cl$ at 200 K in dichloromethane showed a singlet resonance at δ 198 ppm. The complex $[YBr_2(Ph_3AsO)_4]Br$ exhibited a singlet at δ 224 ppm, whilst $[YI_2(Ph_3AsO)_4]I_5$ had a resonance at δ 254 ppm. It was noticable that when compared to ^{89}Y NMR spectra for the compounds $[YX_2(Ph_3PO)_4]X$ (See Tables 3.3 and 3.8, X = Cl, Br or I), the value of δ was between 5 and 10 ppm to higher frequency for arsine oxide species for constant X. No evidence of a tris(arsine oxide) species was observed in any of the spectra. In an attempt to form "$[YCl_3(Ph_3AsO)_3]$" in situ, one molar equivalent of $YCl_3.6H_2O$ was added to a solution of $[YCl_2(Ph_3AsO)_4]Cl$ in acetone. However, no new resonance was apparent. All three complexes were 1 : 1 electrolytes in dichloromethane.

Table 3.8 ^{89}Y NMR spectroscopy data for the YX_3 / Ph_3AsO system.

Complex	δ (^{89}Y)	T/K
$[YCl_2(Ph_3AsO)_4]Cl$	198 (s)	200
$[YBr_2(Ph_3AsO)_4]Br$	224 (s)	200
$[YI_2(Ph_3AsO)_4]I_5$	254 (s)	200

3.2.6 Complexes of yttrium chloride with trimethylarsine oxide

Hydrated YCl_3 reacted with Me_3AsO in ethanol to form $[Y(Me_3AsO)_6]Cl_3$. No evidence for other compounds was observed. As for $[Y(Me_3PO)_6]X_3$ (Section 3.2.3), the compound was insoluble in acetone, ethanol and chlorocarbon solvents but was slightly soluble in $MeNO_2$. The infrared spectrum contained $v(AsO) = 877$ cm^{-1} (identical to that of $[Y(Me_3AsO)_6](NO_3)_3$, structurally characterised in Section 2.2.8).[21] The compound had $\Lambda_m = 224$ $ohm^{-1}cm^2mol^{-1}$ in nitromethane, consistent with a 3 : 1 electrolyte.[20] The ^{89}Y NMR spectrum at 200 K (in $EtNO_2/d_6$-acetone) found a singlet resonance at δ 135 ppm, identical to that observed for $[Y(Me_3AsO)_6](NO_3)_3$ and comparing closely to the ^{89}Y NMR spectrum of $[Y(Me_3PO)_6]Cl_3$ which exhibited δ 133 ppm, confirming that the octahedral YO_6 cation was present. $EtNO_2$ was used in place of $MeNO_2$ as the latter has a melting point of 244 K, hindering low temperature ^{89}Y NMR spectroscopy. $EtNO_2$ is chemically the closest solvent to $MeNO_2$, allowing studies at 200 K.

3.2.7 ^{89}Y NMR studies

By comparison of their ^{89}Y NMR spectra, it is apparent that variation of both the halide and the ligand coordinated to the metal centre has a systematic effect on the position of the resonance observed (Fig. 3.9). Changes in the R group of R_3EO (E = As or P) have little effect, whilst changing from P to As results in a shift to higher frequency of $\leq$ 10 ppm. Adding halides into the coordination sphere causes stepwise shifts to high frequency, whilst changing from $Cl{\rightarrow}Br{\rightarrow}I$ leads to stepwise increases in δ.

$[YCl_2(Ph_2MePO)_4]^+ \xrightarrow{64} [YCl_3(Ph_2MePO)_3] \xrightarrow{43} [YBr_3(Ph_2MePO)_3] \xrightarrow{55} [YI_3(Ph_2MePO)_3]$

192   256   299   354

$\downarrow$ -13 $\searrow$ -1 $\downarrow$ -65 $\downarrow$ -79 $\downarrow$ -109

$[YCl(Ph_3PO)_5]^{2+} \xrightarrow{12} [YCl_2(Ph_3PO)_4]^+ \xrightarrow{29} [YBr_2(Ph_3PO)_4]^+ \xrightarrow{25} [YI_2(Ph_3PO)_4]^+$

179   191   220   245

$\downarrow$ -46 $\downarrow$ 7 $\downarrow$ 4 $\downarrow$ 9

$[Y(Me_3PO)_6]^{3+}$

133

$\downarrow$ 2

$[Y(Me_3AsO)_6]^{3+} \xrightarrow{63} [YCl_2(Ph_3AsO)_4]^+ \xrightarrow{26} [YBr_2(Ph_3AsO)_4]^+ \xrightarrow{30} [YI_2(Ph_3AsO)_4]^+$

135   198   224   254
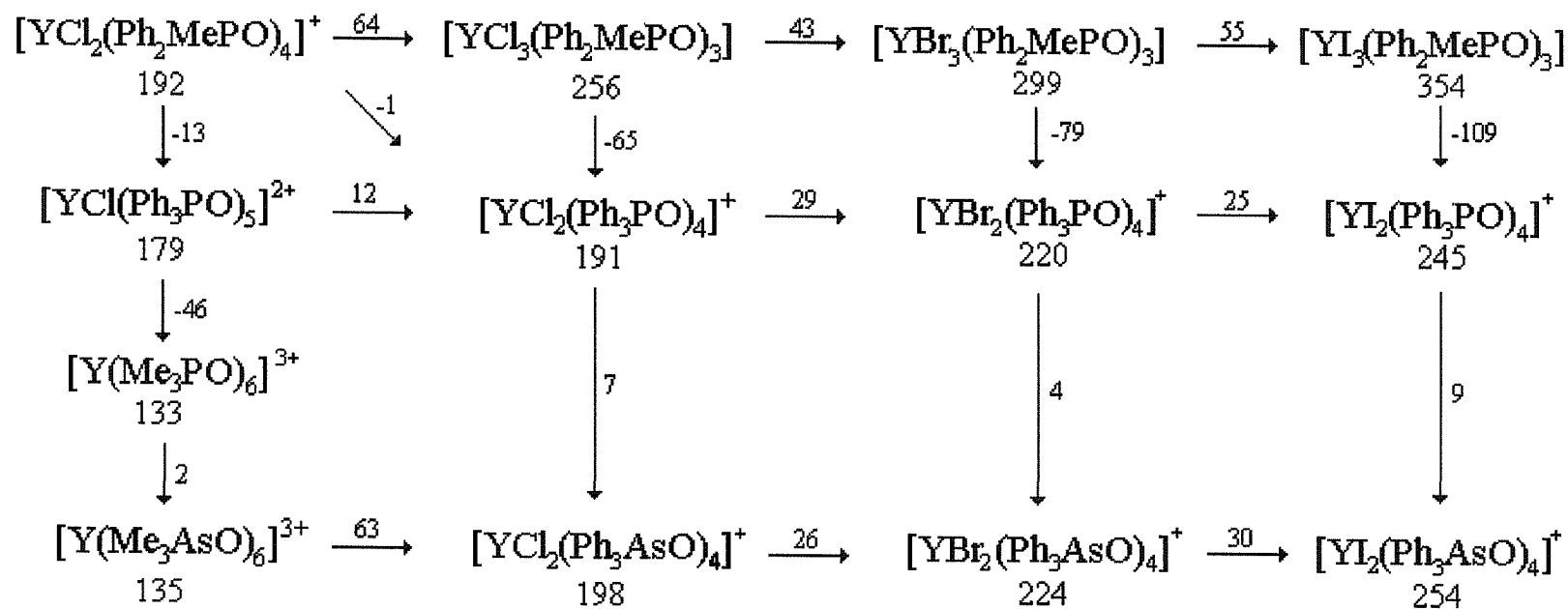
Fig. 3.9 [89]Y NMR chemical shifts of certain cations identified during these studies. Values below species are the chemical shift, whilst values by arrows are the difference in δ between two species. (There is some variation in both solvents used and temperature of observation. However, whilst this may alter specific values slightly, the trends are still valid).

3.2.8 Reaction scheme

$YX_3.nH_2O + Ph_3PO$ (X = Cl, Br or I) $\longrightarrow$ $[YX_2(Ph_3PO)_4]X$

$YX_3.nH_2O + Ph_3PO + NaPF_6$ $\longrightarrow$ $[YX_2(Ph_3PO)_4]PF_6$

$[YCl_2(Ph_3PO)_4]Cl + SbCl_5 + Ph_3PO$ $\longrightarrow$ $[YCl(Ph_3PO)_5][SbCl_6]_2$

$YX_3.nH_2O + Ph_2MePO$ $\longrightarrow$ $[YX_3(Ph_2MePO)_3]$

$YX_3.nH_2O + Ph_2MePO + NaPF_6$ $\longrightarrow$ $[YX_2(Ph_2MePO)_4]PF_6$

$YX_3.nH_2O + Me_3PO$ $\longrightarrow$ $[Y(Me_3PO)_6]X_3$

$YX_3.nH_2O + L$ (L = ppO_2 or dppm-O_2) $\longrightarrow$ $[YCl_2(L)_2]Cl$

$YX_3.nH_2O + Ph_3AsO$ (X = Cl or Br) $\longrightarrow$ $[YX_2(Ph_3AsO)_4]X$

$YI_3.nH_2O + Ph_3AsO$ $\longrightarrow$ $[YX_2(Ph_3AsO)_4]I_5$

$YCl_3.6H_2O + Me_3AsO$ $\longrightarrow$ $[Y(Me_3AsO)_6]Cl_3$
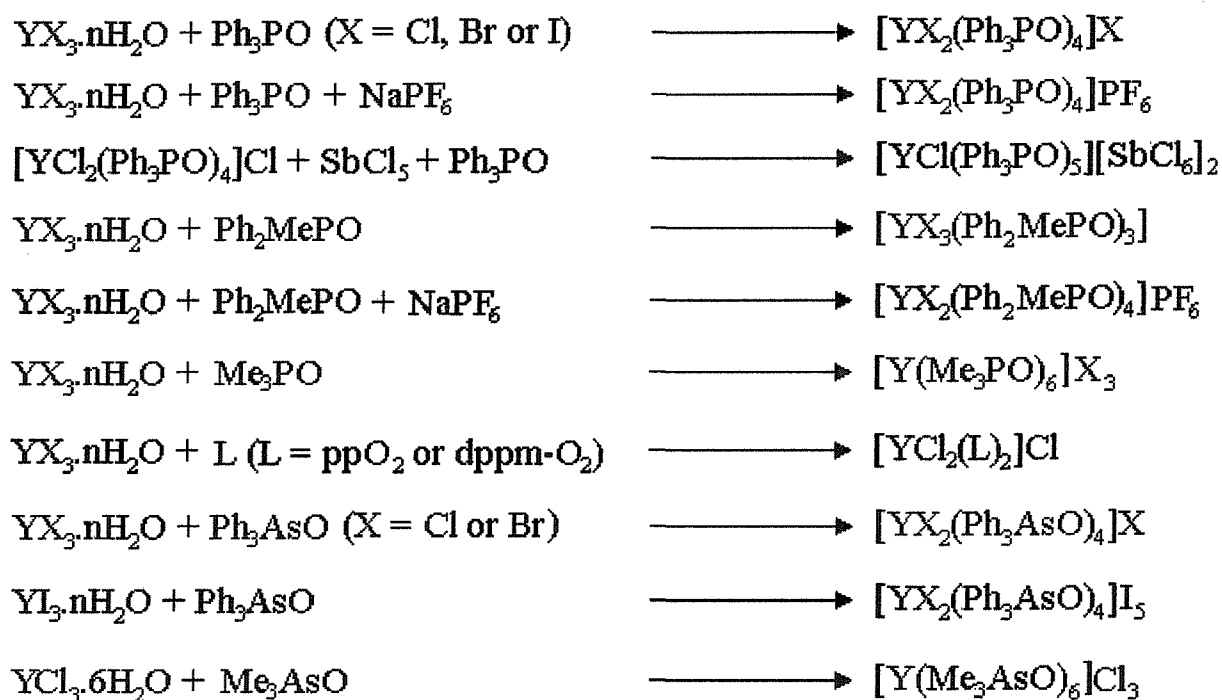
Fig. 3.10 Reaction schemes indicating the products from reaction of $YX_3.nH_2O$ with tertiary pnictogen oxide ligands isolated in this study. 'ppO_2' refers to the ligand o-$C_6H_4\{P(O)Ph_2\}_2$.

3.3 Conclusions

Yttrium halides form complexes with phosphine oxide ligands with an R_3PO : metal ratio ranging from 6 : 1 to 3 : 1, dependent on ligand type, although not all complexes were isolated in the solid state. The chemistry with R_3AsO ligands was similar, except that no tris(arsine oxide) compounds were isolated, with no evidence for their existence in solution observed.

Comparison with the $Y(NO_3)_3$ / R_3EO studies (Chapter 2) indicate that yttrium shows a preference for coordinating to nitrate groups over the halides used here. For example, reactions with trimethylphosphine oxide with yttrium halides yield $[Y(Me_3PO)_6]X_3$ (X = Cl, Br or I) exclusively whilst with yttrium nitrate, no homoleptic compound was isolated. Crystallographic studies revealed that all the YX_3 / R_3EO compounds contained six-coordinate yttrium with a *pseudo*-octahedral geometry. These are the first structural reports for yttrium halide / R_3PO systems. This contrasted with the nitrate system where both coordination number and geometry were seen to vary. The 4 : 1 complexes characterised here disagree with literature reports suggesting that these are seven-coordinate species. Both X-ray and molar conductance data (indicating species are 1 : 1 electrolytes) strongly suggest that six- coordinate Y(III) is present in all cases.[4, 6, 7, 9]

Solution NMR and conductance studies showed that compounds often exist as a mixture of species in solution, with the equilibrium position easily altered by addition of ligand or $YX_3.nH_2O$ salt. However, as observed for the nitrate systems, single pure species generally crystallise from solution under suitable conditions. In contrast to the studies on the nitrate species in Chapter 2, the halide species studied here did not demonstrate fluxionality in solution, probably because of the six-coordinate geometry (fluxionality is relatively rare in six-coordinate species). Studies also revealed that the [89]Y NMR chemical shift varied systematically depending on the number and nature of both X and R_3EO (E = As or P) ligands. In comparison, whilst the analogous nitrate system shows that the chemical shift moves to higher frequency as NO_3 groups are replaced by R_3EO ligands, trends are less regular due to the varying coordination

numbers. $^{31}P-\{^{1}H\}$ NMR showed far less variation in chemical shift with such changes, making it a less useful tool for identifying complexes in solution. For example, $[YCl_2(Ph_3PO)_4]^+$ and $[YCl_3(Ph_3PO)_3]$ differ by just 1.5 ppm in the $^{31}P-\{^{1}H\}$ NMR spectrum, whilst the ^{89}Y NMR resonances were 50 ppm apart.

3.4 Experimental

Ph$_3$PO, Ph$_2$MePO, Ph$_3$AsO, YCl$_3$.6H$_2$O (Aldrich) and Me$_3$PO (Alfa) were used as received. Me$_3$AsO was prepared by oxidation of trimethylarsine in diethyl ether by hydrogen peroxide, with sublimation of the product *in vacuo* used to purify the product.[22] YF$_3$.1/2H$_2$O was synthesized by precipitation from aqueous solutions of Y(NO$_3$)$_3$.6H$_2$O and NaF. YBr$_3$.6H$_2$O was afforded by reaction of Y$_2$O$_3$ and 48% HBr in boiling water, with the resultant solution concentrated yielding white crystals (Found: Br, 54.8. Calc. For YBr$_3$.6H$_2$O: Br, 54.9%). Attempts to produce YI$_3$.8H$_2$O by the same method consistently gave compounds containing excess diiodine which could not be removed. Hence, a 1 : 3 ratio of aqueous solutions of yttrium sulfate and barium iodide were mixed, with the BaSO$_4$ precipitate filtered off. The resultant solution was evaporated to dryness, producing a fawn solid. (Found: I, 61.9. Calc. For YI$_3$.8H$_2$O: I, 62.0%). DPPM-O$_2$ was produced by iodine oxidation of DPPM in toluene, followed by base hydrolysis using NaOH.[23] o-C$_6$H$_4$(POPh$_2$)$_2$ was synthesized by literature methods (v(PO) = 1200 cm^{-1}, ^{31}P-{^{1}H} NMR (300 K, CH$_2$Cl$_2$/CDCl$_3$) δ 33.6).[23]

3.4.1 Complexes of yttrium halides with triphenylphosphine oxide

[YCl$_2$(Ph$_3$PO)$_4$]Cl

Solutions of YCl$_3$.6H$_2$O (0.20 g, 0.66 mmol) and Ph$_3$PO (1.11 g, 4.0 mmol) in ice cold ethanol (5 cm^3) were mixed with the resultant solution refrigerated overnight. Colourless crystals were deposited which were filtered off and dried *in vacuo*. Yield 0.56 g, 60%. (Found: C, 65.7; H, 4.5. Calc. for C$_{72}$H$_{60}$Cl$_3$O$_4$P$_4$Y: C, 66.1; H, 4.6%.) IR (cm^{-1})(Nujol mull): 1310m, 1188w, 1150vs (PO), 1119s, 1087s, 1074m, 997w, 975w, 749s, 692s, 543s, 420w, 398w, 353w, 310m, 260m. ^{31}P-{^{1}H} NMR (300 K, CH$_2$Cl$_2$/CDCl$_3$): 35.0 (d) $^2J(^{31}$P-^{89}Y) = 12 Hz. ^{1}H NMR (300 K, CDCl$_3$): 7.1 – 7.9 (m). Λ_m (10^{-3} mol dm^{-3} CH$_2$Cl$_2$) = 30 ohm^{-1} cm^2 mol^{-1}.

[YCl$_2$(Ph$_3$PO)$_4$]PF$_6$

A solution of YCl$_3$.6H$_2$O (0.30 g, 1.0 mmol) in warm (60°C) ethanol (10 cm^3) was added to a solution of NH$_4$PF$_6$ (0.16 g, 1.0 mmol) in ethanol and stirred for 1 h. To

this, a solution of triphenylphosphine oxide (1.11 g, 4.0 mmol) in ethanol (10 cm^3) was added, affording a fine white precipitate. The solid was filtered off and dried *in vacuo*. Yield 1.09 g, 75%. (Found: C, 61.1; H, 4.4. Calc. for $C_{72}H_{60}Cl_2F_6O_4P_5Y$: C, 61.0; H, 4.3%.) IR (cm^{-1})(CsI disc): 3061w, 1439m, 1318m, 1192w, 1150vs (PO), 1122s, 1092s, 1028m, 999m, 839s, 750m, 725s, 693s, 559s, 543s, 459m, 446m, 421m, 305m, 267s. ^{31}P-{^{1}H} NMR (300 K, CH$_2$Cl$_2$/CDCl$_3$): 35.0 (d) ($^2J(^{31}$P-^{89}Y) = 13 Hz), -145 (septet) PF$_6^-$. ^{1}H NMR (300 K, CDCl$_3$): 7.1 – 7.9 (m). A_m (10^{-3} mol dm^{-3} CH$_2$Cl$_2$) = 21 ohm^{-1} cm^2 mol^{-1}.

[YBr$_2$(Ph$_3$PO)$_4$]Br

Prepared similarly to [YCl$_2$(Ph$_3$PO)$_4$]Cl. Yield 0.75 g, 52%. (Found: C, 59.6; H, 4.2. Calc. for $C_{72}H_{60}Br_3O_4P_4Y$: C, 59.9; H, 4.2%.) IR (cm^{-1})(CsI disc): 1307m, 1188w, 1140vs (PO), 1119s, 1087s, 1084m, 998w, 973w, 763m, 693s, 543s, 449m, 417w, 305m, 262m. ^{31}P-{^{1}H} NMR (300 K, CH$_2$Cl$_2$/CDCl$_3$): 36.0 (d) ($^2J(^{31}$P-^{89}Y) = 11 Hz). ^{1}H NMR (300 K, CDCl$_3$): 7.2 – 7.9 (m). A_m (10^{-3} mol dm^{-3} CH$_2$Cl$_2$) = 20 ohm^{-1} cm^2 mol^{-1}.

[YBr$_2$(Ph$_3$PO)$_4$]PF$_6$

Prepared similarly to [YCl$_2$(Ph$_3$PO)$_4$]PF$_6$. Yield 1.40 g, 90%. (Found: C, 57.9; H, 4.2. Calc. for $C_{72}H_{60}Br_2F_6O_4P_5Y$: C, 57.4; H, 4.2%.) IR (cm^{-1})(CsI disc): 3061w, 1439m, 1359m, 1191w, 1147vs (PO), 1123s, 1089s, 1029m, 1000m, 839s, 750m, 726s, 693s, 559sh, 543s, 449m, 417m, 305m, 250w. ^{31}P-{^{1}H} NMR (300 K, CH$_2$Cl$_2$/CDCl$_3$): 36.0 (d) ($^2J(^{31}$P-^{89}Y) = 11 Hz), -145 (septet) PF$_6^-$. ^{1}H NMR (300 K, CDCl$_3$): 7.2 – 7.9 (m). A_m (10^{-3} mol dm^{-3} CH$_2$Cl$_2$) = 19 ohm^{-1} cm^2 mol^{-1}.

[YI$_2$(Ph$_3$PO)$_4$]I

Prepared similarly to [YCl$_2$(Ph$_3$PO)$_4$]Cl, yielding a pale yellow powder. Yield 0.30 g, 38%. (Found: C, 54.2; H, 3.8. Calc. for $C_{72}H_{60}I_3O_4P_4Y$: C, 54.6; H, 3.8%.) IR (cm^{-1})(CsI disc): 1485w, 1438m, 1359m, 1188w, 1136vs(PO), 1121s, 1083s, 1027w, 1000w, 749m, 725s, 696s, 543s, 460m, 449m, 421w, 299m. ^{31}P-{^{1}H} NMR (300 K, CH$_2$Cl$_2$/CDCl$_3$): 37.2 (d, $^2J(^{31}$P-^{89}Y) = 13 Hz). ^{1}H NMR (300 K, CDCl$_3$): 7.1 – 7.6 (m). A_m (10^{-3} mol dm^{-3} CH$_2$Cl$_2$) = 25 ohm^{-1} cm^2 mol^{-1}.

$[YI_2(Ph_3PO)_4]PF_6$

Prepared similarly to $[YCl_2(Ph_3PO)_4]PF_6$, producing a pale yellow powder. Yield 0.35 g, 39%. (Found: C, 53.8; H, 3.7. Calc. for $C_{72}H_{60}I_2F_6O_4P_5Y$: C, 54.0; H, 3.8%.) IR $(cm^{-1})(CsI$ disc): 3061w, 1439m, 1318m, 1192w, 1144vs (PO), 1122s, 1092s, 1028m, 999m, 839s, 750m, 725s, 693s, 559s, 543s, 459m, 446m, 421m, 305m, 267s. $^{31}P\text{-}\{^1H\}$ NMR (300 K, $CH_2Cl_2/CDCl_3$): 35.0 (d, $^2J(^{31}P\text{-}^{89}Y)$ = 13 Hz), -145 (septet) PF_6^-. ^1H NMR (300 K, $CDCl_3$): 7.1 – 7.9 (m). Λ_m (10^{-3} mol dm^{-3} CH_2Cl_2) = 21 ohm^{-1} cm^2 mol^{-1}.

$[YCl(Ph_3PO)_5][SbCl_6]_2$

Under a dry nitrogen atmosphere, $SbCl_5$ (0.05 g, 0.17 mmol) was added dropwise to a solution of $[YCl_2(Ph_3PO)_4]Cl$ (0.11 g, 0.08 mmol) in anhydrous dichloromethane (5 cm^3). A solution of triphenylphosphine oxide (0.02 g, 0.08 mmol) in CH_2Cl_2 was then added, affording a milky white suspension. The solution was concentrated to $ca.$ 5 cm^3, the white powder filtered off and dried $in\ vacuo$. Yield 0.12 g, 56%. (Found: C, 49.6; H, 3.3. Calc. for $C_{90}H_{75}Cl_{13}O_5P_5Sb_2Y$: C, 49.4; H, 3.5%.) IR $(cm^{-1})(CsI$ disc): 2975w, 1484w, 1437m, 1357m, 1191w, 1141s (PO), 1121s, 1090m, 1027w, 995m, 745s, 692s, 543s, 347s ($SbCl_6^-$). ^1H NMR (300 K, $CDCl_3$): 7.2 – 7.7 (m). Λ_m (10^{-3} mol dm^{-3} CH_2Cl_2) = 42 ohm^{-1} cm^2 mol^{-1}.

3.4.2 Complexes of yttrium halides with diphenylmethylphosphine oxide

$[YCl_3(Ph_2MePO)_3]$

A solution of yttrium(III) chloride hexahydrate (0.30 g, 1.0 mmol) in boiling ethanol (10 cm^3) was added to a solution of diphenylmethylphosphine oxide (0.22 g, 1.0 mmol) in ethanol (5 cm^3) with the resultant solution stirred for 1 h. The solution was concentrated to $ca.$ 5 cm^3 and refrigerated overnight, yielding a white solid which was filtered off and dried $in\ vacuo$. Yield 0.28 g, 88%. (Found: C, 54.5; H, 4.1. Calc. for $C_{39}H_{39}Cl_3O_3P_3Y$: C, 55.5; H, 4.7%.) IR $(cm^{-1})(CsI$ disc): 1709w, 1641m, 1439m, 1363w, 1225w, 1148vs (PO), 1127m, 1101m, 999w, 896m, 783w, 752m, 696m, 614m, 515s, 306w, 254s. ^1H NMR (300 K, $CDCl_3$): 2.29(br)[9H], 7.4-7.7(m)[30H]. Λ_m (10^{-3} mol dm^{-3} CH_2Cl_2) = 2 ohm^{-1} cm^2 mol^{-1}.

[YBr₃(Ph₂MePO)₃]

Made similarly to the above using a 1:3 molar ratio of $YBr_3.6H_2O$ to ligand. Yield 0.45 g, 46%. (Found: C, 48.2; H, 4.1. Calc. for $C_{39}H_{39}Br_3O_3P_3Y$: C, 47.9; H, 4.0%.) IR $(cm^{-1})(CsI$ disc): 1591w, 1439m, 1358w, 1178sh, 1144vs (PO), 1127sh, 1098s, 998m, 894s, 782w, 750s, 720m, 694m, 515s, 503sh, 392w, 312w. ^1H NMR (300 K, $CDCl_3$): 2.18(br)[9H], 7.3-7.7(m)[30H]. Λ_m (10^{-3} mol dm^{-3} CH_2Cl_2) = 7 ohm^{-1} cm^2 mol^{-1}.

[YI₃(Ph₂MePO)₃]

Made similarly to [YCl₃(Ph₂MePO)₃] using a 2:1 ratio of Ph₂MePO to $YI_3.8H_2O$, yielding a yellow powder. Yield 0.31 g, 28%. (Found: C, 42.5; H, 3.7. Calc. for $C_{39}H_{39}I_3O_3P_3Y$: C, 41.9; H, 3.5%.) IR $(cm^{-1})(CsI$ disc): 2896w, 1592w, 1439m, 1359w, 1178sh, 1140vs (PO), 1125s, 1093s, 1071m, 1029m, 996m, 895s, 786w, 749s, 720m, 696m, 519s, 478m, 421m, 383w. ^1H NMR (300 K, $CDCl_3$): 2.0(d)[9H], 7.2-7.7(m)[30H]. Λ_m (10^{-3} mol dm^{-3} CH_2Cl_2) = 5 ohm^{-1} cm^2 mol^{-1}.

[YCl₂(Ph₂MePO)₄]PF₆

NH_4PF_6 (0.082 g, 0.5 mmol) was added to a boiling ethanolic solution of $YCl_3.6H_2O$ (0.15 g, 0.5 mmol). The mixture was stirred and allowed to cool to room temperature, following which a solution of Ph₂MePO (0.43 g, 2.0 mmol) in ethanol (5 cm^3) was added, immediately forming a precipitate. The mixture was left to stand for 2 h, with the solid filtered off and dried *in vacuo*. Yield 0.28 g, 43%. (Found: C, 53.0; H, 4.4. Calc. for $C_{52}H_{52}Cl_2F_6O_4P_5Y$: C, 53.4; H, 4.5%.) IR $(cm^{-1})(CsI$ disc): 1591w, 1486w, 1440m, 1305w, 1165sh, 1151s (PO), 1126m, 1101w, 1075w, 1031w, 1000m, 903s, 840s, 782s, 756s, 748s, 720m, 698s, 559s, 511s, 498s, 455m, 418m, 387w, 312m, 264s. ^1H NMR (300 K, $CDCl_3$): 1.92 (br)[12H], 7.2-7.7(m)[40H]. Λ_m (10^{-3} mol dm^{-3} CH_2Cl_2) = 20 ohm^{-1} cm^2 mol^{-1}.

3.4.3 Complexes of yttrium halides with trimethylphosphine oxide

[Y(Me₃PO)₆]Cl₃

To an ethanolic solution (10 cm³) of YCl₃.6H₂O (0.15 g, 0.5 mmol), a solution of trimethylphosphine oxide (0.28 g, 3.0 mmol) in ethanol (10 cm³) was added, with the mixture stirred for 1 h. Refrigeration overnight produced a white precipitate. Yield 0.34 g, 90%. (Found: C, 28.9; H, 7.6. Calc. for $C_{18}H_{54}Cl_3O_6P_6Y$: C, 28.9; H, 7.2%.) IR (cm⁻¹)(CsI disc): 2960w, 1423w, 1358w, 1299w, 1111vs, br (PO), 960m, 872m, 762m, 396m, 364w, 332m. ¹H NMR (300 K, d³-MeNO₂): 1.60 (d, $^2J(^{31}P-^1H)$ = 14 Hz). Λ_m (10⁻³ mol dm⁻³ MeNO₂) = 225 ohm⁻¹ cm² mol⁻¹.

[Y(Me₃PO)₆]Br₃

Solutions of yttrium(III) bromide hexahydrate (0.44 g, 1.0 mmol) and trimethylphosphine oxide (0.37 g, 4.0 mmol) in boiling ethanol (10 cm³) were mixed, resulting in a milky suspension in which the solid was seen to redissolve upon stirring. Refrigeration overnight deposited white needles. These were filtered off and dried *in vacuo*. Yield 0.39 g, 66%. (Found: C, 24.2; H, 6.1. Calc. for $C_{18}H_{54}Br_3O_6P_6Y$: C, 24.5; H, 6.1%.) IR (cm⁻¹)(CsI disc): 2962w, 2896w, 1358m, 1299m, 1111s, br (PO), 959s, 872m, 761m, 395s, 364m, 330m. ¹H NMR (300 K, d³-MeNO₂): 1.69 (d, $^2J(^{31}P-^1H)$ = 13 Hz). Λ_m (10⁻³ mol dm⁻³ MeNO₂) = 207 ohm⁻¹ cm² mol⁻¹.

[Y(Me₃PO)₆]I₃

A solution of YI₃.8H₂O (0.31 g, 0.5 mmol) in boiling ethanol (10 cm³) was added to a solution of Me₃PO (0.18 g, 2.0 mmol) in ethanol affording a yellow suspension. Refrigeration overnight deposited a solid which was filtered off and dried *in vacuo*. Yield 0.21 g, 50%. (Found: C, 20.9; H, 5.4. Calc. for $C_{18}H_{54}I_3O_6P_6Y$: C, 21.2; H, 5.3%.) IR (cm⁻¹)(CsI disc): 2964w, 2897w, 1421w, 1358m, 1299m, 1110s, br (PO), 957s, 871m, 761m, 396s, 364m, 331m. ¹H NMR (300 K, d³-MeNO₂): 1.73 (d, $^2J(^{31}P-^1H)$ = 13 Hz). Λ_m (10⁻³ mol dm⁻³ MeNO₂) = 228 ohm⁻¹ cm² mol⁻¹.

3.4.4 Complexes of yttrium chloride with diphosphine dioxides

[YCl₂(DPPM-O₂)₂]Cl

To a solution of $YCl_3.6H_2O$ (0.076 g, 0.25 mmol) in boiling ethanol (5 cm³), a solution of DPPM-O₂ (0.10 g, 0.25 mmol) in ethanol (10 cm³) was added, immediately affording a white precipitate. The mixture was left to stand for 1 h, the precipitate filtered off and dried *in vacuo*. Yield 0.06 g, 47%. (Found: C, 57.9; H, 4.4. Calc. for $C_{50}H_{44}Cl_3O_4P_4Y$: C, 58.4; H, 4.3%.) IR (cm⁻¹)(CsI disc): 3042w, 1437m, 1410s, 1368m, 1167s (PO), 1120m, 1071w, 997w, 843s, 790s, 742m, 692m, 572w. ¹H NMR (300 K, CDCl₃): 2.2(s)[2H], 7.2-7.8 (m)[20H]. Λ_m (10⁻³ mol dm⁻³ CH₂Cl₂) = 21 ohm⁻¹ cm² mol⁻¹.

[YCl₂(o-C₆H₄{P(O)Ph₂}₂)₂]Cl

Made similarly to [YCl₂(DPPM-O₂)₂]Cl. Yield 0.16 g, 55%. (Found: C, 62.9; H, 4.3. Calc. for $C_{60}H_{48}Cl_3O_4P_4Y$: C, 62.6; H, 4.2%.) IR (cm⁻¹)(CsI disc): 2960w, 1439m, 1410s, 1359m, 1171br,s (PO), 1121m, 1073w, 1005w, 844m, 750s, 730s, 694s, 562s, 549s, 534m. ¹H NMR (300 K, CDCl₃): 7.2-7.8 (m). Λ_m (10⁻³ mol dm⁻³ CH₂Cl₂) = 19 ohm⁻¹ cm² mol⁻¹.

3.4.5 Reaction of yttrium halides with tertiary arsine oxide ligands

[YCl₂(Ph₃AsO)₄]Cl

Yttrium(III) chloride hexahydrate (0.30 g, 1.0 mmol) and triphenylarsine oxide (1.28 g, 4.0 mmol) were dissolved separately in boiling ethanol (10 cm³), with the solutions mixed together and stirred for 1 h. The reaction mixture was refrigerated overnight, resulting in white crystals which were filtered off and dried *in vacuo*. Yield 0.32 g, 20%. (Found: C, 57.7; H, 3.9. Calc. for $C_{72}H_{60}As_4Cl_3O_4Y$: C, 58.3; H, 4.1%.) IR (cm⁻¹)(CsI disc): 1440m, 1359m, 1186w, 1089m, 1071w, 1026w, 999w, 894vs (AsO), 744s, 693s, 553w, 481s, 376m, 365s, 273m, 260s. ¹H NMR (300 K, CDCl₃): 7.3 – 7.8 (m). Λ_m (10⁻³ mol dm⁻³ CH₂Cl₂) = 31 ohm⁻¹ cm² mol⁻¹.

[YBr$_2$(Ph$_3$AsO)$_4$]Br

Prepared similarly to [YCl$_2$(Ph$_3$AsO)$_4$]Br. Yield 0.89 g, 55%. (Found: C, 53.0; H, 3.8. Calc. for C$_{72}$H$_{60}$As$_4$Br$_3$O$_4$Y: C, 53.4; H, 3.7%.) IR (cm^{-1})(CsI disc): 1440m, 1359m, 1089m, 1071w, 1025w, 999w, 893vs (AsO), 744s, 691s, 478s, 368s, 338sh, 272m, 243m. ^{1}H NMR (300 K, CDCl$_3$): 7.2 – 7.8 (m). Λ_m (10^{-3} mol dm^{-3} CH$_2$Cl$_2$) = 23 ohm^{-1} cm^2 mol^{-1}.

[YI$_2$(Ph$_3$AsO)$_4$]I$_5$

Prepared similarly to [YCl$_2$(Ph$_3$AsO)$_4$]Cl, yielding dark brown crystals. Yield 0.56 g, 25%. (Found: C, 38.2; H, 2.9. Calc. for C$_{72}$H$_{60}$As$_4$I$_7$O$_4$Y: C, 38.1; H, 2.7%.) IR (cm^{-1})(CsI disc): 1484m, 1440m, 1360w, 1186w, 1088s, 1025w, 999m, 893vs (AsO), 740s, 691s, 477s, 457m, 367m, 356m, 273w, 244w. ^{1}H NMR (300 K, CDCl$_3$): 7.2 – 7.8 (m). Λ_m (10^{-3} mol dm^{-3} CH$_2$Cl$_2$) = 41 ohm^{-1} cm^2 mol^{-1}.

[Y(Me$_3$AsO)$_6$]Cl$_3$

10 cm^3 boiling ethanolic solutions of YCl$_3$.6H$_2$O (0.15 g, 0.5 mmol) and Me$_3$AsO (0.41 g, 3.0 mmol) were mixed and allowed to cool to room temperature. The solvent was removed *in vacuo* leaving a pale yellow oil. This was dissolved in ice-cold acetone and on standing for 1 h produced a white powder which was filtered off and dried *in vacuo*. Yield 0.22 g, 43%. (Found: C, 21.0; H, 5.2. Calc. for C$_{18}$H$_{54}$As$_6$Cl$_3$O$_6$Y: C, 21.3; H, 5.4%.) IR (cm^{-1})(CsI disc): 2896w, 1418m, 1359s, 1269m, 1097w, 925w, 877s (AsO), 648s, 344s, 285m. ^{1}H NMR (300 K, d$_3$-MeNO$_2$): 2.0(s). Λ_m (10^{-3} mol dm^{-3} MeNO$_2$) = 224 ohm^{-1} cm^2 mol^{-1}.

3.4.6 Crystallographic studies

Details of the crystallographic data collection and refinement parameters are given in Table 3.9.

[YCl$_2$(Ph$_3$PO)$_4$]Cl.2.5EtOH.H$_2$O

Plate-like crystals were obtained by vapour diffusion of Et$_2$O into a CH$_2$Cl$_2$ solution of [YCl$_2$(Ph$_3$PO)$_4$]Cl in a refrigerator. Refinement on F^2 was conducted using SHELXL 97 and was routine.[25] Data processing used the SORTAV absorption

correction. Phenyl H atoms were introduced in calculated positions. Solvent molecules appeared during refinement, with one ethanol molecule given a reduced occupancy in order to obtain adp's similar to the other two EtOH molecules.

[YBr$_2$(Ph$_3$PO)$_4$]PF$_6$.Et$_2$O

Plate-like crystals were formed by vapour diffusion of Et$_2$O into a dichloromethane solution of the compound, the recrytallisation cell held in a refrigerator. Full-matrix least squares refinement on F was carried out in TEXSAN.[26] One Et$_2$O molecule appeared in the electron density map and was modelled. Phenyl H atoms were added in calculated positions.

[Y(Me$_3$PO)$_6$]Br$_3$

Small block crystals were obtained from the synthesis. Refinement using the DIRDIF[27] program was straightforward. Methyl H atoms were added in calculated positions.

Table 3.9 Crystallographic data collection and refinement parameters

	$[YCl_2(Ph_3PO)_4]Cl.2.5EtOH.H_2O$	$[YBr_2(Ph_3PO)_4]PF_6.Et_2O$	$[Y(Me_3PO)_6]Br_3$
Formula	$C_{72}H_{60}Cl_3O_4P_4Y + C_5H_{17}O_{3.5}$	$C_{72}H_{60}Br_2F_6O_4P_5Y$	$C_{18}H_{54}Br_3O_6P_6Y$
Formula weight	1441.53	1580.96	881.08
Crystal system	Monoclinic	Triclinic	Monoclinic
Space group	$P2_1/c$ (No. 14)	$P\bar{1}$ (No. 2)	$C2/c$ (No. 15)
a / Å	14.3599(3)	13.1913(1)	17.5730(9)
b / Å	17.5316(4)	14.9556(2)	16.9269(9)
c / Å	29.1891(7)	18.1360(2)	12.5446(7)
α / °	90	98.1110(4)	90
β / °	97.748(1)	94.1310(4)	95.304(3)
γ / °	90	96.2750(8)	90
U / Å^3	7281.3(3)	3506.99(6)	3715.5(3)
Z	4	2	4
μ(Mo-K$_\alpha$) / cm^{-1}	10.52	21.57	50.93
No. unique reflections	13067	14107	18877
R_{int}	0.099	0.087	-
No. of obs. reflections [a]	13067	9456	8505
No. parameter/restraint	847/0	856/0	156/0
R [b]	0.068	0.079	0.079
wR_2 [c]	0.175	-	-
wR [d]	-	0.086	0.078

[a] Observed if $[I_o > 2\sigma(I_o)]$ [b] $R = \sum (|F_{obs}|_i - |F_{calc}|_i) / \sum |F_{obs}|_i$ [c] $wR_2 = [\sum w(F_{obs}^2 - F_{calc}^2)^2 / \sum w(F_{obs}^2)^2]^{1/2}$ [d] $wR = \sqrt{[\sum w_i(|F_{obs}|_i - |F_{calc}|_i)^2 / \sum w_i |F_{obs}|_i^2}$

3.5 References

1. L. R. Melby, N. J. Rose, E. Abramson and J. C. Carris, *J. Am. Chem. Soc.*, 1964, **86**, 5117.

2. D. R. Cousins, F. A. Hart, *J. Inorg. Nucl. Chem.*, 1967, **29**, 1745.

3. D. R. Cousins, F. A. Hart, *J. Inorg. Nucl. Chem.*, 1967, **29**, 2965.

4. D. R. Cousins, F. A. Hart, *J. Inorg. Nucl. Chem.*, 1968, **30**, 3009.

5. J. V. Kingston, E. M. Krankovitz, R. J. Magee, *Inorg. Nucl. Chem. Lett.*, 1969, **5**, 485.

6. T. S. Lobana in *The Chemistry of Organophosphorus Compounds*, ed. F. R. Hartley, Wiley, New York, 1992, Volume 2, p. 409.

7. E. Giesbrecht, *Pure Appl. Chem.*, 1979, **51**, 925.

8. H.-K. Wang, M.-J. Zhang, X.-Y. Jing, J.-T. Wang, R.-J. Wang, H.-G. Wang, *Inorg. Chim. Acta*, 1989, **163**, 19.

9. H. Gehrke Jr., R. De Jong, *Proc. S. Dak. Acad. Sci.*, 1968, **47**, 210 (Chem. Abs. **71** (1969) 108605f).

10. P. Sobota, S. Szafert, J. Utko, *Inorg. Chem.*, 1994, **33**, 5203.

11. Q. Chen, Y. D. Chang, J. Zubieta, *Inorg. Chim. Acta*, 1997, **258**, 257.

12. G. R. Willey, P. R. Meehan, P. A. Salter, W. Errington, *Polyhedron*, 1996, **15**, 3193.

13. J.-S. Li, B. Neumuller, T. Dehnicke, *Zeit. Anorg. Alrg. Chem.*, 2002, **628**, 45.

14. S. Joseph, P. K. Radhakrishnan, *Polyhedron*, **18**, 1881.

15. M. K. M. Nair, P. K. Radhakrishnan, *Synth. React. Inorg. Met.-Org. Chem.*, 1996, **26**, 529.

16. R. Pastorek, *Chem. Zvesti*, 1979, **33**, 74.

17. G. M. Begun, A. C. Rutenberg, *Inorg. Chem.*, 1967, **6**, 2212.

18. I. R. Beattie, T. Gilson, K. Livingston, V. Fawcett and G. A. Ozin, *J. Chem. Soc. A.*, 1967, 712.

19. B. Neumuller, R. Meyer, Z. Kocher and K. Dehnicke, *Z. Krystallogr.*, 1994, **209**, 90.

20. W. J. Geary, *Coord. Chem. Rev.*, 1971, 7, 81.

21. W. Levason, B. Patel, M. C. Popham, G. Reid and M. Webster, *Polyhedron*, 2001, **20**, 2711.

22. A. Merijanian, R. A. Zingaro, *Inorg. Chem.*, 1966, **5**, 187.

23. F. Canziani, F. Zingales and U. Sartorelli, *Gazz. Chim. Ital.*, 1964, **94**, 848.

24. A. R. J. Genge, W. Levason, G. Reid, *Inorg. Chim. Acta*, 1999, **288**, 142.

25. G. M. Sheldrick, SHELXL 97, Crystal structure refinement program, University of Göttingen, 1997.

26. TEXSAN, Single crystal structure analysis software, Version 1.7-1, Molecular Structure Corporation, The Woodlands, TX, 1995.

27. P. T. Beurskens, G. Admiraal, G. Beurskens, W. P. Bosman, S. Garcia-Granda, R. O. Gould, J. M. M. Smits and C. Smykalla, The DIRDIF program system, University of Nijmegen, 1992.

Chapter 4

Complexes of Scandium Halides with Tertiary Phosphine and Arsine Oxide Ligands

4.1 Introduction

Whilst studies into the chemistry of scandium have accelerated in recent years, it is still the least studied 3d element. Indeed, no complexes of scandium halides with phosphine or arsine oxide ligands have been structurally characterized, although *in situ* ^{45}Sc NMR studies of $ScCl_3$ / $(RO)_3PO$ systems do include a brief mention of complexes with Ph_3PO, with the species $[ScCl_3(Ph_3PO)_3]$ (both *mer* and *fac* isomers), $[ScCl_3(MeCN)_2(Ph_3PO)]$ and $[ScCl_3(MeCN)(Ph_3PO)_2]$ identified.[1] However, with this exception, no studies of R_3PO ligands with scandium halides were found in the literature.

Further ^{45}Sc NMR studies of scandium halide–phosphate systems have been conducted,[2, 3] whilst other solution studies examining the extraction of scandium from aqueous HCl solutions using phosphates have been conducted.[4] Similar extraction experiments with sulfoxides have been examined and a series of complexes of scandium salts with Ph_2SO have been reported.[5, 6]

Tetrahydrofuran complexes of scandium halides have received a relatively large amount of attention, ranging from the synthesis and characterisation of anhydrous $[ScCl_3(THF)_3]$[7, 8] (Fig. 4.1), formed by gently warming anhydrous $ScCl_3$ in an excess of dry THF, to the controlled hydrolysis of the THF adduct to replace the coordinated solvent with H_2O in a stepwise fashion.[9] By halide abstraction in THF, further solvent molecules can be coordinated to the scandium centre.[10]
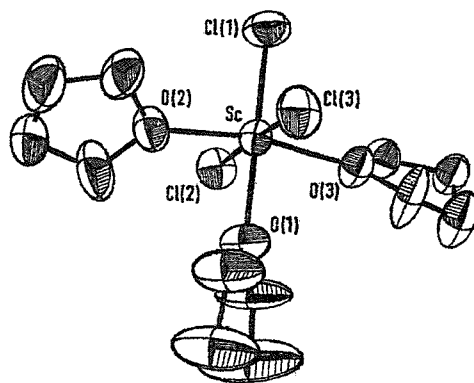
Fig. 4.1 View of the complex $[ScCl_3(thf)_3]$.[8]

Further oxygen donor chemistry is examined in a series of papers by Willey et al., exploring complexes of crown ethers with scandium chloride, demonstrating different coordination numbers around scandium centres from the eight-coordinate sandwich cation $[Sc([12]\text{-crown-4})_2]^{3+}$ to seven-coordinate $[ScCl_2([15]\text{-crown-5})]^+$ and including ^{45}Sc NMR studies (see Chapter 5).[11-14]

As seen for yttrium halides, some Schiff base chemistry has been examined. For example, the compound $[Sc(2,6\text{-diacetylpyridine})H_2O]Cl_3.5H_2O$ (Ligand shown in Fig. 4.2) has been reported.[15] Pyridine adducts of scandium derived from $[ScCl_3(thf)_3]$ have also been studied.[16] For example, the complex $[[(Me_3Si)_2N]_3Sc(THF)]$ was initially prepared by reaction of $[ScCl_3(thf)_3]$ with three equivalents $Na(SiMe_3)$ in hexane. Addition of pyridine to a solution of $[[(Me_3Si)_2N]_3Sc(THF)]$ in hexane produced the complex $[[(Me_3Si)_2N]_3Sc(py)]$.[16]
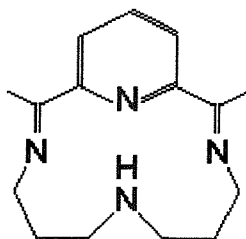
Fig. 4.2 The ligand "2,6-diacetylpyridine" which reacts with hydrated scandium chloride in ethanol to afford the complex $[Sc(2,6\text{-diacetylpyridine})H_2O]Cl_3.5H_2O$.[15]

This study aims to reveal the coordination chemistry of scandium halides with R_3PO and R_3AsO ligands. With no previous studies into compounds of this type, the initial aim was to probe what complexes could be synthesised. The results would allow a simple comparison of the coordination chemistry of scandium with that of yttrium, given results detailed in Chapter 3. In addition, further examination of the ligating powers of R_3PO and R_3AsO would be possible. Finally, the study offered a chance to examine how these complexes behave in solution, probed by molar conductance and multinuclear NMR spectroscopy.

4.2 Results and Discussion

4.2.1 Complexes of scandium halides with triphenylphosphine oxide

The reaction of $ScCl_3.6H_2O$ with three to six molar equivalents of triphenylphosphine oxide in ethanol yielded white $[ScCl_2(Ph_3PO)_4]Cl$. Similar reactions with $ScBr_3.6H_2O$ and $ScI_3.8H_2O$ yielded white $[ScBr_2(Ph_3PO)_4]Br$ and yellow $[ScI_2(Ph_3PO)_4]I$. Attempts to isolate $[ScCl_3(Ph_3PO)_3]$ were unsuccessful, even when using 1:1 metal to ligand ratios used in ethanol and acetone, but evidence for its existence was seen in solution (see below). $ScF_3.1/2H_2O$ did not react with Ph_3PO in boiling ethanol or acetone, even with longer reaction times.

The IR spectrum of $[ScCl_2(Ph_3PO)_4]Cl$ exhibited $v(PO) = 1152$ cm^{-1} (compared to 1195 cm^{-1} for the 'free' ligand), $[ScBr_2(Ph_3PO)_4]Br.CH_2Cl_2$ had $v(PO) = 1137$ cm^{-1} whilst the iodide complex had a strong band at 1132 cm^{-1}, with water identified by a broad band at 3466 cm^{-1} and a sharp band at 1624 cm^{-1}. It was apparent that moving along the halide series Cl→Br→I, the value of $v(PO)$ shifts to lower wavenumbers, as seen for the analogous yttrium halide complexes described in Section 3.2.1.

The $^{31}P-\{^1H\}$ NMR spectrum of $[ScCl_2(Ph_3PO)_4]Cl$ in CH_2Cl_2 contained a strong resonance at 34.5 ppm, with weaker features at 34.0, 33.0 (ratio of integrals approximately 2:1) and 26.0 (Ph_3PO) ppm. Addition of an excess of Ph_3PO to this solution resulted in the loss of the weaker resonances at 34.0 and 33.0 ppm, suggesting they could be assigned to the axial and equitorial ligands in *mer*-$[ScCl_3(Ph_3PO)_3]$, formed by decomposition in solution. The ^{45}Sc NMR spectrum of the initial solution contained a broad resonance at δ 75 ppm ($W_{1/2} = 850$ Hz), with a weaker and broader resonance at δ 121 ppm ($W_{1/2} = 1400$ Hz). Following addition of Ph_3PO, the resonance at 121 ppm was not observed, consistent with its assignment as $[ScCl_3(Ph_3PO)_3]$. The complex had $\Lambda_m = 17$ ohm^{-1}cm^{2}mol^{-1}, rising to 22 ohm^{-1} cm^2 mol^{-1} following addition of Ph_3PO, helping to confirm the presence of the non-electrolyte $[ScCl_3(Ph_3PO)_3]$ in small quantities in solution. A summary of the multinuclear NMR data for the ScX_3 / Ph_3PO system can be found in Table 4.1.

^{31}P-$\{^1$H$\}$ NMR spectroscopy for a CH_2Cl_2 solution of [ScBr$_2$(Ph$_3$PO)$_4$]Br exhibited a single resonance at δ 35.8 ppm, remaining unchanged upon addition of excess Ph$_3$PO (demonstrating that no tris(phosphine oxide) complex exists in solution). This contrasted with the decomposition observed for solutions of [ScCl$_2$(Ph$_3$PO)$_4$]Cl. The ^{45}Sc NMR spectrum had a very broad resonance at δ 108 ppm ($W_{1/2}$ = 4500 Hz), with no change occurring after addition of further Ph$_3$PO, confirming only a single species existed in solution. Similarly, the ^{31}P-$\{^1$H$\}$NMR spectrum for [ScI$_2$(Ph$_3$PO)$_4$]I.2H$_2$O contained a single resonance (δ 38.0 ppm) which remained unchanged after addition of Ph$_3$PO. In contrast to the chloro- and bromo-complexes, the ^{45}Sc NMR spectrum was extremely broad ($W_{1/2}$ = 20000 Hz), centred at ca. 200 ppm. This seems a reasonable chemical shift for [ScI$_2$(Ph$_3$PO)$_4$]I by comparison with other ^{45}Sc data (Table 4.1 and Fig. 4.5). Owing to the large line width, further resonances could conceivably be obscured or masked, although given the ^{31}P-$\{^1$H$\}$ NMR data and molar conductance data this seems unlikely. The presence of water was confirmed by a broad singlet at δ 1.7 ppm in the ^{1}H NMR spectrum. The large line widths observed in the ^{45}Sc NMR spectra indicate a significant electric field gradient, allowing fast quadrupolar relaxation at the ^{45}Sc nucleus, with increasing line width along the series from Cl→Br→I. This behaviour is explained by the increasing difference in electronic environment between the hard O of the R$_3$EO ligand and the softer halides.

The molar conductances for dichloromethane solutions of both [ScBr$_2$(Ph$_3$PO)$_4$]Br and [ScI$_2$(Ph$_3$PO)$_4$]I were consistent with 1 : 1 electrolytes (Λ_m = 21 and 22 ohm^{-1} cm^2 mol^{-1}),[17] with no significant change upon addition of Ph$_3$PO.

Table 4.1 Multinuclear NMR spectroscopic data for complexes of scandium(III) halides with triphenylphosphine oxide.

Complex	δ (^{31}P-$\{^1$H$\}$)	δ (^{45}Sc)	$W_{1/2}$ (Hz)
[ScCl$_2$(Ph$_3$PO)$_4$]Cl	34.5	75	850
[ScCl$_3$(Ph$_3$PO)$_3$][a]	34.0, 33.0	121	1400
[ScBr$_2$(Ph$_3$PO)$_4$]Br	35.8	108	4500
[ScI$_2$(Ph$_3$PO)$_4$]I	38.0	ca. 200	ca. 20000

[a] Identified in solution only.

The structure of $[ScBr_2(Ph_3PO)_4]Br.1/2Et_2O$ (Fig. 4.3) reveals a six coordinate scandium centre with *trans* octahedral geometry. The angles were close to the idealised values (Br-Sc-Br = 179.04°, Br-Sc-O = 88.6(3)-91.3(3)°). The Sc-Br distances seem to be the first reported examples (Sc-Br = 2.652(1) and 2.661(1) Å). The Sc-O-P angles range from 153.6(2) to 166.5(2)° (Ave. = 160.6°), showing less variation than the analogous yttrium cation for which Y-O-P(ave.) = 164.1° (see 3.2.1). Selected bond lengths and angles are given in Table 4.2.
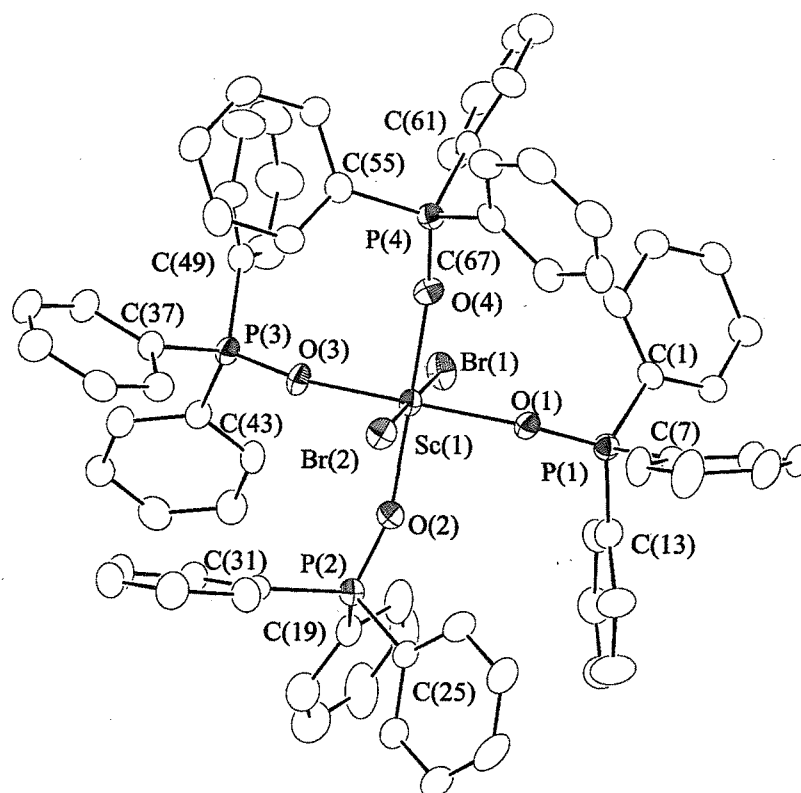
Fig. 4.3 The structure of the cation in $[ScBr_2(Ph_3PO)_4]Br.1/2Et_2O$. H atoms omitted for clarity. Ellipsoids are drawn at 40% probability.

Table 4.2 Selected bond lengths (Å) and angles (°) for the structure of [ScBr$_2$(Ph$_3$PO)$_4$]Br.1/2Et$_2$O.

Sc-O(1)	2.090(4)	Sc-Br(1)	2.652(1)
Sc-O(2)	2.057(4)	Sc-Br(2)	2.661(1)
Sc-O(3)	2.059(4)	O(n)-P(n)	1.504(4)-1.512(4)
Sc-O(4)	2.074(4)		
Sc-O(1)-P(1)	153.6(2)	Sc-O(3)-P(3)	163.0(2)
Sc-O(2)-P(2)	159.1(3)	Sc-O(4)-P(4)	166.5(2)
Br(1)-Sc-Br(2)	179.04(5)	O(n)-Sc-Br(n)	88.6(3)-91.3(3)

4.2.2 Complexes of scandium halides with diphenylmethylphosphine oxide

When ScCl$_3$.6H$_2$O was reacted with three molar equivalents of Ph$_2$MePO in boiling acetone, the product isolated was [ScCl$_3$(Ph$_2$MePO)$_3$].H$_2$O. In contrast, reaction of ScBr$_3$.6H$_2$O with diphenylmethylphosphine oxide in ice-cold acetone yielded [ScBr$_2$(Ph$_2$MePO)$_4$]Br. No pure iodo-complexes could be isolated. The complex [ScCl$_2$(Ph$_2$MePO)$_4$]Cl could not be isolated, despite observation of the [ScCl$_2$(Ph$_2$MePO)$_4$]$^+$ cation in solution.

The infrared spectrum of [ScCl$_3$(Ph$_2$MePO)$_3$].H$_2$O contained ν(PO) = 1143 cm^{-1}, with water apparent from the broad band at 3420 cm^{-1}, and a sharper peak at 1643 cm^{-1}. The presence of H$_2$O was confirmed by a broad singlet at 1.7 ppm in the ^{1}H NMR spectrum. The IR spectrum of [ScBr$_2$(Ph$_2$MePO)$_4$]Br exhibited ν(PO) = 1138 cm^{-1}.

The ^{31}P-{^{1}H} NMR spectrum of [ScCl$_3$(Ph$_2$MePO)$_3$] in CH$_2$Cl$_2$ contained resonances at δ 29.0 (Ph$_2$MePO), 40.5, 42.4 and 42.5 ppm. The peaks at 40.5 and 42.5 ppm had integrals of 1:2, leading to their assignment to the inequivalent phosphine oxide resonances of mer-[ScCl$_3$(Ph$_2$MePO)$_3$]. Addition of Ph$_2$MePO to this solution led to complete conversion to the species with the resonance at δ 42.4 ppm, suggesting this could be due to [ScCl$_2$(Ph$_2$MePO)$_4$]$^+$. The ^{45}Sc NMR spectrum of [ScCl$_3$(Ph$_2$MePO)$_3$] . contained two peaks at δ 80 and 123 ppm, the latter significantly stronger. Addition of Ph$_2$MePO to the solution caused growth of the minor peak, leading to the

assignment of the resonance at δ 80 as $[ScCl_2(Ph_2MePO)_4]Cl$, with the species at δ 123 being $[ScCl_3(Ph_2MePO)_3]$. Multinuclear NMR spectroscopic data are summarised in Table 4.3. The molar conductance data for a CH_2Cl_2 solution of $[ScCl_3(Ph_2MePO)_3]$ supported these conclusions with $\Lambda_m = 8$ $ohm^{-1}cm^2mol^{-1}$, consistent with a non-electrolyte. Addition of Ph_2MePO led to $\Lambda_m = 23$ $ohm^{-1}cm^2$ mol^{-1} (typical of a 1:1 electrolyte).

In contrast to the chloro-complex, the $^{31}P\text{-}\{^1H\}$ NMR spectrum of $[ScBr_2(Ph_2MePO)_4]Br$ contained a resonance at δ 41.0 ppm, and remained unchanged upon addition of excess ligand to the solution. Similarly, the ^{45}Sc NMR spectrum exhibited a single resonance at δ 100 ppm. The molar conductance was 22 ohm^{-1} cm^2 mol^{-1} for a 10^{-3} mol dm^{-3} dichloromethane solution of this complex, indicating the compound was a 1:1 electrolyte, confirming that $[ScBr_3(Ph_2MePO)_3]$ was not present in any significant quantity.

Table 4.3 Multinuclear NMR spectroscopic data for complexes of scandium(III) halides with diphenylmethylphosphine oxide.

Complex	δ ($^{31}P\text{-}\{^1H\}$)	δ (^{45}Sc)	$W_{1/2}$ (Hz)
$[ScCl_3(Ph_2MePO)_3]$	40.5, 42.5	123	1100
$[ScCl_2(Ph_2MePO)_4]Cl^a$	42.4	80	2000
$[ScBr_2(Ph_2MePO)_4]Br$	41.0	100	8000

[a] Identified in solution only.

4.2.3 Complexes of scandium halides with trimethylphosphine oxide

The reaction of $ScCl_3.6H_2O$ with six molar equivalents of Me_3PO afforded $[ScCl(Me_3PO)_5]Cl_2$. In contrast, reactions with $ScBr_3.6H_2O$ or $ScI_3.8H_2O$ with Me_3PO yielded $[Sc(Me_3PO)_6]X_3$ (X = Br or I). In common with all the homoleptic Me_3PO complexes isolated throughout these studies, the bromo- and iodo-complexes were poorly soluble in chlorocarbons, ethanol or acetone but dissolved in $MeNO_2$. An

attempt to abstract the coordinated chloride in $[ScCl(Me_3PO)_5]Cl_2$ with antimony pentachloride in anhydrous MeCN was unsuccessful, with no reaction apparent.

The infrared spectra of all three compounds were simple:- $[ScCl(Me_3PO)_5]Cl_2$ contained $v(PO) = 1109$ cm^{-1}, $[Sc(Me_3PO)_6]Br_3$ had $v(PO) = 1110$ cm^{-1} and $[Sc(Me_3PO)_6]I_3$ exhibited $v(PO) = 1108$ cm^{-1}.

The $^{31}P\text{-}\{^1H\}$ NMR spectrum of $[ScCl(Me_3PO)_5]Cl_2$ in nitromethane showed a mixture of species present, with resonances at δ 36.5 (Me_3PO), 54.0, 54.5 and 56.0 ppm. The intensities of the peaks at 54.5 and 56.0 ppm were in a 1 : 4 ratio, suggesting they could be attributed to the inequivalent phosphorus centres in $[ScCl(Me_3PO)_5]Cl_2$. The resonance at 54.0 disappeared following addition of Me_3PO, leading to its tentative assignment as $[ScCl_2(Me_3PO)_4]Cl$. The ^{45}Sc NMR spectrum of this complex in $MeNO_2$ consisted of resonances at δ 47.0 and 84.5 ppm. On addition of excess Me_3PO, only $[ScCl(Me_3PO)_5]Cl_2$ (δ 47.0 ppm) remained, along with very minor resonances at δ 11 and 4 ppm. The latter was attributed to a very small quantity of $[Sc(Me_3PO)_6]Cl_3$. The peak at δ 11 ppm was apparent in the spectra of all three scandium halide / Me_3PO complexes. On addition of Me_3PO this resonance disappeared, whilst it was absent if the spectra were run in acetone (although the solubility of the complexes in Me_2CO is poor). Hence, the peak was tentatively assigned as $[Sc(Me_3PO)_{6-n}(MeNO_2)_n]^{3+}$. The ^1H NMR spectrum of $[ScCl(Me_3PO)_5]Cl_2$ was complex, indicating a mixture of species was present in solution. The molar conductance in nitromethane solution was 117 ohm^{-1} cm^2 mol^{-1}, a value in between that of a 1:1 and 2:1 electrolyte, rising to 180 ohm^{-1} cm^2 mol^{-1} upon addition of Me_3PO, typical of a 2:1 electrolyte.[17]

The $^{31}P\text{-}\{^1H\}$ NMR spectrum of $[Sc(Me_3PO)_6]Br_3$ in $MeNO_2$ contained four resonances at δ 36.5 (Me_3PO), 56.5 $([Sc(Me_3PO)_6]Br_3)$, 56.0 and 55.0 ppm (in a 4:1 ratio, suggesting $[ScBr(Me_3PO)_5]Br_2$). On addition of excess Me_3PO, the resonance at 56.5 ppm grew, with coupling observed with eight lines of equal intensity due to coupling to ^{45}Sc. The resonances at 56.0 and 55.0 remained as weak features. The

^{45}Sc NMR spectrum of the solution prior to addition of Me$_3$PO exhibited resonances at δ 4.5 ([Sc(Me$_3$PO)$_6$]Br$_3$), 11.0 ([Sc(Me$_3$PO)$_{6-n}$(MeNO$_2$)$_n$]$^{3+}$) and 51.5 ppm ([ScBr(Me$_3$PO)$_5$]Br). Following Me$_3$PO addition, the equilibrium position was shifted towards [Sc(Me$_3$PO)$_6$]Br$_3$, with well defined septet coupling (Fig. 4.4), indicating the scandium metal centre is in a cubic environment of six equivalent phosphorus nuclei with slow relaxation as a result. Multinuclear NMR data are summarised in Table 4.4.

δ / ppm
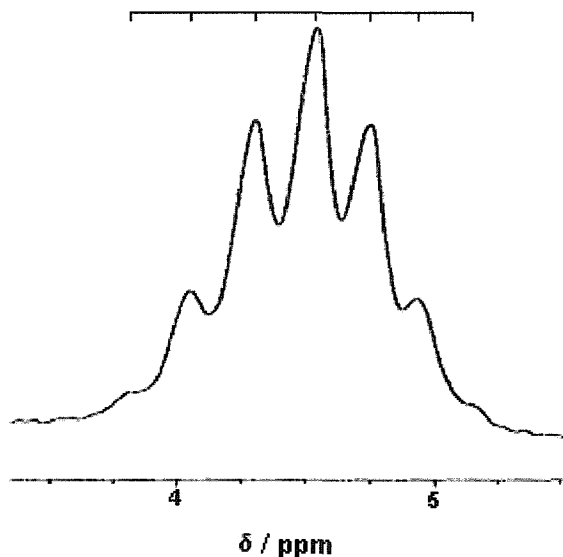
Fig. 4.4 ^{45}Sc NMR spectrum of [Sc(Me$_3$PO)$_6$]Br$_3$ in MeNO$_2$ with excess Me$_3$PO showing a binomial septet.

The ^{31}P-{^{1}H} NMR spectrum of [Sc(Me$_3$PO)$_6$]I$_3$ in MeNO$_2$ was simple, with a single species present at δ 57.5 ppm, the spectrum remaining unchanged after addition of Me$_3$PO. The ^{45}Sc NMR spectrum contained two resonances at δ 4.0 and 9.0 ppm, the former attributable to [Sc(Me$_3$PO)$_6$]$^{3+}$. When excess Me$_3$PO was added, the resonance at 9.0 ppm disappeared, suggesting it was due to [Sc(Me$_3$PO)$_{6-n}$(MeNO$_2$)$_n$]$^{3+}$.

Table 4.4 Multinuclear NMR spectroscopic data for complexes of scandium(III) halides with trimethylphosphine oxide.

Complex	δ (^{31}P-{^{1}H})	δ (^{45}Sc)	$W_{1/2}$ (Hz)	^{2}J(^{31}P-^{45}Sc)/Hz
[ScCl(Me$_3$PO)$_5$]Cl$_2$	56.0, 54.5	47.0	250	-
[ScCl$_2$(Me$_3$PO)$_4$]Cl[a]	54.0	85.0	360	-
[Sc(Me$_3$PO)$_6$]Br$_3$	56.5 (octet)	4.4 (septet)	-	19.0
[ScBr(Me$_3$PO)$_5$]Br$_2$[a]	56.0, 55.0	51.5	850	-
[Sc(Me$_3$PO)$_6$]I$_3$	57.0 (octet)	4.2 (septet)	-	19.0

[a] Identified in solution only.

4.2.4 Complexes of scandium halides with triphenylarsine oxide

The reaction of ScCl$_3$.6H$_2$O with four molar equivalents Ph$_3$AsO in ethanol gave *trans*-[ScCl$_2$(Ph$_3$AsO)$_4$]Cl.2EtOH. The analogous reaction with scandium bromide afforded [ScBr$_2$(Ph$_3$AsO)$_4$]Br.5H$_2$O. No analytically pure iodide compound could be isolated, although spectroscopic data appeared to suggest the cation was similar to the bromo- and chloro-complexes. Both [ScCl$_2$(Ph$_3$AsO)$_4$]Cl.2EtOH and [ScBr$_2$ (Ph$_3$AsO)$_4$]Br.5H$_2$O appeared to be air and moisture stable whilst the pale yellow iodo-complexes darkened in colour upon exposure to air, due to liberation of diiodine. Hence, the varying analyses for iodo-compounds were attributed to differing iodide/polyiodide anions.

The infrared spectrum of [ScCl$_2$(Ph$_3$AsO)$_4$]Cl.2EtOH had v(AsO) = 908 cm^{-1}, with ethanol of solvation apparent as a broad band centred at 3407 cm^{-1}, its presence confirmed by the characteristic resonances in the ^{1}H NMR spectrum. [ScBr$_2$(Ph$_3$AsO)$_4$]Br.5H$_2$O contained v(AsO) = 883 cm^{-1}, water apparent by a broad band at 3400 cm^{-1} and a sharper band at 1654 cm^{-1}. The ^{1}H NMR spectrum had a broad singlet at δ 1.8 ppm, with the integrals confirming five H$_2$O molecules were present. The iodo-compound exhibited v(AsO) = 883 cm^{-1}.

The ^{45}Sc NMR spectrum of [ScCl$_2$(Ph$_3$AsO)$_4$]Cl in CH$_2$Cl$_2$ had a single, broad resonance at δ 96 ppm ($W_{1/2}$ = 4000 Hz), with no evidence observed for decomposition to [ScCl$_3$(Ph$_3$AsO)$_3$], contrasting with the solution behaviour of [ScCl$_2$(Ph$_3$PO)$_4$]Cl (see 4.2.1). The ^{45}Sc NMR spectrum of the bromide complex contained a significantly broader ($W_{1/2}$ = 18000 Hz) resonance centred at ca. 140 ppm. No resonances were observed for a solution of the iodo-complex, presumably because the line widths were unobservably broad. The ^{45}Sc NMR data is summarised in Table 4.5, with data for the Ph$_3$PO analogues also included for comparison. The line widths moving from Cl→Br→I were broader than for the Ph$_3$PO system, with the iodide compound noticeably too broad for observation. This behaviour is due to a greater disparity between the harder O of Ph$_3$AsO and the increasingly softer halides compared to the difference when Ph$_3$PO was the ligand, causing faster quadrupolar relaxation because of the greater electric field asymmetry (see Chapter 1 for explanation). It is also clear that the ^{45}Sc NMR chemical shift increases when Ph$_3$AsO is the donor ligand (compared to shifts for Ph$_3$PO complexes). All three compounds were 1:1 electrolytes in dichloromethane solutions. The conductivities were unaffected on addition of further Ph$_3$AsO.

Table 4.5 ^{45}Sc NMR spectroscopic data for complexes of scandium(III) halides with Ph$_3$EO ligands (E = As or P) in dichloromethane solution.

Complex	δ (^{45}Sc)	$W_{1/2}$ (Hz)
[ScCl$_2$(Ph$_3$AsO)$_4$]Cl	96	4000
[ScCl$_2$(Ph$_3$PO)$_4$]Cl	75	850
[ScCl$_3$(Ph$_3$PO)$_3$][a]	121	1400
[ScBr$_2$(Ph$_3$AsO)$_4$]Br	ca. 140	18000
[ScBr$_2$(Ph$_3$PO)$_4$]Br	108	4500
[ScI$_2$(Ph$_3$AsO)$_4$]I	-	Unobservably broad
[ScI$_2$(Ph$_3$PO)$_4$]I	ca. 200	ca. 20000

[a] Identified in solution only.

The structure of $[ScCl_2(Ph_3AsO)_4]Cl.2EtOH$ was determined (Fig. 4.5), revealing *trans*-chlorides, with the geometry around the scandium centre octahedral, with angles close to those of an idealised octahedron (Cl-Sc-Cl = 179.8(1)°, O(n)-Sc-Cl(n) = 88.6(3)-91.3(3)°). The Sc-Cl bond lengths (2.562(4) & 2.545(4) Å) were *ca.* 0.15 Å longer than those observed for $[ScCl_3(thf)_3]$ or some reported $ScCl_3$ / crown ether complexes.[8, 12, 13] The Sc-O-As angles were more acute than the Sc-O-P angles observed for $[ScBr_2(Ph_3PO)_4]Br$ (Table 4.6) presumably owing to a combination of steric hindrance caused by the greater bulk of Br compared to the lighter Cl, and the added steric bulk of As compared to P. The Sc-O(As) distances were similar to those observed for $[Sc(Ph_3AsO)_3(NO_3)_2]NO_3$ (For $[Sc(Ph_3AsO)_3(NO_3)_2]NO_3$, Sc-O(As) = 1.996(4) to 2.030(4) c.f. 2.059(7) to 2.089(7) Å).
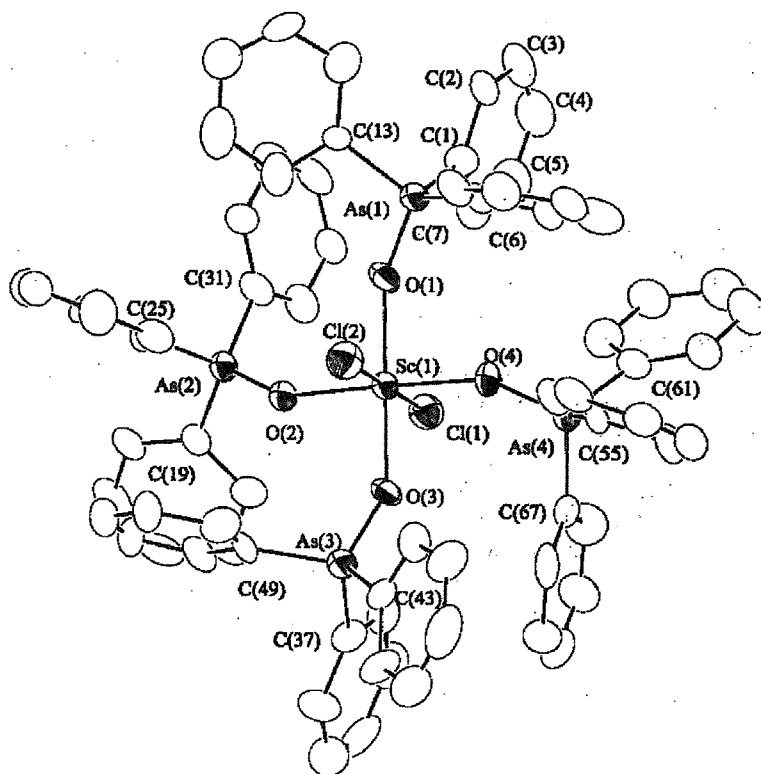
Fig. 4.5 The structure of the cation in $[ScCl_2(Ph_3AsO)_4]Cl$ showing the atom numbering scheme. Ellipsoids are drawn at the 40% probability level and H atoms are omitted for clarity.

Table 4.6 Selected bond lengths (Å) and angles (°) for the structure of [ScCl$_2$(Ph$_3$AsO)$_4$]Cl.

Sc-O(1)	2.079(7)	Sc-Cl(1)	2.562(4)
Sc-O(2)	2.089(7)	Sc-Cl(2)	2.545(4)
Sc-O(3)	2.059(7)	O(n)-As(n)	1.651(7)-1.668(7)
Sc-O(4)	2.063(7)		
Sc-O(1)-As(1)	146.6(4)	Sc-O(3)-As(3)	147.3(5)
Sc-O(2)-As(2)	145.4(5)	Sc-O(4)-As(4)	147.5(5)
Cl(1)-Sc-Cl(2)	179.8(1)	O(n)-Sc-Cl(n)	88.6(3)-91.3(3)

4.2.5 Complexes of scandium halides with trimethylarsine oxide

The reaction of Me$_3$AsO with ScCl$_3$.6H$_2$O in a 6 : 1 molar ratio in ethanol yielded white [Sc(Me$_3$AsO)$_6$]Cl$_3$, contrasting with the analogous reaction with Me$_3$PO which yielded the pentakis species [ScCl(Me$_3$PO)$_5$]Cl$_2$. Similar hexakis(arsine oxide) products were seen when using ScBr$_3$.6H$_2$O and ScI$_3$.8H$_2$O.

The infrared spectrum of the chloro-complex contained three strong bands at 924, 874 and 844 cm^{-1}, attributed to v(AsO) and methyl rocking modes (it is difficult to distinguish between these). The spectrum for [Sc(Me$_3$AsO)$_6$]Br$_3$ was similar, with bands at 926, 874 and 846 cm^{-1}, whilst the spectrum of [Sc(Me$_3$AsO)$_6$]I$_3$.3H$_2$O had bands at 921, 872 and 844 cm^{-1} in addition to absorptions assigned to water at 3440 (broad) and 1647 cm^{-1}. The presence of water was confirmed by a broad singlet at 1.7 ppm in the ^{1}H NMR spectrum.

The ^{45}Sc NMR spectum of [Sc(Me$_3$AsO)$_6$]Cl$_3$ in MeNO$_2$ contained a major resonance at δ 56.0 ppm, with a much weaker broad feature at δ 84 ppm. Addition of Me$_3$AsO to the solution caused the weak feature to disappear, suggesting it was due to [ScCl(Me$_3$AsO)$_5$]Cl$_2$. Molar conductance data in nitromethane solution supported this assignment, with addition of Me$_3$AsO to the solution causing Λ_m to rise from 214 ohm^{-1}cm^{2}mol^{-1} to 251 ohm^{-1}cm^{2}mol^{-1}, the latter typical of a 3 : 1 electrolyte.[17] In addition, two methyl resonances were observed in the ^{1}H NMR spectrum, singlets at

δ 2.1 and 2.05 ppm, the latter significantly weaker, suggesting the presence of a second (minor) complex. The spectra for both $[Sc(Me_3AsO)_6]Br_3$ and $[Sc(Me_3AsO)_6]I_3.3H_2O$ in $MeNO_2$ contained a single ^{45}Sc resonance in each at δ 56 ppm which remained unchanged on addition of Me_3AsO in both cases. ^{45}Sc NMR data are presented in Table 4.7, with the homoleptic compounds exhibiting narrower line widths than for $[ScCl(Me_3AsO)_5]Cl_2$ and other non-homoleptic complexes identified in this chapter. This strongly suggests that the scandium centres are in cubic symmetry environments. Both showed an increase in molar conductance when excess ligand was added, suggesting some (minor) coordinated halide species exist prior to this (although not enough to be detected by ^{45}Sc NMR spectroscopy).

Table 4.7 ^{45}Sc NMR spectroscopy data for the scandium halide-Me_3AsO complexes in nitromethane solution.

Complex	δ (^{45}Sc)	$W_{1/2}$ (Hz)
$[Sc(Me_3AsO)_6]Cl_3$	56	80
$[ScCl(Me_3AsO)_5]Cl_2{}^a$	84	400
$[Sc(Me_3AsO)_6]Br_3$	56	70
$[Sc(Me_3AsO)_6]I_3$	56	70

[a] Identified in solution only.

The structure of $[Sc(Me_3AsO)_6]Br_3$ was determined (Fig. 4.6) and as expected, the bond lengths and angles within the cation were very similar to those of $[Sc(Me_3AsO)_6][NO_3]_3$.
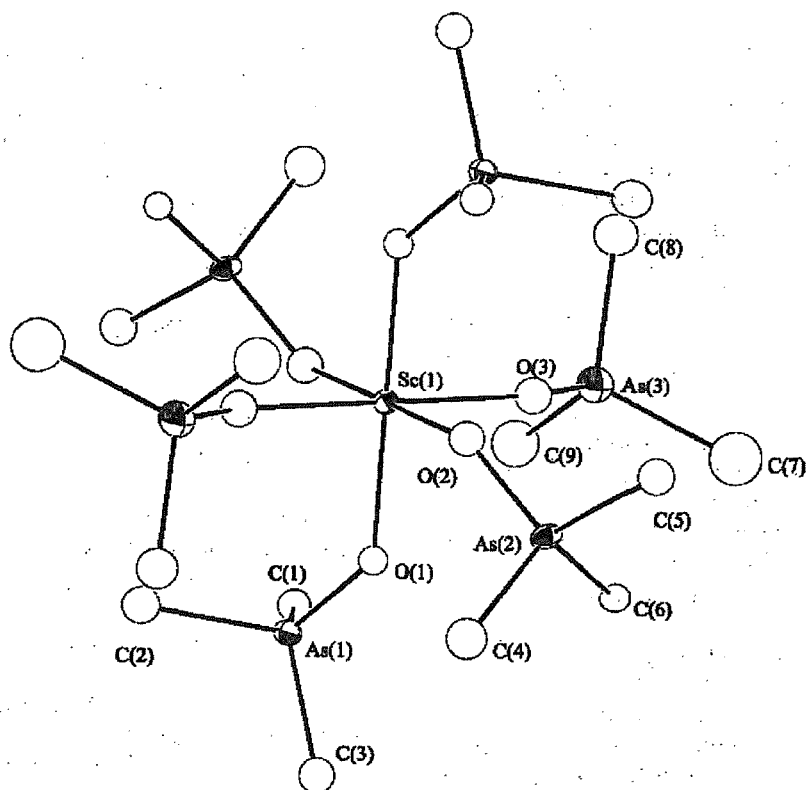
Fig. 4.6 View of the cation in $[Sc(Me_3AsO)_6]Br_3$ showing the atom numbering scheme. Ellipsoids are drawn at the 40% probability level and H atoms are omitted for clarity.

Table 4.8 Selected bond lengths (Å) and angles (°) for $[Sc(Me_3AsO)_6]Br_3$.

Sc-O(1)	2.08(2)	Sc-O(3)	2.11(2)
Sc-O(2)	2.11(2)	O(n)-As(n)	1.65(2)-1.69(2)
Sc-O(1)-As(1)	133.8(9)	O(1)-Sc-O(2)	89.5(6)
Sc-O(2)-As(2)	132.6(10)	O(1)-Sc-O(3)	90.5(7)
Sc-O(3)-As(3)	146.3(10)	O(2)-Sc-O(3)	88.3(6)

4.2.6 ^{45}Sc NMR studies

Whilst the ^{31}P nucleus is very sensitive, the chemical shifts were seen to vary very little between complexes in each ScX_3 / R_3PO system resulting in resonances which can be difficult to resolve owing to near coincidence. In contrast, the ^{45}Sc NMR chemical shifts

and line widths vary significantly (Table 4.9). For example, when the ^{45}Sc nucleus is in a high symmetry environment such as the ScO_6 species, resonances are relatively sharp whilst in contrast it was concluded that the resonance in $[ScI_2(Ph_3AsO)_4]I$ was unobservably broad. There is a possibility that resonances may be hidden underneath broader features. The line widths were seen to increase along the series Cl→Br→I, whilst changing from P to As also causes an increase in $W_{1/2}$.

Table 4.9 Comparison of ^{45}Sc NMR line widths between related R_3PO and R_3AsO complexes.

Complex	$W_{1/2}$ (Hz)	Complex	$W_{1/2}$ (Hz)
$[ScCl_2(Ph_3PO)_4]Cl$	850	$[ScBr(Me_3PO)_5]Br_2$	850
$[ScCl_3(Ph_3PO)_3]$	1400	$[ScCl_2(Ph_3AsO)_4]Cl$	4000
$[ScBr_2(Ph_3PO)_4]Br$	4500	$[ScBr_2(Ph_3AsO)_4]Br$	18000
$[ScI_2(Ph_3PO)_4]I$	*ca.* 20000	$[ScI_2(Ph_3AsO)_4]I$	Unobservable
$[ScCl_3(Ph_2MePO)_3]$	1100	$[Sc(Me_3AsO)_6]Cl_3$	80
$[ScCl_2(Ph_2MePO)_4]Cl$	2000	$[ScCl(Me_3AsO)_5]Cl_2$	400
$[ScBr_2(Ph_2MePO)_4]Br$	8000	$[Sc(Me_3AsO)_6]Br_3$	70
$[ScCl(Me_3PO)_5]Cl_2$	250	$[Sc(Me_3AsO)_6]I_3$	70
$[ScCl_2(Me_3PO)_4]Cl$	360		

The ^{45}Sc NMR chemical shifts exhibit systematic trends with donor set (Fig. 4.5). It was apparent that moving from Cl→Br→I, δ moves to higher frequency, whilst moving from R_3PO to R_3AsO also causes an increase in the value of δ. Similar behaviour was seen for the YX_3 / R_3EO system (Chapter 3). In contrast to the ^{89}Y NMR spectra, coupling patterns were not observed, with the exception of the highly symmetrical $[Sc(Me_3PO)_6]^{3+}$ species where the cubic environment causes slow relaxation of the

quadrupolar ^{45}Sc nucleus. It was evident through these studies that intermolecular exchange with added R_3EO (E = As or P) was slow on the NMR time scales.

$[Sc(OPMe_3)_6]^{3+}$ $\xrightarrow{43}$ $[Sc(OPMe_3)_5Cl]^{2+}$ $\xrightarrow{4.5}$ $[Sc(POMe_3)_5Br]^{2+}$

4   47   51.5

$\downarrow 52$ $\downarrow 37$ $\searrow 38$

                               $[Sc(OPMe_3)_4Cl_2]^{+}$

                                 85

$[Sc(OAsMe_3)_6]^{3+}$ $\xrightarrow{28}$ $[Sc(OAsMe_3)_5Cl]^{2+}$

56   84

$[ScCl_6]^{3-}$ $[ScBr_6]^{3-}$

249   288

$\uparrow 128$ $\uparrow 180$

$[Sc(OPPh_3)_3Cl_3]$ $\xrightarrow{-46}$ $[Sc(OPPh_3)_4Cl_2]^{+}$ $\xrightarrow{33}$ $[Sc(OPPh_3)_4Br_2]^{+}$ $\xrightarrow{90}$ $[Sc(OPPh_3)_4I_2]^{+}$

121   75   108   ~200

                        $\downarrow 21$ $\downarrow 32$

                  $[Sc(OAsPh_3)_4Cl_2]^{+}$ $[Sc(OAsPh_3)_4Br_2]^{+}$

                       96   140
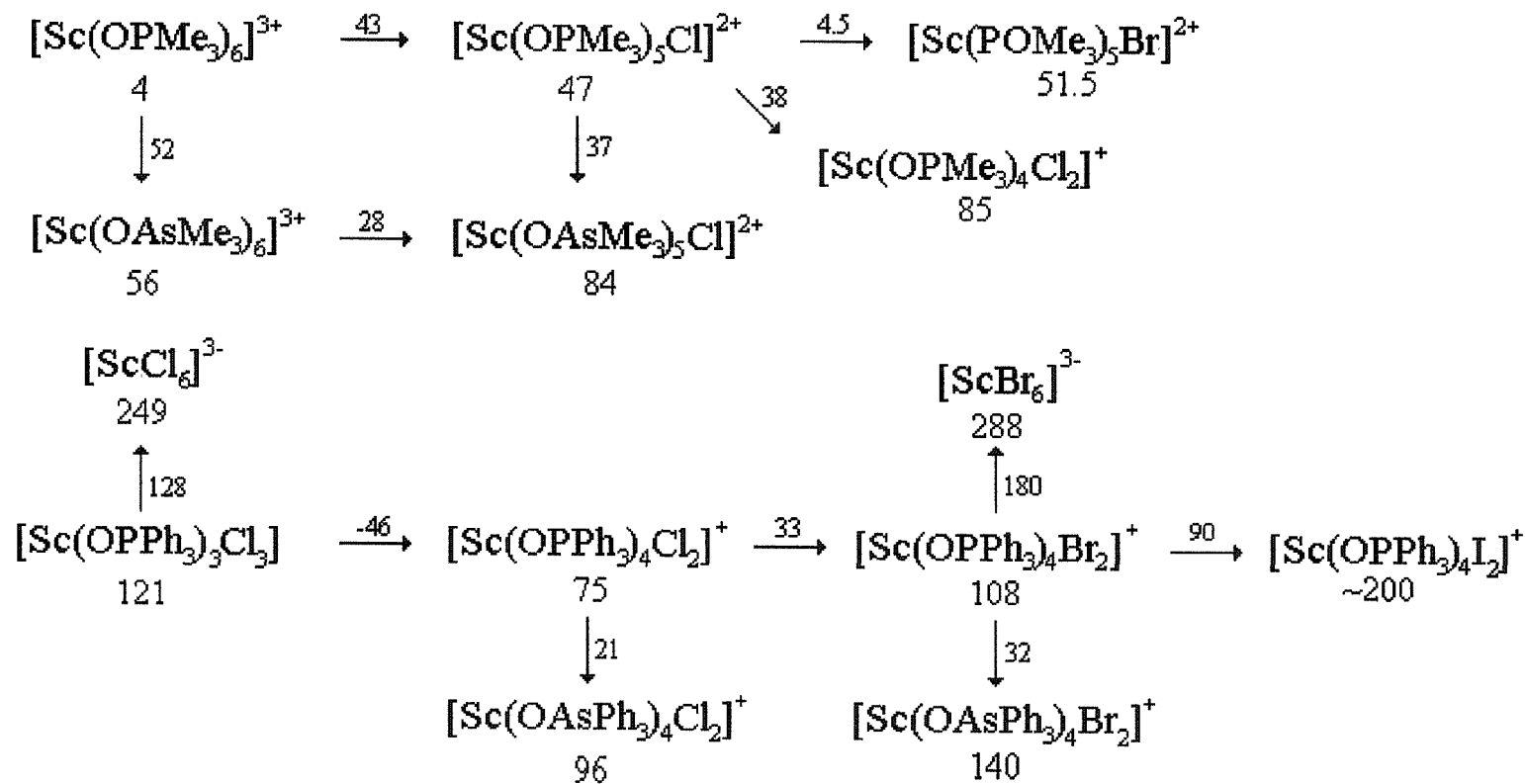
Fig. 4.7 Scheme showing systematic trends in [45]Sc NMR chemical shifts. Numbers under species are the chemical shift whilst values by arrows are the difference in chemical shift. The values for $[ScX_6]^{3-}$ ions obtained from Ref. 18. (There is some variation in the temperature of observation and solvents used. However, whilst this may alter specific values slightly, the trends are still valid).

4.2.7 Reaction scheme

$ScX_3.nH_2O$ (X = Cl, Br or I) + Ph_3PO $\longrightarrow$ $[ScX_2(Ph_3PO)_4]X^*$

$ScCl_3.6H_2O + Ph_2MePO$ $\longrightarrow$ $[ScCl_3(Ph_2MePO)_3].H_2O$

$ScBr_3.6H_2O + Ph_2MePO$ $\longrightarrow$ $[ScBr_2(Ph_2MePO)_4]Br$

$ScCl_3.6H_2O + Me_3PO$ $\longrightarrow$ $[ScCl(Me_3PO)_5]Cl$

$ScX_3.nH_2O + Me_3PO$ (X = Br or I) $\longrightarrow$ $[Sc(Me_3PO)_6]X_3^*$

$ScX_3.nH_2O + Ph_3AsO$ (X = Cl, Br or I) $\longrightarrow$ $[ScX_2(Ph_3AsO)_4]X^\times$

$ScX_3.nH_2O + Me_3AsO$ (X = Cl, Br or I) $\longrightarrow$ $[Sc(Me_3AsO)_6]X_3^*$
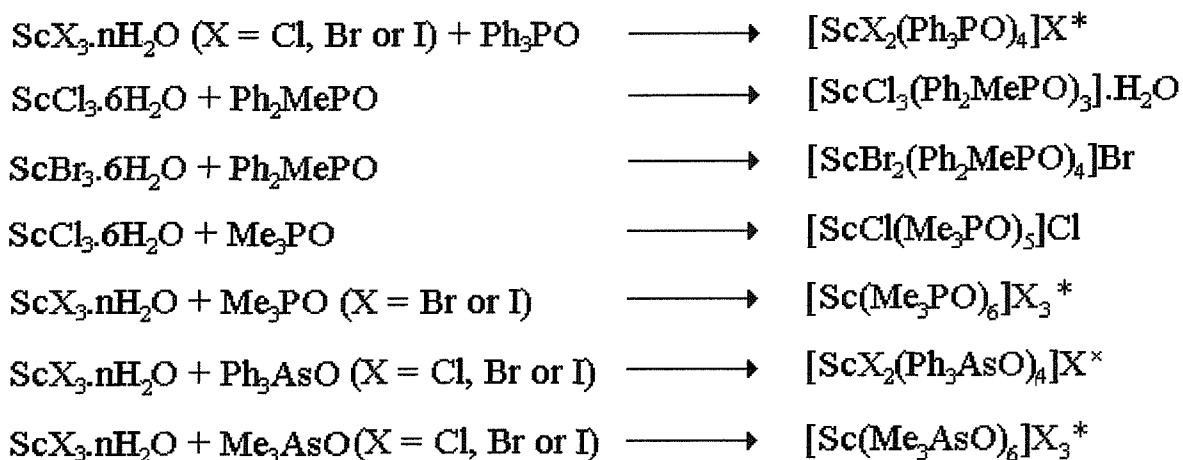
$*$ = Solvents of crystallisation present in some complexes

$\times$ = $*$ + iodo complex not analytically pure

Fig. 4.8 Reaction scheme indicating the compounds isolated in this study from reactions of hydrated scandium halide salts with tertiary phosphine and arsine oxide ligands.

4.3 Conclusions

When scandium halides were reacted with phosphine oxide ligands, complexes were formed with a ligand to metal ratio ranging from 3:1 to 6:1, although only some stoichiometries form with each ligand. With arsine oxide ligands, no 3:1 or 5:1 complexes were isolated, although some evidence for the existence of $[ScCl(Me_3AsO)_5]^{2+}$ in solution was observed. In all cases, the compounds isolated contained six-coordinate scandium centres, as seen in the analogous yttrium halide systems (Chapter 3). The results suggest scandium has a greater affinity for the lighter halides, as predicted on the basis of their greater electronegativity. For example, in the Me_3PO systems, $[ScCl(Me_3PO)_5]Cl_2$ was isolated, whilst similar reactions with $ScX_3.nH_2O$ (X = Br or I) afforded hexakis(phosphine oxide) compounds. Similarly, $[ScCl_3(Ph_3PO)_3]$ was observed in solution, whilst the bromide and iodide species showed no evidence for similar complexes. As for yttrium, scandium exhibits a greater affinity for nitrate groups than halides. This is demonstrated by the formation of $[Sc(Ph_3PO)_4X_2]X$ compared to $[Sc(Ph_3PO)_2(NO_3)_3]$. Further evidence is provided by the Ph_3AsO systems, for which scandium halides consistently form tetrakis(arsine oxide) compounds, whilst for scandium nitrates, both $[Sc(Ph_3AsO)_2(NO_3)_3]$ and $[Sc(Ph_3AsO)_3(NO_3)_2]NO_3$ are produced.

Like yttrium, scandium also demonstrated a greater affinity for R_3AsO than R_3PO ligands. For example, whilst the pentakis species $[ScCl(Me_3PO)_5]Cl_2$ is formed, from the analogous reaction $[Sc(Me_3AsO)_6]Cl_3$ was isolated. Similarly, evidence was observed for $[ScCl_3(Ph_3PO)_3]$ in solution whilst the lowest ligand to metal ratio arsine oxide complexes detected were of the type $[ScX_2(Ph_3AsO)_4]X$ (X = Cl, Br or I).

Comparison of results with the yttrium halide system reveals a tendency to lower ligand to metal ratios for scandium complexes, presumably due to the smaller radius of Sc^{3+}

(0.83 compared with 1.06 Å for yttrium). For example, evidence for $[YCl(Ph_3PO)_5]^{2+}$ was seen in solution whilst no resonances attributable to a pentakis(Ph$_3$PO) species were observed for scandium halides.

4.4 Experimental

Ph_3PO, Ph_2MePO, Ph_3AsO (Aldrich) and Me_3PO (Alfa) were used as received. Me_3AsO was prepared by oxidation of trimethylarsine in diethyl ether by hydrogen peroxide, with sublimation of the product *in vacuo* used to purify the product.[19] $Sc_2(SO_4)_3$ was prepared by addition of Sc_2O_3 (1.4 g, 10 mmol) to a solution of 98% H_2SO_4 in water (100 cm^3) with the reaction mixture heated to reflux for 48 h. The solution was evaporated to *ca.* 10 cm^3 then left to stand. The white solid was filtered off and dried *in vacuo*. Yield 88%. $ScF_3.1/2H_2O$ was prepared by precipitation from aqueous solutions of $Sc_2(SO_4)_3$ and NaF, with the solid filtered off, washed with water and then dried *in vacuo*. $ScCl_3.6H_2O$ was produced by addition of barium chloride solution to an aqueous solution of $Sc_2(SO_4)_3$ in a 3 : 1 molar ratio. The precipitated $BaSO_4$ was removed by filtration, with the filtrate evaporated to dryness *in vacuo* to leave a cream hygroscopic solid. Yield 90%. (Found: Cl, 40.8. Calc. for $ScCl_3.6H_2O$: Cl, 41.0%). $ScI_3.8H_2O$ was made similarly, yielding a fawn coloured hygroscopic product that was stored in a dessicator. Yield 86%. (Found: I, 66.7. Calc. for $ScI_3.8H_2O$: I, 66.8%). In contrast, $ScBr_3.6H_2O$ was formed by reaction of Sc_2O_3 with an aqueous solution of 48% HBr, with a 1 : 6 molar ratio of metal salt to acid. The mixture was refluxed until all scandium oxide had dissolved. The solution was evaporated to *ca.* 10 cm^3 then left to stand. The pale orange solid produced was filtered off and dried *in vacuo*. Yield 79%. (Found: Br, 60.8. Calc. for $ScBr_3.6H_2O$: Br, 61.0%).

4.4.1 Complexes of scandium halides with triphenylphosphine oxide

[Sc(Ph₃PO)₄Cl₂]Cl

In warm (60 °C) ethanol (10 cm^3), scandium chloride hexahydrate (0.13 g, 0.5 mmol) and triphenylphosphine oxide (0.55 g, 2 mmol) were dissolved separately, the solutions mixed well then refrigerated overnight. The solution was concentrated to *ca.* 10 cm^3, then refrigerated for 1 h, following which the white solid formed was filtered off and

dried *in vacuo*. Yield 0.35 g, 50%. (Found: C, 68.4; H, 4.7. Calc. for $C_{72}H_{60}Cl_3O_4P_4Sc$:

C, 68.4; H, 4.8%). IR (cm^{-1}) (CsI disc): 3055w, 1624w, 1591w, 1439m, 1358w, 1191w,

1152s (PO), 1122s, 1091s, 1046w, 1029w, 999m, 751m, 726s, 697s, 544s, 473m, 460m,

445m, 430m. ^{31}P-{^1H} NMR (300 K, CH_2Cl_2): 34.5, 34.0, 33.0, 26.0. ^{45}Sc NMR (300

K, CH_2Cl_2): 76 ($W_{1/2}$ = 1000 Hz), 121 ($W_{1/2}$ = 1000 Hz). ^1H NMR (300 K, CDCl$_3$): 7.0

- 7.9(m). Λ_m (10^{-3} mol dm^{-3}, CH_2Cl_2) = 17 ohm^{-1} cm^2 mol^{-1}, + excess Ph$_3$PO 22.

[Sc(Ph₃PO)₄Br₂]Br.CH₂Cl₂

A solution of scandium bromide hexahydrate (0.39 g, 1.0 mmol) was dissolved in ice-

cold ethanol (10 cm^3) and added to Ph$_3$PO (1.11 g, 4 mmol) in ethanol (5 cm^3) with the

mixture stirred for 1 h. The solution was refrigerated for 1 h, affording a white solid

which was filtered off and dried *in vacuo*. This was recrystallised by vapour diffusion of

diethyl ether into a dichloromethane solution of the solid. Yield 0.84 g, 60 %. (Found: C,

59.0; H, 4.5. Calc. for $C_{73}H_{62}Br_3Cl_2O_4P_4Sc$: C, 59.1; H, 4.2%). IR (cm^{-1}) (CsI disc):

3056w, 1620w, 1591w, 1438m, 1358w, 1188w, 1137s (PO), 1120s, 1084s, 1028m,

1000m, 750m, 725s, 692s, 547s, 465m, 454m, 426w, 317m, 306m, 269m, 255m.

^{31}P-{^1H} NMR (300 K, CH_2Cl_2): 35.8. ^{45}Sc NMR (300 K, CH_2Cl_2): 108 ($W_{1/2}$ = 4000

Hz). ^1H NMR (300 K, CDCl$_3$): 7.0-7.6(m), 5.2(s). Λ_m (CH_2Cl_2, 10^{-3} mol dm^{-3}) = 21

ohm^{-1} cm^2 mol^{-1}, + excess Ph$_3$PO = 23.

[Sc(Ph₃PO)₄I₂]I.2H₂O

This was made similarly to the chloride analogue, as a pale yellow solid. Yield 0.35 g,

44%. (Found: C, 54.7; H, 3.7. Calc. for $C_{72}H_{64}I_3O_6P_4Sc$: C, 54.9; H, 4.1 %). IR (cm^{-1})

(CsI disc): 3466br, 3054w, 1624w, 1590w, 1438m, 1359w, 1187w, 1132s (PO), 1122s,

1073s, 1027m, 999m, 750m, 725s, 693s, 543s, 464m, 452m, 425w. ^{31}P-{^1H} NMR

(300 K, CH_2Cl_2): 38.0. ^{45}Sc NMR (300 K, CH_2Cl_2): *ca.* 200 ($W_{1/2}$ = 10000 Hz). ^1H

NMR (300 K, CDCl$_3$): 7.0-7.7(m), 1.7 (H$_2$O). Λ_m (10^{-3} mol dm^{-3} CH$_2$Cl$_2$) = 22 ohm^{-1} cm^2 mol^{-1}.

4.4.2 Complexes of scandium halides with diphenylmethylphosphine oxide

[ScCl$_3$(Ph$_2$MePO)$_3$].H$_2$O

A solution of diphenylmethylphosphine oxide (0.16 g, 0.75 mmol) in boiling acetone (10 cm^3) was added to a solution of scandium chloride hexahydrate (0.06 g, 0.25 mmol) in acetone (5 cm^3) resulting in a white suspension. Hexane (10 cm^3) was added affording a sticky solid which was separated and stirred with diethyl ether for 24 h. The white powder produced was filtered off and dried *in vacuo*. Yield 0.17 g, 59%. (Found: C, 56.8; H, 5.1. Calc. for C$_{39}$H$_{41}$Cl$_3$O$_4$P$_3$Sc: C, 57.2; H, 5.0 %). IR (cm^{-1})(CsI disc): 3420br, 3056w, 2913w, 1643m, 1439s, 1359w, 1143s (PO), 1127sh, 1099m, 1028w, 998w, 901s, 783m, 746s, 720m, 696s, 517s, 507sh, 429w. ^{45}Sc NMR (300 K, CH$_2$Cl$_2$): 123, 80 (w). ^{31}P-{^{1}H} NMR (300 K, CH$_2$Cl$_2$): 40.5, 42.4, 42.5. ^{1}H NMR (300 K, CDCl$_3$): 1.7 br[2H], 1.9 (d, $^2J_{PH}$ = 13 Hz)[3H], 2.5 (d, $^2J_{PH}$ = 13 Hz)[6H], 7.3-7.9 (m)[30H]. Λ_m (CH$_2$Cl$_2$, 10^{-3} mol dm^{-3}) = 8 ohm^{-1} cm^2 mol^{-1}, + excess Ph$_3$AsO = 23.

[ScBr$_2$(Ph$_2$MePO)$_4$]Br

To a solution of Ph$_2$MePO (0.22 g, 1.0 mmol) in ice-cold acetone (10 cm^3), a solution of scandium bromide hexahydrate (0.09 g, 0.25 mmol) in acetone (5 cm^3) was added, and the resultant mixture stirred for 1 h. Concentration of the solution to *ca.* 5 cm^3 followed by refrigeration overnight precipitated a white solid. This was filtered off and dried *in vacuo*. Yield 0.14 g, 49%. (Found: C, 55.3; H, 4.8. Calc. for C$_{52}$H$_{52}$Br$_3$O$_4$P$_4$Sc: C, 54.3; H, 4.6 %). IR (cm^{-1}) (CsI disc) 3420br, 3050w, 2908w, 1638m, 1486m, 1438s, 1363w, 1138s (PO), 1094m, 1073w, 1028m, 998w, 894s, 787m, 746s, 719m, 695s, 515s. ^{45}Sc NMR (300 K, CH$_2$Cl$_2$): 100 ($W_{1/2}$ = 5000 Hz). ^{31}P-{^{1}H} NMR (300 K, CH$_2$Cl$_2$): 41.0,

40.3 (w). ^{1}H NMR (300 K, CDCl$_3$): 1.92 (d, $^2J_{PH}$ = 13 Hz)[12H], 7.3-7.9 (m)[40H]. Λ_m (CH$_2$Cl$_2$, 10^{-3} mol dm^{-3}) = 22 ohm^{-1} cm^2 mol^{-1}.

4.4.3 Complexes of scandium halides with trimethylphosphine oxide

[Sc(Me$_3$PO)$_5$Cl]Cl$_2$

Ice-cold ethanolic solutions (10 cm^3) of ScCl$_3$.6H$_2$O (0.13 g, 0.5 mmol) and Me$_3$PO (0.28 g, 3 mmol) were mixed together, stirred for 1 h, then concentrated to *ca.* 5 cm^3 and refrigerated overnight. The white solid formed was filtered off and dried *in vacuo*. Yield 0.24 g, 63%. (Found: C, 29.7; H, 8.1. Calc. for C$_{15}$H$_{45}$Cl$_3$O$_5$P$_5$Sc: C, 29.4; H, 7.4%). IR (cm^{-1}) (CsI disc): 2964w, 2896w, 1421w, 1360w, 1299m, 1182w, 1109br,vs (PO), 959s, 872s, 845m, 762s, 682m, 559w, 427s. ^{31}P-{^{1}H} NMR (300 K, MeNO$_2$): 36.5, 54.0, 54.5, 56.0. ^{45}Sc NMR (300 K, MeNO$_2$): 47 ($W_{1/2}$ = 4000 Hz), 84.5. ^{1}H NMR (300 K, d^3-MeNO$_2$): 1.5(d, $^2J(^{31}$P-^{1}H) = 14 Hz); 1.7(d), 1.8(d, $^2J(^{31}$P-^{1}H) = 14 Hz), 1.90(d, $^2J(^{31}$P-^{1}H) = 14 Hz). Λ_m (10^{-3} mol dm^{-3} MeNO$_2$) = 117 ohm^{-1} cm^2 mol^{-1}, + excess Me$_3$PO 180.

[Sc(Me$_3$PO)$_6$]Br$_3$

To a solution of scandium bromide hexahydrate (0.20 g, 0.5 mmol) in ice-cold ethanol (10 cm^3), trimethylphosphine oxide (0.28 g, 3 mmol) in ethanol (5 cm^3) was added, immediately affording a white precipitate. The mixture was left to stand for 1 h, the precipitate filtered off and dried *in vacuo*. Yield 0.29 g, 54%. (Found: C, 25.2; H, 6.6. Calc. for C$_{18}$H$_{54}$Br$_3$O$_6$P$_6$Sc: C, 25.8; H, 6.5%). IR (cm^{-1}) (CsI disc): 2964w, 2897w, 1422m, 1361w, 1312m, 1299m, 1183w, 1110v br (PO), s, 960s, 872s, 762m, 682m, 428s, 418s. ^{31}P-{^{1}H} NMR (300 K, MeNO$_2$): 36.5, 55.0, 56.0, 56.5(m). ^{45}Sc NMR (MeNO$_2$): 4.5, 51.5. ^{1}H NMR (300 K, d^3-MeNO$_2$): 1.5(d) $^2J(^{31}$P-^{1}H) = 14 Hz), 1.85 (d, $^2J(^{31}$P-^{1}H) = 14 Hz), 1.70(d), 1.85(d, $^2J(^{31}$P-^{1}H) = 14 Hz). Λ_m (10^{-3} mol dm^{-3} MeNO$_2$) = 179 ohm^{-1} cm^2 mol^{-1}, + excess Me$_3$PO 221.

[Sc(Me₃PO)₆]I₃.EtOH

Solutions of $ScI_3.8H_2O$ (0.11 g, 0.25 mmol) and Me_3PO (0.14 g, 1.5 mmol) in boiling ethanol (10 cm³) were mixed well, yielding a pale yellow precipitate. The precipitate was filtered off and dried *in vacuo*. Yield 0.14 g, 67%. (Found: C, 24.2; H, 6.1. Calc. for $C_{20}H_{60}I_3O_7P_6Sc$: C, 23.6; H, 5.9%). IR (cm⁻¹) (CsI disc): 3480br, 2964w, 2898w, 1421m, 1360w, 1312m, 1299m, 1184w, 1108vbr, s (PO), 957s, 871s, 761m, 681m, 427s. $^{31}P-\{^1H\}$ NMR (300K, $MeNO_2$): *ca.* 57.5(s). ^{45}Sc NMR (300 K, $MeNO_2$): 4.0, 9.0. ^1H NMR (300 K, d^3-$MeNO_2$): 1.1(t), 3.4(q), 1.88(d, $^2J(^{31}P-^1H) = 13$ Hz), 1.78-1.82(br). Λ_m (10⁻³ mol dm⁻³ $MeNO_2$) = 189 ohm⁻¹ cm² mol⁻¹, + excess Me_3PO 242.

4.4.4 Complexes of scandium halides with triphenylarsine oxide

[Sc(Ph₃AsO)₄Cl₂]Cl.2EtOH

To a solution of $ScCl_3.6H_2O$ (0.06 g, 0.25 mmol) in boiling ethanol (5 cm³), an ethanolic solution (5 cm³) of Ph_3AsO (0.32 g, 1.0 mmol) was added and the mixture stirred for 1 h. The solution was then concentrated to *ca.* 5 cm³ and refrigerated for 24 h. The white solid was filtered off and dried *in vacuo*. Yield 0.16 g, 45%. (Found: C, 58.9; H, 4.5. Calc. for $C_{76}H_{72}As_4Cl_3O_6Sc$: C, 59.5; H, 4.7 %). IR (cm⁻¹)(CsI disc): 3407br, 3055w, 1583w, 1485m, 1440m, 1358w, 1187w, 1162w, 1089s, 1070w, 1027m, 999m, 908vs (AsO), 883m, 745s, 692s, 480s, 458m. ^{45}Sc NMR (300 K, CH_2Cl_2): 96 ($W_{1/2}$ = 4000 Hz). ^1H NMR (300 K, $CDCl_3$): δ 7.0-7.7(m)[60H], 1.2(t)[6H], 3.4(q)[4H] (EtOH). Λ_m (CH_2Cl_2, 10⁻³ mol dm⁻³) = 20 ohm⁻¹ cm² mol⁻¹, + excess Ph_3AsO = 24.

[Sc(Ph₃AsO)₄Br₂]Br.5H₂O

Was made similarly to the chloride analogue, furnishing a pale yellow solid. Yield 0.22 g, 54%. (Found: C, 51.4; H, 3.6. Calc. for $C_{72}H_{70}As_4Br_3O_9Sc$: C, 51.9; H, 4.3 %). IR (cm⁻¹) (CsI disc): 3400br, 3051w, 1654m, 1582w, 1485m, 1440s, 1354w, 1185m,

1162w, 1088s, 1027w, 999m, 883s (AsO), 762s, 744s, 691s, 482s, 473s, 457m, 413m. ^{45}Sc NMR (300 K, CH_2Cl_2): $ca.$ 140 ($W_{1/2}$ = 20000 Hz.). ^{1}H NMR (300 K, $CDCl_3$): 7.1-6.6 (m)[60H], 1.8 br[10H]. Λ_m (CH_2Cl_2, 10^{-3} mol dm^{-3}) = 19 ohm^{-1} cm^2 mol^{-1}, + excess Ph_3AsO = 23.

"[ScI$_2$(Ph$_3$AsO)$_4$]I"

Was made similarly to the chloride analogue, yielding an ochre solid. Yield 0.20 g, 46%. An analytically pure sample could not be obtained (see 4.2.4). IR (cm^{-1}) (CsI disc): 3300m, 1636w, 1439m, 1359w, 1185w, 1161w, 1088s, 1027w, 998m, 883s, br (AsO), 739s, 690s, 477m, 457m, 419m. ^{45}Sc NMR (300 K, CH_2Cl_2): Not observed. ^{1}H NMR (300 K, $CDCl_3$): 7.15-7.7 (m). Λ_m (CH_2Cl_2, 10^{-3} mol dm^{-3}) = 20 ohm^{-1} cm^2 mol^{-1}, + excess Ph_3AsO = 23.

4.4.5 Complexes of scandium halides with trimethylarsine oxide

[Sc(Me$_3$AsO)$_6$]Cl$_3$

$ScCl_3 \cdot 6H_2O$ (0.05 g, 0.19 mmol) was dissolved in boiling ethanol (10 cm^3) and added to an ethanolic solution (10 cm^3) of Me_3AsO (0.21 g, 1.5 mmol), affording a white suspension. The solution was concentrated to $ca.$ 10 cm^3, with the resultant white solid filtered off and dried in $vacuo.$ Yield 0.13 g, 71%. (Found: C, 22.1; H, 5.6. Calc. for $C_{18}H_{54}As_6Cl_3O_6Sc$: C, 22.3; H, 5.6 %). IR (cm^{-1}) (CsI disc): 2981w, 2904w, 1418m, 1359w, 1295w, 1269m, 1114w, 924s, 874s, 844s, 647s, 420m. ^{45}Sc NMR (300 K, MeNO$_2$): 56.0, 84 (vw). ^{1}H NMR (300 K, d^3-MeNO$_2$): 2.1 (s), 2.05 (w). Λ_m (MeNO$_2$, 10^{-3} mol dm^{-3}) = 214 ohm^{-1} cm^2 mol^{-1}, + excess Me_3AsO = 251.

[Sc(Me$_3$AsO)$_6$]Br$_3$

Was made similarly to the chloride analogue. Yield 0.13 g, 62%. (Found: C, 19.0; H, 5.0. Calc. for $C_{18}H_{54}As_6Br_3O_6Sc$: C, 19.6; H, 5.0 %). IR (cm^{-1}) (CsI disc): 2982w,

2920w, 1653w, 1418m, 1359m, 1268m, 1088m, 926s, 874s, 846s, 648s, 420m. ^{45}Sc NMR (300 K, MeNO$_2$): 56.0. ^{1}H NMR (300 K, d^3-MeNO$_2$): 2.05 (s). Λ_m (MeNO$_2$, 10^{-3} mol dm^{-3}) = 239 ohm^{-1} cm^2 mol^{-1}, + excess Me$_3$AsO = 281.

[Sc(Me$_3$AsO)$_6$]I$_3$.3H$_2$O

Solutions of ScI$_3$.8H$_2$O (0.10 g, 0.17 mmol) and Me$_3$AsO (0.14 g, 1.0 mmol) in warm (60°C) ethanol (10 cm^3) were mixed, yielding a pale yellow solid immediately, which was filtered off and dried *in vacuo*. Yield 0.11 g, 53%. (Found: C, 15.8; H, 3.9. Calc. for C$_{18}$H$_{60}$As$_6$I$_3$O$_9$Sc: C, 16.7; H, 4.6 %). IR (cm^{-1}) (CsI disc): 3440br, 2978w, 2902w, 1647w, 1417m, 1359w, 1265m, 1088w, 921s, 872s, 844s, 646s, 420m. ^{45}Sc NMR (300 K, MeNO$_2$): 56.0. ^{1}H NMR (300 K, d^3-MeNO$_2$): 2.1 (s), 2.05 (w). Λ_m (MeNO$_2$, 10^{-3} mol dm^{-3}) = 253 ohm^{-1} cm^2 mol^{-1}, + excess Me$_3$AsO = 280.

4.4.6 Crystallographic studies

Details of the crystallographic data collection and refinement parameters are given in Table 4.10.

[ScBr$_2$(Ph$_3$PO)$_4$]Br.1/2Et$_2$O

Colourless plate crystals were grown by vapour diffusion of Et$_2$O into a CH$_2$Cl$_2$ solution of [ScBr$_2$(Ph$_3$PO)$_4$]Br.CH$_2$Cl$_2$ in a refrigerator. Full-matrix least squares refinement on F was carried out in TEXSAN.[20, 21]

[ScCl$_2$(Ph$_3$AsO)$_4$]Cl

Plate-like crystals were grown by vapour diffusion from a CH$_2$Cl$_2$ – Et$_2$O system with the recrystallisation cell held in a refrigerator. Solution on F^2 was carried out using SHELXL 97.[22, 23] Initially, refinement was conducted in the triclinic space group P$\bar{1}$ (No. 2) with $Z = 4$. However, the value of Z caused some concern[24] and examination

of data revealed systematic absences consistent with a monoclinic space group. Hence, refinement was carried out in $P2_1/c$ (No. 14).

$[Sc(Me_3AsO)_6]Br_3$

Small block crystals were obtained by vapour diffusion of Et_2O into a $MeNO_2$ solution of the complex containing an excess of Me_3AsO to prevent any decomposition into $[ScBr(Me_3AsO)_5]^{2+}$. Refinement on F was carried out,[20, 21] with anisotropic refinement giving some O and C atoms non-positive definite thermal parameters. As a result, all O and C atoms were refined isotropically.

Table 4.10 Crystallographic data collection and refinement parameters

	[ScBr$_2$(Ph$_3$PO)$_4$]Br.1/2Et$_2$O	[ScCl$_2$(Ph$_3$AsO)$_4$]Cl	[Sc(Me$_3$AsO)$_6$]Br$_3$
Formula	C$_{72}$H$_{60}$Br$_3$O$_4$P$_4$Sc + ½(C$_4$H$_{10}$O)	C$_{72}$H$_{60}$As$_4$Cl$_3$O$_4$Sc	C$_{18}$H$_{54}$As$_6$Br$_3$O$_6$Sc
Formula weight	1434.89	1440.19	1100.82
Crystal system	Triclinic	Monoclinic	Monoclinic
Space group	$P\bar{1}$ (No. 2)	$P2_1/c$ (No. 14)	$C2/c$ (No. 15)
a / Å	14.2119(4)	18.436(2)	17.7475(5)
b / Å	14.7923(4)	18.946(3)	16.9358(5)
c / Å	17.6032(5)	18.393(3)	12.5771(4)
α / °	66.695(2)	90	90
β / °	80.919(1)	90.04(1)	96.643(1)
γ / °	89.302(1)	90	90
U / Å^3	3351.0(2)	6424.5(18)	3754.9(2)
Z	2	4	4
μ(Mo-K$_\alpha$) / cm^{-1}	20.5	23.33	86.7
No. unique reflections	15012	9826	4371
R_{int}	0.054	0.16	0.093
No. of obs. reflections	8868[e]	9826[a]	1581[e]
No. parameter/restraint	777/0	758/0	96/0
R [b]	0.059	0.081	0.065
wR_2 [c]	-	0.217	-
wR [d]	0.073	-	0.114

[a] Observed if [$I_o > 2\sigma(I_o)$]   [b] $R = \Sigma$ (|F$_{obs}$|$_i$ - |F$_{calc}$|$_i$) / Σ |F$_{obs}$|$_i$ [c] $wR_2 = [\Sigma w(F_{obs}^2 - F_{calc}^2)^2 / \Sigma w(F_{obs}^2)^2]^{1/2}$ [d] $wR = \sqrt{[\Sigma w_i(|F_{obs}|_i - |F_{calc}|_i)^2 / \Sigma w_i|F_{obs}|_i^2}$ [e] Observed if [$I_o > 3\sigma(I_o)$]

4.5 References

1. G. A. Kirakosyan, V. P. Tarasov, Y. A. Buslaev, *Mag. Res. Chem.*, 1989, **27**, 103.

2. Y. A. Buslaev, G. A. Kirakosyan, V. P. Tarasov, *Dokl. Akad. Nauk. SSSR*, 1982, **264**, 1405.

3. V. Y. Korovin, S. B. Randerevich, Y. N. Pogorelov, S. V. Bodaratskii, *Koord. Khim.*, 1996, **22**, 597.

4. S. S. Korovin, P. G. Berezhko, A. M. Reznik, G. S. Filatov, *Khim. Khim. Tekhnol.*, 1969, **12**, 1607.

5. S. A. Semenov, A. M. Reznik, L. D. Yurchenko, *Khim. Khim. Tekhnol.*, 1983, **26**, 251.

6. F. Kutek, I. Sebkova, B. Dusek, *Anorg. Chem. Technol.*, 1977, **22**, 25.

7. O. V. Kravchenko, S. E. Kravchenko, V. D. Makhaev, V. B. Polyakova, G. V. Slobodenchuk, K. M. Semenenko, *Koord. Khim.*, 1982, **8**, 1356.

8. J. L. Atwood, K. D. Smith, *J. Chem. Soc., Dalton Trans.*, 1974, 921.

9. G. R. Willey, P. R. Meehan, M. G. B. Drew, *Polyhedron*, 1997, **16**, 3485.

10. G. R. Willey, T. J. Woodman, W. Errington, *Trans. Met. Chem. (London)*, 1998, **23**, 387.

11. G. R. Willey, P. R. Meehan, M. G. B. Drew, *Polyhedron*, 1996, **15**, 1397.

12. G. R. Willey, P. R. Meehan, M. D. Rudd, M. G. B. Drew, *J. Chem. Soc., Dalton Trans.*, 1995, 811.

13. G. R. Willey, M. T. Lakin, N. W. Alcock, *J. Chem. Soc., Dalton Trans.*, 1993, 3407.

14. P. R. Meehan, G. R. Willey, *Inorg. Chim. Acta*, 1999, **284**, 71.

15. W. Radecka-Paryzek, V. Patroniak-Krzyminiewska, *Pol. J. Chem.*, 1995, **69**, 1.

16. K. J. Covert, D. R. Neithamer, M. C. Zonnevylle, R. E. LaPointe, C. P. Schaller, P. T. Wolczanski, *Inorg. Chem.*, 1991, **30**, 2494.

17. W. J. Geary, *Coord. Chem. Rev.*, 1971, **7**, 81.

18. D. Rehder in *Transition Metal NMR*, P. S. Pregosin (Ed.), Elsevier, New York, 1991, Ch. 1, p4.

19. A. Merijanian, R. A. Zingaro, *Inorg. Chem.*, 1966, **5**, 187.

20. TEXSAN, Single crystal structure analysis software, Version 1.7-1, Molecular Structure Corporation, The Woodlands, TX, 1995.

21. P. T. Beurskens, G. Admiraal, G. Beurskens, W. P. Bosman, S. Garcia-Granda, R. O. Gould, J. M. M. Smits and C. Smykalla, The DIRDIF program system, University of Nijmegen, 1992.

22. G. M. Sheldrick, SHELXS 97, Program for crystal structure solution, University of Göttingen, 1997.

23. G. M. Sheldrick, SHELXL 97, Crystal structure refinement program, University of Göttingen, 1997.

24. R. E. Marsh, *Acta Crystallogr., Sect. B*, 1999, **55**, 931.

Chapter 5

Complexes of Scandium Halides

with Crown Ether Ligands

5.1 Introduction

In 1967, Pedersen reported a range of crown ethers and their complexes with Group I and Group II metals.[1] Surprisingly, the work was not extended to lanthanide ions for several years. The ionic radii of the lanthanide ions (and Group III metal ions) appeared favourable for coordination to crown ether ligands but the large hydration energy of Ln^{3+} may have hindered research (which often leads to lanthanide-crown complex dissociation in aqueous solvents).[2]

Research into lanthanide – crown complexes has now received much attention with study conducted into complexes with a range of lanthanide salts. For example, compounds based on lanthanide nitrates, halides and perchlorates have all been structurally characterised.[2] However, in this chapter, only the most relevant examples, namely lanthanide halide complexes of [12]-crown-4, [15]-crown-5 and [18]-crown-6 are discussed.

Numerous complexes with [12]-crown-4 have been structurally characterised, with distinct geometries observed, both the lanthanide used and reaction temperature affecting the result.[3] Compounds of the type $[Ln(H_2O)_5([12]\text{-crown-4})]Cl_3.2H_2O$ have been observed where Ln = Y, Ce (Fig. 5.1), Nd, Sm, Eu, Gd, Dy-Er and Yb. The geometry of the cation is a monocapped tetragonal antiprism, with the anions all showing hydrogen bonding to the coordinated water molecules.
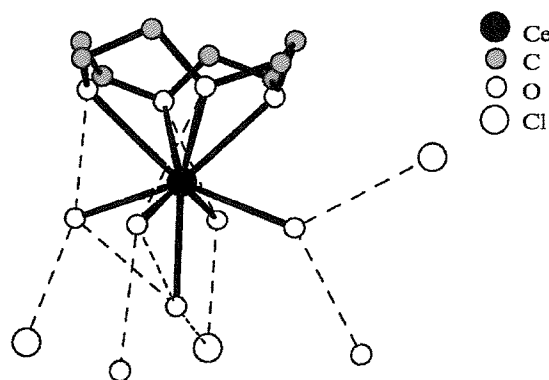
Fig. 5.1 View of the complex $[Ce(H_2O)_5([12]\text{-crown-4})]Cl_3.2H_2O$.[4]

A second geometry observed was that in [LnCl$_2$(H$_2$O)$_2$([12]-crown-4)]Cl (Fig. 5.2) for Ln = Ho-Lu, the coordination environment about Ln being a bicapped trigonal prism.[3]
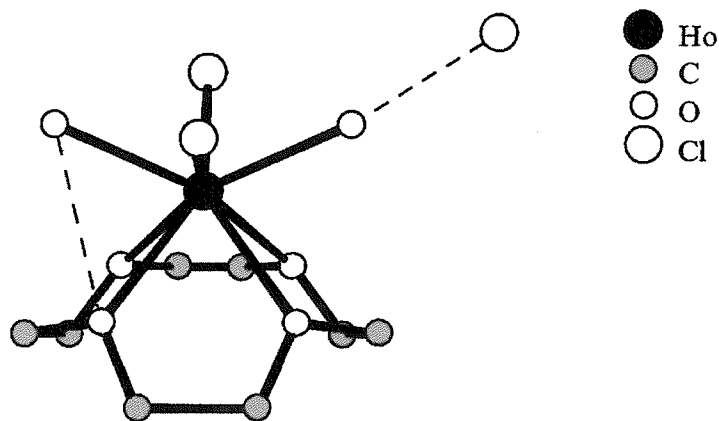
Fig. 5.2 View of the complex [HoCl$_2$(H$_2$O)$_2$([12]-crown-4)]Cl.[5]

Further complex types were observed, namely [YCl$_2$(H$_2$O)(CH$_3$OH)([12]-crown-4)]Cl (Fig. 5.3),[6] [PrCl$_3$(H$_2$O)([12]-crown-4)].[12]-crown-4.CH$_3$OH (Fig. 5.4) and [PrCl$_3$(CH$_3$OH)([12]-crown-4)].[7]
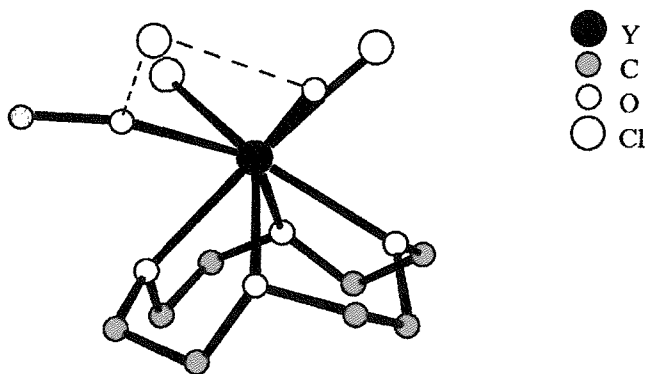
Fig. 5.3 View of the compound [YCl$_2$(H$_2$O)(CH$_3$OH)([12]-crown-4)]Cl.[6]
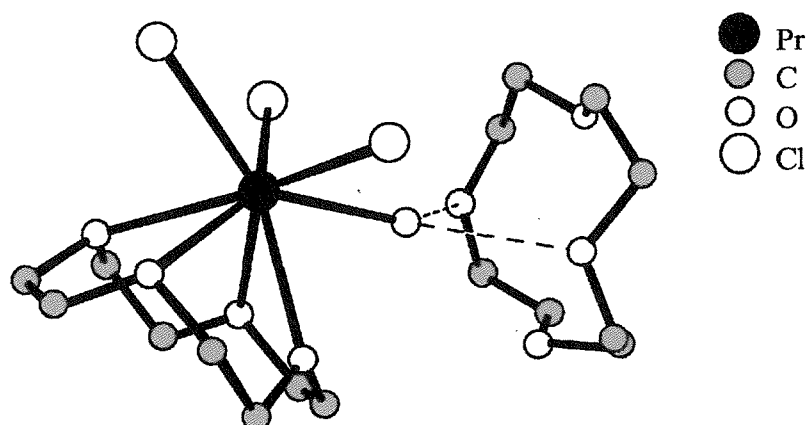
Fig. 5.4 View of the structure [PrCl₃(H₂O)([12]-crown-4)].[12]-crown-4.CH₃OH.[7]

Reactions of [15]-crown-5 with LnCl₃ yielded two main complex types, dependent on whether anhydrous metal salts were used. When anhydrous PrCl₃, NdCl₃ or SmCl₃ were used, the product was [LnCl₃([15]-crown-5)].[8, 9] When hydrated yttrium, gadolinium or lutetium salts were employed, the product was [Ln(H₂O)₈]Cl₃.[15]-crown-5.nH₂O.[10-13] The structures of these aquo complexes revealed a distorted dodecahedral coordination polyhedron around the metal centres, with complex systems of OH...O and OH...Cl hydrogen bonding.

When [18]-crown-6 was reacted with LnCl₃ in a methanol – acetonitrile mixture, the product was [LnCl(H₂O)₂([18]-crown-6)]Cl₂.2H₂O for Ln = Pr, Nd, Sm-Gd, Tb (Fig. 5.5).[14, 15] The metal centre is coordinated to all six oxygens of the crown. When lanthanum chloride was used, the products observed were [LaCl₂(CH₃OH)([18]-crown-6)]Cl.1.5H₂O and [LaCl₂(H₂O)([18]-crown-6)]Cl.[15]
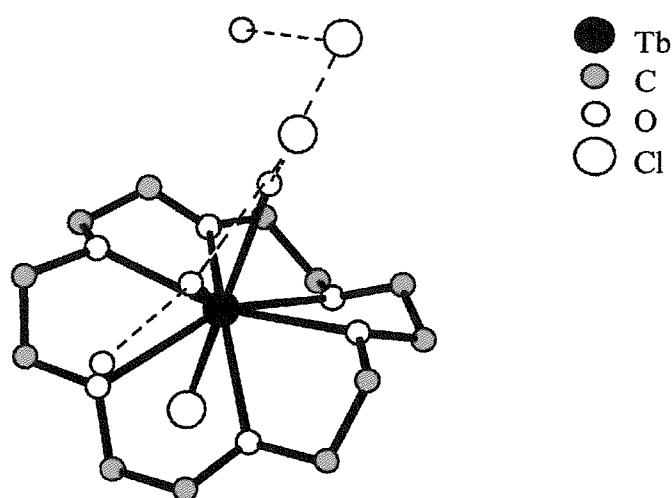
Fig. 5.5 View of the structure [TbCl(H$_2$O)$_2$([18]-crown-6)]Cl$_2$.2H$_2$O.[15]

In a series of papers examining reactions of scandium halides with crown ethers using a reaction system of anhydrous [ScCl$_3$(thf)$_3$], SbCl$_5$ (acting as a halide abstractor), crown ether and acetonitrile as a solvent, Willey et al. describe formation of an array of complexes. Reaction of [ScCl$_3$(thf)$_3$] with antimony pentachloride in acetonitrile, followed by addition of [12]-crown-4 affords the compound [Sc(12-crown-4)$_2$][SbCl$_6$][Sb$_2$Cl$_8$(MeCN)$_2$].2MeCN (Fig. 5.6), the scandium centre sandwiched between two crown ligands.[16] Synthesis of [ScCl$_2$([12]-crown-4)(MeCN)][SbCl$_6$] has also been reported.[17] The same report documents synthesis of [M([12]-crown-4)(MeCN)$_5$][SbCl$_6$]$_3$ and [M([18]-crown-6)(MeCN)$_3$][SbCl$_6$]$_3$ where M = Y or La.[17] Reaction of [ScCl$_3$(thf)$_3$] with one molar equivalent of SbCl$_5$ followed by addition of [15]-crown-5 yields [ScCl$_2$([15]-crown-5)]SbCl$_6$. A second synthetic approach by Belsky et al. uses CuCl$_2$ as a halide abstractor, with formation of [ScCl$_2$([15]-crown-5)]$_2$[CuCl$_4$] reported.[18] Willey et al. report synthesis of the [18]-crown-6 complex [ScCl$_2$([18]-crown-6)][SbCl$_6$] (Fig. 5.7) by reaction of [ScCl$_3$(thf)$_3$] with SbCl$_5$ in dry acetonitrile followed by addition of the crown ether, in a paper which also describes structural characterisation of [ScCl$_2$(benzo-[15]-crown-5)][SbCl$_6$].[17] Willey et al. have also reported crystal structures of the compounds [ScCl$_2$(dibenzo-[24]-crown-8)(H$_2$O)][SbCl$_6$] and [ScCl$_2$(dibenzo-[30]-crown-10)(H$_2$O)$_2$][SbCl$_6$].[19] In addition, the

same author has conducted solution studies of the scandium chloride – crown ether systems, with species identified by ^{45}Sc NMR spectroscopy (discussed in Section 5.2).[20]
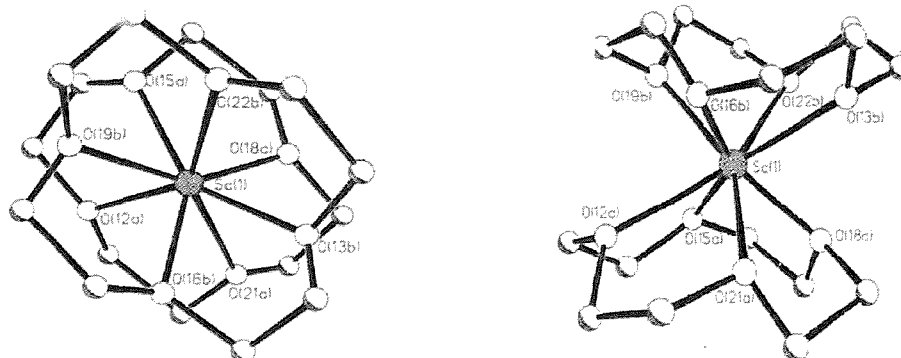
Fig. 5.6 Views of the cation $[Sc([12]\text{-crown-4})_2]^{3+}$ perpendicular and parallel to the plane of the crown ether ligands.[16]
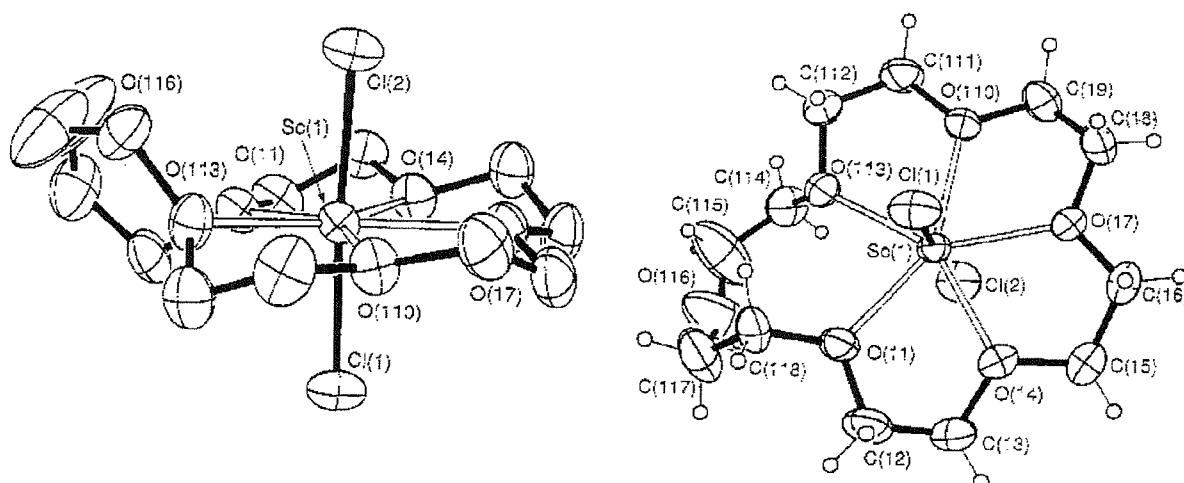
Fig. 5.7 Views of the cation of $[ScCl_2([18]\text{-crown-6})][SbCl_6]$.[17]

A number of studies examining complexes of other scandium salts with crown ether ligands have been reported. For example, the structures of both $[Sc(NO_3)_3(H_2O)_3]\cdot[18]\text{-crown-6}$ (Fig. 5.8)[21-23] and $[Sc(NO_3)_3(H_2O)_2]\cdot[15]\text{-crown-5}$ have been reported.[24]
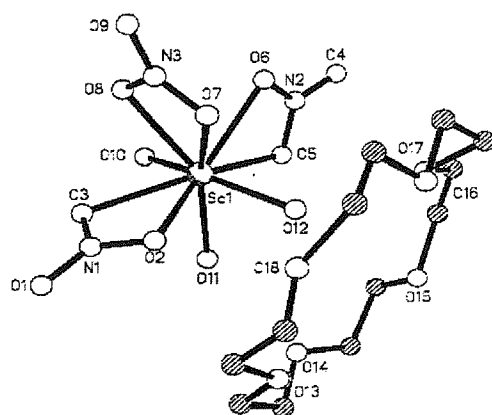
Fig. 5.8 View of hydrated scandium nitrate [Sc(NO$_3$)$_3$(H$_2$O)$_3$] exhibiting hydrogen bonding to [18]-crown-6.[21]

In this chapter, the aim was to explore reactions of anhydrous [ScCl$_3$(thf)$_3$] with crown ether ligands in the presence of a halide abstractor. Whilst previous studies have revealed complexes of this type, it seemed likely that further compounds could be synthesised beyond those reported in the literature. Additionally, attempts to bond a mixed donor macrocycle ([15]aneS$_2$O$_3$) to a scandium centre would be made, possibly giving the first reported example of bonding between Sc^{3+} and a thioether group. Compounds formed by reaction of hydrated scandium salts with crown ethers would then be investigated, and finally the hydrolysis pathway of anhydrous products would be examined, allowing comparison of all three systems. Additionally, behaviour of all the isolated complexes in solution would be covered, using ^{45}Sc NMR spectroscopy as a probe. The study would allow comparison of the affinity of the scandium centre for chloride, crown ethers and water (where appropriate).

5.2 Results and Discussion

5.2.1 Reactions of [ScCl$_3$(thf)$_3$] with crown ether ligands

When [ScCl$_3$(thf)$_3$] was reacted with SbCl$_5$ and [15]-crown-5 in a 1:2:1 molar ratio in anhydrous MeCN, colourless crystals of [ScCl(MeCN)([15]-crown-5)][SbCl$_6$]$_2$. MeCN were produced. Reaction of [ScCl$_3$(thf)$_3$] with 1 molar equivalent of both FeCl$_3$ and [18]-crown-6 in MeCN produced yellow-green crystals of [ScCl$_2$([18]-crown-6)]FeCl$_4$. The same reaction, using [15]aneS$_2$O$_3$ as the ligand produced yellow [ScCl$_2$([15]aneS$_2$O$_3$)][FeCl$_4$]. Attempts to isolate complexes with no coordinated chlorides using excess SbCl$_5$ (to act as a halide extractor) were unsuccessful.

The IR spectrum of [ScCl(MeCN)([15]-crown-5)][SbCl$_6$]$_2$.MeCN contained bands corresponding to both coordinated and lattice MeCN at $v = 2332$ and 2303 cm^{-1}. Additionally, [SbCl$_6$]$^-$ was apparent by a very strong band at 344 cm^{-1}, attributed to the v_3 mode.[17] The strong band at 441 cm^{-1} was assigned as v(Sc-Cl).

The ^{45}Sc NMR spectrum in anhydrous MeCN exhibited a single resonance at δ 99.5 ppm. The dichloro-cation of [ScCl$_2$([15]-crown-5)][SbCl$_6$] has been reported previously, synthesised using a 1:1:1 molar ratio of the same reagents, and was claimed to have a single ^{45}Sc NMR resonance at δ 130 ppm.[17] Attempts were made to synthesise a complex with no coordinated chlorides using an excess of antimony pentachloride. However, *in situ* ^{45}Sc NMR studies of the products within this system only contained resonances at 99.5 ppm, corresponding to the monochloro-cation.

The structure of [ScCl(MeCN)([15]-crown-5)][SbCl$_6$]$_2$.MeCN was determined by single crystal X-ray diffraction, revealing a seven coordinate pentagonal bipyramidal scandium cation (Fig. 5.9). The scandium metal centre was located in the centre of the crown, with MeCN and Cl in *trans* positions perpendicular to the axis of the crown ether. Selected bond lengths and angles are presented in Table 5.1. The structure of [ScCl$_2$([15]-crown-5)]$_2$[CuCl$_4$] has been reported previously, allowing comparison of structural data.[18] The [ScCl(MeCN)([15]-crown-5)]$^{2+}$ cation exhibits a shorter Sc-Cl bond length (2.361(2) Å) than observed for [ScCl$_2$([15]-crown-5)]$^+$ (2.426(8) Å). The

two complexes have similar Sc-O bonds lengths, the monochloro-cation having Sc-O = 2.135(3) to 2.176(3) Å compared with 2.109(2) and 2.150(1) Å for $[ScCl_2([15]\text{-}crown\text{-}5)]^+$.
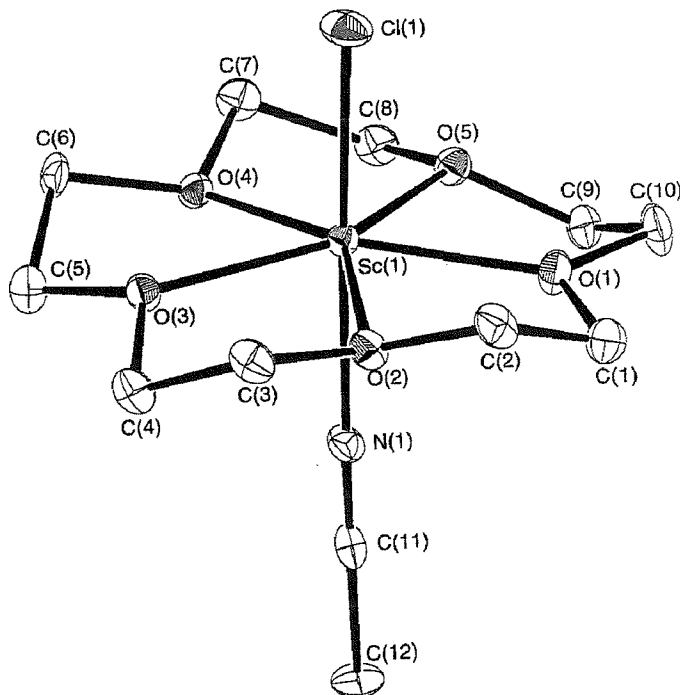
Fig. 5.9 The structure of the cation in [ScCl(MeCN)([15]-crown-5)][SbCl₆]₂.MeCN, showing the atom numbering scheme. Ellipsoids are drawn at the 40% probability level, whilst H atoms are omitted for clarity.

Table 5.1 Selected bond lengths (Å) and angles (°) for the structure of [ScCl(MeCN)([15]-crown-5)][SbCl₆]₂.MeCN.

Sc-Cl(1)	2.361(2)	Sc-N(1)	2.272(4)
Sc-O(1)	2.135(3)	Sc-O(2)	2.155(3)
Sc-O(3)	2.164(3)	Sc-O(4)	2.154(3)
Sc-O(5)	2.176(3)	C-O	1.444(6)-1.469(6)
C-C(crown)	1.477(7)-1.501(7)		
O(1)-Sc-O(2)	71.2(1)	O(2)-Sc-O(3)	72.1(1)
O(3)-Sc-O(4)	71.5(1)	O(4)-Sc-O(5)	72.5(1)
O(5)-Sc-O(1)	71.7(1)	N(1)-Sc-Cl(1)	178.2(1)
O(5)-Sc-Cl(1)	92.14(9)	O(4)-Sc-Cl(1)	95.7(1)

The IR spectrum of [ScCl$_2$([18]-crown-6)][FeCl$_4$] contained the characteristic v_3 mode for [FeCl$_4$]$^-$, a strong band at 389 cm^{-1}, confirming halide abstraction from Sc(III) had occurred.[25] The ^{45}Sc NMR spectrum contained a single resonance at δ 132 ppm (W$_{1/2}$ = 600 Hz), which by comparison with the results for the [15]-crown-5 system suggested a Cl$_2$O$_5$ donor set. Interestingly, previous ^{45}Sc NMR studies of [ScCl$_2$([18]-crown-6)][SbCl$_6$] report multiple resonances.[17, 20] However, cooling this NMR solution did not reveal further peaks. Addition of 1 molar equivalent aliquots of FeCl$_3$ to the NMR solution (in an attempt to abstract further chlorides from the Sc centre) led to the appearance of new features at δ 101 and –2 ppm. The former appeared when a single aliquot was added, remaining until the Sc:FeCl$_3$ ratio reached 1:4. By comparison with the [15]-crown-5 system, this resonance can be attributed to the cation [ScCl([18]-crown-6)]$^{2+}$, whilst the resonance at –2 ppm is presumably [Sc([18]-crown-6)]$^{3+}$ (probably with coordinated MeCN, as six coordinate scandium seems unlikely for this system when the results in this Chapter and those of Willey et al. are considered).

The analogous reaction using SbCl$_5$ as a halide abstractor has been reported, with a 1:1:1 molar ratio of [ScCl$_3$(thf)$_3$], SbCl$_5$ and [18]-crown-6 affording [ScCl$_2$([18]-crown-6)]SbCl$_6$.[17] Attempts to remove further chlorines in this case (by addition of further SbCl$_5$) gave complex mixtures.[17] When monitored *in situ* using ^{45}Sc NMR spectroscopy, the results were difficult to interpret.[20] It seems possible that SbCl$_5$ is such a strong Lewis acid that it reacts not only by abstracting chlorine, but also reacts with other bases in the reaction mixture. Hence, controlling the Sc:SbCl$_5$ ratio proves extremely difficult. However, when the ^{45}Sc NMR results for the system using the weaker Lewis acid FeCl$_3$ are considered, the data for the SbCl$_5$ system begin to make sense. *In situ* ^{45}Sc NMR experiments were conducted on the [ScCl$_3$(thf)$_3$] / [18]-crown-6 / SbCl$_5$ system (in anhydrous MeCN), with the quantity of SbCl$_5$ varied. Resonances were observed at δ 130, 95 and –19 ppm, although their relative intensities were not obviously related to the quantity SbCl$_5$ added. It seems probable that the first two resonances correspond to [ScCl$_2$([18]-crown-6)]$^+$ and [ScCl([18]-crown-6)]$^{2+}$ (presumably with coordinated MeCN) by comparison of shift with the FeCl$_3$ system (see above). The third resonance is absent in the FeCl$_3$ system, but could

be the species $[Sc([18]\text{-crown-6-SbCl}_5)(MeCN)_x]^{3+}$, with the $SbCl_5$ coordinated to the 'free' oxygen in the crown ether.

The crystal structure of $[ScCl_2([18]\text{-crown-6})][FeCl_4]$ shows two similar independent cations, differing only in the conformation of the crown ether at the uncoordinated oxygen O(4). The cation containing Sc(1) is shown in Fig. 5.10, with selected bond lengths and angles reported in Table 5.2. The cation shows the Sc centre bonded to five of the six available crown ether oxygen atoms in a pentagonal bipyramidal geometry, the oxygens in the pentagonal plane, with *trans* chlorines. Comparison of this structure with that of $[ScCl_2([18]\text{-crown-6}][SbCl_6]$ (Fig. 5.7) reveals little difference between the cations, apart from some minor variations in bond lengths and angles.[17] For example, the Sc-Cl bond lengths in $[ScCl_2([18]\text{-crown-6})][FeCl_4]$ range from 2.402(1) to 2.435(1) Å, whilst the $[SbCl_6]^-$ salt had Sc-Cl = 2.402(3) and 2.418(3) Å. The Sc-O$_{bonded}$ distances in the $[FeCl_4]^-$ complex again show noticable variation, ranging from 2.192(3) to 2.264(2) Å. In contrast, the $[SbCl_6]^-$ salt has a narrower distribution of bond lengths, from 2.190(5) to 2.229(5) Å.[17]
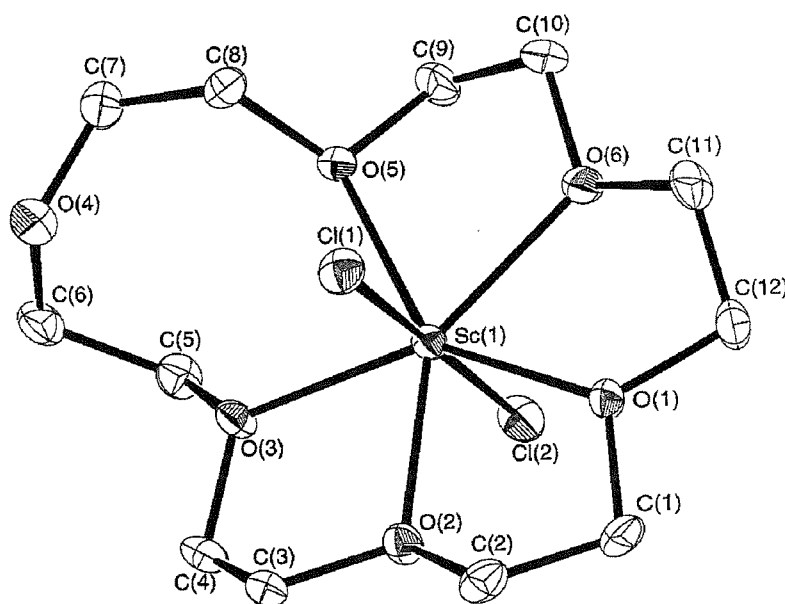
Fig. 5.10 View of the cation containing Sc(1) in $[ScCl_2([18]\text{-crown-6})][FeCl_4]$ showing the atom labelling scheme. Ellipsoids are drawn at the 50% probability level, with H atoms omitted for clarity. The species containing Sc(2) is similar, differing only in the conformation at C(7) and O(4).

Table 5.2 Selected bond lengths (Å) and angles (°) for the structure of [ScCl₂([18]-crown-6)][FeCl₄].

Sc(1)-Cl(1)	2.435(1)	Sc(1)-Cl(2)	2.413(1)
Sc(1)-O(1)	2.195(2)	Sc(1)-O(2)	2.192(2)
Sc(1)-O(3)	2.230(2)	Sc(1)-O(5)	2.243(2)
Sc(1)-O(6)	2.210(2)	Sc(2)-Cl(3)	2.425(1)
Sc(2)-Cl(4)	2.402(1)	Sc(2)-O(7)	2.264(2)
Sc(2)-O(9)	2.216(2)	Sc(2)-O(10)	2.200(2)
Sc(2)-O(11)	2.213(2)	Sc(2)-O(12)	2.202(2)
C-C(crown)	1.483(5)-1.503(5)	C-O	1.417(4)-1.473(4)
O(1)-Sc(1)-O(2)	70.76(9)	O(2)-Sc(1)-O(3)	71.68(8)
O(3)-Sc(1)-O(5)	77.50(9)	O(5)-Sc(1)-O(6)	71.72(8)
O(6)-Sc(1)-O(1)	69.60(9)	Cl(1)-Sc(1)-Cl(2)	177.96(5)
O(1)-Sc(1)-Cl(1)	85.58(7)	O(3)-Sc(1)-Cl(1)	95.50(7)
O(7)-Sc(2)-O(9)	77.85(9)	O(9)-Sc(2)-O(10)	70.66(8)
O(10)-Sc(2)-O(11)	71.11(9)	O(11)-Sc(2)-O(12)	68.96(9)
O(12)-Sc(2)-O(7)	72.28(9)	Cl(3)-Sc(2)-Cl(4)	176.35(4)
O(11)-Sc(2)-Cl(3)	86.47(7)	O(9)-Sc(2)-Cl(3)	95.12(7)

The IR spectrum of the mixed thia-oxa crown complex [ScCl₂([15]aneS₂O₃][FeCl₄] contained the v_3 mode of [FeCl₄]⁻ as a strong band at 382 cm⁻¹. The ¹H NMR spectrum of this complex in CD₂Cl₂ contained overlapping multiplets from 3.35 to 3.70 ppm. When compared to the spectrum of the 'free' ligand, for which resonances are observed at δ 2.72(t), 2.87(s) (both CH_2S), 3.64(s) and 3.75(t) (both CH_2O),[26] it appears that the ligand has coordinated through the sulfur atoms, resulting in the resonances attributable to CH_2S shifting to higher frequency. Further evidence of donation throughout the sulfur atoms is given by the ⁴⁵Sc data, with a single resonance present in an acetonitrile solution at δ 200 ppm. In comparison, the ⁴⁵Sc NMR spectrum of the [ScCl₂([15]-crown-5)]⁺ cation contains a single resonance at δ 130 ppm. Crystals suitable for study by single crystal X-ray diffraction could not be grown, but it appears that scandium has bonded through the softer S donor. This is the first reported example of coordination of a thioether donor to a Sc(III) centre.

Whilst no novel anhydrous ScCl₃ / [12]-crown-4 compounds were synthesised, ⁴⁵Sc NMR spectroscopy was conducted on this system of compounds to investigate behaviour in solution. The complex [Sc([12]-crown-4)₂][SbCl₆][Sb₂Cl₈(MeCN)₂].

2MeCN has been produced by reaction of [ScCl$_3$(thf)$_3$], SbCl$_5$, SbCl$_3$ and [12]-crown-4 in a 1:1:2:2 molar ratio in anhydrous MeCN.[16] The compound has been structurally characterised (Fig. 5.6) revealing the scandium centre sandwiched between two [12]-crown-4 ligands in a square antiprismatic conformation. In this study, the species was observed as a single resonance at δ 25 ppm in the [45]Sc NMR spectrum.[16] A second compound, [ScCl$_2$([12]-crown-4)(MeCN)]SbCl$_6$ has also been reported, synthesised by reaction of a 1:1:1 molar ratio of [ScCl$_3$(thf)$_3$], [12]-crown-4 and SbCl$_5$ in dry MeCN.[17] An *in situ* NMR study of this compound revealed two resonances in the [45]Sc NMR spectrum at δ 25 and 153 ppm, attributed to [Sc([12]-crown-4)$_2$]$^{3+}$ and [ScCl$_2$([12]-crown-4)]$^+$ respectively.[20] However, no structural data exist for the second complex. In the work described in this thesis, a resonance at δ 153 ppm was encountered for all solutions containing the hydrolysis product [ScCl$_3$(H$_2$O)$_3$] (see 5.2.2). Given that the cavity in [12]-crown-4 is too small to encapsulate Sc^{3+}, it would behave differently to the larger crowns studied. Along with this [45]Sc NMR data, attempts were made to confirm the identity of the product of the 1:1:1 molar equivalent reaction. Following the synthetic route reported by Willey *et al.*, a complex with similar spectroscopic data to "[ScCl$_2$([12]-crown-4)(MeCN)]SbCl$_6$" was isolated, although crystals suitable for single crystal X-ray diffraction could not be grown. The [45]Sc NMR spectrum of a solution of the complex in rigorously dried MeCN contained resonances at δ 25 and 205 ppm, the ratio of integrals being approximately 1:1. The latter resonance is very similar to that given by a solution of [ScCl$_3$(thf)$_3$] in dry MeCN. When treated with an excess of LiCl, this resonance is converted to a sharper peak at δ 217 ppm, possibly due to formation of [ScCl$_4$(MeCN)$_2$]$^-$. However, in the absence of excess Cl$^-$, this species probably decomposes to form [ScCl$_3$(MeCN)$_3$]. The resonance observed for this species in this study compares well with the literature value of δ 201 ppm.[27] Hence, whilst in the absence of an X-ray crystal structure any assignment is made tentatively, it seems possible that the species isolated is in fact [Sc([12]-crown-4)$_2$][SbCl$_6$]$_2$[ScCl$_4$(MeCN)$_2$] and not [ScCl$_2$([12]-crown-4)]SbCl$_6$.

5.2.2 Reactions of hydrated scandium chloride with crown ether ligands

The anhydrous scandium chloride systems proved extremely moisture sensitive. For example, when a solution of $[ScCl_2([18]\text{-crown-6})]SbCl_6$ in dry MeCN was left to evaporate exposed to air, crystals of $mer\text{-}[ScCl_3(H_2O)_3].[18]\text{-crown-6}$ were obtained. When $ScCl_3.6H_2O$ was reacted with one molar equivalent of [18]-crown-6 in ethanol, the same product was isolated. The reaction of $ScCl_3.6H_2O$ with [12]-crown-4, [15]-crown-5 or [18]-crown-6 in a 2:1 ratio in ethanol afforded complexes of the type $[ScCl_3(H_2O)_3]_2.crown$. All of these '2:1' products proved highly soluble to the extent that isolation of crystals or powders was difficult. All the complexes isolated in this system were spectroscopically similar.

The ^{45}Sc NMR spectra of all of the complexes containing $[ScCl_3(H_2O)_3]$ contained a resonance at $ca.$ 153 ppm, $W_{1/2}$ ranging from 500 to 1100 Hz. The resonances were both concentration and solvent dependent (spectra were recorded in ethanol, acetonitrile and acetone). When $ScCl_3.6H_2O$ was dissolved in ethanol, a similar resonance was observed (at 150 ppm), and as $[ScCl_3(H_2O)_3]$ is the only scandium containing species formed, this result strongly suggested that the resonances observed in all these NMR solutions were caused by this scandium group.

The ^1H NMR spectra of all the hydrated complexes contained singlets at δ $ca.$ 3.6 ppm, corresponding to 'free' crown ether. A second, broad singlet was also present in all spectra, corresponding to water. The chemical shift of this second peak varied for each complex ($[ScCl_3(H_2O)_3]_2.[12]\text{-crown-4}$ δ 4.0 (br, s), $[ScCl_3(H_2O)_3]_2.[15]\text{-crown-5}$ δ 4.7 (br, s), $[ScCl_3(H_2O)_3]_2.[18]\text{-crown-6}$ δ 4.6 (br, s), $[ScCl_3(H_2O)_3].[18]\text{-crown-6}$ δ 4.2 (br, s)). The presence of water in these compounds was confirmed by two bands in each infra-red spectrum, namely a broad band found between 3410 and 3300 cm^{-1}, and a sharper band lying between 1620 and 1636 cm^{-1}.[25] Bands at $ca.$ 1100 and 950 cm^{-1} in these complexes indicated v(C-O-C) and v(C-C-O) of the crown ethers respectively.[12]

The crystal structure of $mer\text{-}[ScCl_3(H_2O)_3].[18]\text{-crown-6}$ is shown in Figs. 5.11 and 5.12, with selected bond lengths and angles given in Table 5.3. Fig. 5.11 shows the

neutral [ScCl$_3$(H$_2$O)$_3$] unit, with a plane of symmetry passing through Cl(2), Sc(1) and O(4). The arrangement of ligands around the scandium centre is approximately octahedral. Fig. 5.12 shows an extended network of [ScCl$_3$(H$_2$O)$_3$] groups, hydrogen bonded to [18]-crown-6 ligands through three O-H....O bonds (depicted by the thinner black lines). All three water groups of each scandium group are involved in bonding to three oxygens of a single crown. The other three oxygens of the crown ether group bond in the same fashion to a second [ScCl$_3$(H$_2$O)$_3$] group. As a result, an infinite chain of alternating [ScCl$_3$(H$_2$O)$_3$] and [18]-crown-6 groups is formed. The hydrogen bond lengths are all approximately 2.8 Å. The H-atoms of these water groups were convincingly identified in later electron density maps. The [18]-crown-6 group has a crystallographic centre of symmetry.
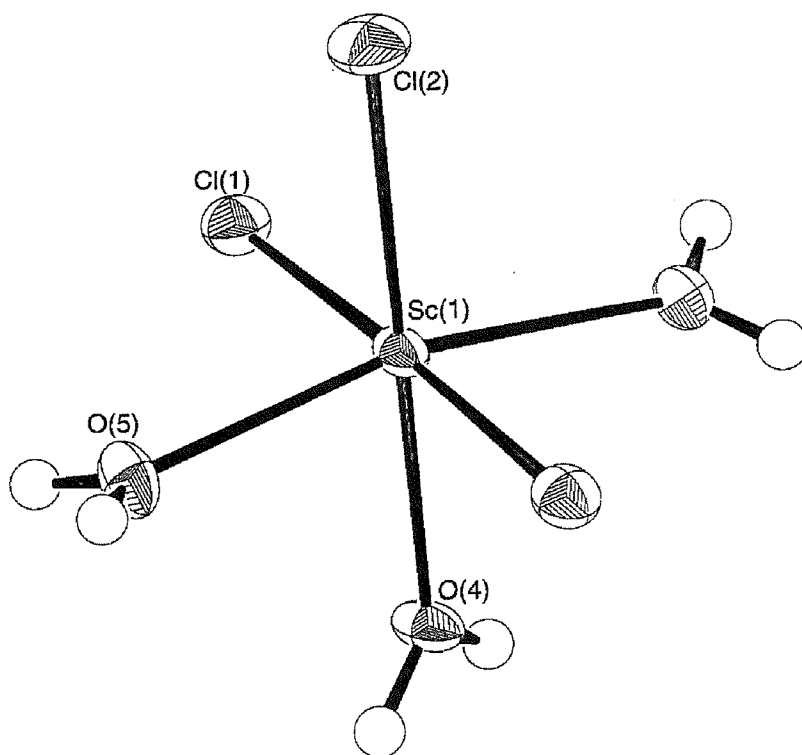
Fig. 5.11 View of the structure of [ScCl$_3$(H$_2$O)$_3$].[18]-crown-6, showing the Sc(1) group and demonstrating the atom numbering scheme adopted. The 2-fold symmetry along O(4), Sc(1) and Cl(2) is identified. Ellipsoids are drawn at the 50% probability level.
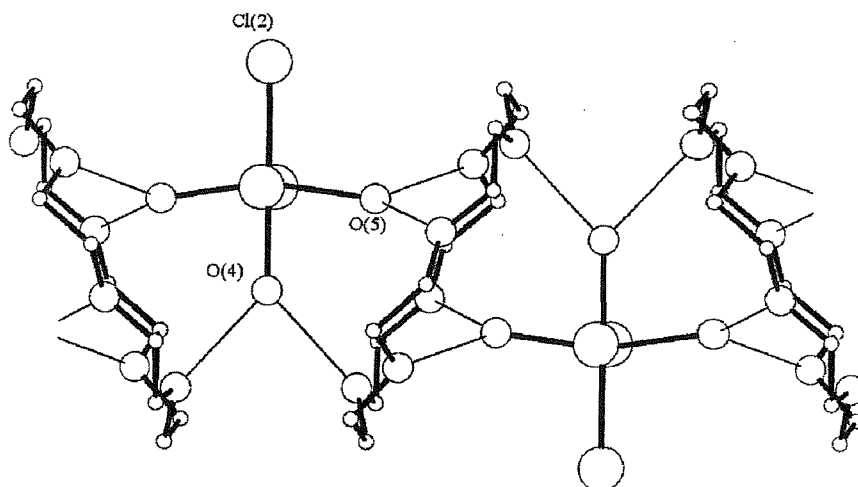
Fig. 5.12 View of [ScCl₃(H₂O)₃].[18]-crown-6 along the *a* direction showing the OH....O bonding between Sc groups and the crown parallel to the *c* direction. H-bonding is indicated by single lines. H-atoms omitted for clarity.

Table 5.3 Selected bond lengths (Å) and angles (°) for the structure of [ScCl₃(H₂O)₃].[18]-crown-6 ('H---O(crown)' distances are hydrogen bond lengths).

Sc-Cl(1)	2.4403(6)	Sc-Cl(2)	2.4267(8)
Sc-O(4)	2.177(2)	Sc-O(5)	2.142(1)
C-C	1.441(3)-1.484(4)	C-O	1.444(6)-1.469(6)
H---O(crown)	2.768(2) – 2.798(2)		
O(4)-Sc-O(5)	81.89(4)	O(5)-Sc-O(5i)[a]	163.78(8)
Cl(1)-Sc-Cl(2)	91.86(2)	Cl(1)-Sc-Cl(1i)[a]	176.27(3)
O(4)-Sc-Cl(1)	88.14(2)	O(4)-Sc-Cl(2)	180.00
O(5)-Sc-Cl(1)	89.79(5)	O(5)-Sc-Cl(2)	98.11(4)

[a] Symmetry operation:- i = -x, y, -z +3/2

The observed hydrolysis pathway by traces of water was unexpected, the displacement of the crown ether group by H₂O indicating a strong preference of the Sc(III) centre for both chloride and water over [18]-crown-6. The crown was hydrogen bonded to the scandium centres (via water) in the secondary coordination sphere. This contrasts with the hydrolysis mechanism observed for the next element in the periodic table, titanium. For example, hydrolysis of [TiCl₄([18]-crown-6)] by trace

quantities of water results in the loss of chlorines, replaced by μ-O bridges. However, the crown remains bonded to the metal centre (see Chapter 6).

5.2.3 Reactions of hydrated scandium nitrate with crown ether ligands

When scandium nitrate pentahydrate was reacted with one molar equivalent of [18]-crown-6 in ethanol, the product was the white solid $[Sc(H_2O)_3(NO_3)_3].[18]$-crown-6. The same reaction using [15]-crown-5 afforded the white powder $[Sc(H_2O)_4(NO_3)_2]NO_3.[15]$-crown-5. Slow evaporation of a solution of $Sc(NO_3)_3.5H_2O$ and [12]-crown-4 in the minimum amount of ethanol yielded several crystals of $[Sc(H_2O)_2(NO_3)_3].([12]$-crown-4$)_2$ suspended in a thick gum. Crystallisation over a longer period yielded a few small crystals of the hydroxy-bridged dimer $[Sc_2(H_2O)_6(OH)_2(NO_3)_2](NO_3)_2.[12]$-crown-4, with the yield so poor that only single crystal X-ray diffraction studies could be carried out. In an attempt to improve the yield, the same reaction was carried out in the presence of several drops of 1 molar NaOH in order to improve formation of the hydroxy-bridged dimer. Several crystals were formed from the reaction, identified by X-ray diffraction as $[Sc_2(NO_3)_4(H_2O)_4(OH)_2].[Na([12]$-crown-4$)_2]NO_3.(H_2O)_3$. All of the complexes were extremely soluble in ethanol, meaning solids proved difficult to isolate in large yields, with the [12]-crown-4 species particularly hard to extract from solution.

The IR spectrum of $[Sc(H_2O)_3(NO_3)_3].[18]$-crown-6 contained a weak band at 810 cm^{-1}, assigned as v_2 of a coordinated nitrate group. In addition, water was apparent from the broad absorption at 3400 cm^{-1} and a sharp band at 1645 cm^{-1}.[25] Further bands assignable to bonded nitrate groups were obscured by absorptions of the crown ether.[25]

The ^1H NMR spectrum of $[Sc(H_2O)_3(NO_3)_3].[18]$-crown-6 in deuterated acetone contained resonances assigned as uncoordinated crown ether (a singlet at 3.6 ppm) and water (a broad singlet at 4.0 ppm). The ^{45}Sc NMR spectrum in acetone contained a single resonance at δ 5.0 ppm. This value seems reasonable when compared to literature values of scandium centres in oxygen donor environments. For example, it compares closely to the hexaaquo ion which is the accepted 'zero reference', whilst in

this study, scandium surrounded by eight O-donors in the complex [Sc(NO$_3$)$_3$(Ph$_3$PO)$_2$] has δ -7.5 ppm (Chapter 2).[28] Crystals of the [18]-crown-6 compound [Sc(NO$_3$)$_3$(H$_2$O)$_3$].[18]-crown-6 were isolated, and a unit cell determined. A search of the Cambridge Crystallographic Database revealed that the structure of this complex had been determined previously, with the unit cell the same (Fig. 5.8).[21] Initially, this refinement had been carried out using the space group P*na*2$_1$, then later, the solution was conducted in the centrosymmetric space group P*nma*. The latter solution revealed a scandium residue with a plane of symmetry, the Sc atom being nine-coordinate (with three bidentate nitrate groups and three waters coordinated (in a *mer* configuration, if the bidentate nitrate groups are conceptually replaced by monodentate ligands)). The Sc-O$_{water}$ distances were 2.205(3) and 2.228(3) Å, whilst the Sc-O$_{nitrate}$ distances range from 2.249(4) to 2.363(5) Å. Atomic coordinates of hydrogen atoms were not supplied, but calculation of O...O distances between crown oxygens and the waters bonded to scandium revealed four potential H-bond lengths of less than 3.0 Å. This system of H-bonding would produce an infinite chain, similar to that observed for [ScCl$_3$(H$_2$O)$_3$].[18]-crown-6.

The IR spectrum of [Sc(NO$_3$)$_2$(H$_2$O)$_4$]NO$_3$.[15]-crown-5 contained two weak ν_2 nitrate modes, at 808 cm^{-1} (corresponding to coordinated nitrate) and at 833 cm^{-1} (ionic nitrate).[25] Absorption bands at 1098 and 944 cm^{-1} were assigned as ν(C-O-C) and ν(C-C-O) respectively.[12] The ^{1}H NMR spectrum of this compound was similar to that of [Sc(H$_2$O)$_3$(NO$_3$)$_3$].[18]-crown-6, containing a singlet at 3.6 ppm ('free' crown) and a broad singlet at 4.4 ppm (coordinated water). The [45]Sc NMR spectrum was also similar, exhibiting a resonance at δ 2 ppm. The crystal structure of [Sc(H$_2$O)$_4$(NO$_3$)$_2$]NO$_3$.[15]-crown-5 was determined (Fig. 5.13). The structure contains an eight coordinate scandium centre, with two coordinated nitrate groups. However, the crystals isolated were of rather poor quality. Whilst the structure did not refine well, a clear picture of the hydrogen bonding network was revealed. A summary of the crystal data is given in Table 5.7. The cation exhibits an eight coordinate scandium centre, with two bidentate nitrate groups and four water groups coordinated. The geometry around the Sc centre is octahedral (if the nitrate groups are conceptually replaced by monodentate ligands). Sc-O$_{water}$ bond lengths range from

2.134(8) to 2.232(7) Å, whilst Sc-O$_{nitrate}$ lengths lie between 2.184(8) and 2.249(7) Å. Disorder was seen in the [15]-crown-5 group, with the non-bonded oxygen and the adjacent carbon atoms exhibiting high thermal parameters. Whilst this was partially caused by fractionally occupied atoms, the high values of the atomic displacement paramaters (adp's) indicated that disorder was more extensive. As a result, no attempt was made to introduce H atoms into the structure, including those of the coordinated water groups. The proposed hydrogen bonding scheme is hence derived from the O....O distances (*ca.* 2.8 Å), with bonds apparent between two *trans* water groups and four oxygens of the crown ether. As a result, a chain of alternating scandium cations and crown ether groups is formed. H-bonding is also apparent between the ionic nitrate groups and the waters containing O(10) and O(11). A previous scandium nitrate – [15]-crown-5 complex has been structurally characterised by Gan *et al.* and had the composition [Sc(H$_2$O)$_2$(NO$_3$)$_3$].[15]-crown-5.[23]
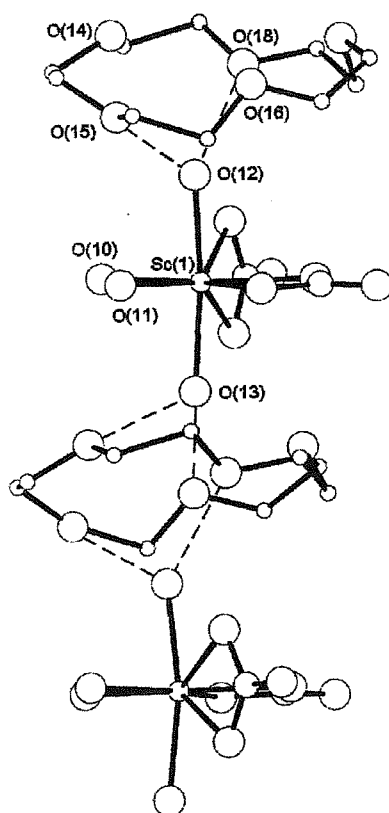
Fig. 5.13 The structure of [Sc(NO$_3$)$_2$(H$_2$O)$_4$](NO$_3$).[15]-crown-5, indicating the OH...O H-bonding chain between the Sc cation and the crown ether lying parallel to the *b* direction. H bonding is shown by dotted lines. H atoms are omitted for clarity.

The IR spectrum of $[Sc(H_2O)_2(NO_3)_3].([12]$-crown-4$)_2$ contained a broad band at 3580 cm^{-1} and a sharp absorption at 1650 cm^{-1}, confirming the presence of water. No bands corresponding to ionic nitrate groups were present. The ^1H NMR spectrum in d^6-acetone contained singlets at δ 3.6 and 4.5 ppm, the latter broad. These corresponded to 'free' crown ether and water respectively. The corresponding ^{45}Sc NMR spectrum revealed a broad resonance at δ -1.0 ppm.

Insufficient quantity of either $[Sc_2(NO_3)_4(H_2O)_4(OH)_2][Na([12]$-crown-4$)_2]$ $(NO_3).(H_2O)_3$ or $[Sc_2(H_2O)_6(OH)_2(NO_3)_2](NO_3)_2.[12]$-crown-4 were isolated to allow either spectroscopic or analytical analysis.

The structure of $[Sc(NO_3)_3(H_2O)_2].([12]$-crown-4$)_2$ was determined by single crystal X-ray diffraction, revealing an eight coordinate scandium centre (Fig. 5.14), with [12]-crown-4 in its second coordination sphere. Fig. 5.15 shows the hydrogen bonded species. Selected bond lengths and angles are given in Table 5.4. The neutral eight coordinate scandium unit contains three nitrate groups bonded in the symmetrical bidentate mode. The scandium group exhibits 2-fold symmetry. The two coordinated water molecules form an O-Sc-O bond angle of 153.64(9)°. Each water forms hydrogen bonds with [12]-crown-4, exhibiting OH....O bond lengths of *ca.* 2.7 Å. Only two oxygens of each crown ether group are involved in H-bonding, meaning a discrete species is formed, contrasting with the chain-like networks observed for both of $[Sc(NO_3)_2(H_2O)_4](NO_3).[15]$-crown-5 and $[Sc(H_2O)_3(NO_3)_3].[18]$-crown-6. The H atoms were located in later electron density maps in convincing positions.
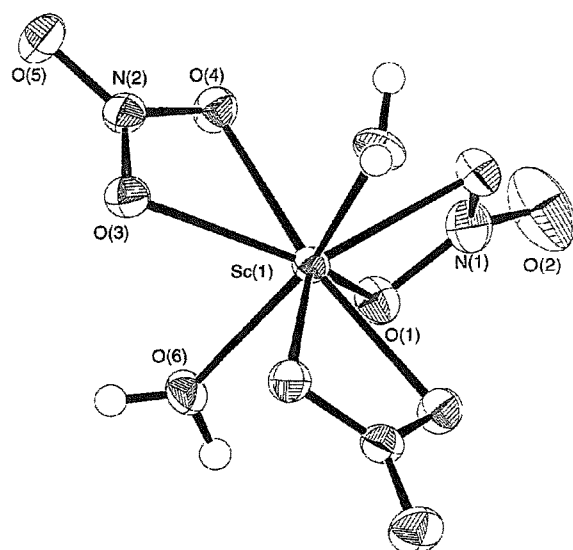
Fig. 5.14 View of [Sc(NO$_3$)$_3$(H$_2$O)$_2$].([12]-crown-4)$_2$ showing the Sc(1) group, indicating the atom numbering scheme adopted. The 2-fold symmetry along the c direction passing through Sc(1), N(1) and O(2) is identified. Ellipsoids are drawn at 50%.
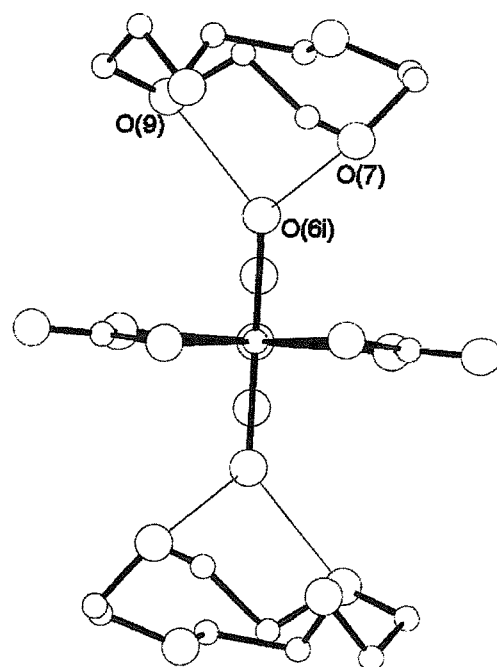
Fig. 5.15 View of [Sc(NO$_3$)$_3$(H$_2$O)$_2$].([12]-crown-4)$_2$ along the c direction showing the OH...O bonds, identified by thin lines, between O(6i) of the Sc group, and the crown ether. Ellipsoids are drawn at the 50% probability level.

Table 5.4 Selected bond lengths (Å) and angles (°) for the structure of $[Sc(NO_3)_3(H_2O)_2].([12]$-crown-4$)_2$. ('H---O(crown)' distances are hydrogen bond lengths).

Sc-O(1)	2.252(2)	Sc-O(3)	2.268(1)
Sc-O(4)	2.201(2)	Sc-O(6)	2.105(2)
C-C	1.492(3)-1.505(4)	C-O	1.417(3)-1.444(3)
H---O(crown)	2.684(2) & 2.689(2)		
O(1)-Sc-O(1i)[a]	56.98(7)	O(3)-Sc-O(4)	57.58(5)
O(6)-Sc-O(6i)[a]	153.64(9)		

[a] Symmetry operation: - i = -x, -y, z

A few crystals of $[Sc_2(NO_3)_2(H_2O)_6(OH)_2](NO_3)_2.[12]$-crown-4 were obtained, the structure revealing a centrosymmetric cation containing two scandium metal centres, bridged by OH groups (Fig. 5.16). Selected bond lengths and angles are presented in Table 5.5. In addition to two OH groups, each scandium centre had a single nitrate group coordinated (in the symmetrical bidentate mode of coordination) and three waters, giving rise to a seven-coordinate metal centre. The Sc-O distances vary considerably depending on the functional group involved. For example, the Sc-O_{bridge} values were 2.050(2) and 2.064(2) Å compared with the longer Sc-$O_{nitrate}$ lengths of 2.261(2) and 2.366(2) Å. The Sc-O_{water} bond lengths range from 2.101(2) to 2.186(2) Å. The crown ether group was also centrosymmetric, with all the oxygens involved in hydrogen bonding to the cation through the coordinated water groups, indicated by O...O distances of less than 3.0 Å. Indeed, all of the hydrogens of the cation were involved in H-bonding to either the crown oxygens, or the oxygens of an ionic nitrate group. Fig. 5.17 shows the extended H-bonding network in this structure, showing chains aligned in the c direction, linked by H-bonding to ionic nitrate groups to form a 2-dimensional network.
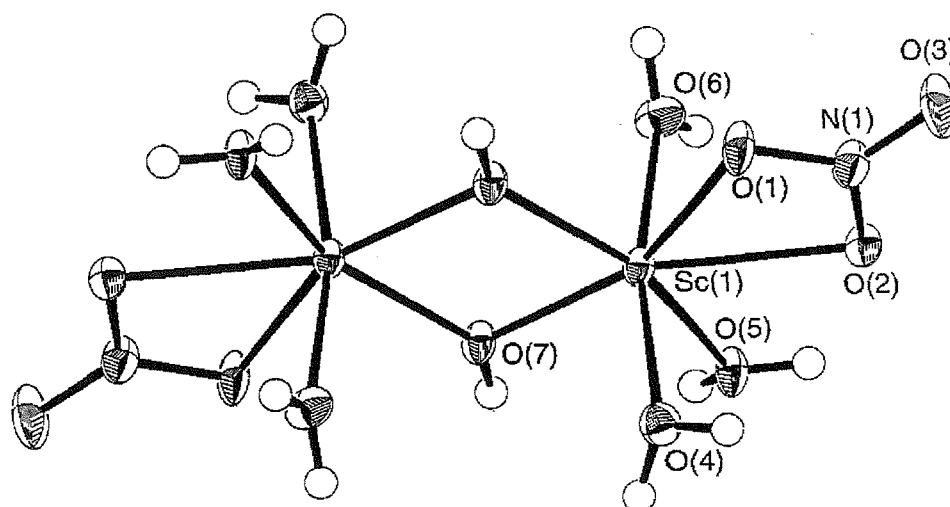
Fig. 5.16 The structure of $[Sc_2(NO_3)_2(H_2O)_6(OH)_2](NO_3)_2.[12]$-crown-4, showing the centrosymmetric cation with the atom numbering scheme identified. Ellipsoids are drawn at the 50% probability level, whilst H atoms are omitted for clarity.
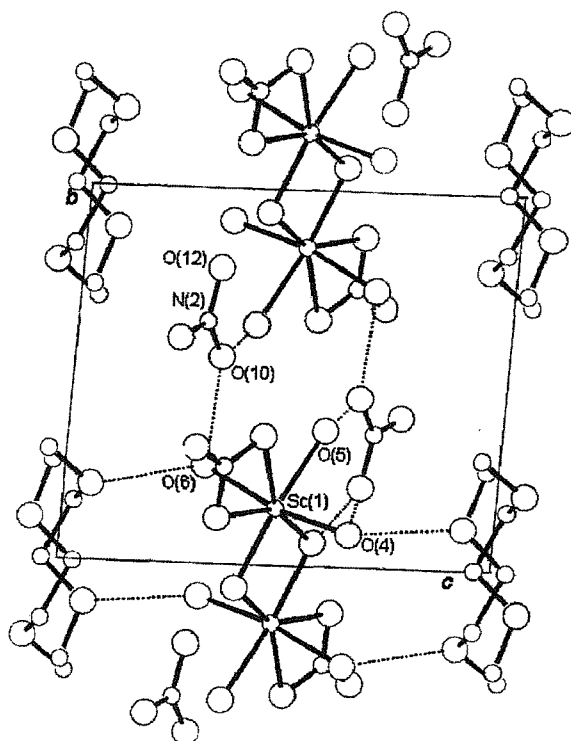
Fig. 5.17 View of $[Sc_2(NO_3)_2(H_2O)_6(OH)_2](NO_3)_2.[12]$-crown-4 showing the 2-dimensional sheet formed by OH...O hydrogen bonding (indicated by dashed lines).

Table 5.5 Selected bond lengths (Å) and angles (°) for the structure of $[Sc_2(NO_3)_2(H_2O)_6(OH)_2](NO_3)_2.[12]$-crown-4. ('H---O(crown)' distances are hydrogen bond lengths).

Sc(1)-O(1)	2.261(2)	Sc(1)-O(2)	2.366(2)
Sc(1)-O(4)	2.128(2)	Sc(1)-O(5)	2.186(2)
Sc(1)-O(6)	2.101(2)	Sc(1)-O(7)	2.050(2)
Sc(1)-O(7i)[a]	2.064(2)	Sc(1)...Sc(1i)[a]	3.296(1)
C(1)-C(2)	1.511(4)	C(3)-C(4)	1.488(4)
C-O	1.431(3)-1.435(3)	H---O(crown)	2.723(3) – 2.904(2)
O(1)-Sc-O(2)	55.23(6)	O(7)-Sc(1)-O(7i)[a]	73.54(7)
Sc(1)-O(7)-Sc(1i)[a]	106.46(7)		

[a] Symmetry operation: - i = 1-x, -y, 1-z

A third scandium nitrate – [12]-crown-4 species was identified by single crystal X-ray diffraction. The structure of $[Sc_2(NO_3)_4(H_2O)_4(OH)_2][Na([12]$-crown-4$)_2]$ $(NO_3).(H_2O)_3$ contained another 'hydroxy-bridged dimer', shown in Fig. 5.18. Selected bond lengths and angles are given in Table 5.6. In this example, the scandium centres are again linked by two hydroxy bridges. In addition, each scandium centre has two coordinated water molecules and two nitrate groups bonded in the symmetrical bidentate fashion, giving an eight-coordinate metal centre. In contrast to the structure of $[Sc_2(NO_3)_2(H_2O)_6(OH)_2](NO_3)_2.[12]$-crown-4, in this example the crown ether groups are bonded to a sodium ion, with two crowns per metal centre leading to an eight-coordinate Na centre. Since all of the ether groups are involved in bonding to the sodium ions, the crown is not involved in secondary coordination to the hydroxy bridged dimer. H-bonding was observed between coordinated water, solvate water and bridging hydroxy groups, the shortest O...O distances being *ca.* 2.7 to 2.8 Å in length. All of the hydrogen atoms were located in convincing positions during refinement except for those coordinated to O(32A)/(32B), a disordered water group. In addition, this solvate water overlapped with the ionic nitrate group, causing disorder in N(5A)/(5B). Figure 5.19 depicts the supramolecular structure of $[Sc_2(NO_3)_4(H_2O)_4(OH)_2][Na([12]$-crown-4$)_2](NO_3).(H_2O)_3$. The sodium cation has been reported previously, and is not uncommon (Fig. 5.20).[29, 30]
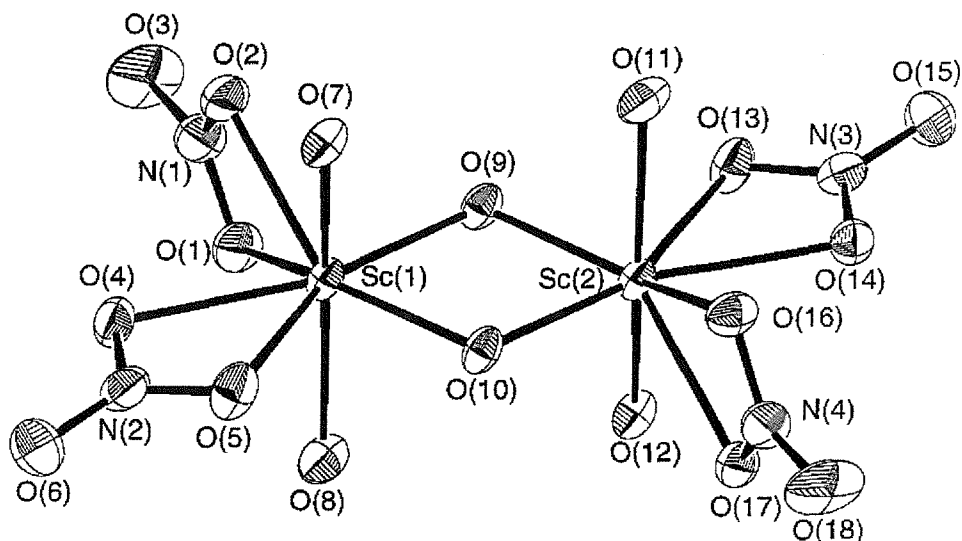
Fig. 5.18 View of $[Sc_2(NO_3)_4(H_2O)_4(OH)_2][Na([12]\text{-}crown\text{-}4)_2](NO_3).(H_2O)_3$, showing the scandium dimer, and indicating the atom numbering scheme adopted. Ellipsoids are drawn at the 50% probability level, with H atoms omitted for clarity.

Table 5.6 Selected bond lengths (Å) and angles (°) for the structure of $[Sc_2(NO_3)_4(H_2O)_4(OH)_2][Na([12]\text{-}crown\text{-}4)_2](NO_3).(H_2O)_3$.

Sc(1)-O(1)	2.346(2)	Sc(1)-O(2)	2.345(2)
Sc(1)-O(4)	2.298(3)	Sc(1)-O(5)	2.337(2)
Sc(1)-O(7)	2.170(2)	Sc(1)-O(8)	2.153(3)
Sc(1)-O(9)	2.039(2)	Sc(1)-O(10)	2.087(2)
Sc(2)-O(9)	2.089(2)	Sc(2)-O(10)	2.033(2)
Sc(2)-O(11)	2.155(3)	Sc(2)-O(12)	2.174(2)
Sc(2)-O(13)	2.352(2)	Sc(2)-O(14)	2.291(2)
Sc(2)-O(16)	2.341(2)	Sc(2)-O(17)	2.355(2)
Sc(1)...Sc(2)	3.324(1)	Na(1)-O(19)	2.465(3)
Na(1)-O(20)	2.490(3)	Na(1)-O(21)	2.503(3)
Na(1)-O(22)	2.431(3)	Na(1)-O(23)	2.499(3)
Na(1)-O(24)	2.449(3)	Na(1)-O(25)	2.449(3)
Na(1)-O(26)	2.475(3)	C-O	1.416(4)-1.436(4)
C-C	1.502(5)-1.518(5)		
O(1)-Sc(1)-O(2)	54.38(9)	O(4)-Sc(1)-O(5)	55.02(9)
O(9)-Sc(1)-O(10)	72.52(9)	O(13)-Sc(2)-O(14)	54.89(9)
O(16)-Sc(2)-O(17)	54.28(9)	O(9)-Sc(2)-O(10)	72.61(9)
Sc(1)-O(9)-Sc(2)	107.3(1)	Sc(1)-O(10)-Sc(2)	107.6(1)
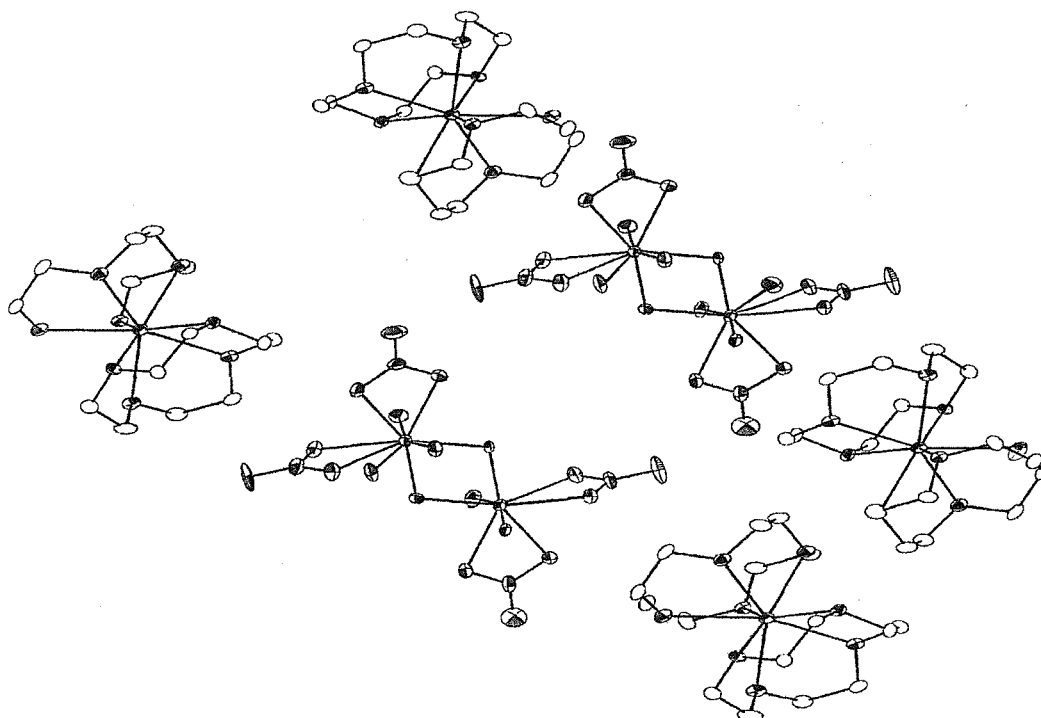
Fig. 5.19 View of the supramolecular structure of [Sc₂(NO₃)₄(H₂O)₄(OH)₂][Na([12]-crown-4)₂](NO₃).(H₂O)₃, with ionic nitrate groups, non-coordinated waters and H atoms omitted for clarity. Ellipsoids are drawn at the 50% probability level.
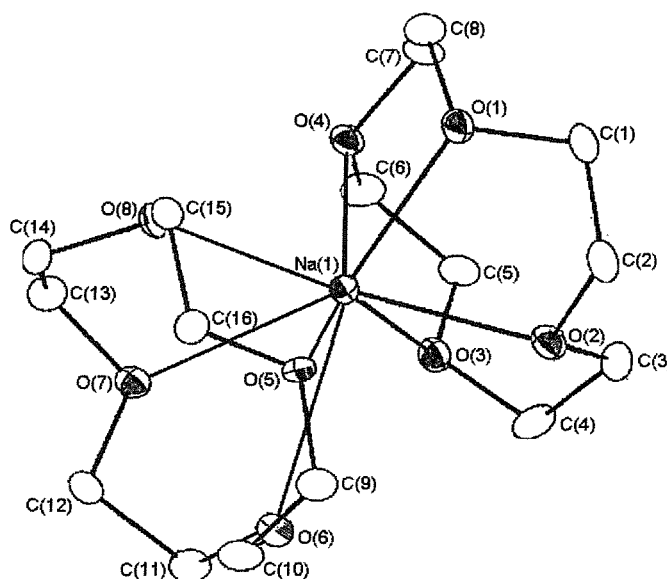
Fig. 5.20 View of [Na([12]-crown-4)₂] showing the atom numbering scheme. Ellipsoids are drawn at the 40% probability level whilst H atoms are omitted for clarity.

5.3 Conclusions

The scandium(III) centre exhibits a stronger affinity for water than the crown ether ligands studied, with a trace amount of water enough to displace a bonded crown (in an anhydrous complex) into the secondary coordination sphere. For example, exposure of $[ScCl_2([18]\text{-crown-}6)]SbCl_6$ to small quantities of H_2O yielded $[ScCl_3(H_2O)_3].[18]\text{-crown-}6$. The Sc^{3+} ion also coordinates preferentially to both chloride and nitrate groups over crown ethers. This contrasts with the behaviour of the next element in the periodic table, titanium, which retains bonding to the crown, losing chlorides in place of oxide groups (Chapter 6).

The results of studies examining reactions of hydrated scandium salts with crown ethers revealed a strong dependence of the supramolecular structure on both reaction conditions and the crown used. However, particular features were observed consistently. For example, when a 1:1 ratio of scandium groups (monomers or dimers) to crown ether was observed, an 'infinite chain' of alternating units was seen. In contrast, a 1:2 ratio resulted in formation of a discrete species. It was apparent that the supramolecular structure is not greatly altered depending on whether chloride or nitrate groups were coordinated to scandium, with the closely related structures of $[ScCl_3(H_2O)_3].[18]\text{-crown-}6$ and $[Sc(H_2O)_3(NO_3)_3].[18]\text{-crown-}6$ providing evidence.[21-23]

Reaction of $[ScCl_3(thf)_3]$ with either [15]-crown-5, [18]-crown-6 or $[15]aneS_2O_3$ in the presence of one molar equivalent of a Lewis acid (to act as a halide abstractor) in rigorously anhydrous conditions affords a cation of the type $[ScCl_2(crown)]^+$. Further halide abstraction can be accomplished by addition of further Lewis acid. However, stronger Lewis acids (in this case $SbCl_5$) may well react with other bases within the reaction mixture, meaning further halide abstraction may not be stoichiometric. All of these ligands encapsulate Sc(III). In contrast, the cavity in [12]-crown-4 is too small to accommodate Sc(III), meaning two ligands sandwich the metal centre. When $[15]aneS_2O_3$ reacts with scandium(III), it appears that coordination through the thioether functions does occur, with this apparently the first reported example of a scandium – thioether linkage. The structures of $[ScCl(MeCN)([15]\text{-crown-}5)]$

[SbCl$_6$]$_2$.MeCN and [ScCl$_2$([18]-crown-6)][FeCl$_4$] both contain seven-coordinate scandium in a pentagonal bypramidal environment. Comparison of these structures with those of the related compounds [ScCl$_2$([15]-crown-5)]$_2$[CuCl$_4$], [ScCl$_2$([15]-crown-5)][SbCl$_6$], [ScCl$_2$(benzo-[15]-crown-5)] [SbCl$_6$] and [ScCl$_2$([18]-crown-6)] [SbCl$_6$] reveals similar geometry in all, showing a strong preference of the metal centre for this environment.

5.4 Experimental

Sc(NO$_3$)$_3$.5H$_2$O (Strem), [12]-crown-4, [15]-crown-5 and [18]-crown-6 (Aldrich) were used as received. ScCl$_3$.6H$_2$O and [ScCl$_3$(thf)$_3$] were synthesised by literature methods.[31, 32] 1,4-dithia-7,10,13-trioxacyclopentadecane ([15]aneS$_2$O$_3$) was made by the literature method shown in Section 1.3.3.[26] Anhydrous tetrahydrofuran was obtained by distillation under nitrogen over sodium / benzophenone.

5.4.1 Reactions of [ScCl$_3$(thf)$_3$] with crown ether ligands

[ScCl(MeCN)([15]-crown-5)][SbCl$_6$]$_2$.MeCN

A solution of SbCl$_5$ (0.24 g, 0.84 mmol) in anhydrous MeCN (5 cm^3) was added to a solution of [ScCl$_3$(thf)$_3$] (0.15 g, 0.42 mmol) in MeCN (10 cm^3). The solution was stirred under nitrogen for 15 min. [15]-crown-5 (0.09 g, 0.42 mmol) was added to the reaction mixture which was left to stand for several days under a nitrogen atmosphere. Colourless crystals formed which were filtered off and dried *in vacuo*. Yield 0.23 g, 84%. (Found: C, 15.9; H, 2.4; N, 1.8. Calc. for C$_{14}$H$_{26}$Cl$_{13}$N$_2$O$_5$Sb$_2$Sc: C, 16.0; H, 2.5; N, 2.7%). IR (cm^{-1})(Nujol mull): 2332w, 2303w, 1349m, 1267m, 1246m, 1128w, 1058s, 965s, 939m, 821m, 449s, 441s, 344vs. ^{1}H NMR (300 K, d^3-MeCN): 4.3(m). ^{45}Sc NMR (300 K, MeCN): 99.5.

[ScCl$_2$([18]-crown-6)][FeCl$_4$]

A solution of FeCl$_3$ (0.08 g, 0.42 mmol) in MeCN (5 cm^3) was added to a solution of [ScCl$_3$(thf)$_3$] (0.15 g, 0.42 mmol) in MeCN (10 cm^3). The solution was stirred under nitrogen for 30 min. A solution of [18]-crown-6 (0.11 g, 0.42 mmol) in MeCN (5 cm^3) was added, with the reaction mixture left to stand for 24 h in a refrigerator. Yellow crystals formed which were filtered off and dried *in vacuo*. Yield 0.09 g, 37%. (Found: C, 24.7; H, 4.1. Calc. for C$_{12}$H$_{24}$Cl$_6$FeO$_6$Sc: C, 24.9; H, 4.1%). IR (cm^{-1}) (Nujol mull): 1261m, 1152w, 1089s, 1020m, 960m, 797m, 449m, 389s. ^{1}H NMR (300 K, d^3-MeCN): 4.3(m). ^{45}Sc NMR (300 K, MeCN): 132.

[ScCl₂([15]aneS₂O₃)][FeCl₄]

Solutions of FeCl₃ (0.08 g, 0.42 mmol) and [ScCl₃(thf)₃] (0.15 g, 0.42 mmol) in MeCN (5 cm³) were mixed together then stirred for 1 h. A solution of [15]aneS₂O₃ (0.11 g, 0.15 mmol) in MeCN (5 cm³) was added. The solution was concentrated to *ca.* 5 cm³ then left to stand for 3 days in a refrigerator, affording a yellow solid which was filtered off and dried *in vacuo*. Yield 0.12 g, 49%. (Found: C, 21.7; H, 3.5. Calc. for C₁₀H₂₀Cl₆FeO₃S₂Sc: C, 21.2; H, 3.5%). IR (cm⁻¹)(Nujol mull): 1302w, 1260m, 1246m, 1169sh, 1111s, 1021sh, 968m, 933m, 839m, 798m, 594m, 466s, 382vs. ¹H NMR (300 K, CD₂Cl₂): 3.35 – 3.70(m). ⁴⁵Sc NMR (300 K, MeCN): 200.

[ScCl₃(H₂O)₃].[18]-crown-6

A solution of [ScCl₃(thf)₃] (0.15 g, 0.42 mmol) in MeCN (10 cm³) was added to a solution of [18]-crown-6 (0.15 g, 0.42 mmol) in MeCN. The solution was left to evaporate in air for 7 days, yielding colourless crystals which were filtered off and dried *in vacuo*. Yield 0.09 g, 46%. (Found: C, 30.8; H, 5.5. Calc. for C₁₂H₃₀Cl₃O₉Sc: C, 30.7; H, 6.4%). IR (cm⁻¹)(Nujol mull): 3410br, 3222br, 1631m, 1300m, 1262w, 1140m, 1101m, 958s, 810m, 439m, 334m. ¹H NMR (300 K, d⁶-acetone): 3.6(s), 4.2(s). ⁴⁵Sc NMR (300 K, EtOH): 152.

5.4.2 Reactions of scandium chloride hexahydrate with crown ether ligands

[ScCl₃(H₂O)₃]₂.[18]-crown-6

A solution of [18]-crown-6 (0.08 g, 0.30 mmol) in boiling ethanol (5 ml) was added to a solution of ScCl₃.6H₂O (0.16 g, 0.60 mmol) in ethanol (10 cm³). The solution was heated to reflux for 1 h, following which all solvent was removed. The residue was washed with ice-cold ethanol (1 cm³), the solid filtered off and then dried *in vacuo*. Yield 0.06 g, 30%. (Found: C, 21.7; H, 5.9. Calc. for C₁₂H₃₆Cl₆O₁₂Sc₂: C, 21.4; H, 5.4%). IR (cm⁻¹)(Nujol mull): 3400br, 3190br, 1635m, 1569w, 1303w, 1259w, 1169m, 1140m, 1093s, 956s, 837m, 768m. ¹H NMR (300 K, d⁶-acetone): 3.6(s), 4.6(s), br. ⁴⁵Sc NMR (300 K, EtOH): 153.

[ScCl₃(H₂O)₃]₂.[15]-crown-5

Was made similarly using $ScCl_3.6H_2O$ (0.14 g, 0.55 mmol) and [15]-crown-5 (0.06 g, 0.27 mmol). Yield 0.085 g, 50%. (Found: C, 19.0; H, 4.9. Calc. for $C_{10}H_{32}Cl_6O_{11}Sc_2$: C, 19.0; H, 5.0%). IR (cm⁻¹)(Nujol mull): 3400br, 1636m, 1304w, 1263w, 1125w, 1060m, 965m, 936m, 919w, 889w, 825m, 771w. ¹H NMR (300 K, d⁶-acetone): 3.6(s), 4.7(s), br. ⁴⁵Sc NMR (300 K, EtOH): 152.

[ScCl₃(H₂O)₃]₂.[12]-crown-4

Was made similarly using $ScCl_3.6H_2O$ (0.22 g, 0.85 mmol) and [12]-crown-4 (0.07 g, 0.42 mmol). Yield 0.08 g, 35%. (Found: C, 16.2; H, 4.6. Calc. for $C_8H_{28}Cl_6O_{10}Sc_2$: C, 16.4; H, 4.8%). IR (cm⁻¹)(Nujol mull): 3300br, 1620m, 1304w, 1166w, 1155w, 1047s, 1021w, 966m, 938m, 908w, 891m, 855m, 810w, 765m. ¹H NMR (300 K, d⁶-acetone): 3.6(s), 4.0(s), br. ⁴⁵Sc NMR (300 K, EtOH): 153.

5.4.3 Reactions of Sc(NO₃)₃.5H₂O with crown ether ligands

[Sc(NO₃)₃(H₂O)₃].[18]-crown-6

A solution of $Sc(NO_3)_3.5H_2O$ (0.15 g, 0.45 mmol) in hot ethanol (15 cm³) was added dropwise to a solution of [18]-crown-6 (0.58 g, 0.22 mmol) in ethanol (5 cm³) and the reaction mixture refluxed for 1 h. The solution was concentrated to ca. 1 cm³ then left to stand for 24 h in a refrigerator producing a white powder. The product was filtered off and dried in vacuo. 0.05 g, 40%. (Found: C, 25.8; H, 5.2; N, 7.2. Calc. for $C_{12}H_{30}N_3O_{18}Sc$: C, 26.2; H, 5.5; N, 7.7%). IR (cm⁻¹)(Nujol mull): 3400br, 3200br, 1645m, 1304w, 1170w, 1153w, 1077w, 1020w, 965m, 936m, 919w, 892m, 844m, 816w, 769m, 562w, 450w. ¹H NMR (300 K, d⁶-acetone): 3.6(s), 4.0(s), br. ⁴⁵Sc NMR (300 K, Me₂CO): 5.

[Sc(NO₃)₂(H₂O)₄]NO₃.[15]-crown-5

A solution of [15]-crown-5 (0.44 g, 0.2 mmol) in ethanol (5 cm³) was added dropwise to a boiling solution of $Sc(NO_3)_3.5H_2O$ (0.12 g, 0.4 mmol) in ethanol (5 cm³), with the reaction mixture refluxed for 1 h. The solution was concentrated to ca. 1 cm³ then refrigerated for 24 h, affording a white solid. The product was filtered off and dried in vacuo. 0.05 g, 50%. (Found: C, 23.0; H, 5.4; N, 8.1. Calc. for $C_{10}H_{28}N_3O_{18}Sc$: C,

22.9; H, 5.3; N, 8.0%). IR (cm^{-1})(Nujol mull): 3400br, 3200br, 1645m, 1537m, 1279m, 1121w, 1098m, 1056w, 1023m, 964w, 944m, 833m, 808m, 757m. ^{1}H NMR (300 K, d^6-acetone): 3.6(s), 4.4(s), br. ^{45}Sc NMR (300 K, Me$_2$CO): 2.

[Sc(NO$_3$)$_3$(H$_2$O)$_2$].([12]-crown-4)$_2$

A solution of [12]-crown-4 (0.18 g, 1.0 mmol) in boiling ethanol (5 cm^3) was added to a solution of Sc(NO$_3$)$_3$.5H$_2$O (0.32 g, 1.0 mmol) in boiling ethanol (15 cm^3) and the mixture refluxed for 1 h. The vessel was left to stand when the solvent evaporated to dryness, producing a gum. The gum was redissolved in the minimum of hot acetone and the solution left to stand. Slow evaporation afforded several crystals along with an oil. The crystals were identifed by single crystal X-Ray diffraction. IR (cm^{-1})(Nujol mull): 3580br, 2665m, 1650m, 1587m, 1305w, 1168w, 1157w, 1088w, 1024w, 972m, 931m, 897m, 852m, 813w, 770m, 637w, 560w, 519w. ^{1}H NMR (300 K, d^6-acetone): 3.6(s), 4.5(s), br. ^{45}Sc NMR (300 K, Me$_2$CO): -1.0, br.

[Sc$_2$(NO$_3$)$_2$(H$_2$O)$_6$(OH)$_2$](NO$_3$)$_2$.[12]-crown-4

On one occasion, the above reaction mixture was left to stand after concentration, depositing a few crystals identified by X-ray crystallography. Insufficient quantities were obtained for spectroscopic study.

5.4.4 Crystallographic Studies

Crystals of the complexes [ScCl(MeCN)([15]-crown-5)][SbCl$_6$]$_2$.MeCN, [ScCl$_2$([18]-crown-6)][FeCl$_4$], [Sc(H$_2$O)$_2$(NO$_3$)$_3$].([12]-crown-4)$_2$, [Sc$_2$(OH)$_2$(H$_2$O)$_6$(NO$_3$)$_2$] (NO$_3$)$_2$.[12]-crown-4 and [Sc$_2$(NO$_3$)$_4$(H$_2$O)$_4$(OH)$_2$][Na([12]-crown-4)$_2$](NO$_3$).(H$_2$O)$_3$ were obtained directly from the reaction mixtures (see above). Crystals of [Sc(H$_2$O)$_4$(NO$_3$)$_2$]NO$_3$.[15]-crown-5 and [ScCl$_3$(H$_2$O)$_3$].[18]-crown-6 were obtained by slow evaporation of ethanolic solutions. A table of crystallographic data is given (Table 5.7). Structure solution and refinement were routine in all cases.[33-36] Methylene hydrogens were added in calculated positions on crown residues, whilst in contrast, H atoms bound to oxygen atoms were located in later electron density maps in all but a

few cases, and were introduced into the model in either fixed or restrained positions (using DFIX command; target 0.84(2) Å).

Table 5.7 Crystallographic data collection and refinement parameters

	[ScCl(MeCN)([15]-crown-5)][SbCl₆]₂.MeCN	[ScCl₂([18]-crown-6)][FeCl₄]	[ScCl₃(H₂O)₃].[18]-crown-6	[Sc(NO₃)₂(H₂O)₄]NO₃.[15]-crown-5
Formula	$C_{14}H_{26}Cl_{13}N_2O_5Sb_2Sc$	$C_{12}H_{24}Cl_6FeO_6Sc$	$C_{12}H_{30}Cl_3O_9Sc$	$C_{10}H_{28}N_3O_{18}Sc$
Formula weight	1051.68	577.82	469.67	523.31
Crystal system	Orthorhombic	Orthorhombic	Orthorhombic	Orthorhombic
Space group	$Pbca$ (No. 61)	$Pna2_1$ (No. 33)	$Pbcn$ (No. 60)	$Pbca$ (No. 61)
a / Å	21.209(2)	19.2026(15)	10.7210(10)	8.666(2)
b / Å	13.4224(10)	11.2156(10)	14.8569(15)	15.767(6)
c / Å	24.800(2)	21.0990(15)	13.2776(15)	31.740(9)
α / °	90	90	90	90
β / °	90	90	90	90
γ / °	90	90	90	90
U / Å³	7060.0(10)	4544.1(6)	2114.9(4)	4337.1(3)
Z	8	8	4	8
μ(Mo-K$_\alpha$) / cm⁻¹	27.19	16.67	7.65	12.63
No. unique reflections	8017	10116	2415	2868
R_{int}	0.107	0.060	0.073	0.11
No. of obs. reflections	8017	10116	2415	1726
No. parameter/restraint	335/0	470/1	125/3	288/18
R [b]	0.042	0.039	0.038	0.12
wR_2 [c]	0.086	0.080	0.092	0.146
wR [d]	0.098	0.065	0.062	0.32

[a] Observed if $[I_o > 2\sigma(I_o)]$ [b] $R = \sum (|F_{obs}|_i - |F_{calc}|_i) / \sum |F_{obs}|_i$ [c] $wR_2 = [\sum w(F_{obs}^2 - F_{calc}^2)^2 / \sum w(F_{obs}^2)^2]^{1/2}$ [d] $wR = \sqrt{[\sum w_i(|F_{obs}|_i - |F_{calc}|_i)^2 / \sum w_i|F_{obs}|_i^2}$

Table 5.7(cont.) Crystallographic data collection and refinement parameters

	$[Sc_2(NO_3)_4(H_2O)_4(OH)_2][Na([12]\text{-crown-4})_2](NO_3).(H_2O)_3$	$[Sc_2(NO_3)_2(H_2O)_6(OH)_2](NO_3)_2.[12]\text{-crown-4}$	$[Sc(NO_3)_3(H_2O)_2].([12]\text{-crown-4})_2$
Formula	$C_{16}H_{48}N_5NaO_{32}Sc_2$	$C_8H_{30}N_4O_{24}Sc_2$	$C_{16}H_{36}N_3O_{19}Sc$
Formula weight	935.50	656.28	619.44
Crystal system	Triclinic	Triclinic	Orthorhombic
Space group	$P\bar{1}$ (No. 2)	$P\bar{1}$ (No. 2)	$P2_12_12$ (No. 18)
a / Å	8.7342(10)	7.5712(15)	11.6362(15)
b / Å	13.4735(15)	9.2350(15)	13.432(3)
c / Å	16.842(3)	9.862(3)	8.7311(10)
α / °	100.341(4)	85.497(7)	90
β / °	98.989(4)	84.869(8)	90
γ / °	93.665(7)	69.545(15)	90
U / Å^3	1917.2(4)	642.7(2)	1364.7(3)
Z	2	1	2
μ(Mo-K$_\alpha$) / cm^{-1}	4.79	6.36	3.58
No. unique reflections	6636	2801	3109
R_{int}	0.058	0.085	0.050
No. of obs. reflections	6636	2801	3109
No. parameter/restraint	493/3	191/6	185/2
R [b]	0.050	0.041	0.041
wR_2 [c]	0.145	0.098	0.088
wR [d]	0.090	0.069	0.060

[a] Observed if $[I_o > 2\sigma(I_o)]$ [b] $R = \Sigma (|F_{obs}|_i - |F_{calc}|_i) / \Sigma |F_{obs}|_i$ [c] $wR_2 = [\Sigma w(F_{obs}^2 - F_{calc}^2)^2 / \Sigma w(F_{obs}^2)^2]^{1/2}$ [d] $wR = \sqrt{[\Sigma w_i(|F_{obs}|_i - |F_{calc}|_i)^2 / \Sigma w_i|F_{obs}|_i^2}$

5.5 References

1. C. J. Pederson, *J. Am. Chem. Soc.*, 1967, **89**, 7017.

2. For a review, see F. A. Hart in *Comprehensive Coordination Chemistry*, G. Wilkinson, J. A. McCleverty, R. D. Gillard (Eds.), Pergamon, Oxford, 1987, Volume 3, p 1091.

3. For a review, see V. K. Belsky, B. M. Bulychev, *Russ. Chem. Rev.*, 1999, **68**, 119.

4. R. D. Rogers, A. H. Bond, S. Aguinaga, A. Reyes, *J. Am. Chem. Soc.*, 1992 **114**, 2967.

5. M. M. Benning, L. K. Kurihara, R. D. Rogers, *J. Less-Common Met.*, 1987, **127**, 269.

6. R. D. Rogers, A. N. Rollins, M. M. Benning, *Inorg. Chem.*, 1988, 27, 3826.

7. R. D. Rogers, L. Nunez, *Inorg. Chim. Acta*, 1990, **172**, 173.

8. L. Nunez, R. D. Rogers, *J. Cryst. Spectr. Res.*, 1992, **22**, 265.

9. N. Hu, Z. Li, Q. Zhou, B. Yang, Z. Jin, J. Ni, *Yingyong Huaxue*, 1987, **4**, 22, *Chem. Abs.*, 1987, **108**, 141082.

10. R. D. Rogers, L. K. Kurihara, *Inorg. Chim. Acta*, 1987, **129**, 277.

11. R. D. Rogers, L. K. Kurihara, *Inorg. Chim. Acta*, 1987, **130**, 131.

12. R. D. Rogers, L. K. Kurihara, *Inorg. Chim. Acta*, 1986, **116**, 171.

13. R. D. Rogers, L. K. Kurihara, *J. Less-Common Met.*, 1987, **127**, 268.

14. R. D. Rogers, L. K. Kurihara, *Inorg. Chem.*, 1987, **26**, 1498.

15. R. D. Rogers, A. N. Rollins, R. D. Etzenhouser, E. J. Voss, C. B. Bauer, *Inorg. Chem.*, 1993, **32**, 3451.

16. G. R. Willey, P. R. Meehan, M. G. B. Drew, *Polyhedron*, 1996, **15**, 1397.

17. G. R. Willey, M. T. Lakin, N. W. Alcock, *J. Chem. Soc., Dalton Trans.*, 1993, 3407; G. R. Willey, M. T. Lakin, N. W. Alcock, *Chem. Commun.*, 1992, 1619.

18. N. R. Strel'tsova, V. K. Belsky, B. M. Bulychev, O. K. Kireeva, *Zh. Neorg. Khim.*, 1992, **37**, 1822.

19. G. R. Willey, P. R. Meehan, M. D. Rudd, M. G. B. Drew, *J. Chem. Soc., Dalton Trans.*, 1995, 811.

20. G. R. Willey, P. R. Meehan, *Inorg. Chim. Acta*, 1999, **284**, 71.

21. Z. Jin, Y. Liu, S. Zhang, F. Yu, J. Ni, *Huaxue Xuebao*, 1987, **45**, 1048, *Chem. Abs.*, 1988, **108**, 105242.

22. M. Tan, X. Gan, N. Tang, J. Zhou, X. Wang, Y. Zhu, *Wuji Huaxue Xuebao*, 1990, **6**, 5, *Chem. Abs.*, 1991, **115**, 221711.

23. N. Seikweng, H. Shengzhi, *Wuji Huaxue Xuebao*, 2000, **16**, 804.

24. X. Gan, N. Tang, Y. Zhu, Y. Zhai, M. Tan, *Zhongguo Xitu Xuebao*, 1989, **7**, 13, *Chem. Abs.*, 1989, **112**, 150561.

25. K. Nakamoto, *Infrared Spectra of Inorganic and Coordination Compounds*, Wiley, New York, 1970.

26. J. S. Bradshaw, G. Y. Hui, B. L. Haymore, J. J. Christensen, *J. Heterocyclic Chem.*, 1973, **10**, 1.

27. G. A. Kirakosyan, V. P. Tarasov, Y, A. Buslaev, *Mag. Res. Chem.*, 1989, **27**, 103.

28. R. K. Harris, B. E. Mann, *NMR and the Periodic Table*, Academic Press, London, 1978.

29. H. Zhang, X. Wang, K. Zhang, B. K. Teo, *Inorg. Chem.*, 1998, **37**, 3490.

30. R. D. Rogers, *Acta Crystallogr., Sect. C*, 1988, **44**, 638.

31. N. J. Hill, W. Levason, M. C. Popham, G. Reid, M. Webster, *Polyhedron*, 2002, **21**, 1579.

32. L. E. Manzer, *Inorg. Synth.*, 1982, **21**, 135.

33. R. H. Blessing, *J. Appl. Cryst.*, 1997, **30**, 421.

34. G. M. Sheldrick, SHELXL 97, Program for crystal structure solution, University of Göttingen, 1997.

35. G. M. Sheldrick, SHELXS 97, Program for crystal structure solution, University of Göttingen, 1997.

36. PATTY, The DIRDIF Program System, P. T. Beurskens, G. Admiraal, G. Beurskens, W. P. Bosman, S. Garcia-Granda, R. O. Gould, J. M. M. Smits, C. Symkalla, *Technical Report of the Crystallographic Laboratory*, University of Nijmegen, The Netherlands, 1992.

Chapter 6

Complexes of Titanium Halides with Crown Ether Ligands

6.1 Introduction

Titanium tetrahalides are often employed as precursors to Ti(IV) compounds. $TiCl_4$ is used most often, whilst frequent examples of complexes synthesised using $TiBr_4$ are encountered. However, very few TiI_4 examples are known. Examples identified include $[TiI_4\{MeSe(CH_2)_2SeMe\}]$, $[TiI_2\{o-C_6H_4(AsMe_2)_2\}_2][I]_2$ and $[TiI_4\{o-C_6H_4(SeMe)_2\}]$.[1, 2] The rarity of iodo-complexes is explained by the poor solubility of TiI_4 in non-coordinating solvents, whilst it is also a much weaker acceptor than the chloro- and bromo-analogues.[3] Previous research into the interactions of titanium halides with crown ether ligands have concentrated on reactions with $TiCl_4$, with no investigations of $TiBr_4$ / crown ether complexes reported in the literature.

A single example of a structurally characterised $TiCl_4$ / [12]-crown-4 compound has been reported in the literature.[4] $TiCl_4$ was reacted with $SbCl_5$ in acetonitrile, yielding $[TiCl_3(MeCN)_3]SbCl_6$. Reaction of this species with [12]crown-4 in dichloromethane afforded the oxygen-bridged hydrolysis product $[\{TiCl(\mu_2-O)([12]-crown-4)\}_2][SbCl_6]_2$ (Fig. 6.1). Each Ti metal centre is seven-coordinate, bonded to the four oxygens of the crown, one chloride and two bridging oxygen atoms. Hence, a planar Ti-O-Ti-O ring links the two metal centres. The Ti-O_{crown} distances vary greatly (Ti-O = 2.121(4) – 2.237(4) Å).[4]

● Ti
○ C
○ O
◯ Cl
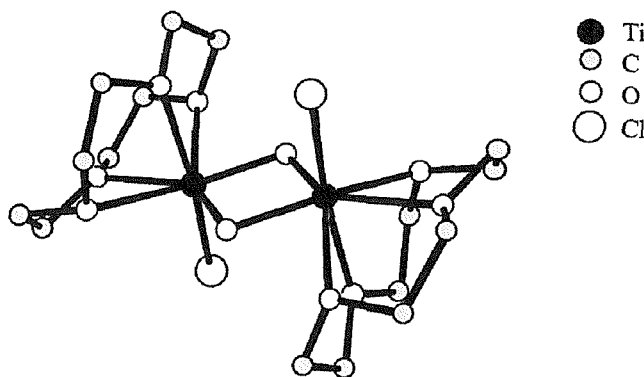
Fig. 6.1 View of the cation $[\{TiCl(\mu_2-O)([12]-crown-4)\}_2]^{2-}$, a hydrolysis product.[4, 5]

Direct reaction of $TiCl_4$ with [15]-crown-5 in acetonitrile produces [TiCl([15]-crown-5)(μ_2-O)(TiCl$_5$)], presumably via adventitious hydrolysis. One Ti centre is located inside the crown ether, coordinated to all five oxygens of the ligand (Fig. 6.2).[6]

● Ti
◐ C
○ O
◯ Cl
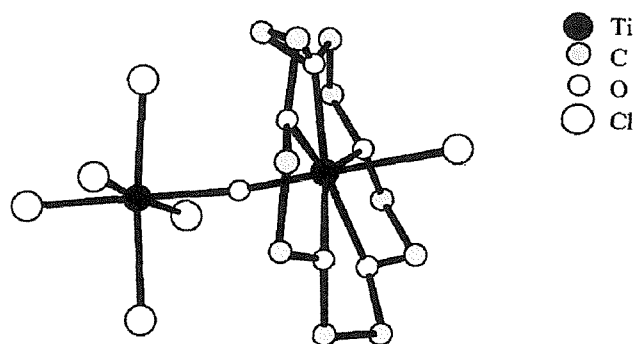
Fig. 6.2 View of the structure [TiCl([15]-crown-5)(μ_2-O)(TiCl$_5$)].[5, 6]

The Ti-O$_{crown}$ distances vary significantly (Ti-O = 2.073(6) – 2.140(5) Å). In the same study, it was found that by addition of metal chlorides with readily ionisable M-Cl bonds, the Ti-O-Ti linkage could be prevented. For example, reaction of $TiCl_4$, $MgCl_2$ and [15]-crown-5 in MeCN yielded [Mg(MeCN)([15]-crown-5)][TiCl$_6$].[6] A second example exhibiting bonding of titanium to a crown ether is [TiCl$_2$([15]-crown-5)][AlCl$_4$], formed using $TiCl_3$ as a precursor, reacted with $AlCl_3$ and [15]-crown-5.[6] The titanium centre lies in the cavity of the crown ether. Ti-O$_{crown}$ distances are seen to vary from 2.12(2) to 2.20(2) Å. The complex [TiCl$_3$([15]-crown-5)(MeCN)][SbCl$_6$] has also been structurally characterised, revealing a six-coordinate Ti(IV) centre, with bonds to two crown ether oxygens, along with three chlorine donors and an acetonitrile, coordinated through nitrogen.[7]

In contrast to reactions with both [12]-crown-4 and [15]-crown-5, when $TiCl_4$ was added to a solution of [18]-crown-6 in dry toluene, no Ti-O-Ti linkage was observed, with [TiCl$_4$(η^2-[18]-crown-6)] formed (Fig. 6.3).[8] The $TiCl_4$ unit is bonded to two adjacent oxygen atoms of the crown ether giving an octahedral coordination geometry. The Ti-O$_{crown}$ distances are 2.125(7) and 2.145(6) Å.
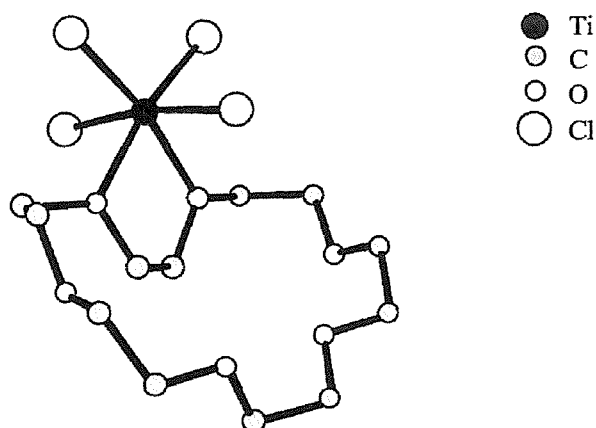
Fig. 6.3 View of the complex [TiCl$_4$(η^2-[18]-crown-6)].[5, 8]

The Ti(III) complex [TiCl$_3$(H$_2$O)([18]-crown-6)] has also been structurally characterised.[9] Reaction of TiCl$_4$ with [18]-crown-6 in ethanol affords the complex [TiCl$_3$(OC$_2$H$_5$)(C$_2$H$_5$OH)$_2$].2([18]-crown-6) (Fig. 6.4). The titanium centre is in an octahedral environment, with two coordinated ethanols showing hydrogen bonding to crown ether ligands through the OH of the ethanol to an oxygen of the crown in a fashion similar to that observed for complexes isolated in Chapter 5 (eg. [Sc(NO$_3$)$_3$(H$_2$O)$_2$].([12]-crown-4)$_2$).[10]
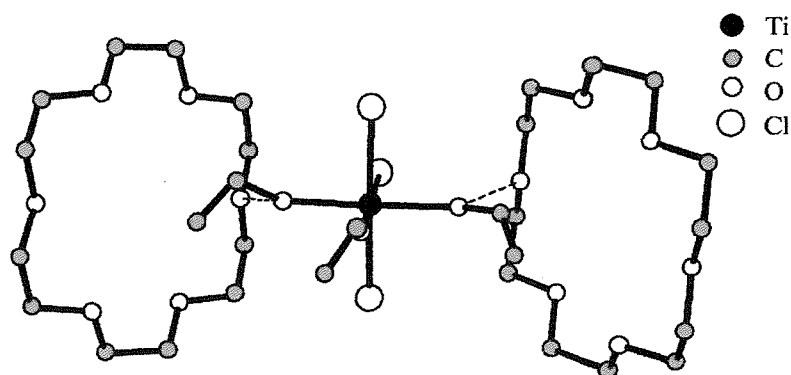
Fig. 6.4 View of the complex [TiCl$_3$(OC$_2$H$_5$)(C$_2$H$_5$OH)$_2$].2([18]-crown-6).[10]

Whilst some studies of complexes of $TiCl_4$ with crown ether ligands have been previously conducted, they are by no means thorough. For example, whilst $[TiCl_4(\eta^2-[18]$-crown-6$)]$ has been reported, analogous complexes of [12]-crown-4 and [15]-crown-5 are not found in the literature.[8] In addition, no examples of $TiBr_4$ compounds with these ligands have been reported. Hence, initially the aim was to examine anhydrous TiX_4/crown ether compounds. Attempts to synthesise compounds exhibiting bonding to the mixed donor macrocycle $[15]aneS_2O_3$ would also be made. The work would then be extended to examining the hydrolysis pathway of these complexes, additionally allowing comparison with the hydrolysis pathway exhibited for analogous complexes of the previous element in the periodic table, scandium (Chapter 5).

6.2 Results and Discussion

6.2.1 Complexes of TiX$_4$ with [12]-crown-4

Reaction of TiCl$_4$ with [12]-crown-4 in anhydrous toluene (chosen in preference to hexane and acetonitrile because of better complex solubility in toluene) under a nitrogen atmosphere yielded a bright yellow solid. However, upon standing, the product decolourised to form a cream compound, which appears to be a hydrolysis product (see below). Similar behaviour was observed when the yellow compound was filtered off and dried *in vacuo*, or when *n*-hexane was employed as the solvent. The solvents were rigorously dried to avoid moisture, whilst the crown ether was pre-dried using SOCl$_2$. Despite these precautions, repeated attempts to isolate the yellow product were unsuccessful. In contrast, reaction of TiBr$_4$ with one molar equivalent [12]-crown-4 in toluene readily afforded the orange - brown compound [TiBr$_4$([12]-crown-4)]. Attempts to react TiI$_4$ with [12]-crown-4 were unsuccessful, possibly due to the poor solubility of TiI$_4$ in non-coordinating solvents and its poor Lewis acidity.

Crystals of the white product gained from attempts to synthesize [TiCl$_4$([12]-crown-4)] suitable for single crystal X-ray diffraction could not be grown owing to the poor solubility in non-coordinating solvents. However, microanalysis results suggested the complex was probably the hydrolysis product [Ti$_2$Cl$_6$O([12]-crown-4)$_2$], a result which seems possible given the hydrolysis product observed for the TiCl$_4$ / [18]-crown-6 system (see 6.2.5). The reason for the vulnerability of the yellow product (presumably [TiCl$_4$([12]-crown-4)]) to hydrolysis was unclear, particularly when the analogous reaction with titanium tetrabromide is considered.

The complex [TiBr$_4$([12]-crown-4)] was identified by microanalysis, whilst the infra-red spectrum contained characteristic bands at 321 and 275 cm^{-1}, attributable to v(Ti-Br).[1, 11] In theory, a cis-bromide arrangement in [TiBr$_4$([12]-crown-4)], which has C$_2$v symmetry, should exhibit four bands in the IR spectrum (2A$_1$ + B$_1$ + B$_2$). Only two bands were observed in practice presumably because the individual bands are close in energy and hence were poorly resolved. The UV/visible spectrum contained the characteristic feature at 21,700 cm^{-1}, assigned as π(Br) → t$_{2g}$(Ti).[1, 11] This compares well with π(Br) → t$_{2g}$(Ti) at *ca.* 22500 cm^{-1} for a series of complexes of titanium tetrabromide with bidentate thio- and seleno- ether ligands

(eg TiBr$_4${MeS(CH$_2$)$_2$SMe}], TiBr$_4${MeSe(CH$_2$)$_2$SeMe}]), given that results must allow for an error of 1000 cm^{-1}.[1] At 300 K, the ^{1}H NMR spectrum exhibited a single, broad resonance at δ 3.66 ppm (compared with 3.60 ppm in the free ligand). Cooling to 220 K did not result in any significant sharpening of the peak, suggesting rapid exchange processes or hydrolysis.

The UV/visible spectrum of the hydrolysis product "[Ti$_2$Cl$_6$O([12]-crown-4)$_2$]" contained a single feature at 28,800 cm^{-1} (compared to *ca.* 28,000 cm^{-1} for the anhydrous TiCl$_4$ / crown ether complexes isolated within this study – see below). The increased wavenumber is caused by a change in the Ti orbital energies due to Ti-O bonding, in turn affecting the π(Cl) $\rightarrow$ t$_{2g}$(Ti) transition energy.

6.2.2 Complexes of TiX$_4$ with [15]-crown-5

Reaction of TiCl$_4$ with [15]-crown-5 in a 1:1 molar ratio in toluene under rigorously anhydrous conditions afforded the complex [TiCl$_4$([15]-crown-5)]. Similar reaction using TiBr$_4$ afforded [TiBr$_4$([15]-crown-5)], yet when TiI$_4$ was used, no reaction was observed.

The IR spectrum of [TiCl$_4$([15]-crown-5)] contained a characteristic very strong, broad band at 394 cm^{-1}, assigned as overlapping terminal ν(Ti-Cl) modes (theory predicts four bands, 2A$_1$ + B$_1$ + B$_2$ which in practice are found in the region 400 - 380 cm^{-1}).[1, 11] The overlapping nature of the bands contrast with a series of TiCl$_4$ / thio- and seleno-ether compounds identified previously, which all exhibit four well-resolved bands.[1] For example, the IR spectrum of [TiCl$_4${*o*-C$_6$H$_4$(SeMe)$_2$}] contained bands at 390, 386, 382 and 379 cm^{-1}, assigned as ν(Ti-Cl).[1] The spectrum of [TiBr$_4$([15]-crown-5)] contained strong bands at 320 and 282 cm^{-1}, assigned as overlapping ν(Ti-Br) modes (again, four bands are expected within the region 320 to 280 cm^{-1}).[1, 11] This contrasted with the spectra of a series of TiBr$_4$ / thio- or seleno-ether complexes which all exhibited four well defined bands. For example, the spectrum of [TiBr$_4${MeSe(CH$_2$)$_3$SeMe}] included bands at 327, 317, 308 and 300 cm^{-1}, assigned as ν(Ti-Br).

The UV/Visible spectroscopy data confirmed the presence of TiX bonds for both the chloro- and bromo-complex. The spectrum of [TiCl$_4$([15]-crown-5)] contained a strong feature at 28,000 cm^{-1}, assigned as π(Cl) $\rightarrow$ t$_{2g}$(Ti).[1, 11] [TiBr$_4$([15]-crown-5)] exhibited a strong feature at 22,000 cm^{-1}, corresponding to π(Br) $\rightarrow$ t$_{2g}$(Ti).[1, 11]

The ^{1}H NMR spectrum of [TiCl$_4$([15]-crown-5)] in anhydrous CD$_2$Cl$_2$ contained resonances at δ 3.60 (br), 4.33, 4.60 and 5.00 ppm, the integrals in a 2 : 1 : 1 : 1 ratio. Hence, the resonance at 5.00 ppm was assigned to CH$_2$ groups bridging the coordinated oxygens whilst the resonance at 4.60 was attributed to the CH$_2$ groups adjacent to these coordinated oxygens. The peak at 4.33 ppm corresponds to the next CH$_2$ groups further away form the coordinated oxygens with the broad resonance at 3.60 assigned to the remaining CH$_2$ groups. Cooling to 220 K had little effect on the spectrum, suggesting that neither dissociation nor fast exchange of 'free' and coordinated ether groups are occurring. When 'wet' CD$_2$Cl$_2$ was used, the yellow colour of the solution was lost, with a white precipitate forming immediately. The resulting spectrum contained only a singlet at δ 3.6, corresponding to the 'free' crown ether ligand. The spectrum of [TiBr$_4$([15]-crown-5)] in dry CD$_2$Cl$_2$ contained a broad resonance at 3.64 ppm, along with overlapping resonances from δ 4.65 to 5.00 corresponding to an exchange broadened equivalent of the spectrum of [TiCl$_4$([15]-crown-5)]. Cooling to 220 K did not affect the spectrum.

6.2.3 Complexes of TiX$_4$ with [18]-crown-6

Reaction of TiCl$_4$ with [18]-crown-6 in a 1 : 1 molar ratio in dry toluene afforded the complex [TiCl$_4$([18]-crown-6)] (a literature method, reported by Atwood et al.),[8] whilst [TiBr$_4$([18]-crown-6)] was obtained from the analogous TiBr$_4$ experiment. In contrast, when TiI$_4$ was used, no reaction occurred. When TiCl$_4$ and the crown were reacted in a 2 : 1 ratio in n-hexane, the product was the 2:1 species [(TiCl$_4$)$_2$([18]-crown-6)].

The crystal structure of [TiCl$_4$(η^2-[18]-crown-6)] has been reported previously.[8] However, no further spectroscopic data were reported. In order to confirm that the

complex isolated in this study was the same compound and was representative of the bulk material, a powder X-ray diffraction pattern was recorded and compared with a simulated pattern calculated from the single crystal X-ray data obtained by Atwood *et al.* The fit between these was very convincing.[8]

The IR spectrum of [TiCl$_4$([18]-crown-6)] contained a broad, very strong resonance at 377 cm^{-1}, corresponding to terminal v(Ti-Cl) modes. The broad nature of the band meant there was a high possibility that further bands might well be obscured or hidden underneath. The spectrum of [(TiCl$_4$)$_2$([18]-crown-6)] was more clearly resolved, with strong bands at 397 and 383 cm^{-1}, the latter broad. The spectrum of [TiBr$_4$([18]-crown-6)] contained three bands attributable to v(Ti-Br) at 321, 312 and 300 cm^{-1}.

The UV/Visible spectra for both TiCl$_4$ complexes contained the characteristic feature at 28,000 cm^{-1}, assigned as π(Cl) $\rightarrow$ t$_{2g}$(Ti). Similarly, the spectrum for [TiBr$_4$([18]-crown-6)] had a broad feature at 21,000 cm^{-1}, attributed to π(Br) $\rightarrow$ t$_{2g}$(Ti).

The ^{1}H NMR spectrum of [TiCl$_4$([18]-crown-6)] in CD$_2$Cl$_2$ at ambient temperature was complex, containing resonances at δ 3.60 in addition to overlapping peaks at *ca.* 3.76, a resonance at 4.00 and a multiplet from 4.23 – 4.60 ppm, in a 3:1:2 ratio. The resonances at higher frequency correspond to the CH$_2$ groups closest to the oxygens coordinated to the Ti centre (See Fig. 6.3), with the frequency dropping progressively moving away from these coordinated oxygens. Cooling to 220 K did not alter the spectrum significantly. The resultant ^{1}H NMR spectrum was more simple, containing three resonances at δ 3.70, 4.00 and 4.52 ppm, the integrals in a 1:1:1 ratio, as observed for [(TiCl$_4$)$_2$([18]-crown-6)]. The ratio of integrals suggests that the structure of this complex probably contains TiCl$_4$ units bridged by the crown ether, as shown in Fig. 6.5.
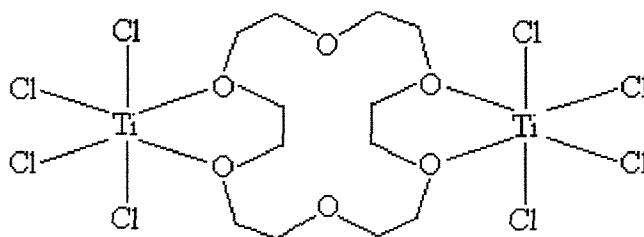
Fig. 6.5 Proposed structure of the compound [(TiCl$_4$)$_2$([18]-crown-6)] given ^{1}H NMR data.

The ^{1}H NMR spectrum of [TiBr$_4$([18]-crown-6)] was simple, containing a single broad resonance at δ 3.72 ppm, remaining unchanged upon cooling to 220 K, indicating rapid exchange on the NMR timescale.

6.2.4 Reaction of TiCl$_4$ with [15]aneS$_2$O$_3$

Reaction of TiCl$_4$ with 1 molar equivalent of [15]aneS$_2$O$_3$ in anhydrous toluene afforded the complex [TiCl$_4$([15]aneS$_2$O$_3$)]. Reactions with TiBr$_4$ and TiI$_4$ were not attempted. Whilst crystals suitable for single crystal X-Ray diffraction could not be grown due to the poor solubility of the product, it is clear that the ligand cooordinates through the sulfur atoms to some extent.

The UV/Visible spectrum contains features at 22,000 and 27,500 cm^{-1}. The latter is consistent with π(Cl) → t$_{2g}$(Ti), whilst by comparison of the spectra with that of [TiCl$_4$(MeSCH$_2$CH$_2$SMe)] it is apparent that the former is caused by π(S) → t$_{2g}$(Ti).[12] Whilst this evidence indicates the presence of Ti-S bonding, it does not determine whether coordination is through two sulfur atoms or mixed donors (Fig. 6.6).
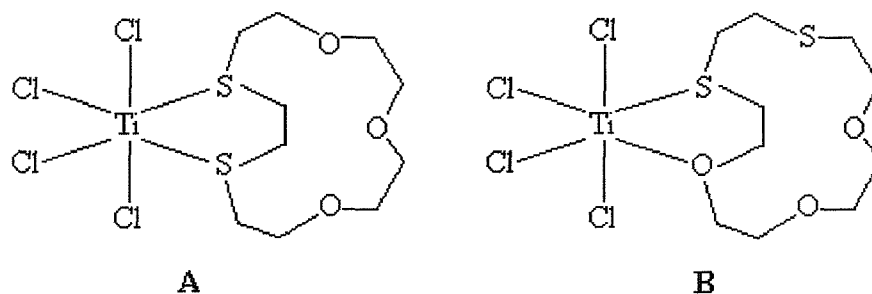
Fig. 6.6 Possible structures of the complex [TiCl$_4$([15]aneS$_2$O$_3$)].

The ^{1}H NMR spectrum in CD$_2$Cl$_2$ at room temperature contained five resonances at δ 2.98, 3.20 and 3.87 ppm along with overlapping resonances at 3.61 and 3.73 ppm. Cooling to 220 K did not alter the spectrum significantly. The integrals were 1:1:1:2, suggesting five CH$_2$ environments. This is consistent with Structure A, indicating that that titanium has chosen coordination to sulfur over oxygen, with both donor atoms in identical environments. This result is interesting given the hard nature of the Ti(IV) centre, meaning coordination through oxygen might be predicted. However, titanium is known to complex readily with softer donors, such as phosphorus, arsenic, sulfur and selenium in anhydrous conditions (the products are very hydrolytically unstable).[1, 11, 12]

6.2.5 Hydrolysis Products

Throughout studies investigating the TiCl$_4$ / crown ether system, it was apparent that samples were extremely vulnerable to hydrolysis. For example, attempts to isolate [TiCl$_4$([12]-crown-4)] proved futile with a hydrolysis product repeatedly formed, whilst all the anhydrous complexes isolated were seen to lose their distinctive yellow colour (caused by π(Cl) → t$_{2g}$(Ti) charge transfer bands) when exposed to air for even a brief period. As a result of this readiness to react with water, attempts to obtain crystals of [TiCl$_4$([18]-crown-6)] (to confirm that the literature complex had been successfully reproduced) by slow evaporation of a toluene solution in a nitrogen filled glove box afforded pale yellow crystals of the oxo-bridged dimer [([18]-crown-6)Cl$_3$Ti(μ-O)TiCl$_3$([18]-crown-6)]. A similar experiment using [TiCl$_4$([15]-crown-5)] yielded several crystals of the tetrameric complex [Ti$_4$Cl$_8$(μ-O)$_4$([15]-crown-5)$_4$]. A

'bulk' sample of the [18]-crown-6 complex was produced by stirring a toluene solution of $TiCl_4$ with one molar equivalent of the ligand under nitrogen for 48 h. A 'bulk' sample of the tetrameric complex could not be prepared.

The IR spectrum of [([18]-crown-6)$Cl_3Ti(\mu$-O)$TiCl_3$([18]-crown-6)] was similar to those of both [$TiCl_4$([18]-crown-6)] and [($TiCl_4$)$_2$([18]-crown-6)]. However, there were variations in ν(Ti-Cl), with vibrations appearing at 394 and 366 cm^{-1} in the former. The Ti-O-Ti linkage has been reported previously, with the ν(Ti-O-Ti) vibrations identified.[13, 14] For example, the compound [Mg(MeCN)$_6$][{$TiCl_4$(MeCN)}$_2(\mu$-O)] exhibits ν_{asym} = 786 cm^{-1}.[14] The crown ether vibrations in the spectrum of the oxo-bridged dimer obscure ν_{sym}, predicted to be a weak band given the Ti-O-Ti angle of 168° (from the single crystal X-ray diffraction (below)) but ν_{asym} was identified by a medium intensity band at 775 cm^{-1}. This assignment compares well with ν_{asym} for [{$TiCl_4$(MeCN)}$_2(\mu$-O)]$^{2-}$, reported at 786 cm^{-1} and that of [{η^5-$C_5H_2(SiMe_3)_3$}$_2Ti_2Cl_4(\mu$-O)], for which ν_{asym} was identified at 762 cm^{-1}.[13, 14]

The UV/Visible spectrum of [([18]-crown-6)$Cl_3Ti(\mu$-O)$TiCl_3$([18]-crown-6)] was noticably different from those of [$TiCl_4$([18]-crown-6)] and [($TiCl_4$)$_2$([18]-crown-6)] with a single feature apparent at 28,600 cm^{-1} compared to 28,000 cm^{-1} for the anhydrous species. The increased wavenumber is caused by a change in the Ti orbital energies due to Ti-O bonding, in turn affecting the π(Cl) $\rightarrow$ t$_{2g}$(Ti) transfer energies.

The structure of [([18]-crown-6)$Cl_3Ti(\mu$-O)$TiCl_3$([18]-crown-6)] was determined (Fig. 6.7), with selected bond lengths and angles presented in Table 6.1. The structure contains two titanium centres bonded to η^2-bound [18]-crown-6 and three chlorines in a *mer* configuration, linked by an oxygen bridge. The Ti centres exhibit a distorted octahedral geometry, with the Cl-Ti-Cl angles ranging from 92.78(2) to 95.50(2)°. The O$_{crown}$-Ti-O$_{crown}$ angles are 73.95(5) and 74.54(5)°, forming the sharp apex of a five-membered ring.

The Ti-O-Ti linkage was non-linear (167.8(8)°), whilst the Ti-O$_{bridge}$ distances differed slightly (1.7993(12) and 1.7948(12) Å). Numerous examples of a Ti-O-Ti

bridge have been reported previously, with the linkage often linear. For example, the structure of [(MeSCH₂CH₂SMe)Cl₃Ti(μ-O)TiCl₃(MeSCH₂CH₂SMe)] has a Ti-O-Ti bond angle of 180°, with the Ti-O$_{bridge}$ bond length 1.788(2) Å.[1] A second example is the Ti-O-Ti bridge reported for the cation [{TiCl₄(MeCN)}₂(μ-O)]²⁻, exhibiting a crystallographically imposed bond angle of 180°, with the Ti-O$_{bridge}$ bond length 1.804(3) Å.[15] Interestingly, a second isomer of this cation has been determined, revealing Ti-O-Ti = 174.7(4)°.[14] A further case containing a bent linkage is the complex [(thf)₂Cl₃Ti(μ-O)TiCl₃(thf)₂], having a Ti-O-Ti angle of 176.7(3)°.[16]

Comparison of Ti-O$_{bridge}$ for the dimer [([18]-crown-6)Cl₃Ti(μ-O)TiCl₃([18]-crown-6)] (1.7993(12) and 1.7948(12) Å) with the bond lengths Ti-O$_{crown}$ which range from 2.1004(12) to 2.1860(13) Å suggests that the bonds in the Ti-O-Ti bridge may have a degree of multiple bond character. At each Ti centre, it is apparent that the Ti-Cl distances are greater when *trans* to a chlorine atom, than when *trans* to an oxygen of the crown ether (Ti-Cl$_{transCl}$ = 2.2893(5) to 2.3329(5) Å c.f. TiCl$_{transOcrown}$ = 2.2551(5) to 2.2582(5) Å). A similar trend is seen in the structure of [TiCl₄([18]-crown-6)].[8]
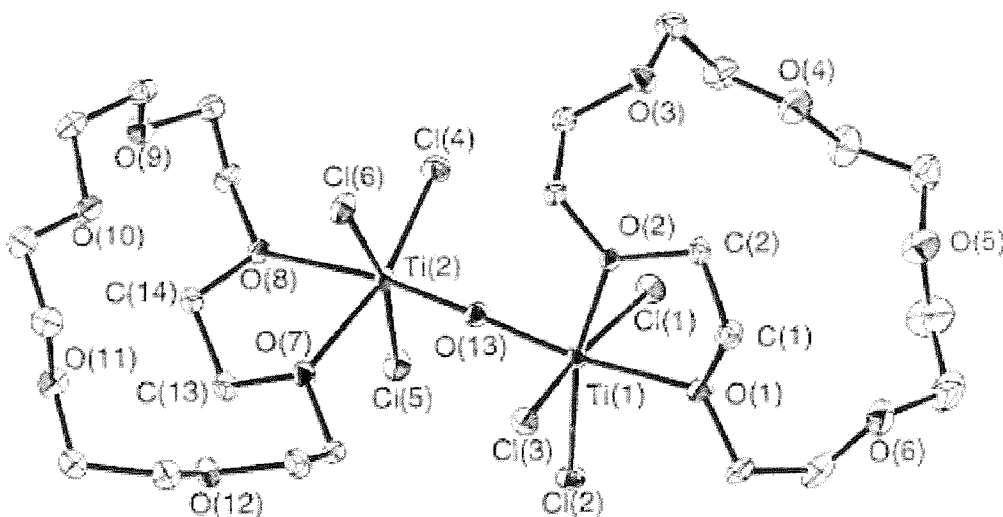
Fig. 6.7 View of the structure of [([18]-crown-6)Cl₃Ti(μ-O)TiCl₃([18]-crown-6)]. H atoms omitted for clarity. Ellipsoids are drawn at 50% probability level.

Table 6.1 Selected bond lengths (Å) and angles (°) for the structure of

[([18]-crown-6)Cl₃Ti(μ-O)TiCl₃([18]-crown-6)].

Ti(1)-O(1)	2.1860(13)	Ti(1)-O(2)	2.1004(12)
Ti(1)-Cl(1)	2.2893(5)	Ti(1)-Cl(2)	2.2582(5)
Ti(1)-Cl(3)	2.3329(5)	Ti(2)-Cl(4)	2.2551(5)
Ti(2)-Cl(5)	2.3077(5)	Ti(2)-Cl(6)	2.3199(5)
Ti(1)-O(13)	1.7993(12)	Ti(2)-O(13)	1.7948(12)
Ti(2)-O(7)	2.1334(13)	Ti(2)-O(8)	2.1856(12)
Ti(1)-O(13)-Ti(2)	167.75(8)	O(13)-Ti(1)-O(2)	94.50(5)
O(13)-Ti(1)-O(1)	168.28(5)	O(1)-Ti(1)-O(2)	73.95(5)
O(13)-Ti(1)-Cl(2)	99.32(4)	O(13)-Ti(1)-Cl(1)	95.55(4)
O(13)-Ti(1)-Cl(3)	93.49(4)	O(2)-Ti(1)-Cl(2)	166.18(4)
O(1)-Ti(1)-Cl(2)	92.23(4)	O(1)-Ti(1)-Cl(1)	85.78(4)
O(2)-Ti(1)-Cl(3)	85.26(4)	Cl(2)-Ti(1)-Cl(1)	92.78(2)
O(1)-Ti(1)-Cl(3)	83.78(4)	Cl(2)-Ti(1)-Cl(3)	93.54(2)
Cl(1)-Ti(1)-Cl(3)	167.99(2)	O(13)-Ti(2)-O(7)	95.70(5)
O(13)-Ti(2)-O(8)	170.17(5)	O(7)-Ti(2)-O(8)	74.54(5)
O(13)-Ti(2)-Cl(4)	99.98(4)	O(7)-Ti(2)-Cl(4)	164.30(4)
O(8)-Ti(2)-Cl(4)	89.80(4)	O(13)-Ti(2)-Cl(5)	93.85(4)
O(7)-Ti(2)-Cl(5)	83.81(4)	O(8)-Ti(2)-Cl(5)	86.34(4)
Cl(4)-Ti(2)-Cl(5)	94.24(2)	O(13)-Ti(2)-Cl(6)	92.21(4)
O(7)-Ti(2)-Cl(6)	84.68(4)	O(8)-Ti(2)-Cl(6)	85.83(4)
Cl(4)-Ti(2)-Cl(6)	95.50(2)	Cl(5)-Ti(2)-Cl(6)	167.46(2)

The structure of the tetrameric compound [{TiOCl₂([15]-crown-5)}₄] is shown in Fig. 6.8, with selected bond lengths and angles given in Table 6.2. The compound contains an eight-membered ring of alternating Ti and O atoms, with the titanium centres forming the corners of a near planar square. The structure exhibits S₄ symmetry. The Ti-O-Ti 'bridges' are non-linear, with a bond angle of 169.2(3)°. The eight-membered Ti-O ring is surprisingly common, with over forty structurally determined examples reported in the literature.[14, 17, 18] The geometry at each Ti centre is close to octahedral, with bonds to two chlorines (in *cis* positions), two bridging oxygen atoms and two oxygens of the crown ether. The Ti-O$_{bridge}$ bond lengths differ notably, depending on which group is *trans* to the oxygen. Ti-O(6), for which a crown ether oxygen is in the *trans* position, is shorter (1.690(5) Å) whilst the symmetry expanded Ti-O(6'), *trans* to a chlorine, exhibits a bond length of 2.001(5) Å, demonstrating the strong *trans* effect of chlorine. As observed for [([18]-crown-6)Cl₃Ti(μ-O)TiCl₃([18]-crown-6)], the Ti-O$_{bridge}$ distances (1.690(5) Å if *trans* to an

oxygen, 2.001(5) Å if *trans* to a Cl) are considerably shorter than Ti-O$_{crown}$ bond lengths (2.244(5) Å if *trans* to O, 2.117(5) if *trans* to Cl). Inequivalent Ti-O bond lengths are not standard for Ti-O-Ti bridges, although examples do exist. For example, the tetramer [{TiOCl$_2$(MeCN)$_2$}$_4$] exhibits non-symmetrical Ti-O-Ti bridges.[14] The structure is similar to that of [{TiOCl$_2$([15]-crown-5)}$_4$], (with MeCN replacing crown ether groups) with the donors *trans* to the bridging oxygen greatly affecting the Ti-O$_{bridge}$ bond length. By analysis of the structures of both [{TiOCl$_2$([15]-crown-5)}$_4$] and [([18]-crown-6)Cl$_3$Ti(μ-O)TiCl$_3$([18]-crown-6)] it is apparent that the *trans* influence of the donors on Ti(IV) is O(oxide) > Cl > O(crown).
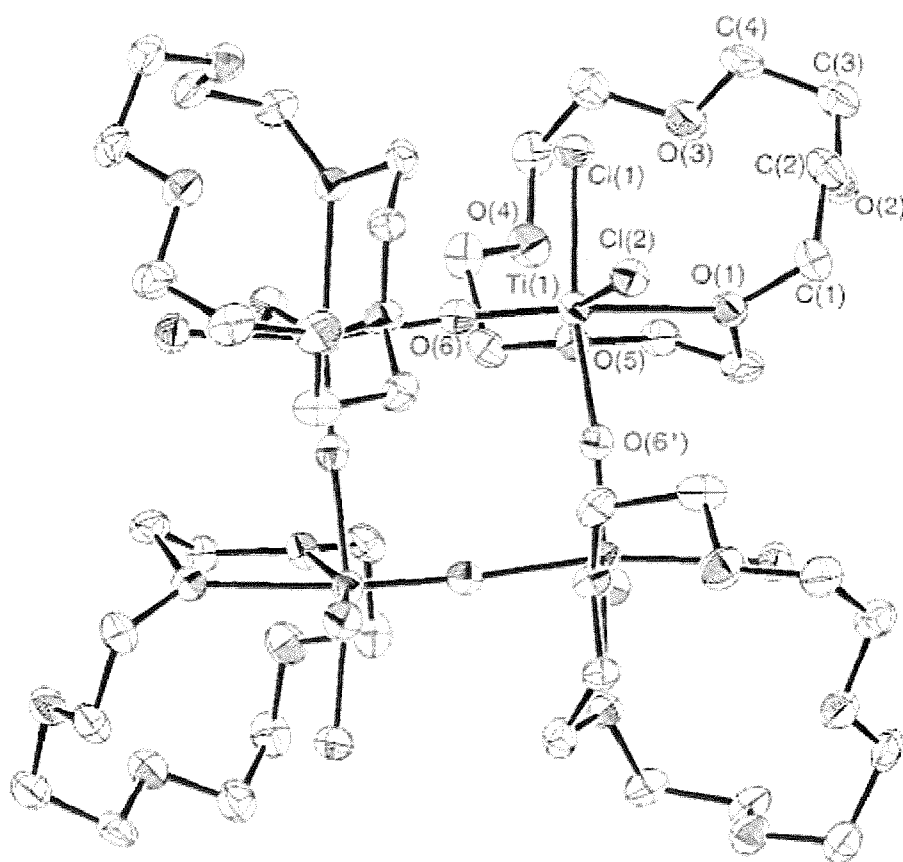
Fig. 6.8 View of the structure of [Ti$_4$Cl$_8$(μ-O)$_4$([15]-crown-5)$_4$], showing the atom numbering scheme. H atoms omitted for clarity. Ellipsoids are drawn at 40% probability level.

Table 6.2 Selected bond lengths (Å) and angles (°) for the structure of $[Ti_4Cl_8(\mu-O)_4([15]-crown-5)_4]$.

Ti-O(1)	2.244(5)	Ti-O(5)	2.117(5)
Ti-O(6)	1.690(5)	Ti-O(6')	2.001(5)
Ti-Cl(1)	2.351(2)	Ti-Cl(2)	2.312(2)
Ti-O(6)-Ti'	169.2(3)	O(6)-Ti-O(6')	94.3(3)
O(5)-Ti-O(6)	96.4(2)	O(5)-Ti-O(6')	83.9(2)
O(1)-Ti-O(6)	169.1(2)	O(1)-Ti-O(6')	82.3(2)
O(1)-Ti-O(5)	73.0(2)	O(6)-Ti-Cl(2)	102.7(2)
O(6')-Ti-Cl(2)	91.1(2)	O(5)-Ti-Cl(2)	160.6(2)
O(1)-Ti-Cl(2)	87.7(2)	O(6)-Ti-Cl(1)	95.6(2)
O(6')-Ti-Cl(1)	168.4(2)	O(5)-Ti-Cl(1)	89.1(2)
O(1)-Ti-Cl(1)	86.9(2)	Cl(1)-Ti-Cl(2)	92.6(1)

6.3 Conclusions

Reaction of TiX_4 (X = Cl or Br) with the crown ethers [12]-crown-4, [15]-crown-5 and [18]-crown-6 in anhydrous toluene yields compounds of the type $[TiX_4(\eta^2 - crown)]$. However, the complexes are extremely sensitive to hydrolysis, to the extent that isolating [TiCl$_4$([12]-crown-4)] was not possible. Two examples of hydrolysis were structurally characterised, representing two different stages of the process. The first stage is demonstrated by [([18]-crown-6)Cl$_3$Ti(μ-O)TiCl$_3$([18]-crown-6)], with formation of a single Ti-O-Ti linkage replacing one chlorine per Ti centre. Further hydrolysis removes a second chlorine from each Ti centre leading to formation of a tetrameric species, [Ti$_4$Cl$_8$(μ-O)$_4$([15]-crown-5)$_4$]. A third step would presumably involve formation of further Ti-O-Ti bridges accompanied by loss of a third chlorine. A likely geometry would be a cube, with Ti centres situated at the corners, a theory supported by the reported structure of the hydrolysis product [Ti$_8$O$_{12}$(H$_2$O)$_{24}$]$^{8+}$ which exhibits such a cubic arrangement (see Fig. 6.9).[19]
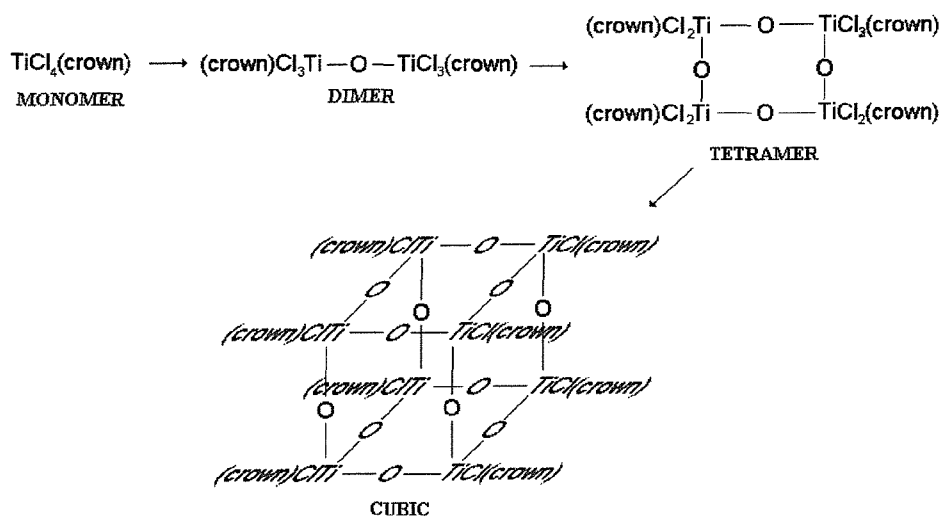
Fig. 6.9 Scheme showing the probable progressive hydrolysis pathway for compounds of the type TiCl$_4$(crown).

Comparison of the [TiCl$_4$(crown)] hydrolysis pathway with the analogous system of the preceeding element in the Periodic Table, scandium, proves interesting. In the former, oxygen replaces terminal chlorines, whilst the crown ether ligand is retained.

In contrast, the findings in Chapter 5 indicate that compounds of the type $[ScCl_3(crown)]^{(3-x)+}$ retain the halide whilst the crown is displaced in favour of water, to form $[ScCl_3(H_2O)_3]$, with the crown ether hydrogen bonded to the coordinated water. The highly polarising Ti(IV) centre is better suited to oxo-group coordination, with π-interactions possible, whilst the larger Sc(III) centre prefers coordination by aquo-ligands. However, for both systems, the ethers show a surprisingly low affinity for the hard d^0 Sc(III) and Ti(IV) metal centres.

$TiCl_4$ reacts with [15]aneS$_2$O$_3$ to form $[TiCl_4([15]aneS_2O_3)]$, with bonding through the sulfur donor atoms. Given the choice of S or O donors in identical environments, the hard Ti(IV) centre surprisingly prefers the softer donor ligand.

6.4 Experimental

$TiCl_4$, $TiBr_4$, TiI_4, [12]-crown-4, [15]-crown-5 and [18]-crown-6 were obtained from Aldrich and used as received, with the exception of [12]-crown-4, which was dried *in vacuo* or by treatment with $SOCl_2$ prior to use. $[15]aneS_2O_3$ was synthesised by literature methods (see 1.3.3).[20] X-ray powder diffraction data were collected over a 2θ range of 10-70° with a step size of 0.02° using a Siemens D5000 diffractometer in reflecting geometry and $Cu-K_{\alpha l}$ radiation. The powder pattern for the literature structure was predicted using the Atoms program.[21]

6.4.1 Reactions of $TiCl_4$ with crown ether ligands

[$TiCl_4$([18]-crown-6)]

To a solution of [18]-crown-6 *(0.26 g, 1.0 mmol)* in toluene (10 cm^3), $TiCl_4$ *(0.19 g, 1.0 mmol)* was added dropwise, affording a yellow precipitate. The mixture was stirred for 30 mins, with the soild then filtered off and washed with *n*-hexane (10 cm^3). The product was then dried *in vacuo*. Yield 0.095 g, 42%. (Found: C, 30.5; H, 5.8. Calc. for $C_{12}H_{24}Cl_4O_6Ti$: C, 31.8; H, 5.3%). IR (cm^{-1})(Nujol mull): 1303w, 1261w, 1208w, 1168m, 1144s, 1134m, 1073m, 1037s, 972m, 932m, 901m, 842m, 804m, 733m, 566w, 467w, 377s, br. UV/Vis. (cm^{-1})(DR, $BaSO_4$): 28000. ^1H NMR (300 K, CD_2Cl_2): 3.60, 3.76 (overlapping) [12 H], 4.00 [4H], 4.23-4.60 [8H]; (220 K): No change; (With added $TiCl_4$, 300 K): No resonances observed.

[($TiCl_4$)$_2$([18]-crown-6)]

Was made similarly using a 2:1 molar ratio of $TiCl_4$: ligand in *n*-hexane. Yield 70 %. (Found: C, 20.4; H, 4.0. Calc. for $C_{12}H_{24}Cl_8O_6Ti_2$: C, 21.7; H, 3.6%). IR (cm^{-1})(Nujol mull): 1300m, 1272w, 1249w, 1169w, 1144s, 1131m, 1068s, 1033s, 932m, 918m, 839m, 804m, 781m, 565w, 397vs, 383vs, br. UV/Vis. (cm^{-1})(DR, $BaSO_4$): 28000. ^1H NMR (300 K, CD_2Cl_2): 3.70 [8H], 4.00 [8H], 4.52 [8H]; (200 K): 3.3 – 4.5 complex pattern.

[([18]-crown-6)TiCl₃OTiCl₃([18]-crown-6)]

Was made similarly to [TiCl₄([18]-crown-6)], except the reaction mixture was stirred for 48 h under nitrogen prior to filtration. Yield 60%. (Found: C, 33.3; H, 5.8. Calc. for $C_{24}H_{48}Cl_6O_{13}Ti_2$: C, 33.8; H, 5.6%). IR (cm^{-1})(Nujol mull): 1303w, 1260w, 1250w, 1144m, 1121w, 1098m, 1081s, 1037m, 1020s, 942s, 917m, 894m, 851m, 828w, 775w, 540m, 439w, 394s, 366s, 307m. UV/Vis. (cm^{-1})(DR, BaSO₄): 28600. ^{1}H NMR (300 K, CD₂Cl₂): 3.60, 3.65 (overlapping) [12 H], 3.99 [4H], 4.43-4.70 [8H]; (200 K): 3.42, 3.49, 3.77, 4.50, 4.53.

[TiCl₄([15]-crown-5)]

To a solution of [15]-crown-5 (0.22 g, 1.0 mmol) in toluene (10 cm³), TiCl₄ (0.19 g, 1.0 mmol) was added dropwise, affording a bright yellow precipitate. The mixture was stirred for 30 mins under a nitrogen atmosphere, following which the solid was filtered off and washed with *n*-hexane (10 cm³). The powder was dried *in vacuo*. Yield 0.16 g, 40%. (Found: C, 29.5; H, 5.2. Calc. for $C_{10}H_{20}Cl_4O_5Ti$: C, 29.3; H, 4.9%). IR (cm^{-1})(Nujol mull): 1305s, 1261w, 1168w, 1130s, 1062s, 1020w, 978s, 930m, 907m, 848s, 827m, 769w, 565w, 546w, 519w, 430m, 394s, 363s, 339s, 321m. UV/Vis. (cm^{-1})(DR, BaSO₄): 28000. ^{1}H NMR (300 K, CD₂Cl₂): 3.60 br [8H], 4.33 [4H], 4.60 [4H], 5.00 [4H]; (220 K): No change; (With added TiCl₄, 300 K): 4.4 v. br. (220 K) 3.68, 3.72, 3.94, 4.11, 4.39, 4.60, 4.87, 5.02, 5.20.

[TiCl₄([15]aneS₂O₃)]

TiCl₄ (0.19 g, 1.0 mmol) was added dropwise to a solution of [15]aneS₂O₃ (0.25 g, 1.0 mmol) in toluene (10 cm³), yielding an orange precipitate. The product was filtered off and washed with toluene (5 cm³) then dried *in vacuo*. Yield 70%. (Found: C, 26.8; H, 4.8. Calc. for $C_{10}H_{20}Cl_4O_3S_2Ti$: C, 27.2; H, 4.6%). IR (cm^{-1})(Nujol mull): 1303s, 1255w, 1169w, 1155w, 1080m, 1021w, 968m, 933m, 918m, 889s, 848m, 805m, 770m, 566w, 482s, 472m, 409s, 385s, 377s, 353sh. UV/Vis. (cm^{-1})(DR, BaSO₄): 27500, 22000. ^{1}H NMR (300 K, CD₂Cl₂): 2.98 [4H], 3.20 [4H], 3.61, 3.73 [8H], 3.87 [4H]; (220 K): No change.

6.4.2 Reactions of TiBr$_4$ with crown ether ligands

[TiBr$_4$([18]-crown-6)]

To a solution of [18]-crown-6 (0.13 g, 0.5 mmol) in toluene (10 cm^3), a solution of TiBr$_4$ (0.19 g, 0.5 mmol) in toluene (10 cm^3) was added, affording a red-brown precipitate. The product was filtered off, washed with toluene (5 cm^3) and dried *in vacuo*. Yield 60 %. (Found: C, 22.6; H, 4.0. Calc. for C$_{12}$H$_{24}$Br$_4$O$_6$Ti: C, 22.8; H, 3.8%). IR (cm^{-1})(Nujol mull): 1302m, 1258w, 1168w, 1150m, 1081s, 1039s, 953s, 921w, 891w, 836w, 803w, 770w, 562w, 467sh, 334s, 321s, 312m, 300m. UV/Vis. (cm^{-1})(DR, BaSO$_4$): 21000. ^{1}H NMR (300 K, CD$_2$Cl$_2$): 3.72 [16H]; (220 K): No change.

[TiBr$_4$([15]-crown-5)]

Solutions of [15]-crown-5 (0.11 g, 0.5 mmol) and TiBr$_4$ (0.19 g, 0.5 mmol) in toluene (10 cm^3) were mixed, producing a red-brown precipitate. The product was filtered off, washed with toluene (5 cm^3) and dried *in vacuo*. Yield 50%. (Found: C, 20.3; H, 3.4. Calc. for C$_{10}$H$_{20}$Br$_4$O$_5$Ti: C, 20.4; H, 3.4%). IR (cm^{-1})(Nujol mull): 1305m, 1260w, 1169m, 1150s, 1138s, 1119s, 1104m, 1013m, 975s, 951s, 921s, 904m, 845s, 821m, 767w, 565w, 544w, 438w, 320s, 282vs. UV/Vis. (cm^{-1})(DR, BaSO$_4$): 22000. ^{1}H NMR (300 K, CD$_2$Cl$_2$): 3.64 br [16H], 4.65-5.00 (overlapping) [8H]; (220 K): No change; (With added TiBr$_4$, 300 K): 3.8, 4.6 v. br. (1:1 integrals); (220 K): 3.55, 3.82, 4.38, 4.59, 4.78, 5.05.

[TiBr$_4$([12]-crown-4)]

Was made similarly to [TiBr$_4$([15]-crown-5)]. Yield 60%. (Found: C, 17.6; H, 2.8. Calc. for C$_8$H$_{16}$Br$_4$O$_4$Ti: C, 17.7; H, 3.0%). IR (cm^{-1})(Nujol mull): 1303m, 1261w, 1169s, 1151m, 1092m, 1021m, 973m, 936m, 919w, 846m, 821m, 803m, 562w, 416w, 394w, 348w, 321m, 275s, 242m. UV/Vis. (cm^{-1})(DR, BaSO$_4$): 21700. ^{1}H NMR (300 K, CD$_2$Cl$_2$): 3.66 br; (220 K): No change.

6.4.3 Crystallographic studies

Details of the crystallographic data collection and refinement parameters are given in Table 6.3.

[([18]-crown-6)Cl₃Ti(μ-O)TiCl₃([18]-crown-6)]

Pale yellow block crystals were grown by slow evaporation of the toluene mother-liquor from the synthesis of [TiCl₄([18]-crown-6)] under a nitrogen atmosphere. Structure solution and refinement were carried out using SHELXL 97, and were straightforward.[22-24] During refinement, a 50% occupied toluene solvent molecule was identified in the asymmetric unit. This was symmetry related to a second 50% occupancy toluene such that the methyl carbon of one molecule is sumperimposed on the ipso carbon of the other. As a result, six carbon atoms were refined, five with occupancy = ½, and one with occupancy = 1.
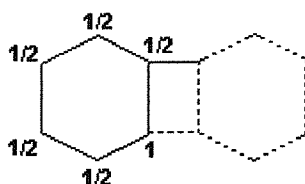
Fig. 6.10 Model of the two symmetry related 50% occupied toluene molecules in the structure of [([18]-crown-6)Cl₃Ti(μ-O)TiCl₃([18]-crown-6)] showing the occupancy of each specific carbon.

[Ti₄Cl₈(μ-O)₄([15]-crown-5)₄]

Pale yellow block crystals were isolated by slow evaporation of the toluene filtrates obtained from the synthesis of [TiCl₄([15]-crown-5)] under a nitrogen atmosphere. Refinement using SHELXL 97 was routine.[22-24] During solution, a fully occupied toluene molecule and a water molecule with occupancy = ½ were identified per Ti centre in the tetrameric complex.

Table 6.3 Crystallographic data collection and refinement parameters

	$[Ti_2Cl_6(\mu\text{-O})([18]\text{-crown-6})_2].1/2C_7H_8$	$[Ti_4Cl_8(\mu\text{-O})_4([15]\text{-crown-5})_4].4C_7H_8.4(1/2H_2O)$
Formula	$C_{27.5}H_{52}Cl_6O_{13}Ti_2$	$C_{68}H_{116}Cl_8O_{26}Ti_4$
Formula weight	899.19	1824.8
Crystal system	Triclinic	Tetragonal
Space group	$P\bar{1}$ (No. 2)	P4/n (No. 85)
a / Å	10.2483(5)	20.353(3)
b / Å	13.835(1)	20.353(3)
c / Å	14.721(1)	10.739(2)
α / °	84.669(3)	90
β / °	81.909(3)	90
γ / °	79.892(3)	90
U / Å^3	2029.3(2)	4448.6(12)
Z	2	2
μ(Mo-K$_\alpha$) / cm^{-1}	0.844	0.655
No. unique reflections	9239	3883
R_{int}	0.046	0.14
No. of obs. reflections	8071	1722
No. parameter/restraint	451/0	356/0
R [b]	0.0346	0.0733
wR_2 [c]	0.0873	0.1671

[a] Observed if $[I_o > 2\sigma(I_o)]$ [b] $R = \sum (|F_{obs}|_i - |F_{calc}|_i) / \sum |F_{obs}|_i$ [c] $wR_2 = [\sum w(F_{obs}^2 - F_{calc}^2)^2 / \sum w(F_{obs}^2)^2]^{1/}$

6.5 References

1. R. Hart, W. Levason, B. Patel, G. Reid, *Eur. J. Inorg. Chem.*, 2001, 2927.

2. R. J. H. Clark, W. Errington, J. Lewis, R. S. Nyholm, *J. Chem. Soc. (A)*, 1966, 989.

3. M. F. Lappert, *J. Chem. Soc. (A)*, 1966, 1496.

4. G. R. Willey, J. Palin, N. W. Alcock, *J. Chem. Soc., Dalton Trans.*, 1992, 1117.

5. V. K. Belsky, B. M. Bulychev, *Russ. Chem. Rev.*, 1999, **68**, 119.

6. V. K. Belsky, B. M. Bulychev, N. R. Strel'tsova, *Zh. Neorg. Khim.*, 1992, **37**, 1531.

7. M. Plate, G. Frenzen, K. Dehnicke, *Z. Naturforsch., B*, 1993, **48**, 149.

8. S. G. Bott, H. Prinz, A. Alvanipour, J. L. Atwood, *J. Coord. Chem.*, 1987, **16**, 303

9. S. G. Bott, U. Kynast, J. L. Atwood, *J. Inclusion Phenom.*, 1986, **4**, 241.

10. N. R. Strel'tsova, L. V. Ivakina, V. K. Belsky, P. A. Storozhenko, B. M. Bulychev, A. I. Gorbunov, *Zh. Obshch. Khim.*, 1988, **58**, 861.

11. A. B. P. Lever, *Inorganic Electronic Spectrscopy*, 2nd Edition, Elsevier, 1984.

12. W. Levason, B. Patel, G. Reid, V.-A. Tolhurst, M. Webster, *J. Chem. Soc., Dalton Trans.*, 2000, 3001.

13. J. Okuda, E. Herdtweck, *Inorg. Chem.*, 1991, **30**, 1516.

14. G. R. Willey, J. Palin, M. G. B. Drew, *J. Chem. Soc., Dalton Trans.*, 1994, 1799.

15. V. Krug, U. Müller, *Acta Crystallogr., Sect. C*, 1990, **46**, 547.

16. N. R. Strel'tsova, L. V. Ivakina, V. K. Bel'skii, P. A. Storozhenko, B. M. Bulychev, *Koord. Khim.*, 1988, **14**, 421.

17. Y. Pelihua, T. Pape, I. Uson, M. A. Said, H. W. Roesky, M. L. Montero, H. –G. Schmidt, A. Demsar, *Inorg. Chem.*, 1998, **37**, 5117.

18. U. Thewalt, K. Doppert, *J. Organomet. Chem.*, 1987, **320**, 177.

19. M. G. Reichmann, F. J. Hollander, A. T. Bell, *Acta Crystallogr., Sect. C*, 1987, **43**, 1681.

20. J. S. Bradshaw, G. Y. Hui, B. L. Haymore, J. J. Christensen, *J. Heterocyclic Chem.*, 1973, **10**, 1.

21. ATOMS 5.0.1, Eric Dowty, 1999.

22. R. H. Blessing, *J. Appl. Cryst.*, 1997, **30**, 421.

23. G. M. Sheldrick, SHELXL 97, Program for crystal structure solution, University of Göttingen, 1997.

24. PATTY, The DIRDIF Program System, P. T. Beurskens, G. Admiraal, G. Beurskens, W. P. Bosman, S. Garcia-Granda, R. O. Gould, J. M. M. Smits, C. Symkalla, *Technical Report of the Crystallographic Laboratory*, University of Nijmegen, The Netherlands, 1992.

Chapter 7

Appendix

7.1 Experimental Techniques

The hard metal centres used in these studies show a preference towards hard donor ligands. For studies into reactions of hydrated Sc, Y or La salts with pnictogen oxide ligands this did not cause experimental problems. However, for reactions of anhydrous scandium chloride (Chapter 5) or titanium halides (Chapter 6) with crown ether ligands, products were likely to be both air and moisture sensitive. Hence, during both synthesis and characterisation, precautions to avoid exposure to air and water were taken. Anhydrous solvents were prepared by distillation under nitrogen over specific reagents (Table 7.1), whilst sample preparation was carried out in a continuously nitrogen purged dry glove box. Schlenk techniques were adopted where appropriate.

Table 7.1 Reagents adopted for anhydrous solvent preparation.

Solvent	Reagents
Ethanol	Mg turnings / Trace iodine
Acetonitrile	Calcium hydride
Dichloromethane	Calcium hydride
Tetrahydrofuran	Sodium / Benzophenone[a]
Hexane	Sodium / Benzophenone[a]
Toluene	Sodium / Benzophenone[a]

[a] Trace diglyme added to solubulise sodium.

Throughout these studies, a range of spectroscopic techniques have been employed. Brief descriptions of the methods used follow. In addition, microanalysis for carbon, hydrogen and where appropriate nitrogen has been carried out using the University of Strathclyde microanalytical service.

7.1.1 IR Spectroscopy

Spectra were recorded on a Perkin Elmer 1710 spectrometer over the range 4000-220 cm^{-1}. Samples were prepared as Nujol mulls between CsI plates, or, when absorptions caused by Nujol masked regions of the spectrum that were of interest, CsI discs were

prepared. Some problems were experienced when adopting the latter method when using metal halide salts as reagents with halide exchange observed (apparent by distinct colour change of the disc) for certain samples.

7.1.2 UV/Visible Spectroscopy

Spectra were recorded for the titanium halide – crown ether system using a Perkin Elmer Lambda 19 spectrometer. Owing to both the poor solubility of these compounds in all solvents throughout these studies, spectra were recorded by diffuse reflectance using dry $BaSO_4$ as an inert diluent. Data were displayed using F(R) (the Kubelka-Munk function).

The titanium centre is d^0 and hence lacks d-d and metal to ligand charge transfer transitions. As a result, for the ligands studied, observed transitions could be assigned to ligand to metal charge transfer transitions.

7.1.3 Molar Conductance Experiments

Conductivities were measured on a Pye 1700 conductance bridge for 10^{-3} mol dm^{-3} solutions of the complexes in anhydrous CH_2Cl_2 or $MeNO_2$, the former chosen when solubility permitted. For reference, standard solutions were prepared in CH_2Cl_2 to assess typical values of 1:1, 2:1 and 3:1 electrolytes. For example, the value of Λ_m was measured for a 10^{-3} mol dm^{-3} solution of $^nBu_4NBF_4$ to indicate values for a 1:1 electrolyte (found to be 22.5 $ohm^{-1}cm^2mol^{-1}$). For $MeNO_2$ solutions, literature values were used.[1]

7.1.4 Nuclear Magnetic Resonance Spectroscopy

Multinuclear NMR spectroscopy was used extensively in these studies to examine behaviour in solution. In many cases, variable temperature studies were conducted to allow observation of dynamic processes occurring. Spectra were recorded using either a Bruker AM360 or a Bruker DPX400 NMR spectrometer, with the exception of both ^1H and ^{13}C NMR spectra, which were measured on a Bruker AM300 machine. ^1H NMR spectra were recorded at 300 MHz in $CDCl_3$, CD_2Cl_2, d^6-acetone, d^3-acetonitrile

or d^3-nitromethane in 5 mm tubes. Spectra obtained for other nuclei were recorded from samples in 10 mm tubes.

^{31}P-$\{^1$H$\}$ NMR spectroscopy

Spectra were recorded from solutions containing 10% deuterated solvent. The majority of spectra were from CH_2Cl_2 – 10% $CDCl_3$ solutions, although $MeNO_2$, $EtNO_2$, MeCN or EtOH based solutions were also used where necessary. Spectra were recorded at 145.5 MHz (when using AM360 NMR spectrometer) or 162.0 MHz (DPX400 NMR spectrometer), referenced to external 85% H_3PO_4.

The ^{31}P nucleus has 100% natural abundance, with spin I = ½. In addition, the nucleus has a good receptivity (D_p = 0.0663) and a reasonably high magnetic moment (μ = 1.9581 μ_n) making it a favourable nucleus for NMR spectroscopy studies.[2, 3]

^{89}Y NMR spectroscopy

Information about ^{89}Y NMR spectroscopy, including properties of the nucleus is given in Sections 1.2.2 and 1.4.1. Here, the experimental conditions used to record data are described. Spectra were recorded in 10mm tubes from concentrated solutions. The compound 2,2,6,6-tetramethylpiperidin-1-oxyl (TEMPO) was added to act as a relaxation agent, with a 2 s pulse delay at 17.65 MHz (when using the AM360 NMR spectrometer) or at 19.6 MHz (for DPX400 NMR spectrometer) and a sweep width of 25 KHz. Long collection times were often required owing to the properties of the ^{89}Y nucleus. A 2 mol dm^{-3} solution of YCl_3 at pH 1 was used as a zero reference.[4]

^{45}Sc NMR spectroscopy

Properties of the ^{45}Sc nucleus and a discussion of previous ^{45}Sc NMR studies are described in Sections 1.2.1 and 1.4.2. Here, the experimental conditions used to record data are described. ^{45}Sc NMR spectra were recorded at 87.5 MHz (when using the AM360 NMR spectrometer) or at 97.2 MHz (when the DPX400 spectrometer was employed), referenced to a 0.1 mol dm^{-3} solution of $Sc(NO_3)_3$ at pH 1.[4]

7.1.5 Single Crystal X-Ray Diffraction

Data were routinely collected on either a Rigaku AFC7S four-circle diffractometer or an Enraf Nonius-Kappa CCD diffractometer fitted with Mo-Kα radiation and a graphite monochromator. Cell dimensions were taken directly from the diffractometer software, with the fact that e.s.d. values for data collected with the CCD are unreasonably small acknowledged.[5] The reflections collected were sorted, with data quality determined by percentage of expected unique reflections that were observed. In addition, R_{int}, the internal residual factor, can be calculated. Generally, a value of less than 0.1 indicates a good data set.

Structures were solved using either Patterson synthesis methods or direct methods within the TEXSAN package.[6, 7, 8] DIRDIF is best suited for structures containing one heavy atom and many light atoms whilst direct methods can be used for any structure (they are best suited to a structure containing lots of atoms of similar weight). Most examples within this study contained heavy atoms meaning either method was appropriate. The presence of heavy atoms meant absorption corrections were required. For data collected on the Rigaku, psi-scans were recorded during data collection,[9] whilst for Nonius data, SORTAV software was used to calculate absorption by comparison of symmetry equivalent reflections.[10] Refinement was carried out using full-matrix least-squares refinement cycles,[8] an iterative procedure that achieves the best fit between the observed data and the Fourier transforms of the structure solution. In addition, the least squares cycle offers a range of information, including residual factors such as R and R_w (weighted R-factor) which offer indication as to the quality of the solution Another factor commonly quoted is the reflection:parameter ratio (number of observed reflections per parameter refined). Generally this value should be at least 8 for a satisfactory solution, although for high symmetry complexes slightly lower values may be acceptable. The reflection:parameter difference is accounted for in the goodness of fit (GOF), a standardised comparison with the optimal value being 1.

7.2 References

1. W. J. Geary, *Coord. Chem. Rev.*, 1971, **7**, 81.

2. *Multinuclear NMR*, Ed. J. Mason, Plenum, New York, 1987.

3. R. K. Harris, B. E. Mann, *NMR and the Periodic Table*, Academic Press, London, 1978.

4. A. L. Hector, W. Levason, M. Webster, *Inorg. Chim. Acta*, 2000, **298**, 43.

5. F. H. Herbstein, *Acta Crystallogr., Sect. B*, 2000, **56**, 547.

6. P. T. Beurskens, G. Admiraal, G. Beurskens, W. P. Bosman, S. Garcia-Granda, R. O. Gould, J. M. M. Smits, C. Smykalla, The DIRDIF program system, University of Nijmegen, 1992.

7. G. M. Sheldrick, SHELXL 97, Crystal structure refinement program, University of Göttingen, 1997.

8. TEXSAN, Single crystal structure analysis software, version 1.7-1, Molecular Structure Corporation, The Woodlands, TX, 1995.

9. F. S. Matthews, A. C. T. North, D. C. Phillips, *Acta Crystallogr., Sect. A*, 1995, **51**, 33.

10. SORTAV, R. H. Blessing, *Acta Crystallogr., Sect. A*, 1995, **51**, 33.